Maynooth University
National University of Ireland Maynooth

# The Neural Correlates of Spatial Learning and Memory During Human Navigation

Thesis submitted to the Department of Psychology, Faculty of Science and Engineering, in fulfilment of the requirements for the degree of Doctor of Philosophy, National University of Ireland, Maynooth.

Conor Thornberry B.A. (Hons), M.Sc.

February 2024

**Research Supervisor**: Prof. Seán Commins

**Head of Department**: Dr. Michael Cooke

Publications arising from this thesis:

1. **Thornberry, C.,** Caffrey, M., & Commins, S. (2023). Theta oscillatory power decreases in humans are associated with spatial learning in a virtual water maze task. *European Journal of Neuroscience*, *58*(11), 4341–4356.
2. **Thornberry, C.,** Cimadevilla, J. M., & Commins, S. (2021). Virtual Morris water maze: opportunities and challenges. *Reviews in the Neurosciences*, *32*(8), 887-903.
3. Commins, S., Duffin, J., Chaves, K., Leahy, D., Corcoran, K., Caffrey, M., ... & **Thornberry, C.** (2020). NavWell: A simplified virtual-reality platform for spatial navigation and memory experiments. *Behavior research methods*, *52*(3), 1189-1207.

# Table of Contents

**Chapter 1** ..... **1**
1.1 Theories of Spatial Learning & Memory ..... 2
1.1.1 Cognitive Mapping Theory ..... 2
1.1.2 Associative Learning Theory ..... 4
1.1.3 Multiple Trace Theory & Systems Consolidation ..... 6
1.1.4 Overview of Theoretical Frameworks ..... 8
1.2 Assessment of Spatial Navigation in Animals & Humans ..... 9
1.2.1 The Rat Race: Mazes and Spatial Learning ..... 9
1.2.2 MWM and Navigation Strategy Assessment ..... 11
1.2.3 Virtual Reality in Spatial Navigation Research ..... 14
1.2.4 Virtual Morris Water Maze ..... 15
1.3 The Neural Basis of Spatial Navigation ..... 20
1.3.1 Brain Regions Involved in Spatial Navigation ..... 20
1.3.2 Cellular Networks of Spatial Navigation ..... 22
1.3.3 Brain Oscillations & Spatial Navigation ..... 27
1.4 Oscillations & Human Spatial Navigation ..... 29
1.4.1 Current Understanding of Oscillatory Activity in Human Navigation ..... 29
1.4.2 Low-Frequency Oscillations (Delta & Theta) ..... 30
1.4.3 Alpha Oscillations ..... 34
1.4.4 High-Frequency Oscillations (Beta & Gamma) ..... 35
1.5 Brief Overview of Factors Influencing Brain Activity During Navigation ..... 38
1.5.1 Sex/Gender ..... 38
1.5.2 Ageing ..... 40
1.6 Thesis Objectives ..... 42
**Chapter 2** ..... **44**
2.1 Neuropsychological Assessments ..... 45
2.1.1 National Adult Reading Test (NART) ..... 45
2.1.2 Trail Making Test (TMT) ..... 46
2.1.3 Montreal Cognitive Assessment (MoCA) ..... 47
2.2 Spatial Navigation Task ..... 49
2.2.1 Virtual Morris Water Maze ..... 49
2.2.2 Setup procedure and environment design ..... 51
2.2.1.1 Learning Phase ..... 53
2.2.1.2 Recall Phase ..... 56
2.2.1.3 Practice Phase (Older Adults) ..... 58

2.3 Electroencephalography ..... 59
2.3.1 An overview of measuring EEG ..... 60
2.3.2 Current Approaches for Studying EEG in Human Spatial Navigation ..... 62
2.3.3 Hardware and software ..... 65
2.3.4 Procedure ..... 66
2.3.4.1 COVID-19 precautions ..... 67
2.3.5 EEG Analysis ..... 68
2.3.5.2 Band-Pass Filter Selection ..... 70
2.3.5.3 Bad Channel Removal and Interpolation ..... 72
2.4.3 Independent Component Analysis ..... 72
2.3.5.4 EEG Frequency Band Analysis ..... 74
2.3.5 Statistical Analysis ..... 76
2.3.6 Ethical Approval & Participant Recruitment ..... 77
**Chapter 3 ..... 79**
3.1 Introduction ..... 81
3.2 Methods ..... 85
3.2.1 Participants ..... 85
3.2.4 EEG Pre-Processing ..... 88
3.2.5 EEG Frequency Band Analysis ..... 88
3.2.6 Statistical Analysis ..... 90
3.3. Results ..... 92
3.3.1 Behavioural Results ..... 92
3.3.2 EEG Results ..... 95
3.3.2.1 Trial Start/Route Initiation Phase ..... 95
3.3.2.2 Trial End/Goal Approach Phase ..... 101
3.3.2.3 Exploratory within-groups learning dynamics ..... 106
3.3.2.3.1 Theta Oscillations ..... 108
3.3.2.3.2 Alpha Oscillations ..... 109
3.4 Discussion ..... 110
3.4.1. Hypothesis-driven theta band analysis ..... 110
3.4.3 Exploratory analysis of the alpha band ..... 114
3.4.4 Conclusions ..... 116
**Chapter 4 ..... 117**
4.1 Introduction ..... 119
4.2 Methods ..... 122
4.2.1 Participants ..... 122

4.2.2 Spatial Navigation Task ..... 123
4.2.3 EEG Recording ..... 124
4.2.4 EEG Preprocessing ..... 124
4.2.5 EEG Spectral Analysis ..... 125
4.2.6 Statistical Analysis ..... 126
4.3 Results ..... 127
4.3.1 Behavioural Results ..... 127
4.3.2 EEG Results ..... 130
4.3.2.1 Relative Frequency Band Power ..... 130
4.3.2.3 Behaviour-matched EEG dynamics ..... 138
4.3.2.3.1 Goal-Directed vs Random Behaviour ..... 139
4.3.2.3.2 Switching Behaviour (Learning group) ..... 143
4.4 Discussion ..... 146
4.4.1 Delta-Theta Oscillations ..... 146
4.4.2 Alpha Oscillations ..... 148
4.4.3 Beta-Gamma Oscillations ..... 150
4.4.4 Limitations and Future Directions ..... 152
4.4.5 Conclusion ..... 154
**Chapter 5 ..... 156**
5.1 Introduction ..... 158
5.2 Methods ..... 162
5.2.1 Participants ..... 162
5.2.2 Resting State Task ..... 162
5.2.3 Spatial Navigation Task ..... 163
5.2.4 EEG Recording ..... 164
5.2.5 EEG Preprocessing ..... 165
5.2.6 EEG Spectral Analysis ..... 165
5.2.7 Statistical Analysis ..... 166
5.3 Results ..... 168
5.3.1 Behavioural Results ..... 168
5.3.1.1 Learning Phase ..... 168
5.3.1.2 Recall ..... 171
5.3.1.3 Recent vs Remote Memory ..... 173
5.3.2 EEG Results ..... 175
5.3.2.1 Replication of immediate recall findings ..... 175
5.3.2.2 Task-related differences in recent and remote recall ..... 178
5.3.2.2.1 Immediate vs Recent Recall (24-Hour Group) ..... 179

5.3.2.2.2 Immediate vs Remote Recall (1-Month Group) ..... 183
5.3.2.2.3 Recent vs. Remote memory ..... 188
5.4 Discussion ..... 194
5.4.1 Memory performance ..... 194
5.4.2 Relative dynamics of spatial recall remain similar ..... 195
5.4.3 Overall effort increases with retrieval demands ..... 196
5.4.4. Frontal regions are related to spatial memory retrieval ..... 197
5.4.5. Delta-Theta & Gamma support memory replay during remote retrieval ..... 199
5.5 Conclusions ..... 201
**Chapter 6 ..... 203**
6.1 Introduction ..... 205
6.2 Methods ..... 209
6.2.1 Participants ..... 209
6.2.2 Resting State Task ..... 209
6.2.3 Spatial Navigation Task: Practice Trials ..... 210
6.2.4 Spatial Navigation Task: Experimental Trials ..... 211
6.2.5 EEG Recording ..... 212
6.2.6 EEG Preprocessing ..... 212
6.2.7 EEG Spectral Analysis ..... 213
6.2.8 Statistical Analysis ..... 213
6.3 Behavioural Results ..... 214
6.3.1 Cognitive Tasks ..... 214
6.3.2 Young vs. Old: Learning Phase ..... 215
6.3.3 Older Adults: Learning Phase ..... 217
6.3.4 Young v Old: Immediate Recall Trial ..... 220
6.3.5 Recent & Remote Recall ..... 221
6.3.5.1 Older Adults ..... 221
6.3.5.2 Younger vs. Older Adults ..... 222
6.3.5.3 Performance Change in Older Adults ..... 224
6.4 EEG Results ..... 226
6.4.1 Age-Related Differences in Eyes-Open Resting State ..... 226
6.4.2 Resting State Correlates of Spatial Navigation & Cognition ..... 231
6.4.2.1 All participants ..... 231
6.4.2.2 Group-specific Correlations ..... 232
6.4.3 Immediate Recall: Young vs Old ..... 234
6.4.5 Recent Memory (24-hours): Young vs Old ..... 237
6.4.6 Remote Memory (1-month): Young vs Old ..... 240

6.4.7 Recent vs. Remote Memory in Older Adults ..... 242
6.4.8 Within-group explorative analysis of age-specific performance change ..... 244
6.5 Discussion ..... 247
6.5.1 Behavioural Results ..... 247
6.5.2 Resting State Activity ..... 248
6.5.3 Age-related differences across memory phases ..... 249
6.5.4 Anterior-posterior shift evident within older-adult memory conditions ..... 252
**Chapter 7 ..... 254**
7.1 Overview of thesis findings ..... 255
7.2 Potential implications and future directions ..... 261
7.3 Potential applications ..... 267
7.4 Thesis Difficulties, Limitations and Strengths ..... 273
7.5 Conclusions ..... 277
Appendices ..... 315
Appendix A ..... 316
Appendix B ..... 318

**Acknowledgements**

To my supervisor, Prof. Seán Commins, it has been an absolute privilege to work with you over these many (many) years. You have been an excellent mentor, both personally and academically. This journey would not have been possible without your continuous encouragement and support. To my colleagues and best friends, Dr's Michelle Caffrey and Keith O'Donnell. Without you this experience would have been incredibly challenging. Though our numerous breaks for snacks and tea still made it challenging, it made the journey much more enjoyable. I feel incredibly lucky to have worked with such excellent researchers and friends. To my family, David, Teresa and Niamh, who have supported this journey from very early on. This would not have been possible without you all. I am forever grateful. I promise to actually get a real job soon. To my grandparents, Kathleen & Patrick, who made my journey through the system possible and always supported me along the way. This is for you.

Thank you to the John & Pat Hume scholarship for this opportunity. To the past and present postgrads, who have listened to my insufferable moaning. I appreciate you always being willing to listen. A thank you to all the staff at the Department of Psychology over the years, you have always been incredibly friendly, helpful and welcoming. In particular, thank you to Prof. Richard Roche, Prof. Fiona Lyddy and Dr. Peter Murphy for your life and career advice, support, and direction along this journey. Thank you to all the interns I have worked with over the years with behavioural and EEG data collection, namely Olivia, D'Andra and Caoimhe. To my partner and best friend, Emma – who has always supported me through everything, encouraged me to apply for things I didn't think I could get, and corrected my grammatical errors more times than I care to admit. You are an inspiration, and this is partly yours. Finally, my close friends, Carl, Eamonn, Jamie, Liam, Eoin, Ryan, Warren, James, Dylan and Liam. You have all done nothing but distract me along this journey, but I am incredibly grateful for it. Thank you all, this is for you, but I don't expect you to read it, it's mad boring.

This thesis is dedicated to my grandmother, Kathleen Grehan.

An inspiration in adversity and strength, through health and illness.

Your favourite saying has gotten me through this PhD:

Ah I'll get there.

I am still unsure of where *there* is, but I think this might be close enough for now.

Thank you for everything.

## Thesis Abstract

Spatial navigation is an essential skill for animals and humans alike. It helps us get to a desired place and remember how to get back there in the future. Despite the fact that this process in humans has been well researched, there is still little known about the neural activity underlying spatial navigation processes in humans. Therefore, we aimed to contribute to the current human navigation literature by exploring a number of cognitive factors known to be involved, namely learning and memory. This thesis aims to address gaps in the literature by exploring spatial learning as a dynamic and flexible behavioural process, as well as spatial memory retrieval following recent (24-hours) and remote (1 month) retention intervals. Furthermore, we examined age-related changes in these behavioural and neural underpinnings. Spatial navigation ability was assessed using a virtual water maze task: NavWell (Commins et al., 2020). We also examined brain oscillations, which are rhythmic patterns of neural activity proposed to reflect cognition. We investigated these rhythms at different frequencies using electroencephalography (EEG) in healthy younger and older adults whilst they navigated. Our results suggest that successful spatial learning coincides with the reduction of theta (4-8 Hz) and alpha (8-12 Hz) oscillations. Successful spatial memory retrieval promotes delta (2-4 Hz) and theta (5-7 Hz) increases. When navigation strategies are unsuccessful, these oscillations at frontal areas become enhanced. Recent and remote spatial memory retrieval requires recruitment of the same frequency bands, but greater oscillatory power. However, older adults show reduced power throughout all frequency bands compared to younger adults. They further demonstrated beta (15-29 Hz) and gamma (30-40 Hz) decreases during recent memory retrieval, with delta increases and theta decreases during remote retrieval. Our findings support theories of low-frequency oscillations possessing a mnemonic role, and further contribute to theoretical debates regarding memory consolidation and ageing from the unique perspective of human spatial cognition.

# Chapter 1

# General Introduction

**Publications arising from this chapter:**

Most content from this literature review has been published as:

Thornberry, C., Cimadevilla, J. M., & Commins, S. (2021). Virtual Morris water maze: opportunities and challenges. *Reviews in the Neurosciences*, *32*(8), 887-903.

Where are we and how did we get here? Spatial navigation is the ability to learn, remember and travel to a location in space. This relies on several complex cognitive and neural mechanisms. Spatial memories are formulated and stored to help us recall spatial locations in our environment. This form of memory is closely linked with our ability to navigate. Visual landmarks assist in successful navigation towards a goal. They can help with remembering, especially when distance, direction and appearance of a landmark or goal remain constant (Biegler & Morris, 1996). The spatial relationships between landmarks, goals and place help us recollect spatial memories and in turn, navigate successfully. The recall of these memories relies heavily on the hippocampal brain region (Ekstrom et al., 2005). The hippocampus is thought to communicate with the rest of the brain through rhythmic patterns of neural activity known as oscillations. These waves of electrical activity can occur at multiple frequencies and are thought to reflect the cognition underlying the spatial navigation process. (Buzsáki, 2002, 2005; Buzsáki & Moser, 2013). Humans have a unique history of highly skilled navigation using a combination of the aforementioned cognitive and neural mechanisms (Ekstrom et al., 2018). Therefore, understanding the neural mechanisms underlying *human* spatial navigation could help explain everyday memory-related navigation errors such as getting lost. Uncovering a systematic understanding of these phenomena, will help us understand why symptoms of dementias and stroke typically include disorientation and navigation difficulties.

## 1.1 Theories of Spatial Learning & Memory

### *1.1.1 Cognitive Mapping Theory*

One of the most prominent theoretical accounts of spatial learning and memory is the cognitive map theory (O'Keefe & Nadel, 1978; Tolman, 1948). The concept was first described by Tolman in 1948 as a representation of the environment, including routes and environmental

relationships used to make decisions about where to move. This framework was originally adapted to explain the shortcutting behaviour of rats in Tolman's previous experiments (Tolman et al., 1946). Rats navigated the same environment repeatedly to a goal, before being presented with an altered version of the environment containing multiple alternative routes. During this test phase, rats predominantly chose to use a novel route that led directly to where the reward had previously been experienced. The ability to create short-cuts, which derive from automatically formed cartographic knowledge of the environment, has been cited continuously as evidence in support of cognitive mapping theory. Short-cutting behaviour had also been replicated in hamsters and honeybees (Chapuis et al., 1987; Gould, 1986; Menzel et al., 2005).

The discovery of neurons that fire when an animal occupies a specific location in its environment, termed place cells (O'Keefe & Dostrovsky, 1971; see section 1.3.2) and other spatially tuned neuronal populations in the hippocampus led to the influential 'cognitive mapping' theory, described originally in the book: '*The Hippocampus as a Cognitive Map*' (O'Keefe & Nadel, 1978). They proposed that navigation behaviours have two systems. The first, a simple stimulus response strategy, allowing us respond to landmarks when following a learned route was known as the 'taxon' system. The second, is the 'locale' system, in which we construct a mental representation of the relationships among landmarks and the environment. This theory posits that spatial exploration (encoding) enables the hippocampus to construct mental representations of environmental layouts resembling cartographic maps (see section 1.3.1 for further discussion). These have recently been proposed (Stoewer et al., 2023; Tse et al., 2007) to become integrated with current knowledge to help formulate spatial schemas of our environment. These are generalisable spatial representations of an environment, formed by integrating familiar neural representations that are not specific to any particular location, but allow us to predict what may lie ahead (Farzanfar et al., 2023).

Support for cognitive mapping theory derives from research showing lesions to the hippocampus produce spatial memory deficits across species (Astur et al., 2002; Cave & Squire, 1991; Clark et al., 2005b; Goodrich-Hunsaker et al., 2010; Maguire et al., 2006; Morris et al., 1982; Spiers et al., 2001; Stark & Squire, 2003). Advancement in cellular and behavioural experiments (discussed in section 1.3.2) provided further support for the concept of a cognitive map (O'Keefe & Nadel, 1978). However, the shortcutting evidence remains controversial, with failures to replicate emphasising alternative strategies of view-matching and associative recall (Dhein, 2023; Dyer, 1991; Pearce, 2009; Whishaw, 1991). Recent human research using virtual environments also show goal-proximal landmarks strongly influence shortcutting behaviour and can be explained by associative theories (Wilson & Wilson, 2018). The concept of cognitive mapping theory is promising and fits well with connected neural mechanisms, but it struggles to successfully predict the behavioural flexibility of navigation.

### *1.1.2 Associative Learning Theory*

A second prominent account of spatial learning and memory is – associative learning theory – which proposes that animals learn to associate environmental stimuli with motivationally relevant events such as goal locations or rewards. These associative representations are formed through basic conditioning paradigms that operate via cue competition and determine predictive strength based on reliability (Duval, 2019; McLaren & Mackintosh, 2002; Wagner & Rescorla, 1972). The principles governing the acquisition of navigational cue-goal relationships follow similar rules as classical and operant conditioning paradigms (Pearce, 2009; Jeffrey 2010). Within associative spatial learning frameworks, two primary learning strategies exist. Elemental learning strategies involve a direct association between a cue/landmark and the goal (Rudy, 1991). The navigational aid is derived via recognition, which

promotes retrieval of the formulated spatial relationship, and in turn, the goal location to which it is associated (Sutherland et al., 1988; Pearce, 2002; Farina et al., 2015).

Configural strategies in spatial navigation rely on associations between combinations of multiple environmental cues, bound together into integrated representations (see Figure 1.1 for differences). These configural cue representations form distinct "emergent features" consisting of the combination of individual elements. However, the configural representation itself is treated as separate and independent from any of its constituent parts. In other words, a configural association encoding the co-occurrence of cues A+B forms a novel, singular cue representation that functions independently from the singular elements A or B. This allows locations to be specified through unique arrangements of features in relation to one another, rather than single landmark identities. Hence, associative learning theory can explain the short-cutting behaviour used to support the concept of a cognitive map. However, supporting neuroscientific research has been weaker compared to support for cognitive mapping (Eichenbaum et al., 1999; Muessig et al., 2016; Pfeiffer & Foster, 2013; Rolls et al., 2006). Therefore, associative theory can explain the production of a cognitive map rather than being the sole explanation for successful navigation.

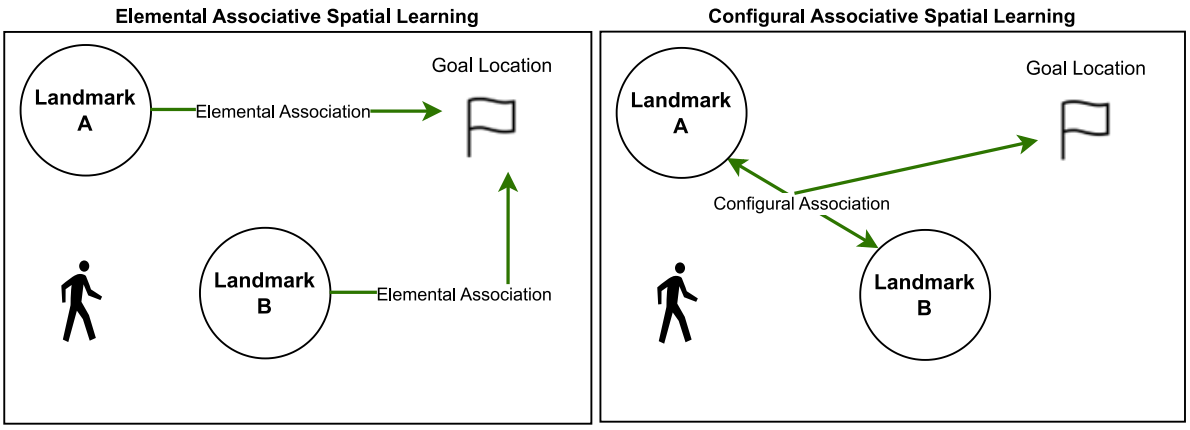


*Figure 1.1:* Conceptual design of two associative learning methods thought to be used during spatial navigation to promote learning and subsequent recall. Elemental learning uses individual cues or landmarks and associates those with a goal location (Left), whereas configural combines two cues or landmarks into a single combined concept which becomes associated with the goal (Right).

### *1.1.3 Multiple Trace Theory & Systems Consolidation*

Much evidence around spatial memory, points to the significant role of the hippocampus in the encoding of new declarative memories (Squire, 2009; also discussed in section 1.2). Both theoretical models of spatial learning described above prescribe their function to the hippocampus and its unique cellular network. However, the mechanisms for the retrieval of spatial memories are still subject to healthy debate within the literature. Proposed by Nadel and Moscovitch (1997), the Multiple Trace Theory (MTT) of spatial memory recall proposed that both recent (recognition and contextual retrieval) and remote (long-term retrieval) require involvement of the hippocampus. Hippocampal networks are proposed to encode memories, with reactivations producing hippocampal-dependent memory traces containing detailed spatial context, whilst cortex-dependent traces of the memory are context-free (Nadel et al., 2000). Therefore, retrieval of remote semantic memories does not require the hippocampus, but retrieval of spatial memories is hippocampal dependent, regardless of memory age.

Alternatively, Systems Consolidation Theory (SC) proposes that the hippocampus (as well as the cortex) is vital for encoding the memory at its early stage, particularly during the learning process. The cortex is initially unable to support the memory, but with repeated replay and retrieval allowing sufficient memory consolidation (e.g., through sleep – see Ji and Wilson (2007)) the cortical memory trace becomes strong enough to no longer require the hippocampus for retrieval. Hence, remote memories should not require the hippocampus, whereas recent memories should as they have not had time to consolidate. In humans, there is some evidence that following damage to the hippocampus both recent and remote memories become impaired (Barry & Maguire, 2019; Spiers et al., 2001). However, in terms of spatial memory, Maguire et al. (2006) demonstrated deficits in detailed remote spatial memories for familiar routes learned long-ago in a taxi-driver with bilateral hippocampal lesions. Based on our knowledge that the hippocampus is involved in storage and retrieval of spatial memory from the study of London taxi drivers (Maguire et al., 2000; Maguire et al., 2003; Weisberg et al., 2019) – we would expect hippocampal involvement regardless, with a deficit in the finer detail of spatial representation. However, the patient in the 2006 study could navigate reasonably well when using main roads – but poorly when using back or side roads. Maguire et al (2006) propose that the representation of the main roads may, over time and with replay, have become "semanticised" (released from the episodic memory requirements of the hippocampus – see section 1.3.2).

Therefore, MTT would explain why these memories had been protected from hippocampal damage. However, imagining spatial scenes (Hassabis et al., 2007; Hassabis & Maguire, 2009) and imagined spatial navigation (Horner et al., 2016) show hippocampal formation activation using functional magnetic resonance imaging (fMRI). Therefore, it is entirely possible that hippocampal involvement in remote spatial memory (and any spatial memory at that) is scene construction rather than reactivation of memory traces, as argued by

Barry and Maguire (2019) and by Sutherland et al. (2020). Most importantly, both theories do suggest hippocampal involvement in the recall of recently formed spatial memories. Hippocampal activity has been found during retrieval of both recent (Rekkas & Constable, 2005; Takehara-Nishiuchi, 2020) and remote (Miller et al., 2020; Schlesiger et al., 2013) memories. It is possible that neurophysiological recordings from the cortex rather than the hippocampus itself may provide the answers to the spatial memory retrieval process.

### *1.1.4 Overview of Theoretical Frameworks*

In summary, we have addressed the two main theoretical debates concerning spatial learning (cognitive mapping theory/associative theory) and spatial memory (multiple trace theory/standard consolidation theory). Cognitive mapping theory proposes that we learn about and form an integrated, map-like representation of our environment, allowing us to navigate flexibly (O'Keefe & Nadel, 1978). However, associative theory suggests that we learn specific stimulus-response associations or route-based strategies, without forming an integrated map of the environment (Pearce, 2009). The evidence discussed above suggests that both cognitive mapping and associative learning processes contribute to spatial learning, but their relative contributions and the conditions under which each dominates are still debated. We hope to address this by providing insights into the neural mechanisms underlying these learning approaches, as specific neural oscillatory dynamics (see section 1.4) have been linked to cognitive mapping (Babiloni et al., 2011; Lithfous et al., 2015; Musaeus et al., 2018) and associative learning processes (Crespo-Garcia et al., 2012; Crespo-García et al., 2016; Greenberg et al., 2015).

In terms of memory systems, Multiple Trace Theory (Nadel et al., 2000) proposes that recent (recognition and contextual retrieval) and remote spatial memories (long-term retrieval)

require the hippocampus. Standard Consolidation Theory (Squire, 1992; Squire et al., 2015) suggests that all remote memories, including spatial memories become independent of the hippocampus through a gradual consolidation process. Some evidence suggests that spatial memories may involve both hippocampus-dependent and hippocampus-independent components, but not much is known about the precise roles and interactions of these systems. We hope that this thesis may reveal some insight into the involvement of specific brain regions (section 1.3) or neural oscillations (see section 1.4) by recording neural activity during spatial memory retrieval at different time points (e.g., recent vs. remote memories). The involvement of particular frequency bands (see section 1.4) during different recall intervals has been shown to be related to the type of consolidation process involved prior to memory retrieval (Barry & Maguire, 2019; Jacobs et al., 2006; Nicolás et al., 2021; Schlesiger et al., 2013).

## 1.2 Assessment of Spatial Navigation in Animals & Humans

### *1.2.1 The Rat Race: Mazes and Spatial Learning*

The assessment of spatial navigation and memory in animal research has a rich tradition. Willard Small was one of the first to develop a maze for rodent learning over 100 years ago (Commins, 2018a; Small, 1901). Edward Tolman (1886-1959) continued this tradition and developed a variety of mazes including the starburst maze, which he used to demonstrate the idea of the cognitive map in rodents (Tolman, 1948). Towards the end of the twentieth century, more sophisticated mazes were developed that allowed for the separation of spatial strategies and their neural substrates including the Radial Maze (Olton & Samuelson, 1976) and the T-Maze (Olton, 1979). The Radial Maze typically has the formation of a centre arena with tunnels or “arms” radiating outwards (see Figure 1.2a). The terminus of these tunnels typically contains a well in which a reward (such as food) can be placed. The ability of an animal to recall which

identical arm contains the reward, relies heavily on spatial learning and memory (Bolhuis et al., 1986; Crusio et al., 1987; Vorhees & Williams, 2014b). The T-Maze generally takes the formation of a long-stretch of maze with two, hidden turning points at the terminus (see Figure 1.2b). Rodents are generally tested for their cognitive ability to recall cue-goal relationships, as each turn has an associated landmark, with only one turn containing a reward. Even when the hippocampus is removed or damaged, rats can still solve simple conditional or alternation reference tasks in the T-Maze (Deacon et al., 2002; Deacon & Rawlins, 2006; Pimentel et al., 2022). However, there is difficulty to use or perceive spatial components and cues to locate the goal, but ability may also depend on the location of the damage (Gammeri et al., 2022; Trivedi & Coover, 2004).

Circular open environments were also developed, allowing more freedom to explore space. Initially designed to examine cognitive mapping theory (O'Keefe et al., 1975), these mazes were soon adapted to different neurophysiological and behavioural studies (Barnes, 1979; Cimadevilla et al., 2000). Thus, the neurobiological substrates of place learning and idiothetic (use of internal sensory cues) and allothetic (use of external physical cues) orientation were extensively studied in circular arenas, under different environmental conditions (Bures & Fenton, 2000; Muela et al., 2022). Though these designs have been incredibly influential in exploring animal learning and spatial memory, the “Gold Standard” of these navigational maze tests is the Morris Water Maze designed by Richard Morris (MWM; Morris, 1984, see Figure 1.2c). The general layout of the maze involves a circular pool filled approximately half-way with water. The animal is tasked with locating and recalling the position of an “escape platform”, which is submerged below the water surface in a fixed location. The platform is generally camouflaged by colouring the water or making the platform from transparent materials. This facilitates the platform to have a low, if any, visual presence in the pool, meaning the location of the platform must be found and recalled (Vorhees & Williams, 2006;

Vorhees & Williams, 2014a, 2014b). The animal can be trained with distal (away from goal) landmarks, proximal (close to goal) landmarks or with their trajectory alone (see Nunez (2008) for an outline of the procedure).

### *1.2.2 MWM and Navigation Strategy Assessment*

The MWM provides a highly controlled environment for landmark manipulation, behavioural observation and lesion studies. The strategy and style of navigation carried out in the water maze can differ depending on the situation. These navigation strategies can be egocentric or allocentric (as mentioned above). Egocentric navigation involves a relationship between the individual and objects or locations. It is typically considered as simple stimulus-response pattern learning, whether it is following a fixed-route or responding to single landmark (Barry & Commins, 2019; Committeri et al., 2020; Ekstrom et al., 2017; Morris et al., 1982; Morris, 1984; Morris, 1981; Sanders et al., 2008). Allocentric navigation refers to mnemonic representations of viewpoint-invariant relations among objects (Harvey et al., 2009; Vorhees & Williams, 2014a), as well as fixed relations between objects or locations independent of the individual. These spatial representations are thought to be stored in memory like a cartographic map (Tolman, 1948; O'Keefe & Nadel, 1978). The recall of large-scale allocentric representations has been shown to be necessary when egocentric information is not readily available (Woollett & Maguire, 2010). Sex differences exist in navigational strategy choice.

In humans navigating a virtual environment, men were more likely to use an allocentric strategy, while women more often used a response-based (egocentric) strategy (Boone et al., 2018; Hegarty et al., 2023; Yu et al., 2021) Ageing also affects navigational strategy. For example in humans, older adults tend to rely on an egocentric strategy or response-based) while

younger adults show no real preference (Zhong et al., 2017). However, the choice of strategy may depend on the environment and availability of information (Hegarty et al., 2023). These different wayfinding strategies are thought to rely on different brain areas (see section 1.3.2) and are an important consideration when using the water maze to examine spatial learning and memory.

A highly replicated finding using the MWM, is that damage to the hippocampus results in impaired allocentric (landmark) navigation (Lissner et al., 2021; Sutherland & Rudy, 1989). However, trajectory learning, or non-landmark dependant (egocentric) search strategies remain preserved (Eichenbaum et al., 1999; Eichenbaum et al., 1990; Lissner et al., 2021). Therefore, the flexibility of protocols and procedures provided by the MWM has led to it becoming one of the most popular tests for spatial navigation (also see section 1.2.3). The assessment of spatial navigation in humans has been more challenging. As a maze-type environment was seen as the most appropriate controllable environment for animals, performing similar tasks with humans on a larger scale has proved difficult. One of the first studies was that by Thorndyke and Hayes-Roth (1982) who examined spatial recall by asking participants to learn a buildings layout from a map or by active navigation around the building. Similar real-world navigation experiments have since proved useful to understand factors underlying human spatial learning and memory such as distance estimation (Commins et al., 2013), environmental orientation (Kimura et al., 2017) and spatial working memory (Nori et al., 2009). However, such large-scale real-world navigation tasks are often difficult to standardise and manipulate (Park et al., 2018). Natural environments are not fully controllable and experiments on this scale can be difficult to organise, resulting in a variation of navigation strategy choice amongst participants as well as numerous confounding variables.

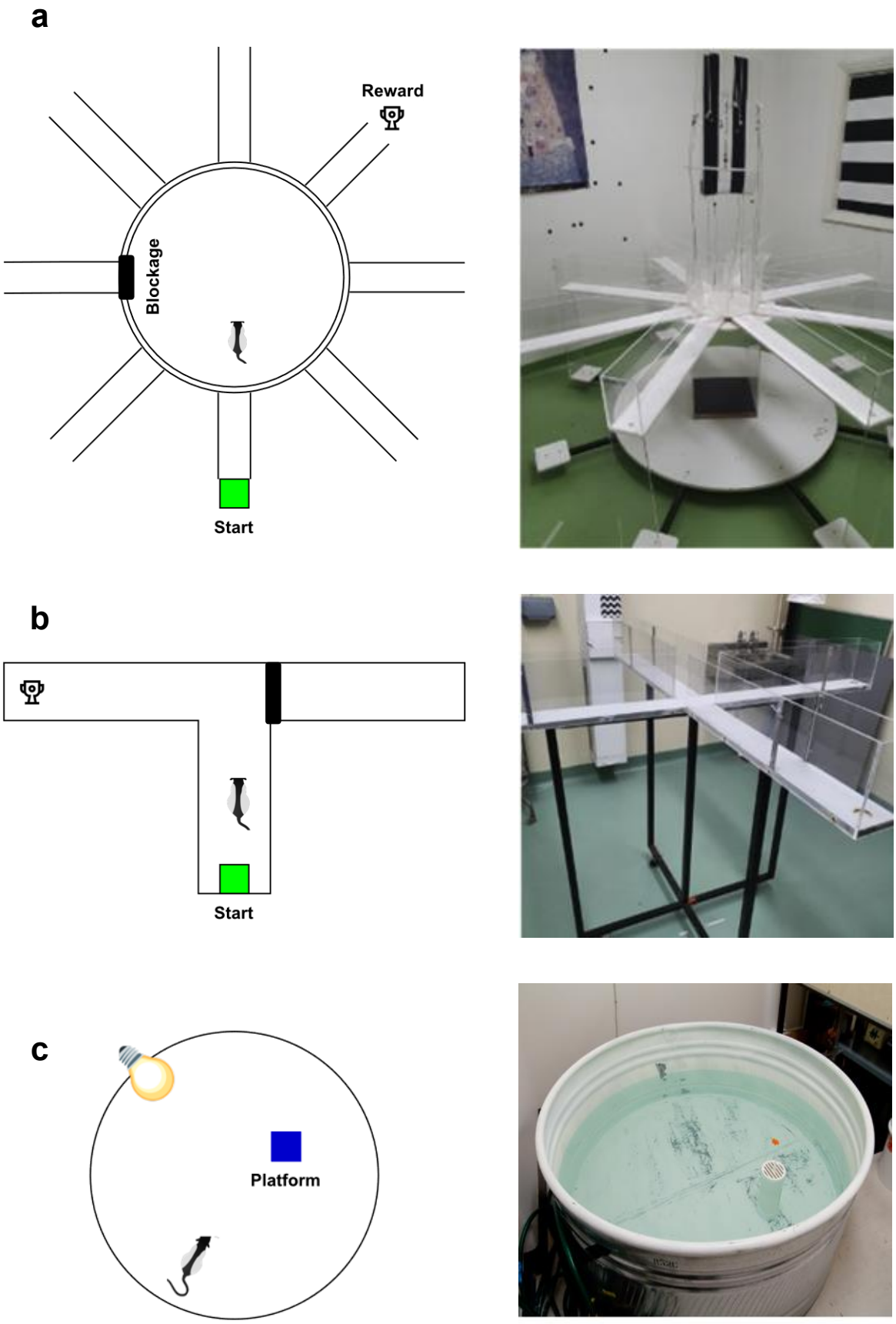


*Figure 1.2:* (a) Diagram (Left) and photograph (Right) of a typical 8-arm radial maze. (b) Diagram (Left) and photograph image (Right) of a typical T-Maze design. (c) Diagram (Left) and photograph (Right) of a typical Morris water maze design, with a lightbulb depicting typical cue/landmark representation. Adapted from Vann (2024) and Bromley-Brits et al. (2011) with permission.

### *1.2.3 Virtual Reality in Spatial Navigation Research*

With the growing popularity of Virtual Reality (VR) in scientific research in the last few decades, behavioural neuroscientists have made use of VR systems to assess spatial memory and navigation in a controlled environment (Maguire et al., 1997; Spiers & Maguire, 2007). The translatability of the animal literature using virtual navigation in humans has shown positive results. For example, navigation performance on a simplistic 2D desktop programme has strongly correlated with real-world navigation performance (Cogné et al., 2017; Santos et al., 2008).

Virtual "mazes" with various designs (see Figure 1.3) have become very successful tools for researching spatial navigation and also helping clinical populations (Thornberry et al., 2021). For example, VR mazes involving navigational and non-navigational skillsets in brain injury patients have shown to be useful for assessments of deficit severity, rehabilitation and also improving community living skills (Aida et al., 2018; Tucker et al., 2018). Impaired spatial navigation has been detected in anxious patients using virtual reality platforms (Cornwell et al., 2012). Additionally, VR applications have aided the detection of cognitive deficits in individuals with mild cognitive impairment (MCI) and aided the assessment of symptomology in psychotic conditions (Kim et al., 2019; Lambe et al., 2020). The use of VR has also facilitated our understanding of the neural correlates of spatial navigation by combining a VR application with a form of neurological measure (such as fMRI or electrophysiological recording of individual cells). The use of VR has provided support for the presence of similar neural mechanisms underlying navigation in humans that were discovered in animals (see section 1.3 below).

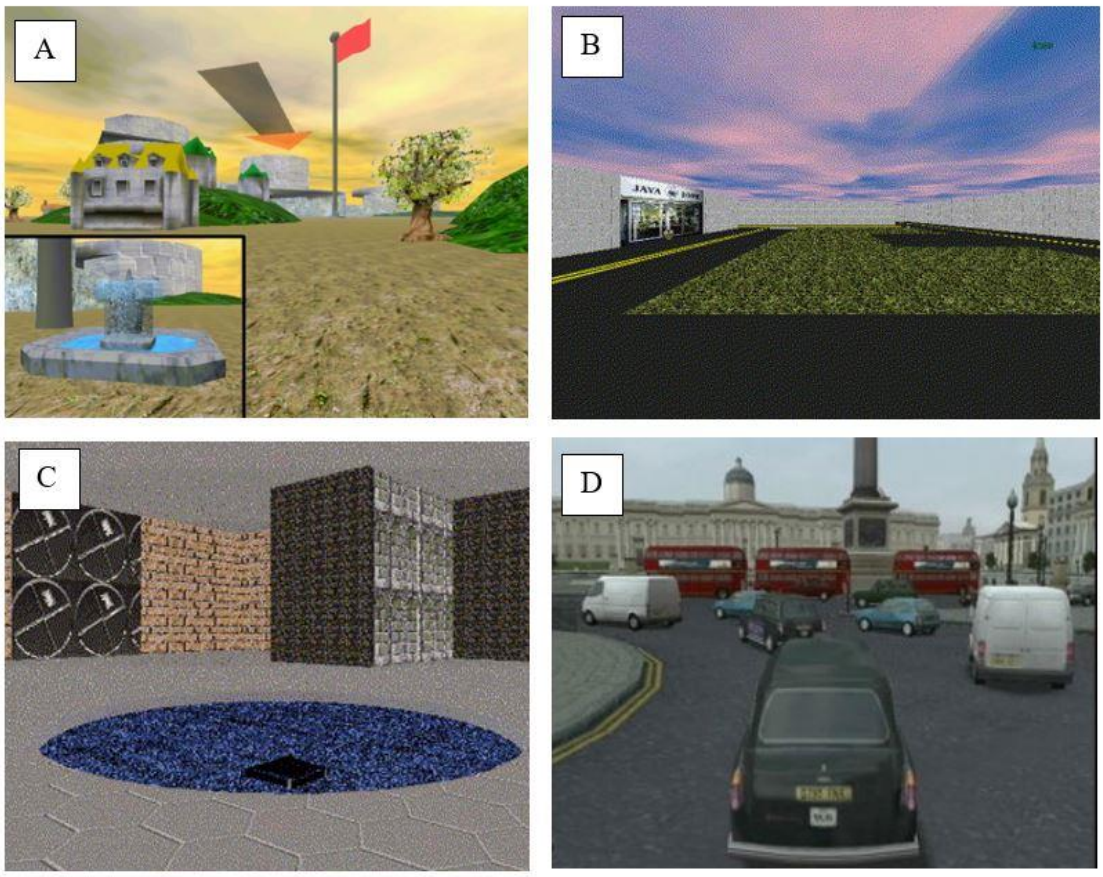


*Figure 1.3:* Examples of virtual mazes from the literature, such as the virtual island 'memory island' (A, from Piper et al. 2010); a virtual town (B, from Newman et al. 2007); an original virtual water maze (C, from Astur et al. 2004) and the virtual taxi simulator based in London (D, from Spiers and Maguire 2008). Full figure adapted from Thornberry et al. (2021).

### *1.2.4 Virtual Morris Water Maze*

Although the MWM is considered the "gold-standard" test for animal navigation, there also exists the need for a standardised testing procedure for *human* spatial memory and navigation. To examine whether animal models of navigation translate to human subjects, researchers have developed a virtual analogue of the water maze (Virtual Water Maze; VWM). Thornberry et al. (2021) found that by far the most popular task used to test human spatial learning and memory was the virtual water maze task, originally developed by Astur et al. (1998) and modelled on

the traditional Morris water maze. The tool has become an incredibly successful method of examining spatial navigation in humans; whilst retaining a similar amount of experimental control and reliability as its rodent counterpart (Astur et al., 1998; Astur et al., 2002; Astur et al., 2004).

Most of the results using VWMs have shown good consistency with the rodent version of the task (Schoenfeld et al., 2014; Schoenfeld et al., 2017). For example, males spend longer in the target zone than females during an invisible platform recall trial (Astur et al., 2004) and during initial trajectory of learning trials (Woolley et al., 2010). Furthermore, the task has been an incredibly popular choice for examining the effect of age on spatial memory and navigation skills; proving effective and consistent for longitudinal and neural measurement studies (Daugherty & Raz, 2017; Daugherty et al., 2015). The VWM has also been a popular choice for spatial memory assessment with clinical samples; demonstrating correlations between performance on a VWM and lower scores on the Montreal Cognitive Assessment (Konishi et al., 2017).

Furthermore, the VWM is capable of investigating both allocentric and egocentric strategies in humans, much like its animal counterpart (Astur et al., 1998; Hölscher, 1999; Morris, 1984; Thornberry et al., 2021). Allocentric strategies are typically examined based on the participants ability to navigate and locate a hidden goal using only the spatial relationships between the goal location and environmental cues. As the number of cues and starting positions can be easily manipulated in the standard water maze protocol (Vorhees & Williams, 2014b); the use of this strategy is further supported following successful navigation to the goal from different starting positions (Ferguson et al., 2019; Mueller et al., 2008). Failure to navigate after alternating the starting positions or rotating the environmental cues supports the use of an egocentric strategy in humans and animals (Grech et al., 2018; Van Gerven et al., 2016). This is because vestibular cues, specific learned routes or a landmark used for initial orientation are

disrupted by these environmental changes (Chamizo et al., 2006; Chamizo et al., 2012; Civile et al., 2014; Lugo et al., 2018). The VWM allows researchers to observe and quantify various measures related to these concepts, such as latency to find the platform, path length. These data provide unique insights into the contributions of allocentric and egocentric strategies during spatial learning and memory.

The basic procedure and look of a VWM generally follows that of the original, with a hidden platform, pool walls and landmarks. Nonetheless, several key factors that influence navigation in the rodent version of the task are removed when made virtual, such as motivation and physical locomotion. Furthermore, there is a lack of consistency both in the environmental design and procedure with the VWM compared to the MWM. For example, many researchers and companies design novel versions of the water maze to make them more 'immersive' or realistic (see Figure 1.4). Some incorporate landmarks from everyday life such as furniture (Thornberry et al., 2021), whilst in others, the original pool of the water maze is instead a circular desert island, in which participants must search for hidden treasure (Piper et al., 2010; Thornberry et al., 2021). In addition, the procedures often differ between labs, including the size of the arena, number of trials and trial length (see Thornberry et al., 2021 for full discussion and Table 1 for an example of this variation). The lack of consistency across designs and protocols poses a problem when attempting to compare research across labs, making replicating experiments difficult. Nevertheless, the VWM remains a popular test and has proven robust for both basic research and clinical work.

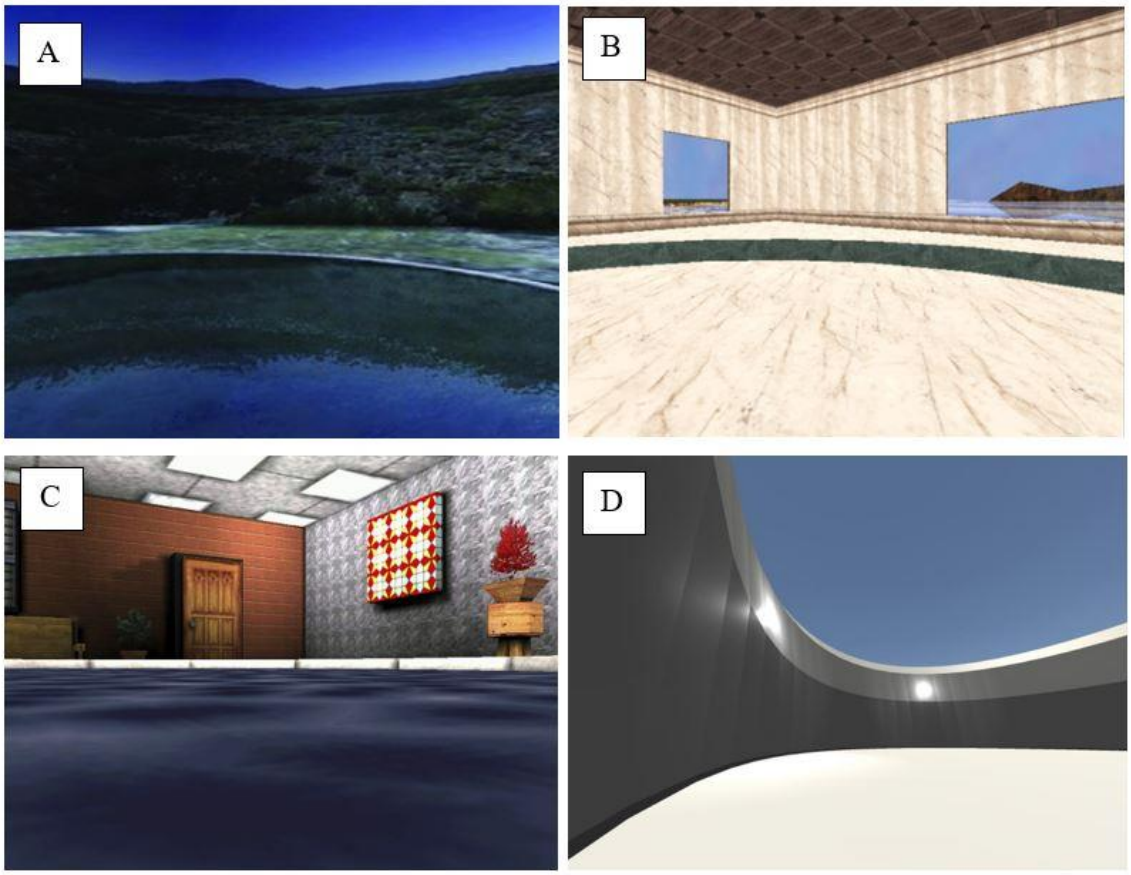


*Figure 1.4:* Examples of virtual water maze layouts from the current literature, such as an outdoor one with forest and mountain landmarks (A, from Machado et al. 2019); an indoor water maze with a window (B, from Livingstone-Lee et al. 2011); a water maze in a room with furniture (C, from Newhouse et al. 2007) and our own open-access maze, 'NavWell' (D, see Commins et al. 2020). Full figure adapted from Thornberry et al. (2021).

*Table 1:* Small sample from the full table in Thornberry et al. (2021) of the variety of different maze designs throughout highly cited literature.

| *Paper* | *Year* | *Arena* | *Indoor/Outdoor* | *Platform Size/Shape* | *Arena Size* |
|---|---|---|---|---|---|
| *Astur et al.* | 2002 | "Pool" | Indoor (Pool in a room) | No Details Provided | No Details Provided |
| *Daugherty et al.* | 2015 | "Pool" | Indoor (Pool in a room) | Approx. 12% of arena size | No Details Provided |
| *Hamilton & Sutherland* | 1999 | Circular | Indoor (square room; pool wall 15% of room height) | Square (Approx. 1.75% of the pool surface area) | Traversal 4s Full rotation 2.5s |
| *Hamilton et al.* | 2009 | Circular | Indoor | 0.66Vu x 0.66Vu (Approx. 20%) | 16Vu x 16Vu x 3Vu |

**NOTE:** Vu represents "virtual units" relative to the paper from which it was retrieved.

## 1.3 The Neural Basis of Spatial Navigation

### *1.3.1 Brain Regions Involved in Spatial Navigation*

Both humans and non-human animals rely extensively on the sea-horse shaped structure known as the hippocampus for spatial navigation (Commins, 2018a; Ekstrom et al., 2018). The hippocampus is located deep within the medial temporal lobe (MTL; Figure 1.5a and 1.5c) and is strongly connected to structures such as the parahippocampal and retrosplenial cortices (see Figure 1.5b and 1.5d). The hippocampus and surrounding structures encode many spatial attributes such as distance, direction and location relative to landmarks (Eichenbaum et al., 1999; Ekstrom et al., 2017; Ekstrom & Ranganath, 2018; O'Keefe, 1993; O'Keefe & Nadel, 1978; Smith & Mizumori, 2006; Stachenfeld et al., 2017). Additionally, humans employ both the parietal and frontal cortical areas to support the integration of sensorimotor information and decision-making respectively (Andersen & Cui, 2009).

Numerous studies in non-human animals report impairments in spatial memory following hippocampal damage (Clark et al., 2005a, 2005b; Morris et al., 1982; Vorhees & Williams, 2024). Morris et al. (1982) demonstrated that hippocampal lesions in rats impaired spatial memory performance in the water maze. Since then, numerous support from neuroimaging studies in humans have reported that damage to the human hippocampus produces retrograde amnesia, in which remote memory is typically spared relative to recent memories (Barry & Maguire, 2019; Rosenbaum et al., 2000; Teng & Squire, 1999) but not necessarily for spatial memories (Broadbent et al., 2006; Clark et al., 2005b). However, Astur et al. (2002) replicated the original findings by Morris et al. (1982) showing that humans with unilateral hippocampal damage were impaired on a virtual spatial navigation task. Bohbot et al. (1998) had previously reported that patients with lesions either to the right or to the left hippocampus were not impaired on spatial memory tasks. Patients with lesions only to the right

parahippocampal cortex showed impairment following a delay between spatial learning and recall. Nevertheless, the finding of spatial impairments due to hippocampal damage has been replicated numerous times since in humans using a virtual water maze (Goodrich-Hunsaker et al., 2010; Kolarik et al., 2016) and other tasks (Maguire et al., 2006; McCormick et al., 2018; McCormick et al., 2017; Miller et al., 2020; Spiers et al., 2001). Although not solely responsible, the hippocampus is the most important structure for spatial navigation in humans.

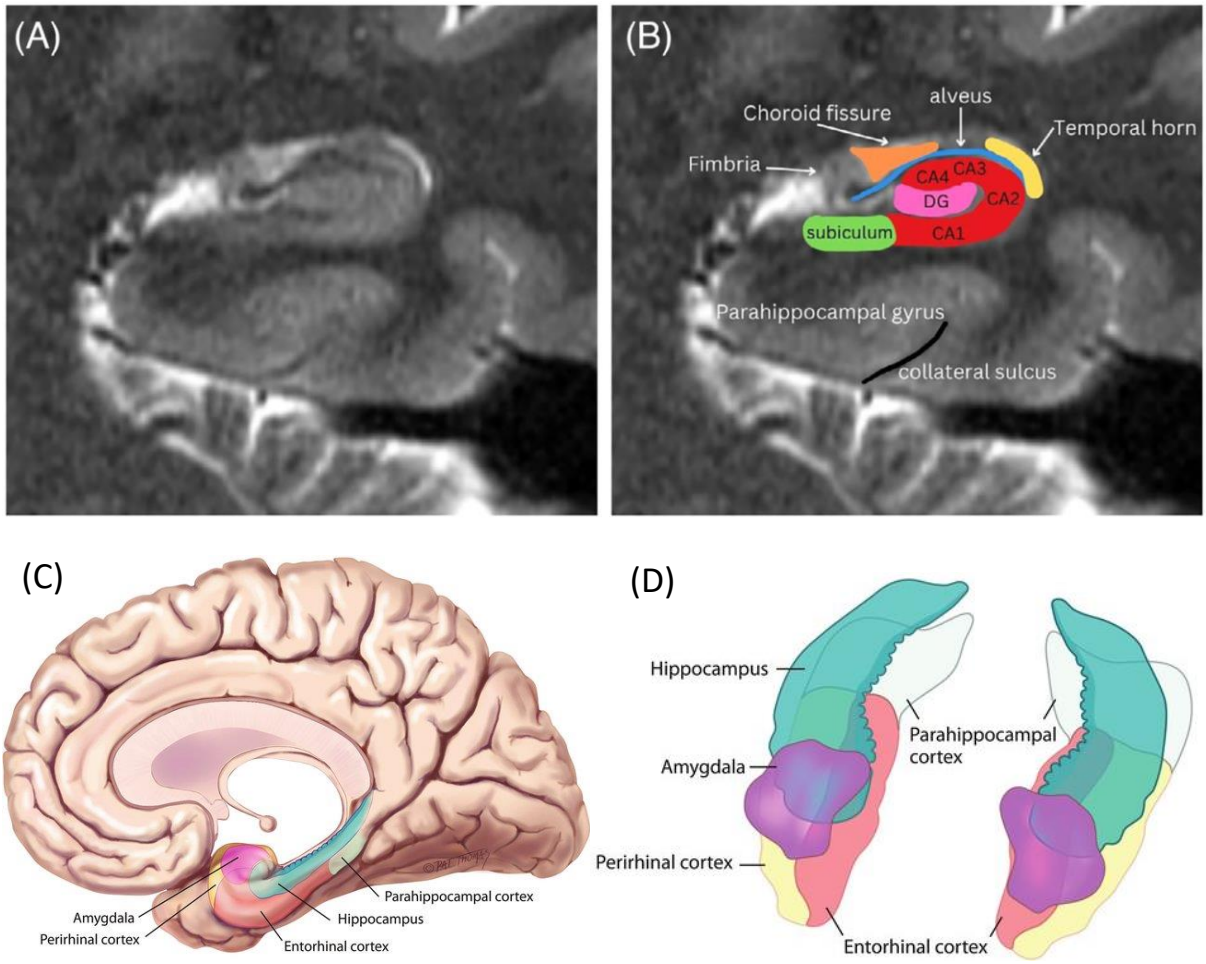


*Figure 1.5:* Coronal T2-weighted MRI images showing normal hippocampal anatomy, unlabelled (A) and labelled (B).The dentate gyrus is shown in pink. The hippocampus is shown in red, which includes the CA1, CA2, CA3, and CA4 subfields and the dentate gyrus. The subiculum is shown in green. A diagram of the brain (C) and isolated sub-cortical structures (D) shows the medial temporal lobe, the hippocampal formation, parahippocampal gyrus, entorhinal and perirhinal cortices, parahippocampal cortex and amygdala. Adapted from Raslau et al. (2015) & Lang et al. (2024).

### *1.3.2 Cellular Networks of Spatial Navigation*

The role of the hippocampus in spatial memory and navigation was further supported by discoveries from the neural networks incorporated within and surrounding the structure. Using single-cell recordings from the surface of subregion CA1 (*Cornu Ammonis*) in the rat hippocampus, O'Keefe and Dostrovsky (1971) recorded extracellular activity during active navigation (see Figure 1.6a and 1.6b). They observed cells that would increase their firing rate from low to high, conditional on the rats' position in the environment, named *place cells.* These are neurons that activate in response to an animal entering a particular location in its environment. Different place cells, were found to have different firing locations, known as place fields (Moser et al., 2008; Moser et al., 2017). These combinations of cells were unique in each different environment, despite their location in the hippocampus – meaning cells nearby were no more related than cells further apart (Moser et al., 2017). The discovery of these cells suggested that the hippocampus may play an important role in co-ordinating, representing and interpreting space. However, more recently it has been suggested that they represent past and future environments as well (Grieves & Jeffery, 2017; Ormond & O'Keefe, 2022; Robinson et al., 2020; Umbach et al., 2020). Place cell maps or firing fields are known to evolve and grow with active exploration and experience of the environment (O'Keefe, 1993; Ormond & O'Keefe, 2022; Pfeiffer & Foster, 2013). It is possible that these cells code for an initial gist-like map of a new environment using predetermined and stable firing fields (as demonstrated by Frank et al. (2004)). This may explain how they become more finely tuned with experience (Bostock et al., 1991; Quirk et al., 1990).

Furthermore, place cells have been found to "replay" their firing pattern during sleep (Wilson & McNaughton, 1994) and upon moments of spatial recall and decision-making (Jai & Frank, 2015; Joo & Frank, 2018; Wu et al., 2017). Replay is a common feature of consolidated memory retrieval and occurs in numerous brain regions, including the

hippocampus, medial temporal lobe and visual cortex (Carr et al., 2011; Klinzing et al., 2019). This suggests a role of place and grid cell system in the *memory* of place. Single-cell recordings from the hippocampus of human patients by Ekstrom et al. (2003) has shown neurons comparable to the place cells found in rodents (see Figure 1.6c). Moreover, recordings from the MTL of patients performing a navigation task demonstrated place cell replay (see Figure 1.6d), with firing corresponding to the location of an item during memory recall (Miller et al., 2013). Recently, Kunz et al. (2021) recorded cells that encode self-centred distances to spatial reference points, alongside "place-like" cells that are involved in episodic memory formation.

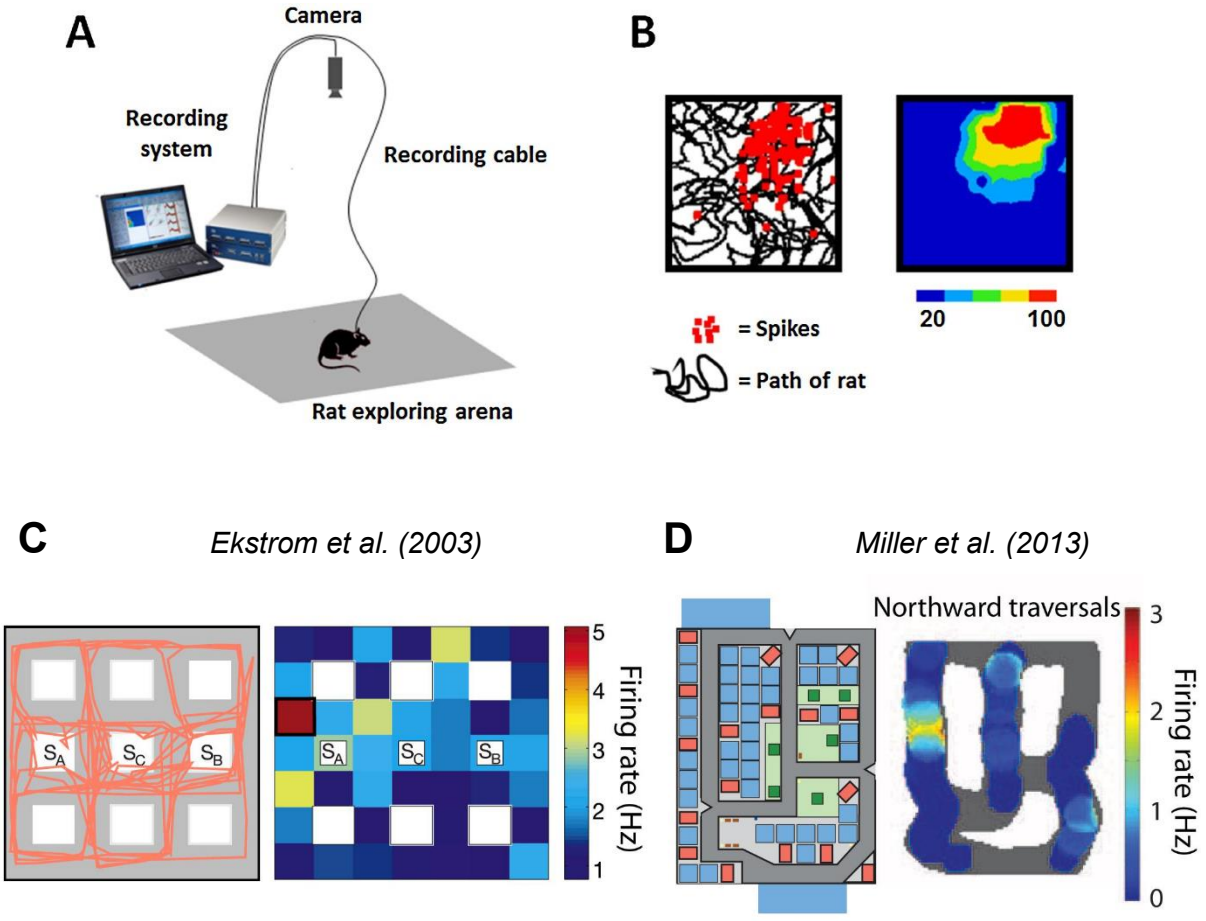


*Figure 1.6:* (A) Experimental setup for recording single neurons from freely exploring rats implanted electrodes. (B) Data from a single hippocampal place cell in a single trial. The left plot shows action potentials (red squares) superimposed on the path of the rat. A spatial map of the cell's firing rate as a function of spatial location, known as a place field, is displayed on the right. (C) Place firing found during virtual navigation in the human hippocampus by Ekstrom et al. (2003). (D) Place cell firing during a virtual task recorded from the MTL in humans by Miller et al. (2013). A & B reused with permission from Grieves & Jeffrey (2017) and C & D adapted from Herweg & Kahana (2018).

In the late 1980's and early 1990's, extracellular recordings from the postsubiculum (PoS) revealed a set of neurons termed *head direction cells* (see Figure 1.7a and 1.7b). These cells have been found throughout the brain in the retrosplenial cortex (RSC) and some parahippocampal regions (Figure 1.7a). Head direction cells fired when a freely moving rat was facing in a particular direction (Taube, 2007; Taube et al., 1990) and are reliant on stable and landmark rich environments (Muller et al., 1987; Page & Jeffery, 2018). Several human neuroimaging studies have found 2D head-direction information coding from spatial-relevant structures such as the RSC (Shine et al., 2016). Kim and Maguire (2019) recently discovered the 2D head-direction system codes vertical and horizontal heading in 3D space in the human thalamus, subiculum and RSC. Recordings from the rodent Medial Entorhinal Cortex (MEC) in 2005 (Moser et al., 2017) revealed more spatially-tuned neurons that fired at multiple locations that were arranged in a periodic triangular or hexagonal grid layout (Figure 1.7a & 1.7c), with consistent spatial fields spanning across an entire environment (Hafting et al., 2005; Moser et al., 2008). The grid-like firing pattern provides a coordinate system for encoding spatial information. These *grid cells* form part of a broader cellular network for successful spatial navigation near and within the hippocampus. Grid-like spiking patterns have also been discovered in humans during a virtual navigation task (Jacobs et al., 2013).

Grid and Head-direction cells work in conjunction with several other unique cells such as boundary vector cells (Figure 1.8a), which are neurons that fire at environmental boundaries and perimeters, found in the rat and more recently the human entorhinal cortex and subiculum (Barry et al., 2006; Bjerknes et al., 2014; Lever et al., 2009; Shine et al., 2019; Solstad et al., 2008). The hippocampus is known to be involved in processes beyond purely spatial navigation including the processing and memory of non-spatial cues such as objects (Cohen et al., 2013). However, there are some cells here that can be spatially tuned to encode the spatial location of an object (Jankowski & O'Mara, 2015). These *object cells* (Figure 1.8b) are modulated

similarly to place cells and fire regardless of the visual availability or appearance of an object (Jankowski & O'Mara, 2015; Nagelhus et al., 2023).

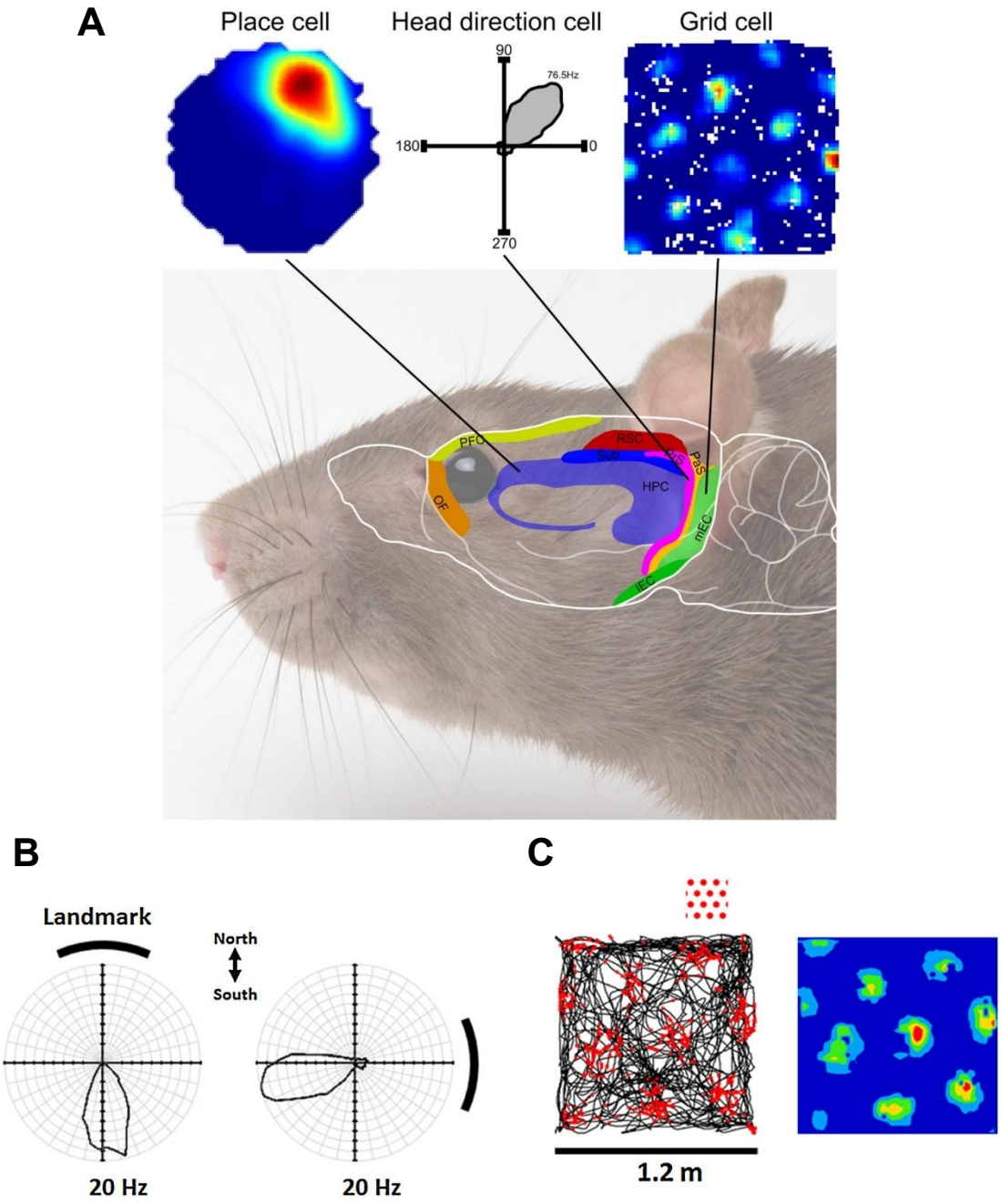


*Figure 1.7:* (A) shows the previously mentioned navigation-related cells and their location within the hippocampus and entorhinal cortex. (B) Shows typical polar plot to track firing patterns of head-direction cells. (C) An example firing rate map of a grid cell produced using the same method as for the place cell in Figure 1.7b. Adapted with from Grieves et al. (2017).

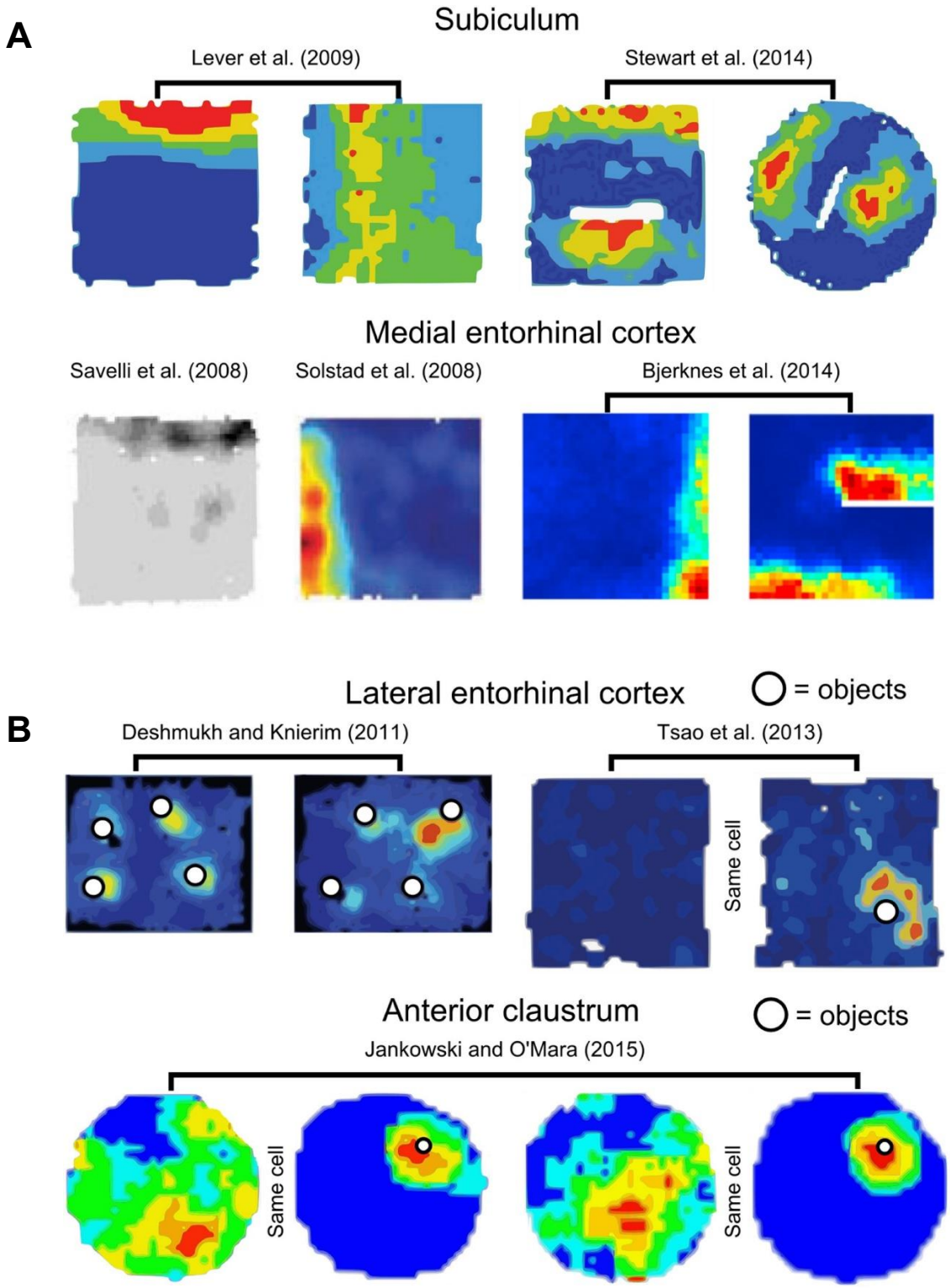


*Figure 1.8:* (A) Border/boundary vector cell firing patterns either firing along the edge of the environment or at a distance from the boundary or border with fewer of these types of cells recorded in the MEC. (B) Firing patterns of cells related to objects in the environment, they fire near a specific object in the Lateral entorhinal cortex. The same object cells recorded by Jankowski & O'Mara (2015) showing place properties until an object is positioned within the place field; in which its firing behaviour switches to object specific. Adapted from Grieves et al. (2017).

The beauty of this cellular network is that it facilitates the generation of memory or navigation-related hypotheses rather elegantly. For example, it has recently been found that place and boundary cells fail to code for environmental connectivity (i.e., doorways or gaps in borders) but instead code for global spatial locations (Duvelle et al., 2021). Perchance, there are cells that are responsible for coding for these connected-spaces, or the functions of boundary-vector cells may differ than once originally thought. Furthermore, the human hippocampus and entorhinal cortex contain *time cells*, which activate at specific moments during an experience (Eichenbaum, 2014; Pastalkova et al., 2008; Umbach et al., 2020). They exhibit the same theta-phase firing precession as place cells (Pastalkova et al., 2008), indicating their possible role of temporally ordering spatial memories at the time of retrieval.

### *1.3.3 Brain Oscillations & Spatial Navigation*

The main disadvantage of single neuron recording is that one can only capture a microscopic snapshot of the brains' activity. There are thousands of neurons firing in synchrony during any cognitive task or event. Prior to the discovery of place cells, early electrophysiological recordings from the rabbit hippocampus in 1938 (Jung & Kornmüller, 1938) followed shortly by the rodent hippocampus in the late 60's (Vanderwolf, 1969) demonstrated a low-frequency signal with different properties to the classic spike activity expected from single neurons. The recording technique is known as Electroencephalography (EEG). This method facilitates the recording of electrical potentials generated by neuronal activity using electrodes placed on the scalp (scalp EEG), the cortex (known as electrocorticography: ECoG) or intracranially, within the brain (iEEG). Vanderwolf (1969) termed the low-frequency activity from the hippocampus occurring at 4-8 Hz as *hippocampal theta oscillations* (see Figure 1.9a and 1.9b). Many early studies focused on theta's role in movement, with later studies demonstrating its role in

modulating synaptic plasticity (Kahana et al., 2001). Specifically, the discovery that theta can regulate the excitability of place cells during navigation (O'Keefe & Recce, 1993) suggested that theta may be involved in the ordering and instructing of place cell firing based on theta phase precession (Burgess & O'Keefe, 2011; Buzsáki, 2002; O'Keefe, 1993). Task-dependent theta oscillations were later found in the human hippocampus during virtual navigation tasks using iEEG (Ekstrom et al., 2005; Kahana et al., 1999). However, they were of lower frequencies than found in the rodent (Kahana et al., 1999; Watrous et al., 2013) and were not as continuous throughout virtual navigation (Caplan et al., 2003). Recently, it has been found that they occur at similar frequencies to rodents during real-world navigation, but match the dynamics of virtual navigation oscillations (Bohbot et al., 2017). Theta oscillations recorded both intracranially and from the scalp have since demonstrated an important role in movement during spatial navigation (Bush et al., 2017; Kaplan et al., 2012; Pereira et al., 2017) but also spatial/episodic memory (Buzsáki, 2005; Buzsáki & Moser, 2013; Greenberg et al., 2015; Herweg, Sharan, et al., 2020; Klimesch, 1999). However, a recent review by Herweg, Solomon, et al. (2020) has demonstrated that we are truly unaware of the dynamics of these rhythms, their role in encoding and/or retrieval of spatial memory and their functional relationship to other rhythms in the brain – regardless of whether they are recorded from the scalp or directly from the hippocampus.

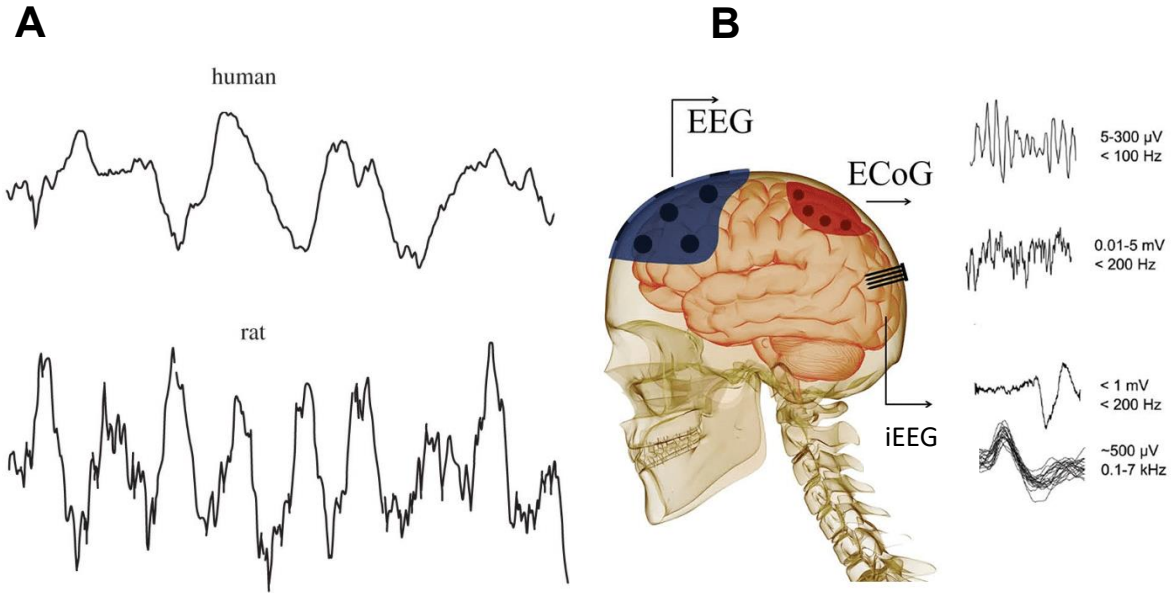


*Figure 1.9:* (A) Theta oscillation recorded from the human hippocampus and the rat hippocampus; adapted with permission from Jacobs (2014). (B) Representation of different electrophysiological recording signals, frequencies and locations of equipment on the human head: adapted with permission from Lago et al. (2017). EEG: Electroencephalography. ECoG: Electrocorticography. iEEG: intracranial Electroencephalography.

## 1.4 Oscillations & Human Spatial Navigation

### *1.4.1 Current Understanding of Oscillatory Activity in Human Navigation*

Oscillations at particular frequencies are responsible for brain-wide cognitive networks related to spatial cognition. For example, theta oscillations allow cell assemblies in the hippocampus to induce and inhibit the firing of cells (Burgess & O'Keefe, 2011) and have been reported to allow cortical regions to communicate with the hippocampus during spatial memory tasks (Jones & Wilson, 2005). Considering the clear theoretical (O'Keefe, 1993; Ormond & O'Keefe, 2022) and neural (Buzsaki, 2006; Buzsáki, 2002; Buzsáki & Moser, 2013) contributions that brain-wide frequency oscillations possess during human spatial navigation, alongside the invention of high-density EEG methodologies (see Chapter 2), much of the literature has only started to focus on investigating these in real-world (Wunderlich & Gramann, 2021), virtual (Du et al., 2023) and integrated environments (Delaux et al., 2021; Jabès et al., 2021).

Therefore, characterising frequency dynamics of oscillatory activity in the brain facilitates our understanding of their contribution during naturalistic behaviour. Oscillations are variations in the excitability of neuronal populations (Buzsáki, 2006). Categorising these different rhythms that simultaneously compose the EEG signal into a spectrum of frequencies allows researchers to characterise the dynamics of individual frequencies. Brain oscillations have been grouped into frequency bands ranging from delta (1-4 Hz), theta (4-8 Hz), alpha (8-12 Hz), beta (15-29 Hz), gamma (30-150 Hz) omega (150+ Hz). Typically, researchers examine the amplitude of the oscillation. This is essentially the amount of energy present in a frequency band and is typically converted to power (squared amplitude). Cognitive processes have been mostly associated with frequency bands ranging from delta to gamma activity. However, as opposed to the functions originally theorised by Berger in 1929, individual frequencies are *not* bound to specific cognitive functions, there can be coupling between frequencies, such as theta and gamma during spatial memory retrieval (Vivekananda et al., 2021) or different dynamics operating at specific frequencies within band, such as the Mu rhythm at approx. 10 Hz in alpha – related to sensorimotor processing (Pfurtscheller et al., 1997). This is imperative to remember, as a brief overview of frequency bands and their contributions to spatial navigation is provided below.

### *1.4.2 Low-Frequency Oscillations (Delta & Theta)*

Low frequency oscillations such as delta (1-4 Hz) are believed to contribute to successful communication between the cortex and the hippocampus in humans during spatial learning and environmental encoding. Delta recorded from the human hippocampus during virtual navigation by Park et al. (2014) revealed delta oscillations were associated with the encoding of environmental novelty, with delta power increasing as the task and environment

became familiar. This built on the findings by Watrous et al. (2011) showing increased delta power in the human hippocampus when participants viewed virtual landmarks – though it also increased with increased movement (matching their role in the rodent). However, more electrodes demonstrated this dynamic during viewing than did for movement. Miller et al. (2018) reported hippocampal delta increases were left lateralised for viewing object-location pairs (supporting evidence of left-lateralisation for spatial information – see Morgan et al. (2011)), with increases during navigation lateralised to the right hippocampus (Jacobs et al., 2010). However, since rodent hippocampal theta have been suggested to operate at higher frequencies compared to humans (e.g., Jacobs (2014) suggest 1-8 Hz for humans and 1-12 Hz for rodents) – authors have recently argued that delta rhythm recorded on the cortex could reflect sub-cortical hippocampal theta activity (De Stefano et al., 2022; Herweg, Solomon, et al., 2020). These range and band suggestions are arbitrary, with theta typically incorporating both delta and alpha bands. With no definitive division of the human EEG frequency range in the literature, there are uncertainties regarding the specific operating frequencies of human and rodent bands (Bazanova & Vernon, 2014). Nevertheless, studies of scalp delta activity (along with theta) during human navigation report sustained increases during the starting phase of a trial in a learning condition, regardless of movement speed – reported by Kline et al. (2014) and again by Delaux et al. (2021). Therefore, it is hypothesised that delta activity is responsible for spatial memory and route-planning through the use of familiarity and landmark recall (Caplan et al., 2003; Lin et al., 2022) and that the rhythm works closely with theta (4-8 Hz).

Theta (4-8 Hz) has been subject to much human navigation research since it was first noted in rodent studies and proposed as an essential neural mechanism for spatial memory and place cell firing (Burgess & Gruzelier, 1997; Buzsáki, 2002, 2005; O'Keefe, 1993; O'Keefe & Recce, 1993). Furthermore, it is consistently reported during human spatial navigation in the hippocampus and on the scalp (Chrastil et al., 2022; Cornwell et al., 2012; Ekstrom et al., 2005;

Lega et al., 2012; Thornberry et al., 2023). Considering the significant amount of research, the general role of theta oscillations during navigation is still relatively unspecified. There are currently two opposing theoretical accounts for theta's role in spatial navigation (Ekstrom & Watrous, 2014). The first is one that theta (4-8 Hz) possesses a potential role in segregating and facilitating spatial encoding and retrieval phases of navigation (Herweg, Solomon, et al., 2020). For example, Chrastil et al. (2022) reported increased scalp theta power during successful spatial decision making in a navigation task, compared to incorrect trials. Recent findings report theta power increases at early parts of trials during which spatial encoding takes place (Chrastil et al., 2022; Du et al., 2023; Liang et al., 2018; Liang et al., 2021; Lin et al., 2022). Specifically, these findings map on to Cornwell et al. (2008), who reported correlations between spatial learning performance in a VWM and theta power in the posterior hippocampus – even when controlling for sensorimotor activity. Enhancement of theta frequency using stimulatory techniques resulted in more accurate encoding and episodic memory retrieval (Roberts et al., 2018).

However, these dynamics of memory-related theta are even disputed. For example, some studies demonstrate *increases* in theta rhythm during navigation related to successful spatial recognition, retrieval of object-place locations and associative memory (Addante et al., 2011; Alekseichuk et al., 2016; Düzel et al., 2005; Khader et al., 2010; Kota et al., 2020; Miyakoshi et al., 2021; Vivekananda et al., 2021), with findings from a virtual water maze probe trial reflecting similar results (Bauer et al., 2021) - supporting a functional role of theta in memory retrieval. Alternatively, some studies report *decreases* in theta rhythms during successful encoding of object-place context (Crespo-García et al., 2016; Herweg, Sharan, et al., 2020), successful place retrieval during spatial tasks (Fellner et al., 2016; Hanslmayr et al., 2009; Lithfous et al., 2015) and associative memory formation (Michelmann et al., 2018). These decreases were typically characterised by localised decreases over the posterior scalp

and hippocampal regions accompanied by increases at the frontal cortex during successful retrieval (Greenberg et al., 2015). However, frontal theta power decreases have recently been demonstrated when episodic memories were tested after 1 and 2 weeks but not after 6–14 months from encoding (Nicolás et al., 2021). This would suggest theta instead plays a role in processing and storing information for consolidation, allowing more information to be encoded through reduction of neural synchrony across the cortex (Greenberg et al., 2015).

The second alternative hypothesis for theta oscillations in navigation, is that they are involved in sensorimotor integration including speed modulation and motor movements. Motor planning has been correlated with hippocampal theta during spatial navigation tasks (Caplan et al., 2003; Kaplan et al., 2012). Theta has also been shown to be modulated by movement speed in humans navigating in virtual and real environments (Bush et al., 2017; Lin et al., 2022). Some researchers argue that they are modulated by acceleration rather than actual movement speed based on observations in rodents (Kropff et al., 2021). Furthermore, theta increases were reported in the medial temporal lobe during real-world walking (Aghajan et al., 2017) with theta in the entorhinal cortex responsible for carrying grid-cell related orientation information (Chen et al., 2018). However, it seems that mainly iEEG studies report movement-based theta, possibly suggesting that mnemonic theta oscillations are more prominent at a cortical level, with a movement, distance and direction role subcortically. There is suggestion that these two theoretical frameworks overlap at different frequencies within the theta rhythm, with different roles at different times (Buzsáki & Moser, 2013; Ekstrom & Watrous, 2014). Overall, the theta rhythm is one of the most studied and reported rhythms during human navigation. Nevertheless, the frequency dynamics and cortical localisation of the rhythm, alongside its true role in human navigation are still unspecified.

### *1.4.3 Alpha Oscillations*

Oscillations at the 8-12 Hz range seemingly overlap with some human definitions of high theta (Newson & Thiagarajan, 2019) and also fall within the typical range of rodent hippocampal theta (Watrous et al., 2013). Furthermore, researchers in the fields outside of spatial cognition, have illustrated essential roles of alpha in attentional processes and access to stored information (Foxe & Snyder, 2011; Hanslmayr et al., 2009; Klimesch, 1999, 2012; Klimesch et al., 1998; Sauseng, Klimesch, Stadler, et al., 2005). Attention is an important part of successful encoding and subsequent retrieval of information. We cannot learn about something without properly attending, but we can also not recall something if we don't attend to mnemonic cues that may aid with recognition. Spatial navigation for example, is a complex task that requires focus and on-demand encoding and retrieval of information (Ekstrom et al., 2018). Alpha power has been demonstrated to increase in power during active but not guided navigation, as active navigation would require greater attention (Chrastil et al., 2022). On the contrary, Ehinger et al. (2014) reported vestibular (alpha suppression) and kinaesthetic (alpha increases) information modulated alpha power, also reported by Gramann et al. (2010) but in terms of egocentric to allocentric positional information.

In terms of spatial information retrieval, increases in alpha power have been found over cortical areas processing irrelevant stimuli during spatial working memory but also virtual navigation tasks (Du et al., 2023; Haegens et al., 2012; Händel et al., 2011; Jensen et al., 2012). Posterior (occipital and parietal) alpha is typically observed during navigation and particularly in conjunction with frontal theta prior to spatial decision-making (Chrastil et al., 2022; Du et al., 2023; Li et al., 2021). However, alpha decreases have been shown in the retrosplenial cortex during spatial learning (Chiu et al., 2012; Lin et al., 2015) and orientation (Do et al., 2021; Gramann et al., 2010). It is thought to support the transformation of spatial information from allocentric to egocentric reference frame. Furthermore, Liang et al. (2018) demonstrate how

posterior alpha becomes suppressed by movement during a navigation task (possibly "cortical idling" during movement via the mu rhythm – see Pfurtscheller et al. (1996)). Therefore, alpha's role may be explained by a form of the inhibition-timing hypothesis – the idea that alpha inhibits processing of irrelevant stimuli, to facilitate efficient information retrieval (Foxe & Snyder, 2011). However, evidence for the core concepts of the inhibition-timing hypothesis have been relatively weak (Morrow et al., 2023). Further work is required to understand the role and dynamics of alpha during spatial navigation and whether it is complementary to mnemonic roles of low-frequency oscillation, or whether it is involved in attention or even movement-related contributions to successful navigation.

### *1.4.4 High-Frequency Oscillations (Beta & Gamma)*

We have decided to incorporate beta (15-29 Hz) and gamma (>30 Hz) oscillations here due to the reduced literature on beta oscillations in navigation, and the overabundance of research on gamma oscillations mainly derived from iEEG experiments – with varying definitions of the gamma band. Henceforth, we define Gamma as any frequency range >30 Hz. Firstly, Beta oscillations (∼12–29 Hz) have been mostly found to support sensorimotor processing. Beta is typically decreased below baseline during "active" states, such as movement. Decreases are typically seen in beta oscillations across sensorimotor areas before or after movement execution (Barone & Rossiter, 2021). Increases (or in some cases a return to a baseline-like state) have typically been reported during rest periods (Jensen et al., 2005) or following movement cessation (Barone & Rossiter, 2021; Engel & Fries, 2010; Kilavik et al., 2013).

Beyond its well-established role in sensorimotor preparation and integration (Barone & Rossiter, 2021), beta is known to reflect activity in alpha oscillations – particularly during spatial tasks (Bauer et al., 2006). For example, in a spatial attention task which cued

participants to orientate themselves in order to interact with a tactile stimulus, suppression of beta occurred in preparation for attention-orientation (Van Ede et al., 2011). Beta activity suppression predicted better performance, with this phenomenon replicated numerous times in studies of decision-making & response inhibition (Enz et al., 2021; Wessel, 2020). In a spatial working memory task, alpha and low-beta suppressions were found to support sustained visuospatial attention, with beta responsible for the active maintenance of spatial location representations (Proskovec et al., 2018). Sutterer et al. (2019) also reported beta (15-20 Hz) increases associated with retrieval of spatial locations from long-term memory, reflecting the same patterns of activation seen during encoding (but see Hanslmayr et al. (2009)). In active virtual navigation studies, beta desynchronisation is typically sustained during straightforward or passive phases of navigation (Delaux et al., 2021; Do et al., 2021; Lin et al., 2015), with successful retrieval of spatial information during active navigation demonstrating beta increases (Chrastil et al., 2022; Sutterer et al., 2019). Hence, it is hypothesised that beta oscillations may also play a role in top-down control and maintenance of spatial information (Engel & Fries, 2010; Spitzer & Haegens, 2017). Furthermore, this period of maintenance can be activated, to facilitate memory retrieval (Hanslmayr et al., 2016; Sederberg et al., 2006). It is thought that it is more likely that beta opens the network (Palmigiano et al., 2017) - facilitating communication between sub-cortical and cortical regions through other oscillations.

Gamma oscillations (>30 Hz) have a detailed research background, with much of the spatial literature demonstrating their complementary role with theta oscillations (Aguilera et al., 2022; Goyal et al., 2020; Seger et al., 2023). They have been linked with numerous high-level cognitive functions such as memory, as well as the proposal that they are responsible for long-range communication between assemblies of neurons. Gamma oscillations exist within a large range with a central frequency between 30-80 Hz, which is incredibly broad and can lead

to many issues with signal-processing – particularly relative power spectrum and baseline contribution (Ray & Maunsell, 2015). It is likely that they have no fixed or specific role (see Ray et al. 2015 for this argument). In spatial navigation research, one of the most frequent findings is the observation of theta-gamma coupling or synchronisation between oscillations, thought to organise the processing of spatial information and memories (Buzsáki & Moser, 2013; Buzsáki & Vanderwolf, 1983). Further research indicated a detailed role of gamma in the hippocampus, reporting that gamma oscillations from CA1 couple inputs from the medial entorhinal cortex (updates information about current position), and area CA3 (stores spatial information) – both gamma phases involved here couple with different theta cycles (Colgin et al., 2009). Further research has hypothesised that the coupling between theta and gamma facilitates the temporal component of information encoding and retrieval (demonstrated in area CA3 by Jenson & Lisman in 1996), and hence co-ordinates the sequence of place cell activation (Burgess & O'Keefe, 2011). There are few human navigation papers that report a specific role of gamma. However, Jacobs et al. (2010) found posterior gamma oscillations during virtual reality navigation using iEEG – with a follow up study by White et al. (2012) confirming posterior gamma oscillations during visuospatial processing in a virtual town using scalp EEG.

Gamma oscillations were found in the left hippocampus during an encoding phase of a virtual navigation task – alongside theta oscillations, with gradually decreasing gamma in higher performing individuals (Park et al., 2014). These results align with non-spatial experimental observations of gamma oscillations relating to successful consolidation of working memory (Mainy et al., 2007) and retrieval of declarative memory (Osipova et al., 2006). Using a virtual Morris water maze task, Pu et al. (2018) found hippocampal gamma oscillations at rest predicted successful consolidation of encoded spatial information. Furthermore, the authors reported hippocampal reactivation accompanied by gamma oscillations immediately after learning, indicating a plausible role in consolidation. Yang et al.

(2021) reported egocentric and allocentric active navigation during a virtual-reality walking task increased scalp gamma oscillations at occipital regions accompanying synchronisations of frontal theta. Therefore, it is highly likely that gamma is involved in successful spatial navigation. Nevertheless, we are uncertain whether the true role of gamma oscillations are for communication between brain regions or sequencing processes. Furthermore, we do not know whether this is navigation-specific or more a general function and whether or not encoding and retrieval have any connection to gamma oscillations.

In short, oscillations are one of the most prominent and important neural correlates of cognitive function. All brain rhythms, delta (1-4 Hz), theta (4-8 Hz), alpha (8-12 Hz), beta (15-29 Hz) & gamma (>30 Hz) maintain distinct but complementary roles in spatial navigation, including spatial learning, information processing, sensorimotor integration, attention and memory. Understanding these oscillations in humans will better shed light on their individual functional roles and help us understand brain function during spatial cognition in health and disease.

## 1.5 Brief Overview of Factors Influencing Brain Activity During Navigation

### *1.5.1 Sex/Gender*

Successful spatial navigation is not the only factor known to influence navigation-related brain oscillations. Behaviourally, there is much evidence of a male advantage in the animal literature (Gaillard et al., 2021; Kolb & Cioe, 1996; Perrot-Sinal et al., 1996; Schoenfeld et al., 2010), which seems to translate well over to virtual water maze paradigms in humans (Astur et al., 1998; Astur et al., 2004; Buckley & Bast, 2018; Newhouse et al., 2007). Nevertheless, there are some studies in humans and non-human animals that demonstrate no sex/gender differences (Commins et al., 2020; Gagnon et al., 2018; Gaillard et al., 2021; Keay et al., 2018; Padilla et

al., 2017). Using a large-scale, widely available mobile app to examine navigation (Sea Hero; Coughlan et al. (2018)) researchers report that any gender difference reported in the global sample of more than 2.5 million people could be explained by the gender inequality of the country from which the population was sampled (Coutrot et al., 2019). Furthermore, Cheng et al. (2022) show that machine learning algorithms exploiting this dataset indicated that men tended to *evaluate* themselves as better navigators. Therefore, the debate regarding sex/gender differences is still active – though much human literature indicates it can be explained by other factors.

With a focus on neural oscillations during navigation and sex/gender differences, similar issues and debates exist. In a virtual maze task, women displayed more theta power increases compared to males (Kober & Neuper, 2011). Since females and males tend to prefer different strategies and landmark-use (Sandstrom et al., 1998) – it has been argued that it may be based on navigation strategy, though no behavioural differences were found. Training spatial skills improves navigation in a virtual task equally, but females showed greater theta power in frontal and parietal regions compared to males prior to training (Ramos-Loyo & Sanchez-Loyo, 2011). Post-training, theta power and coherence was similar in both groups – but promoted previous connection between frontal and parietal cortices, just in different hemispheres (left for males, right for females). Female hippocampal theta does not decrease in familiar or learned environments as it does for males (Pu et al., 2020) – but this could be explained by behavioural differences again.

Further research has supported the idea of a verbal strategy in women and a more spatial strategy in men based on hemispheric differences in both scalp EEG (Ramos-Loyo & Sanchez-Loyo, 2011) and a recent MRI study using virtual navigation tasks (Noachtar et al., 2022). This is all further supported through studies using a virtual water maze in humans such as Piber et al. (2018), demonstrating male advantages in learning phases of the task (which require

learning strategies) but equal performance during retrieval. However, even at rest there are known sex/gender differences in oscillatory activity, which are complex and demonstrate different components within the default network (Jaušovec & Jaušovec, 2010; Kimura, 1996). Therefore, whilst navigation behavioural performance is likely to be similar, it is important to examine and include gender in analyses, which can be done (Jaušovec & Jaušovec, 2010) by including baseline-correction techniques and comparisons from resting state data.

### *1.5.2 Ageing*

Age-related decline in navigation abilities begins as early as the mid 20's, with individual variability shown to be greatest in our early 60's (Coutrot et al., 2019; Klencklen et al., 2012). Furthermore, spatial navigation ability is considered to be one of the first cognitive functions to decline with age, and some of the first early pre-clinical signs of mild cognitive impairment and Alzheimer's disease (Coughlan et al., 2018; Coughlan et al., 2020). The interest in age-related decline in spatial cognition is only beginning to gather interest in human neuroscience. Recently a systematic review by van der Ham and Claessen (2020) of age-related navigation research has demonstrated that there are functional differences, with greater decline in path knowledge, compared to landmark and self-centred location knowledge.

There are also changes in our brain activity and function as we age. There are general slowing of oscillatory activity alongside less phase-coupling between rhythms such as theta and gamma. Interestingly, non-human animal work has demonstrated gamma oscillations typically reduce in speed and intensity within the medial frontal cortex (Insel et al., 2012), suggesting a slowing of overall neuronal communication. There are some general key findings regarding oscillatory activity in older adults: reduction in alpha activity at rest, and a general increase in delta and theta power (Ishii et al., 2018). Reduced amplitude of alpha has been

mainly reported at the posterior part of the scalp of healthy older adults, which sees decline in attention and concentration and can be predictive of conversion to MCI and later Alzheimer's disease (Babiloni et al., 2006; Babiloni et al., 2016; Rempe et al., 2023; Scally et al., 2018). Increases in theta power and theta-gamma synchronisation are correlated with associative memory errors (Crespo-Garcia et al., 2012) and contextual memory impairments during retrieval in older adults (Strunk et al., 2017). Greater theta power at rest is associated with healthy ageing and better cognitive function (Finnigan & Robertson, 2011; Fleck et al., 2017), suggesting that the resting theta rhythm is a sign of healthy cognitive ageing – with older adults with greater cognitive reserve, showing greater theta coherence than those with low cognitive reserve (Fleck et al., 2017). Healthy older adults have greater alpha and theta at rest, compared to those with MCI, Alzheimer's and Vascular Dementia (Moretti et al., 2004). Therefore, ageing research on oscillations has helped us understand the dominant frequencies of general daily cognition, and those that may be related to decline.

Considering spatial navigation skills are one of the first cognitive processes to decline with age-related pathology – understanding the connection between these oscillations and spatial navigation, learning and memory is essential. Decreased theta and gamma oscillations have been observed in older adults during retrieval of spatial (Rondina Ii et al., 2019), with typical spatial learning and retrieval in older adults in virtual and real environments being different or slower to younger adults (Bécu et al., 2020; Moffat et al., 2001). Jabès et al. (2021) reported overall greater power, lower theta & alpha and greater beta & gamma power at rest in older adults. The authors also reported that theta, alpha & beta are associated with spatial working memory in a navigation task. Poor cognitive map formation in older adults, and decreased theta and alpha power have been reported in the older adults compared to young adults at encoding in a virtual maze task (Lithfous et al., 2015), with the main differences being located in frontal regions – known to be associated with spatial memory decline (Lithfous et

al., 2015; Missonnier et al., 2011). This was replicated in theta during a navigation task recorded from the hippocampus, but only in poor elderly performers (Lithfous et al., 2018). This suggests that theta is somehow related to healthy cognitive ageing as suggested above, including spatial cognition. Nonetheless, there is very little research exploring the impact of age on the underlying impacts of neural oscillations related to successful spatial navigation and memory retrieval. Further research is necessary, but incorporating and controlling for age as a factor in all navigation studies with humans is a certain requirement.

### 1.6 Thesis Objectives

The general aim of this thesis was to further investigate the neural oscillations underlying human spatial navigation using a VWM task. More specifically, we aimed to explore key components of spatial navigation - learning (encoding) and memory (retrieval), examining how spatial ability and neural oscillations change during these processes with factors such as age and consolidation time. This paradigm should allow us to examine the discussed theoretical frameworks as well as perform some exploratory investigations using a novel protocol. The current chapter aimed to provide an overview and background to our current understanding of human spatial navigation and neural oscillations. Chapter 2 outlined the methods, analyses and signal processing approaches used throughout the thesis. We then examined spatial encoding during navigation in Chapter 3 in younger adults, using a hypothesis-driven approach to investigate theta and alpha activity during spatial learning, compared to a non-learning control group. The aim of Chapter 4 was to perform an exploratory analysis of *all* oscillatory bands during immediate spatial memory retrieval using the aforementioned learning & non-learning groups. Subsequently, Chapter 5 aimed to examine the impact of memory consolidation time (recent or remote), if any, on spatial memory retrieval and neural oscillations following successful spatial learning in new sample of healthy younger adults. Finally, Chapter 6 aimed

to investigate the differences between older and younger adults during rest, as well as immediate, recent and remote spatial memory retrieval following spatial learning. The impact of this work and its contribution to the current behavioural and neural theoretical frameworks of human spatial learning and memory during navigation are discussed in Chapter 7.

# Chapter 2

# General Methodology

**Publications arising from this chapter:**

The behavioural paradigm and NavWell task have been published as:

Commins, S., Duffin, J., Chaves, K., Leahy, D., Corcoran, K., Caffrey, M., ... & Thornberry, C. (2020). NavWell: A simplified virtual-reality platform for spatial navigation and memory experiments. *Behavior research methods*, *52*(3), 1189-1207.

**Brief Overview**

Many of the methodologies discussed throughout this thesis are used repeatedly over the course of the main experimental paradigms. These methodologies can be broken down into cognitive control measures, spatial navigation task, EEG data collection, signal processing and statistical analyses. The aim of this chapter is to outline each of these procedures and why they were chosen for use in particular paradigms.

## 2.1 Neuropsychological Assessments

A number of standard cognitive tests were given to participants including the National Adult Reading Test (NART), the Trail Making Test (TMT) and the Montreal Cognitive Assessment (MoCA). These were provided to ensure that the various groups tested were matched in their general cognitive abilities. The tasks were generally given between the learning and recall phase, to ensure a sufficient break was given. In addition, as the MoCA is often used to examine Mild Cognitive Impairment (MCI), we wanted to ensure that our older adults all scored within the normal range.

### *2.1.1 National Adult Reading Test (NART)*

The National Adult Reading Test (NART) is a psychological test used to examine premorbid intelligence in adults who are potentially experiencing cognitive or intellectual decline (Nelson & Willison, 1991). The NART is a single word reading test consisting of 50 items, with increasing difficulty. All words on the list violate grapheme-phoneme correspondence rules of typical language comprehension. Participants are requested to read the list aloud, whilst the administrator records any errors in pronunciation. The number of errors is recorded for each

participant and is then used to estimate verbal IQ, performance IQ and full-scale IQ. The NART allows for a good estimation of general intelligence. Reading ability is highly correlated with verbal and overall IQ as it disregards numerical, spatial and logical components (Bright et al., 2002). NART scores also correlate strongly with scores on the WAIS-IQ, suggesting in a neurotypical population, it is a good estimate of a person's general intelligence. A number of papers have demonstrated the usefulness of this task as a control measure in studies of human spatial navigation and cognition (Burgess et al., 2006; Howett et al., 2019; Maguire et al., 2003).

### *2.1.2 Trail Making Test (TMT)*

The Trail Making Test (TMT) is a pen and paper cognitive test that was initially included in the Individual Army Test Battery (U.S. Army Individual Test Battery, 1944) and was retained due to its excellent ability to measure cognitive flexibility, visuo-spatial attention, and inhibition (Reitan & Wolfson, 1995). The widely used and validated TMT contains two sections. The TMT-A contains a page displaying twenty-five circled numbers and requires individuals to connect these series of circles in numerical order without lifting the pen/pencil. The TMT-B contains twenty-five circled numbers *and* letters, requiring participants to alternate between number and letter as they match them consecutively. Participants' time-to-complete each section is recorded and is a commonly used measure of executive function and cognitive flexibility. Part A of the TMT mainly captures visual processing and motor speed skills, while part B measures task-switching ability and working memory, as well as inhibition (Reitan & Wolfson, 1995). The TMTs provide an excellent measure of overall cognitive performance, suggesting it is a logical choice to ensure healthy neurotypical participants are cognitively matched (see Tombaugh, 2004 for a review). The task has been shown to be capable of

accurately detecting neurological impairment and brain injury (Woods et al., 2015). The tasks scoring system controls for education level and age (Tombaugh, 2004). Therefore, we have chosen this task as it is a freely available, easy-to-administer assessment for general cognitive functioning. Particularly due to navigation performance being highly correlated with performance on the TMT (Committeri et al., 2020) and similar tasks in healthy older adults (Sanders et al., 2008), it offers a good test for our experimental design.

### *2.1.3 Montreal Cognitive Assessment (MoCA)*

The MoCA was developed as a screen tool for Mild Cognitive Impairment (MCI). The task has shown excellent validity and performance across the world and in different languages (Nasreddine et al., 2005). The MoCA comprises a single-page test of approximately thirty items that can be administered in ten minutes. Cognitive impairments are detected via a cut-off score of twenty-six. Among the thirty items included within the MoCA are tests of executive functioning, memory, and attention (Julayanont & Nasreddine, 2017). The MoCA has been shown to suffer from a "ceiling effect", causing a lot of scores to cluster towards the higher end of the scoring system (Zadikoff et al., 2008). The MoCA also possesses good cognitive heterogeneity, with several cognitive domains examined in a short task. This makes the MoCA a more favourable measure than other tests, such as the Mini-Mental State Examination (MMSE; Cockrell and Folstein (2002)). However, it has been reported that MCI prevalence is higher on the MoCA than the MMSE (Jia et al., 2021). Interestingly, scores on the MoCA are correlated with performance in virtual navigation tasks (more specifically a virtual water maze) in those with amnestic MCI (aMCI), a pre-dementia stage of Alzheimer's Disease (AD). Nevertheless, researchers do suggest different scoring methods (such as 23.5 as a cut-off instead; see Ilardi et al. (2023)) or the removal of the 1-point correction for education

experience (Carson et al., 2018)). Despite its criticisms, the MoCA tends to contain more frontal tasks than the MMSE, with the MoCA more sensitive to detecting non-AD dementias such as vascular dementia. A relatively recent review demonstrated that in studies examining the impact of age on spatial cognition, the MoCA was one of the most used screening tools for dementia or MCI (van der Ham & Claessen, 2020). The authors recommend screening both younger and older adults using these tools, to control for individual variation in spatial navigation performance. Therefore, we utilise the MoCA throughout Chapter 5 to test for cognitive function in older *and* younger adults for research participation exclusion purposes and general comparisons. Given that our intention is to examine healthy older and younger adults, we found the MoCA to be the most useful for this purpose.

## 2.2 Spatial Navigation Task

### *2.2.1 Virtual Morris Water Maze*

The ability to learn and accurately recall locations in our environment relies on multiple cognitive mechanisms and is essential for everyday life. The experiments in this thesis were carried out on a computer-based program known as NavWell, created in collaboration with Maynooth University Department of Computer Science. The NavWell software can design virtual environments comparable to the Morris Water Maze (MWM; Morris, 1984) in which humans can navigate. The software is based on the standard MWM protocols, with various arena sizes, cues and procedures that can be designed and manipulated by researchers (see Commins et al., 2020).

The original "water maze" developed by Richard Morris in 1981 has been to the forefront of learning and memory research for many years (Alcalá et al., 2020; Morris et al., 1982; Morris, 1984; Morris, 1981; Vorhees & Williams, 2014a, 2014b). The general layout of the maze involves a circular pool filled approximately half-way with water. The animal is tasked with locating and recalling the position of a hidden "platform", which is submerged below the water surface in a fixed location. The platform is generally camouflaged by colouring the water. This facilitates the platform having minimal visual presence in the pool, meaning the location of the platform must be found and recalled from memory. The animal can be trained with distal or proximal landmarks or with their trajectory alone (see Nunez, 2008 for an outline of the procedure). The maze provides a highly controlled environment for behavioural, electrophysiological and lesion studies.

The task is a simple, effective and a relatively cheap test that is primarily used to examine spatial learning and recall in rodents (D'Hooge & De Deyn, 2001). The popularity of the task was cemented when it was shown to be hippocampal-dependent (Morris et al., 1982). Furthermore, it is sensitive to age as well as environmental (Cao et al., 2008; Farina et al.,

2015), behavioural (Fenton et al., 1994; Hölscher, 1999), neural (Broadbent et al., 2006; Packard & McGaugh, 1992) immediate early gene (Farina & Commins, 2020; Shires & Aggleton, 2008) and pharmacological (Morris et al., 1982; Skarsfeldt, 1996) manipulations. In addition, its use across species and with models of different diseases and disorders such as Alzheimer's Disease (Bromley-Brits et al., 2011; Commins & Kirby, 2019); Parkinson's Disease (Pothakos et al., 2009) and Epilepsy (Inostroza et al., 2011) has made it the 'gold standard' tool for animal learning, memory and navigation research over the last 40 years.

Virtual reality and gamified navigation tasks have repeatedly shown to reflect spatial navigation performance in real-world settings (Coutrot et al., 2019; Santos et al., 2008) despite the lack of idiothetic, vestibular and kinaesthetic feedback (Ladouce et al., 2017). These virtual navigation tasks can be used with cognitively healthy and clinical populations, reporting success with depressed patients (Cornwell et al., 2010), Alzheimer's Disease patients (Tu et al., 2015), and can be used to detect and monitor progression in Dementia (Cogné et al., 2017). The NavWell task itself has been validated using several experiments, such as verifying that there are no differences between 2D (desktop) and 3D (head mounted display via Oculus) versions of the maze (Commins et al., 2020, Experiment 1). Further experiments found replication of typical animal behaviours reported in the literature such as successful spatial memory using proximal landmarks (Commins et al., 2020, Experiment 2) and poorer age-related task-performance in older adults (Commins et al., 2020, Experiment 4). The NavWell task also irradicates sex-gender effects typically reported in other VWM's (Astur et al., 1998; Boone et al., 2018; Commins et al., 2020; Weiss et al., 2003). Younger and older adults reported that the task was "not difficult" to use (see Commins et al., 2020). This task was a robust choice for this current thesis. It has been repeatedly validated for use with several populations, provides a more ecologically valid examination of spatial learning and memory whilst remaining incredibly translatable to the animal literature. Virtual water maze tasks such as

NavWell have been reported to be the most used spatial task within the human literature (Thornberry et al., 2021) and have shown promising results in combination with multiple forms of brain imaging (e.g., EEG, iEEG, fMRI; Chrastil et al., 2022; Ekstrom et al., 2003; Maguire et al., 2006). Therefore, the use of VWM can aid in human spatial navigation research but using a peer-reviewed software with a published recommended method and set of procedures, such as NavWell, is essential for translatability and validity. The specific details of the environment and protocols used in this thesis' experimental paradigm are described below.

### *2.2.2 Setup procedure and environment design*

Participants were seated 50 cm from the LCD computer screen on their own in a darkened, electrically shielded and sound-attenuated testing cubicle (150 cm × 180 cm) with access to a joystick for navigating. The same arena design was used for all experiments in this thesis. The reason for this choice is because it is the arena design that elicited the best learning from participants across numerous variations of arenas tested in our lab (Deery & Commins, 2023; Thornberry, 2019). The virtual maze consisted of a medium circular environment (taking 15.75s to traverse, calculated at 75 virtual metres [Vm]). Two cues were used and were located on the wall of the arena: a yellow square (northeast quadrant wall) and a light of 50% luminance (northwest quadrant wall) and can be viewed from a participants perspective in Figure 2.1a. Viewing angle was fixed, participants could only look left and right. This was to prevent the use of extramaze features to navigate and to ensure joystick controls were as straightforward as possible. A square goal was hidden in the middle of the northeast quadrant and was 15% of the total arena size and consisted of a bright blue square that only became visible when the participant crossed it (northwest quadrant wall, see Figure 2.1b). An overall schematic that incorporates task-specific elements from both behavioural phases is available in Figure 2.3.

**a.**

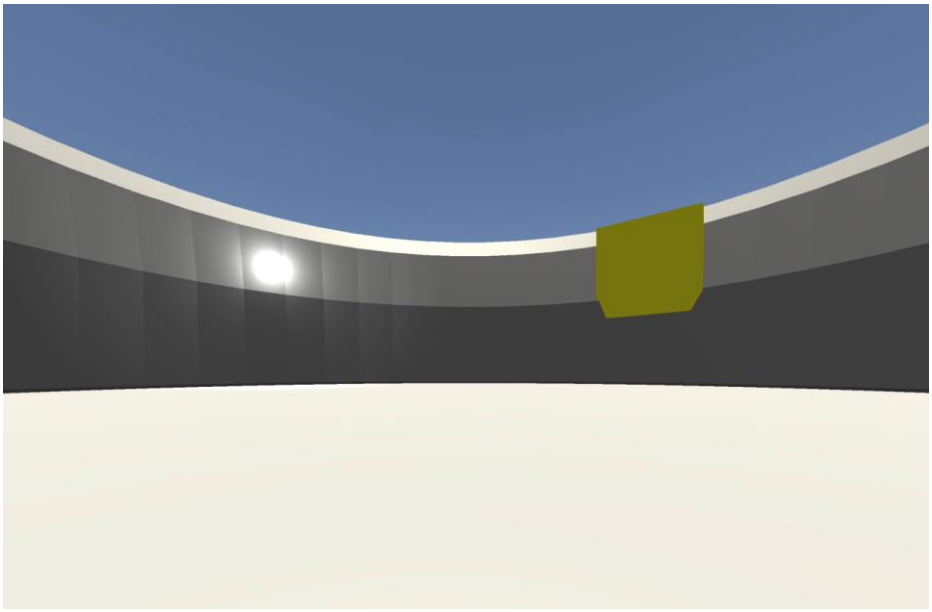

**b.**


*Figure 2.1:* Screenshot of the NavWell environment used in this experiment from the perspective of a participant. The light & square cues on the wall of the environment can be seen from the South starting point. *Figure 2.1b:* The goal location becomes illuminated when a participant walks over it, "congratulations, you reached the goal platform!" message displayed prior to the start of the ITI.

*2.2.1.1 Learning Phase*

The task was programmed so that participants would start from pseudorandom starting positions around the cardinal points of the arena (North, South, East & West). The maximum trial length was set to 60 seconds/trial to locate the goal for all experimental paradigms. Participants were transported to the location of the goal if they failed to locate it. There was a 10s inter-trial interval between each trial. The goal remained in the same location throughout (centre of NE quadrant). Latency (time taken to locate target or complete trial; measured in seconds), path length (distance travelled in virtual metres [Vm]) and percentage time spent in goal quadrant are typical measures of water maze performance (see (Thornberry et al., 2021); Vorhees and Williams (2014a)). These were recorded for each participant during each trial by NavWell (see also Commins et al., 2020).

As previously discussed, the goal of the standard MWM is to locate an invisible platform in a circular pool and to recall its location, examining an animal's spatial navigation and memory (see Morris, 1984; Voorhees & Williams, 2006). NavWell requires participants to locate and recall the location of an invisible platform in a virtual translation of a typical water maze pool. The NavWell environment was also split into four quadrants for the purpose of analysis (see Figure 2.3). Upon traversing the target, it would illuminate blue and present the message: "*Congratulations, you have located the goal platform!*". This would disable movement for the participant, but still permitted them to look around using the joystick (see Figure 2.2). The task data were stored on an administrator cloud system and could be downloaded as a .csv file upon completion of the experiment. NavWell also produced a tracked heatmap and path sketch for each trial, as well as a time percentage spent in each of the four quadrants of the arena. When the environment and experiment was designed, participants were assigned a participant code number for the experiment and randomly assigned to an experimental group for all experiments. Participants data were then anonymised.

Upon starting the experiment, participants were presented with the following message: *"Welcome Participant. Your experiment is about to start. Your goal is to find the platform within the pool. Use the cues in the environment in order to locate yourself. The experiment consists of 12 total trials"*. The first trial began after 10 seconds and presented the following message on screen: *"Your trial #1 is about to start. You will have 60 seconds to find the goal."* Participants were then instructed that their sixty seconds will begin when this message disappears. There was a 10 second Inter Trial Interval (ITI), which facilitated participants to look around and attempt to remember the targets location. When the target was located and illuminated blue, the following message appeared: *"Congratulations. You reached the goal platform!"* followed by *"You can rest for 10 seconds. Look around the environment to learn this location."* (Figure 2.1b).

If participants were unsuccessful in locating the target on any of the trials, the trial would end with the presentation of *"Trial Ended"* on-screen message. NavWell would then relocate them to the platform position during the same duration ITI. They were then prompted to learn the current location and the surrounding environment by presenting the message: *"You have been moved to the platform location. You can rest for 10 seconds. Look around the environment to learn this location."* (Figure 2.2 "Incorrect Trial"). When all twelve learning trials were completed, there was a minimum duration of 10 minutes between this phase and the recall phase (see below). Performance of correct trials produced short latencies and path lengths. However, incorrect trials produced 60-s latency scores, as well as prompting the NavWell software to perform the above procedure during the ITI. For a clear understanding of the two possible trials and the NavWell protocol, see Figure 2.2 below.

## Possible Participant Trials and the Respective Protocol in NavWell

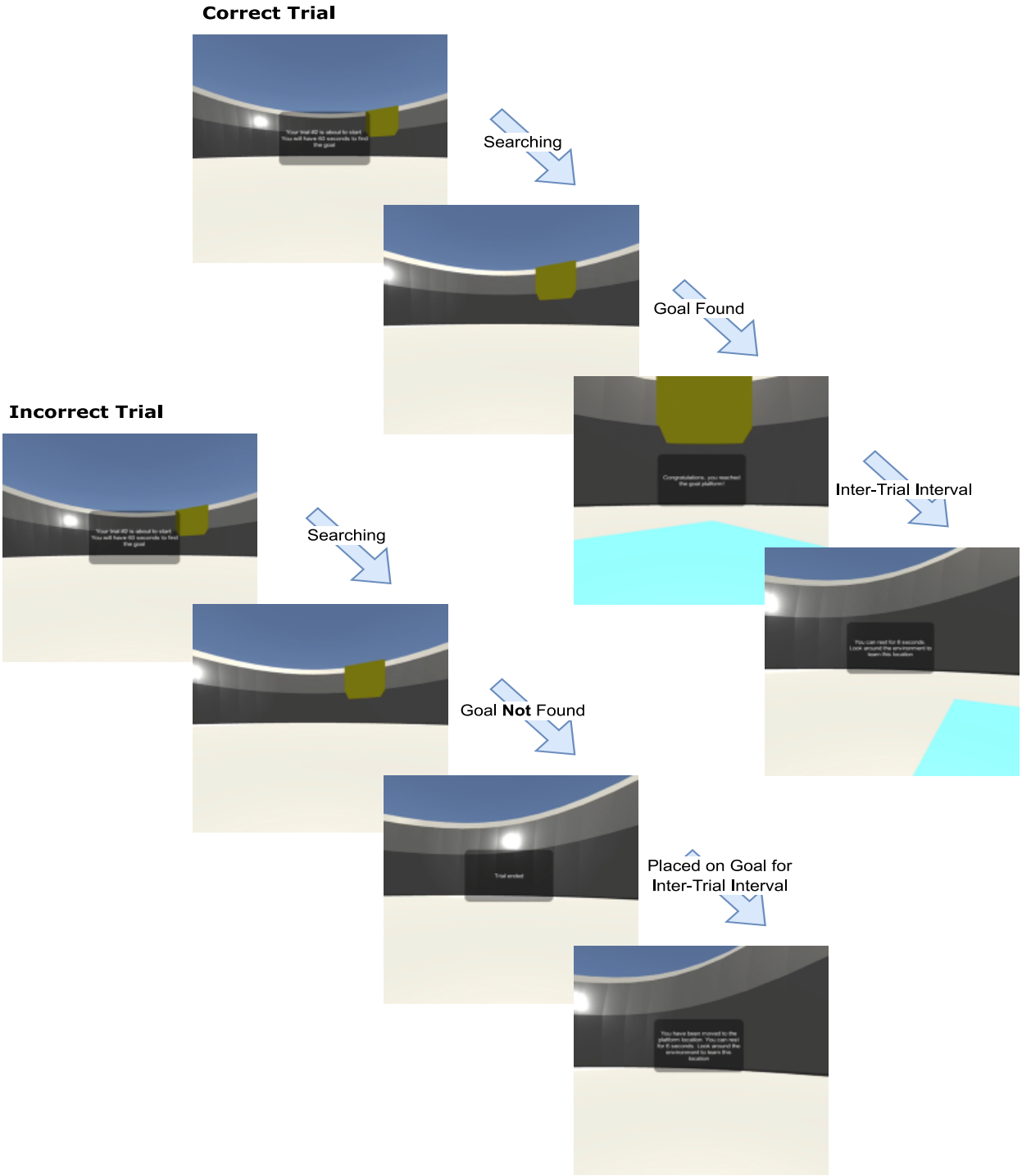


*Figure 2.2*: A breakdown of the two possible trial outputs (Correct Trial and Incorrect Trial) containing different participant behaviour, and the relevant NavWell protocol elicited during each stage.

*2.2.1.2 Recall Phase*

A single recall trial was given some time following completion of the training trials and the neuropsychological assessments. In the standard Morris Water Maze procedure, a "retention" or "probe" trial is carried out following the learning trials to verify learning and examine spatial recall (Morris, 1984; Voorhees & Williams, 2006; Nunez, 2008). The platform is removed from the pool and the search strategy of the animal is examined. Typically, this test can be used to examine hippocampal-dependent spatial memory (Morris et al., 1982; Ekstrom et al., 2003, Barnhart et al., 2015). Lesions to the hippocampus impair recall during animal probe trials (Barkas et al., 2010; Broadbent et al., 2006; de Bruin et al., 1994; Farina & Commins, 2016; Inostroza et al., 2011; Morris et al., 1982; O'Keefe, 1993). A single recall trial is typically used as a measure of spatial memory; the platform is removed from the pool and the percentage of time spent searching in the correct quadrant is measured (Barnhart et al., 2015; Maei et al., 2009; Vorhees & Williams, 2006; Vorhees & Williams, 2014a). For this project, our participants also had to recall the targets' location during a single retention trial to examine hippocampal-dependent memory, however, the target did not illuminate blue if it was traversed (i.e., remained invisible). In Chapter 3, a recall trial was given to participants approximately 10 minutes after completion of their learning phase, which we termed an "immediate recall" (analysed in Chapter 4). To examine recent and remote spatial memory in our subsequent chapters (Chapter 5 & 6) we gave participants an immediate recall trial on the day of the learning phase but were also asked to return 24 hours later (i.e., recent spatial memory – Eichenbaum et al., 1999; Clark et al., 2005) or 1 month later (i.e., remote spatial memory – Clark et al., 2005; Cimadevilla et al., 2000) for a further recall trial. The paradigm of the recall phase is in Figure 2.4.

The recall trial was set to a duration of 60 seconds. All participants started from the Southwest (SW) position, which was a novel starting point not used during the learning phase

(see Figure 2.3). Participants received no feedback during this trial. However, participants were not made aware of this, receiving on-screen instructions to locate the platform as normal. They received further verification of this from the researcher and were debriefed after. Percentage time (of a total 60 seconds) spent in each quadrant including the target (NE) was recorded to measure memory recall. This is standard practice in the animal version of the task and has been used to previously validate the software in Commins et al. (2020). Participants were finally debriefed following the completion of the recall trial and thanked for their participation.

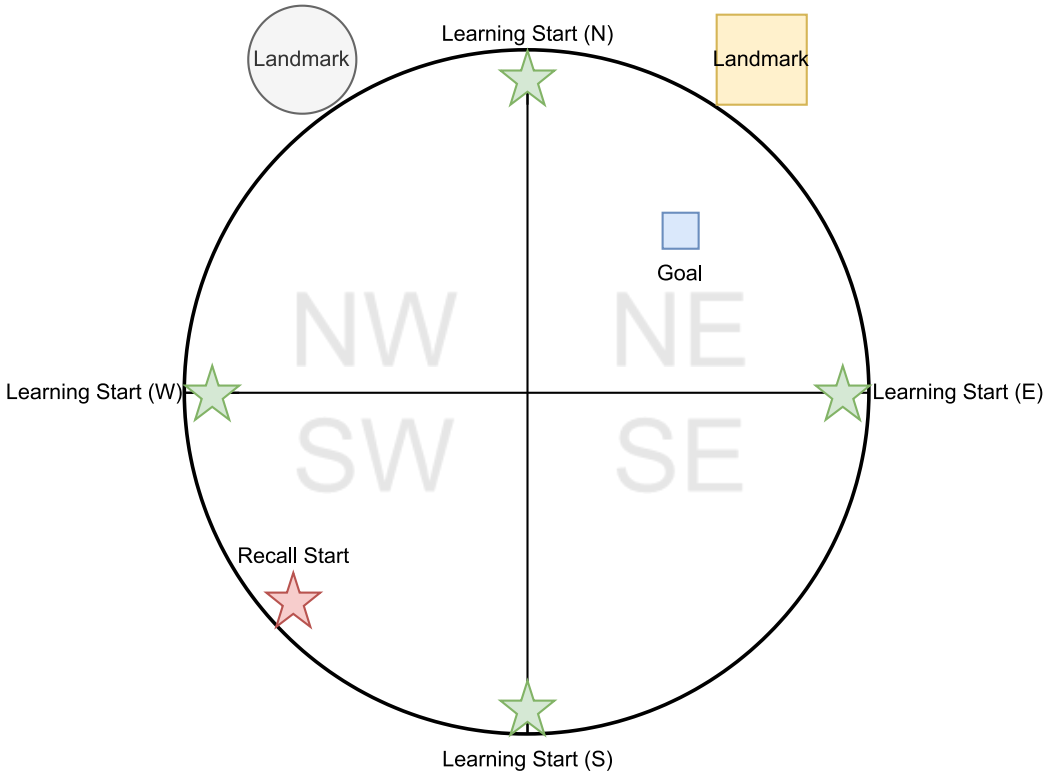


*Figure 2.3*: Schematic of the NavWell Arena including landmark position, goal position, quadrant labels and starting positions for learning trial (green stars) and starting position for the recall phase (red star). The grey circle depicts the light from the previous figures, and the square is depicted as a yellow square.

*2.2.1.3 Practice Phase (Older Adults)*

Older adult participants were to complete a series of four training trials before commencing their twelve experimental trials (Figure 2.4). This is common practice in the virtual water maze literature (Daugherty & Raz, 2017; Daugherty et al., 2015; Dobbels et al., 2020) as it helps older adults familiarise themselves with the controls, the nature of the task and allowed them to get comfortable with the EEG equipment's presence during their navigation. All younger adults in this study were offered four training trials for the same above reasons. No younger adult participant accepted this offer. During these practice trials, the goal remained visible (blue square), and participants simply had to move towards it. The goal did not move location for each of the 4 trials (SE quadrant). The practice trials were also used to control for potential motor, visual or motivational issues. The training maze contained no landmarks, and the participants started each trial from the north, south, east and west positions respectively. The arena was a medium circular pool, as explained above. Each trial was 60 seconds in length or ended when the goal had been reached. This is also discussed in Chapter 6.

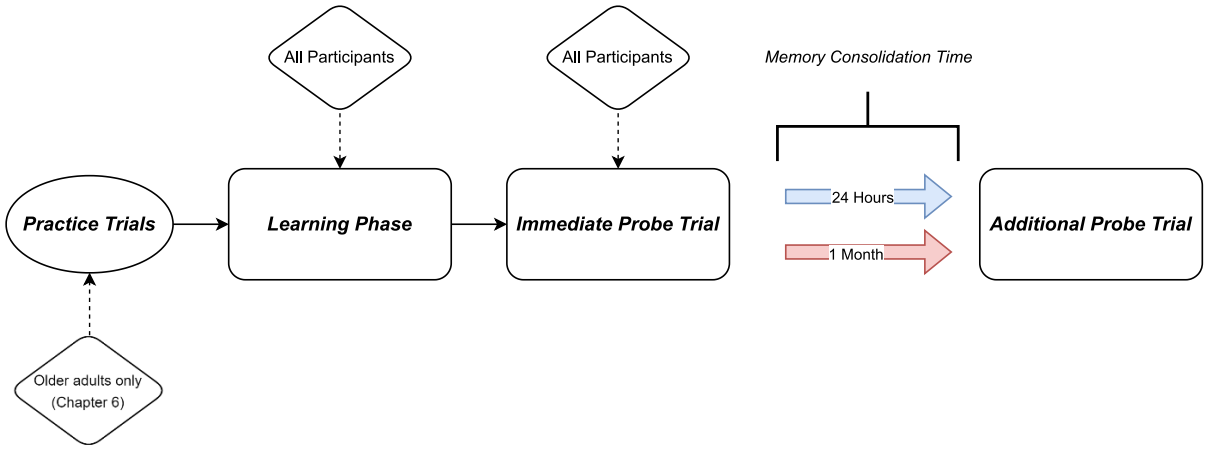


*Figure 2.4*: A breakdown of the recall phase trial paradigms and overall experimental paradigm.

## 2.3 Electroencephalography

Electroencephalography (EEG) is one of the most effective and commonly used techniques for noninvasively investigating the electrophysiological dynamics of cortical neural activity (Cohen, 2014). The discovery of low-level cortical brain activity by Hans Berger in 1924 was revolutionary for neuroscience and neurosurgery. EEG is commonly recorded by placing electrodes on the scalp that are capable of reading voltage fluctuations of the cortex, which are then typically amplified and digitised (Cohen, 2014; Kumar & Bhuvaneswari, 2012). EEG electrodes capture the extracellular activity that derives from excitatory and inhibitory post-synaptic potentials in populations of pyramidal neurons that lie parallel to each other, due to the structure of the cortex (Cohen, 2017). EEG sensors measure the perpendicular electric field that passes through the space between the source of activity and the sensors location. Additionally, EEG sensors capture electrical currents propagated in the conductive medium of the human head due to volume conduction (Cohen, 2017). EEG provides high temporal resolution but has historically possessed poor spatial resolution. However, recent advancements in source localisation techniques and the combination of EEG (Light et al., 2010; Michel & Brunet, 2019) with MRI data (Logothetis, 2008) have improved the overall resolution of neural signal, producing a low-cost technique to examine brain activity.

Synchronized neural activity across substantial groups of cortical neurons can generate ionic currents that are substantial enough to be measured at the scalp via EEG. The firing of cortical pyramidal neurons is triggered by neurotransmitters binding to post-synaptic receptors, which opens ion channels and allows the flow of ions (e.g., sodium) into or out of the cell. This leads to either depolarization or hyperpolarization of the neuron. At the local level, synchronised dendritic activity from neighbouring cortical pyramidal neurons can summate to produce detectable extracellular current flows known as local field potentials (LFPs). Localised firing that generates LFPs can result in synchronized rhythmic patterns across neural

populations in small sections of brain tissue (Cohen, 2017). The presence of these brain rhythms and their amplitude, commonly termed neural oscillations can be observed in bands of frequency such as theta (4-8 Hz) and alpha (8-12 Hz) and recorded from the scalp. The scalp EEG, recorded by a single electrode, is a spatiotemporally smoothed version of the LFP. It has no real relationship with the firing patterns of the contributing individual neurons. This is largely due to the attenuating effects of the brain tissue, skull, and scalp present between the current source and the electrode (Buzsáki et al., 2012; Cohen, 2017). For further information see Chapter 1.

### *2.3.1 An overview of measuring EEG*

EEG produces waveform data that can be analysed in terms of changes in amplitude across (measured in μV) and/or frequency (measured in Hertz: Hz) across time. The power of the signal (i.e., the amount of activity within a frequency or frequency band) is typically measured in $\mu V^2$ within the frequency domain. Analysis of these signals involves digitization and examination of their characteristics in both the time and frequency domains. Time domain analysis focuses on how brain activity changes over time, such as identifying the timing of neural activity peaks (i.e., changes in amplitude) during cognitive or motor tasks (see Figure 2.5a). Frequency domain analysis employs Fourier transformation to break down the recordings into a combination of waves with different frequencies. These wave patterns typically occur at the same time and can be isolated by breaking down these complex signals into distinct frequency bands (2.5b). The power within these frequencies can also change across time and can be analysed using time-frequency methods (Figure 2.5c).

These bands traditionally include delta (1-4 Hz), theta (4-8 Hz), alpha (8-12 Hz), beta (12-30 Hz), lower gamma (30-80 Hz), upper gamma (80-150 Hz), and omega (150+ Hz) waves.

Neural oscillations are the most prominent feature of EEG, linked to multiple spatial locations, time scales and across several species (Cohen, 2017). Cognitive processes are typically known to operate in the oscillatory range of delta to gamma activity (Alekseichuk et al., 2016; Buzsaki, 2006; Fellous & Sejnowski, 2000; Goodman et al., 2018; Lundqvist et al., 2016). However, a single frequency band and such oscillations contained within, in isolation, cannot be responsible for one specific cognitive process (Buzsaki, 2006; Buzsáki & Moser, 2013). Furthermore, it is possible for the function of several frequency bands to overlap, such as theta and gamma oscillations during spatial memory retrieval (Lisman & Jensen, 2013). Therefore, there is no real agreement in the literature on the exact range of these frequency bands.

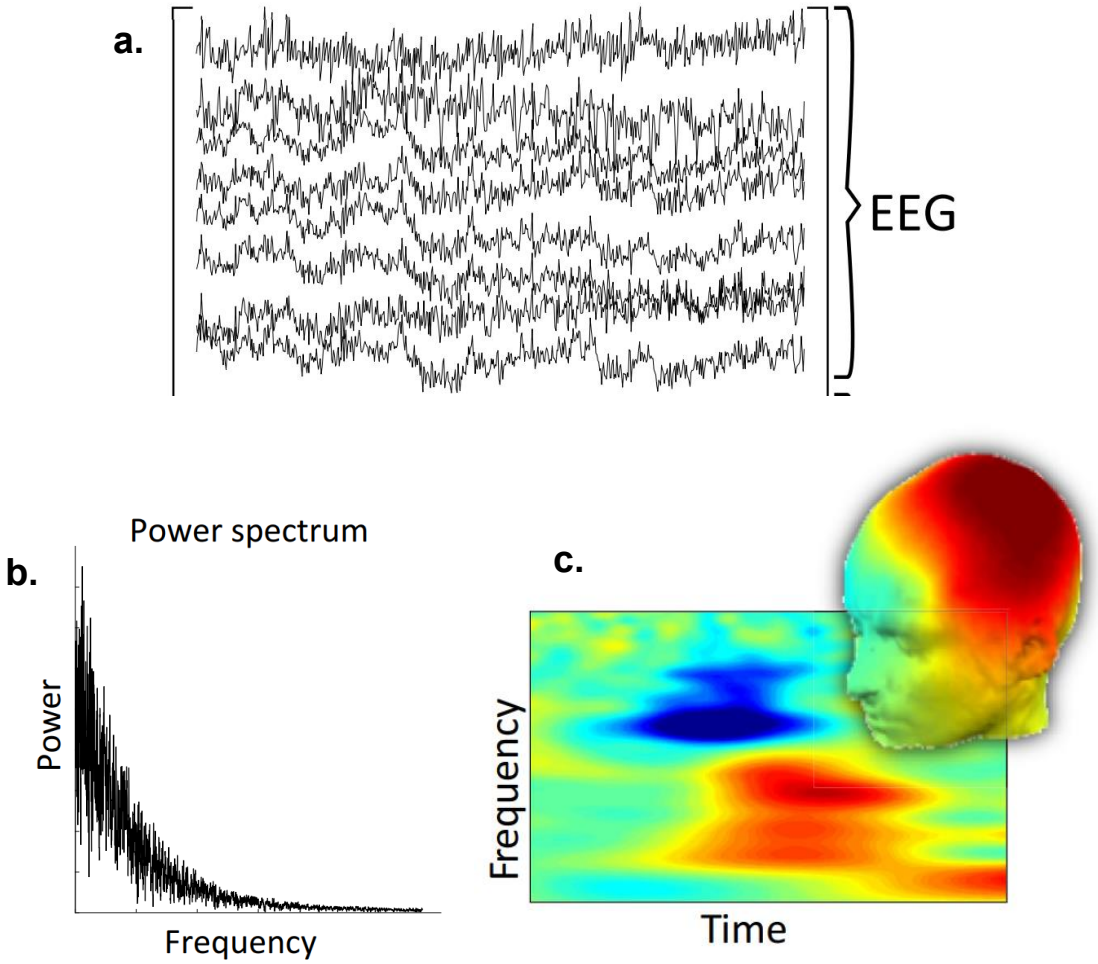


*Figure 2.5:* An image of raw and unfiltered EEG amplitudes recorded from the scalp with the electrode site typically displayed on the y-axis and time displayed on the x-axis (a). A typical diagram of the frequency power spectrum, with the amount of activity (power) on the y-axis and the frequency (in Hertz) on the x-axis (b). A time-frequency plot that uses a time-frequency decomposition method to plot changing power in frequency on the y-axis across time on the x-axis. Scalp topography can show the distribution of this power at particular times (c). This figure has been adapted from Cohen, 2017 with permission.

### *2.3.2 Current Approaches for Studying EEG in Human Spatial Navigation*

As previously discussed in Chapter 1, much of our current knowledge derives from the study of non-human animals and the hippocampus. Some studies have focused on the human hippocampus (Ekstrom et al., 2005). However, what both domains have in common is the presence of oscillatory activity during spatial cognition. One of the easiest and most non-invasive ways of studying cortical activity in humans during navigation is by using high-density scalp EEG combined with VR (see Figure 2.6a & 2.6b). Though, this does not truly reflect the type of spatial accuracy available in iEEG navigation studies (Luck & Gaspelin, 2017) –iEEG is next to impossible to implement on healthy cohorts of participants, typically requiring surgical patients.

Nevertheless, advanced signal processing after a real-world navigation experiment with a mobile EEG system (Jungnickel et al., 2019) or a stationary high-density EEG recording from a virtual navigation experiment (Delaux et al., 2021) requires large amounts of data from time-locked cognitive events, which are not as clear-cut in a fluid ever-changing behaviour such as navigation (see Nyberg et al. (2022) and Erkan (2018)). Participants are typically required to complete many trials while EEG is recorded. Each trial typically consists of a stimulus presentation or the recording of a participant response. Signals of interest (typically timestamped by an event marker) are extracted and the data from multiple trials are averaged together (see Figure 2.6e for an example). Though this is one of the most widely used and significantly supported non-invasive, inexpensive neuroimaging techniques in the literature – it may be impractical (as well as not ecologically valid) to record multiple repetitions of a specific spatial learning or memory event during naturalistic navigation behaviour (see Figure 2.6c and 2.6d for low trial number frequency analysis of navigation data). Acquisition of precisely timed events during a naturalistic learning behaviour, such as spatial encoding and retrieval is incredibly difficult. Recently, there have been statistical methodologies developed

to counteract this (such as independent component extraction, see Figure 2.6d middle). For example, Di Liberto et al. (2021) utilised linear regression-based decoding models to locate the event of steering actions within EEG signal, to investigate continuous action planning within the data. Though this is a useful method, the authors used a driving simulator with a specific set of turns and bends on a predefined driving track. This is very different to the dynamic and fluid nature of active natural spatial navigation. Another approach to EEG data analysis is the extraction of changes in the frequency domain. Using similarly advanced signal processing methods, researchers can extract the contribution of frequencies to recorded but stationary data (Cohen, 2014; Morales & Bowers, 2022; Sanei & Chambers, 2013). Our task and protocol does not map on to any specific EEG literature involving virtual mazes or mobile-EEG tasks – as it involves the continuous recording of spatial navigation using a joystick-controlled virtual water maze task. Therefore, a combination of these processes will be used to best suit our chosen experimental paradigm.

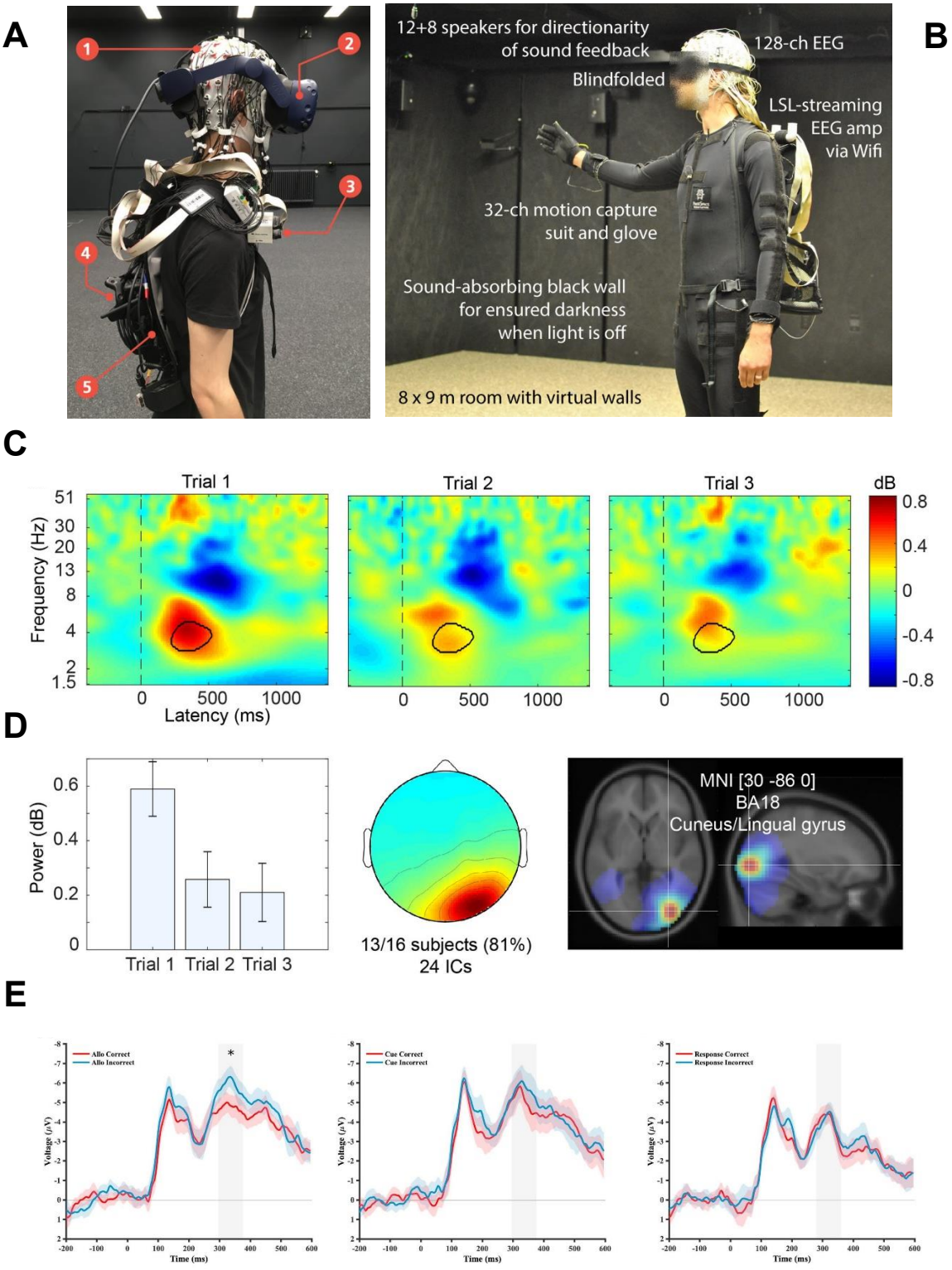


*Figure 2.6:* (A). Photograph of participant's equipment in Delaux et al. (2021) using a combination of VR, EEG and real-world movement. (B) Another example of equipment in VR-EEG experiments from Miyakoshi et al. (2021). (C) Example of time-frequency plots from active navigation experiment from Miyakoshi et al. (2021), in which time 0 represents trial/navigation onset with significant effects circled in black. (D) Examples of analysis of low-trial navigation experiments including theta power comparisons (left), independent component extraction (middle) and source reconstruction (right). (E) An example of ERPs that can be extracted during stationary non-active navigation/spatial tasks – presented in amplitude and time as opposed to power, frequency and time.

*2.3.3 Hardware and software*

EEG was recorded using a BioSemi ActiveTwo system with a 32-electrode cap using a 10-20 layout (see Figure 2.7a, 2.7b & 2.7c). Thirty-two active sintered Ag-AgCl electrodes (Figure 3c) contacted the scalp through an electrolyte gel link (Signa Gel, Parker Laboratories Inc., NJ, USA) which formed a connection between the scalp and the cap in which electrodes were inserted. Use of this electrode material amplifies EEG at the scalp, thus ensuring minimal interference from external noise and a performance preferable to that of passive electrodes at most impedances (Laszlo et al., 2014). Wet electrodes aid in further noise reduction and are considered more comfortable for participants compared to dry electrodes (Mathewson et al., 2017; Oliveira et al., 2016). Vertical eye movements were recorded using electrooculogram (EOG) electrodes (EX1 – EX4) placed above & below the eye and at the lateral canthus of both eyes to record horizontal eye movements (see Figure 2.7d).

Data were recorded continuously throughout the task in a room enclosed by a Faraday cage using a battery-powered amplifier so as to reduce the impact of electrical mains noise on the signal (see Figure 2.6e). Data were relayed to computers in an adjoining room. EEG signals were observed and recorded on a Dell machine with a Windows 7 operating system. A second Dell machine with a Windows 10 operating system was used to administer NavWell to the Faraday cage. Only the computer monitor, and the joystick were present within the Faraday cage; the computer hard drive was situated in the adjacent room. EEG data were sampled at a rate of 1024 Hz and down sampled offline to 512 Hz. The entire experimental setup is available in Figure 2.7f. Data were monitored during collection and saved using ActiView software (BioSemi B.V., Amsterdam, The Netherlands). BioSemi electrode offset tolerance was set to a strict < 20Ω to ensure noise-free signal.

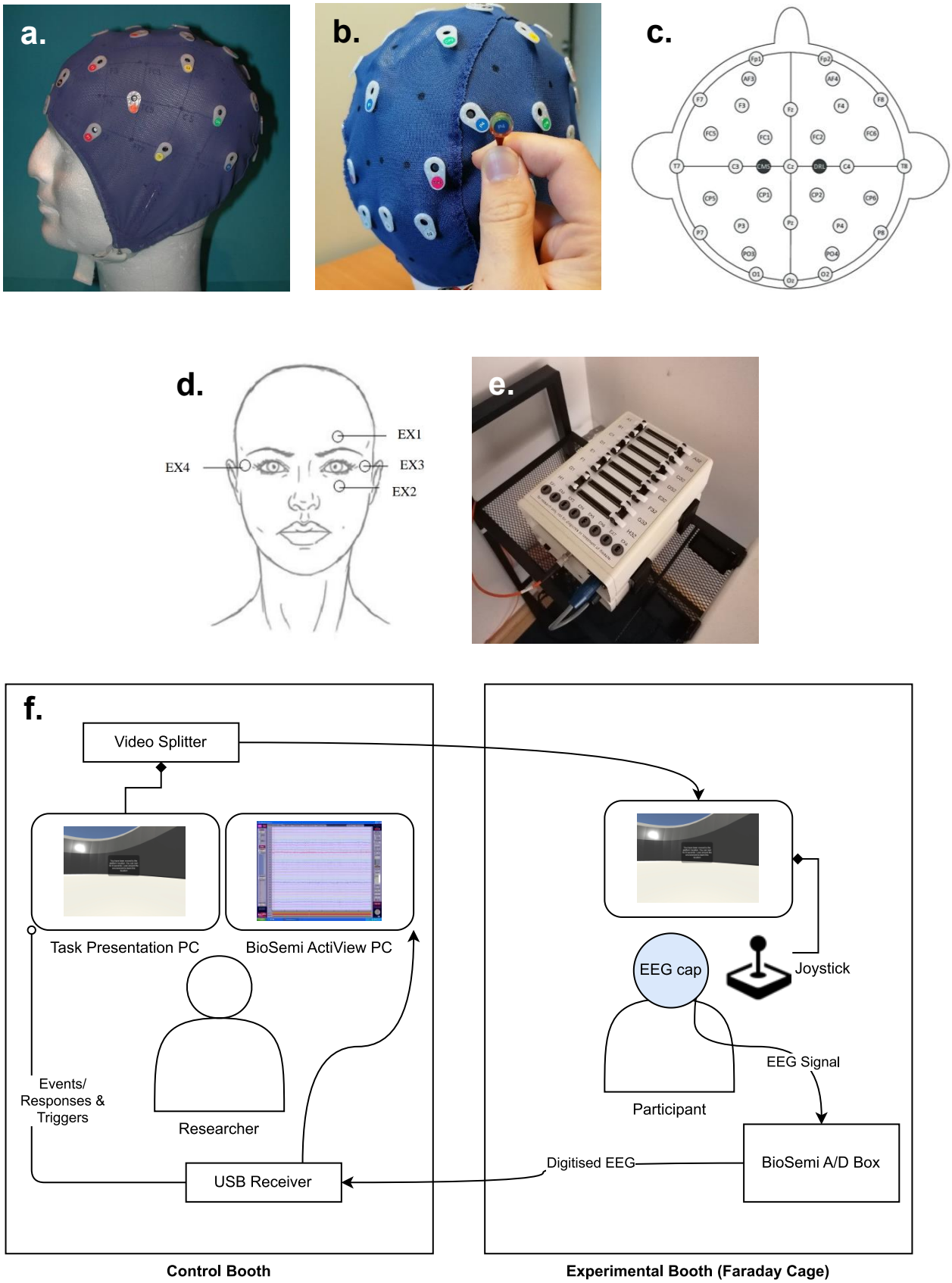


*Figure 2.7:* (a-b) The BioSemi 32-channel caps and electrodes used in the experiment. (c) BioSemi 32 electrode cap using a 10-20 layout system. Adapted from the BioSemi website: http://www.biosemi.com/pics/cap_32_layout_medium.jpg. (d) Positioning of the four EXG electrodes on the face. (e) The BioSemi ActiveTwo System A/D box used to record the EEG data. (f) The setup and design of each EEG testing booth in the EEG laboratory including the control booth (i.e. for the researcher) and the experimental booth (i.e. for the participant).

### *2.3.4 Procedure*

EEG data were collected during all experimental sessions. See Appendix A for amended standard operating procedures (SOP). Participants were seated in a comfortable chair outside of the Faraday cage in a dimly lit EEG testing room. The circumference of the participant's head was measured just above the eyebrows and over the inion at the back of the head. This circumference was used to guide selection of an appropriate cap size. The distance from the nasion to the inion was then measured in centimetres and divided by two to determine the proper location of the Vertex electrode (Cz). The cap was carefully placed on the participant's head. The chin strap was then fitted to ensure that the cap remained in a secure position. After each electrode holder was filled with gel the electrodes were attached. The participant was then moved to the Faraday cage and the electrodes were connected to the A/D box. The hardware and software mentioned previous was now setup for use. Using the ActiView software the trace for each electrode was examined to check for impedance (< 20 Ω). Once any problems with high offset or excessive noise where rectified testing began. Participants were made aware of artefact-related problems induced by blinks, other facial movements, head, and neck movements and the importance of keeping their feet rested flat on the floor. They were asked to keep such movements to a minimum and could request a break at any point.

#### *2.3.4.1 COVID-19 precautions*

The SARS-Cov2 virus was first detected in Republic of Ireland in February 2020. In March 2020 the Irish government announced the closure of all education facilities. Further restrictions included the temporary closure of all non-essential services (Thornberry et al., 2022). Additional physical distancing measures were also later introduced, including a stay-at-home order (people were not to leave their homes except under necessary or exceptional

circumstances), and a travel restriction (exercise only, within 5 km of your home). These periods of 'hard' lockdown occurred between March and October 2020, January and July 2021, & October – December 2021). During this entire period, no experimental work could take place.

Some initial data were collected amid the backdrop of the COVID-19 pandemic (Chapter 3). Even when restrictions were lifted at the end of January 2022, a series of precautionary protocols were introduced to mitigate potential risks for both participants and the researcher. Upon entry and exit, participants were instructed to scan a QR code. This action directed them to a brief form where they provided contact information and noted their entry and exit times. This form was for the purpose of contact tracing. Throughout the study, participants and researchers were required to wear face coverings. Additionally, researchers wore gloves when handling equipment. Used EEG caps were cleaned and isolated for a minimum of three days before potential reuse. All EEG equipment, computers, and shared areas underwent thorough cleaning and disinfection after each use. Interaction between participants and researchers was limited. Researchers only came into direct contact with participants during EEG setup. To view the COVID-19 Standard Operating Procedure (SOP) for EEG during the pandemic used by the lab, see Appendix A.

### *2.3.5 EEG Analysis*

All data were pre-processed and analysed using the methods discussed below. Any change to these methods was based on experimental design and was mentioned in the subsequent methods section within each chapter.

*2.3.5.1 EEG Preprocessing Pipeline*

Continuously recorded EEG data were analysed offline in MATLAB R2021B using the Brainstorm package (Tadel et al., 2011) and custom scripts when necessary. Our plan was to implement spectral analysis in the time and frequency domain, as this was the most appropriate method for the research question and experimental design. The data were first down sampled to 512 Hz. Following this, a band-pass filter containing a 1 Hz high-pass filter and a 40 Hz low-pass filter was applied. Data were visually inspected for bad segments, which were then removed if necessary. Independent Component Analysis (ICA) was performed to remove and correct artifacts, namely eye movements, blinks, and muscle artifacts. We used the EEGLAB *infomax* algorithm callable via brainstorm using the *runica* function. Within this function we correlated the ordering of individual components with patterns within the EOG signals. Components were removed based on visual inspection of topography and/or time-series and the components correlation with EOG electrodes. Bad electrodes that originated from pre-defined regions of interest were interpolated, if possible, using Brainstorm after ICA. Since we did not possess a reference electrode, we re-referenced our signal to the average of the electrodes. This is one of the better re-referencing methods, particularly when applied after ICA (de Cheveigné & Nelken, 2019; Delorme, 2023). However, in further chapters we added two mastoid electrodes to provide two possible re-referencing solutions if needed (Delorme, 2023). A more detailed rationale for certain aspects of this general pipeline (Figure 2.8) is available in the below sections.

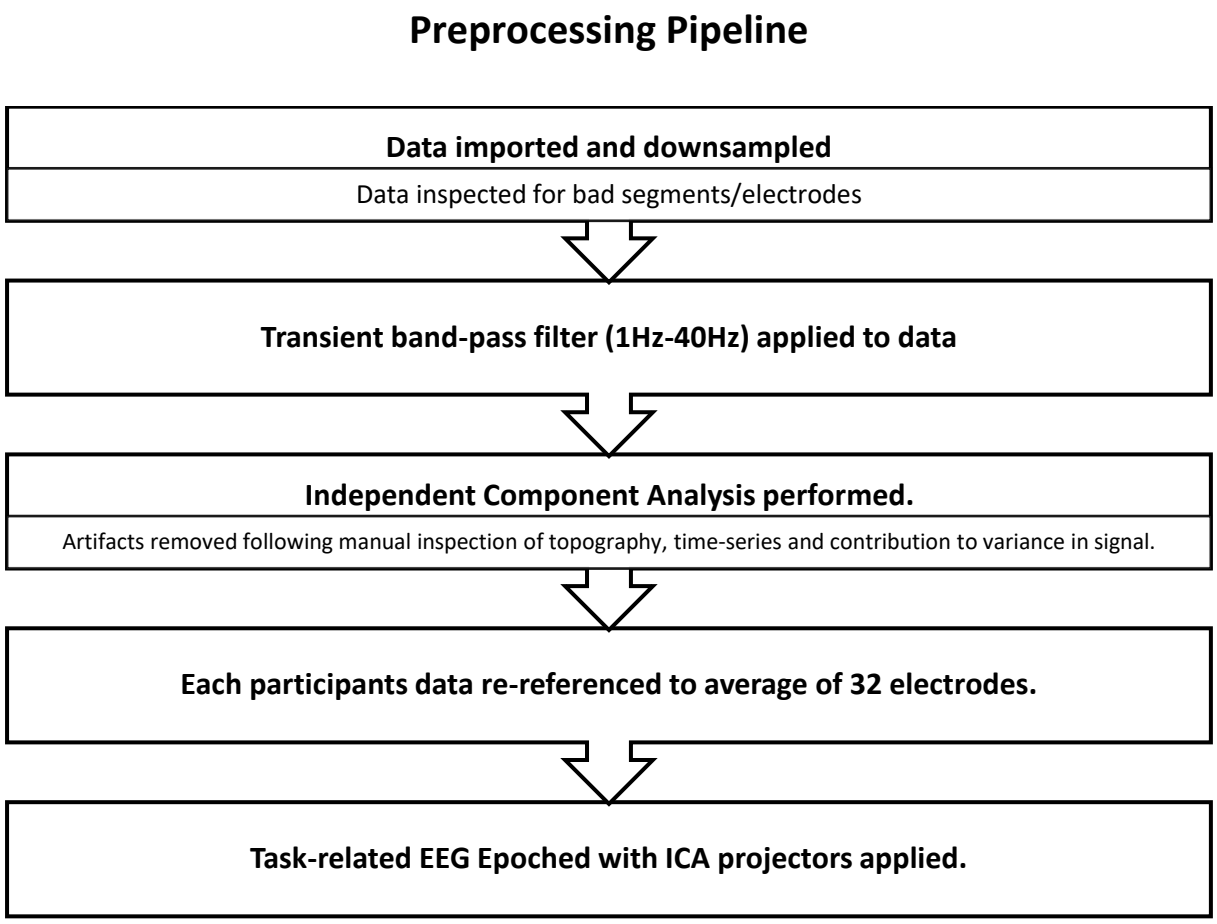


Figure 2.8: Flowchart diagram of EEG preprocessing steps performed on data.

*2.3.5.2 Band-Pass Filter Selection*

Frequency filtering is one of the most essential preprocessing steps in EEG data analysis (Cohen, 2014; McFarland et al., 1997). Filtering data can remove both high-frequency noise (e.g., above 40 Hz) or can remove slow frequency drifts (e.g., 0 Hz "DC" component). This is done through the application of either a low-pass filter for high-frequency filtering and a high-pass filter for low-frequency filtering. Based on recent research, depending on the complexity of the task different filters can have different effects, but all filters greater than 0.1 Hz and up to 1 Hz lead to a significant increase in the amount of clean and usable data (Delorme, 2023). The choice of filter should be directly related to the underlying hypothesis, paradigm constraints, the amount of expected noise and the frequency-bands of interest (Cohen, 2014).

Furthermore, line-noise from the typical electrical mains currents (~50 Hz in Europe) can require a notch filter to fix. However, applying a notch filter is not necessary with the BioSemi system. This is because of the combination of active electrodes, battery power and optic fibre data transfer. Furthermore, all experiments were run in an electrically shielded Faraday cage, meaning that there was no possible interference from the mains current and a notch filer was not necessary.

Another fundamental aspect to consider when filtering data is how they will impact the data in the time domain. Epoched data typically consist of short fragments (e.g., two second time windows) of continuously recorded EEG. These shorter epochs are incredibly susceptible to edge artifacts introduced by low-pass filters (e.g., a 0.1Hz high-pass filter can distort up to 10 seconds of data at the start of an epoch). Considering our methodology and the constraints of our task, this was an important factor to evaluate during filter design. Applying filters early on prior to epoching can help alleviate these issues (see de Cheveigné, 2019). Therefore, we implemented this in our filter design also. However, considering the continuous recording and in some instances, a lack of accurate temporal information, we concluded that a 1 Hz high-pass filter should be sufficient. This is what is typically used in the literature for EEG combined with navigation tasks (Delaux et al, 2021; Thornberry et al., 2023). Furthermore, considering we were trying to base our methodology on navigation/EEG papers available at the time of this protocol design (namely Delaux et al., 2021), we chose a 40 Hz low-pass filter, which matches with much of the literature and is useful in removing the influence of high-frequency peaks. Nevertheless, researchers face a constant battle in the design of filter definitions, with the topic seldom discussed in the rationale for most experiments.

*2.3.5.3 Bad Channel Removal and Interpolation*

The loss of individual channel data from isolated or sometimes multiple electrodes is a common occurrence in EEG research (e.g., damage to wires, insufficient gel application, poor quality contact). Bad channel removal can lead to invalid dimensions between subjects and non-strict group level analysis. Channel interpolation is a method of channel data reconstruction based on the surrounding channels, which possess very similar signals due to spatial volume conduction (Yao et al., 2019). Unfortunately, the success of interpolation algorithms is a direct function of the availability and proximity of surrounding electrodes. Interpolation will perform better and be more reliable from a 256-channel system compared to a 32-channel system, as the 256-channel system electrodes have an inherently proximal and abundant spatial layout.

Considering our low-density EEG recordings are not suited to the precision and data quantity requirements of interpolation algorithms (Dong et al., 2021), we tried not to use interpolation as a channel correction method throughout this thesis unless necessary. We only used interpolation if the channel derived from one of our pre-defined regions of interest. Otherwise, bad channels/segments were removed following visual inspection of the continuous data. When data were epoched, we ran an automatic detection tool within Brainstorm to detect and remove epochs containing bad data not identified in the continuous inspection. Bad epochs were identified using the automatic detection of voltage steps above 100 μV or peak-to-peak signal deflections exceeding 200 μV. These bad epochs were inspected visually by the researcher before confirming their removal.

*2.4.3 Independent Component Analysis*

Independent component analysis (ICA) is a model-based methodology that decomposes patterns of activity within a signal based on maximal differences in terms of time, spectral

activity and topography (Onton et al., 2006). ICA decomposes the signal into the individual sources that comprise the recorded data. Through this decomposition, the algorithm allows for the isolation and identification of noise contributing sources known as independent components (IC), as well as the IC's contribution to the overall signal. It has been shown to be incredibly useful in parsing non-brain related activity from signal and removing prominent non-brain artefacts that contribute to much of the noise in EEG data (Onton et al., 2006). One such typical non-brain artefact is eye-blinks (see Figure 2.9 for an example of this IC). If the quality of the data is good, heavy component removal is sometimes not necessary, and contributes very little to the overall final signal data (Delorme, 2023).

Considering our experimental design contains large amounts of joystick interaction, muscle movement is a likely prominent artifact in much of our recorded data. Furthermore, the continuous nature of our task would also produce more frequent blinks. We would also expect very minimal horizontal eye-movements due to the nature of the task being first-person, with head direction changed via joystick control. Though ICA can be used to divide signal into brain components that may be relevant to a task, the main aim of ICA in this thesis was to isolate and remove noise from our signal. This is a powerful method for data cleaning, but it should be noted that the manual selection and rejection of ICs can result in error. We chose the algorithm *infomax ICA* (Bell & Sejnowski, 1995) which was available in Brainstorm, had the most frequent use in the community, and most importantly has shown the best results at increasing signal-to-noise ratio in EEG setups with few channels (Rejer & Górski, 2015).

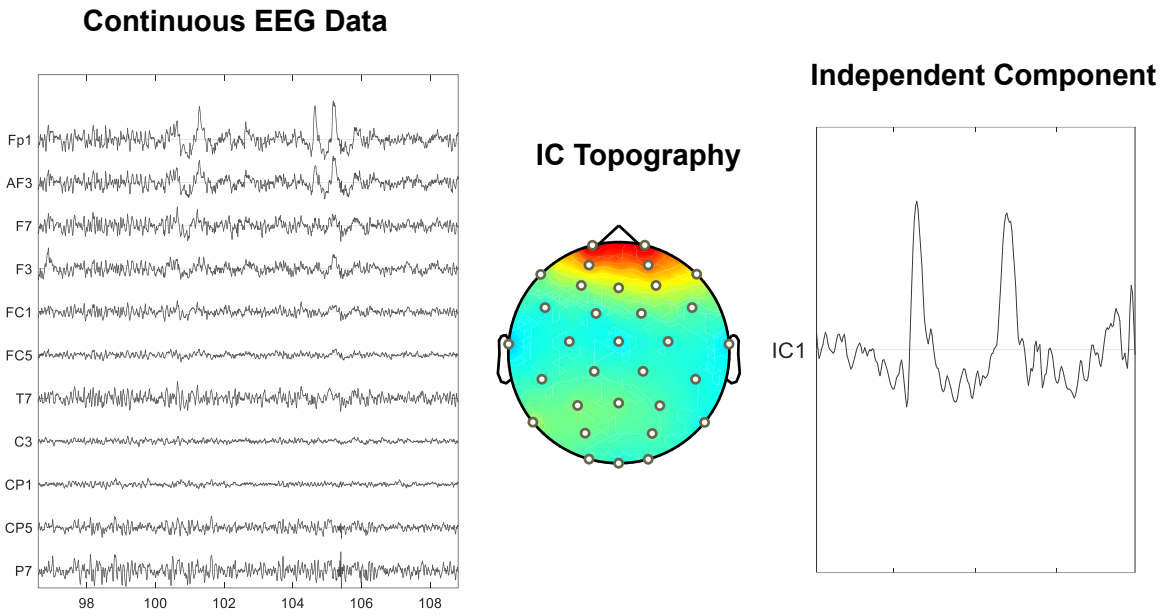


*Figure 2.9*: Independent Component Analysis decomposition of eye blinks related artifacts. The IC can be viewed in the continous data at frontal channels. The spatial (topography) and temporal (Independent Component) occurance of the IC contained within the continous signal has been decomposed into a single signal component. This data and IC have been extracted from a single-subject from Chapter 4.

### *2.3.5.4 EEG Frequency Band Analysis*

Artefact-free data were epoched for the selected time period around each analogue trigger for all trials for all participants. We chose epoch times that were sufficient to perform a good estimation of the overall power spectrum and avoid edge-effect estimation contaminations (see Gyurhovics et al., 2021 for the importance of doing this) near important behaviours (see relevant chapters for details).

For time frequency analysis (Chapter 3), we used a Morlet wavelet time-frequency analysis, with a central frequency of 1Hz & a full width half maximum time resolution of 3 seconds alongside a linear frequency definition from 1 to 30 Hz (1:1:30). A 1/f normalisation was not applied here. Instead, power was then standardised via baseline normalisation (see Chapter 3 for details) and converted to decibels (*dB*) for each individual participant. This

normalisation is done independently for each participant and electrode site. For statistical analysis outside of brainstorm, we averaged the power within each frequency band across time (we used the underlying MATLAB Fast Fourier Transform defaults available via our linear frequency definition if analysing time-frequencies). We then extracted these data for our pre-defined regions of interest (ROIs) for each individual participant.

In Chapter 3 we examined the power at our ROIs, the frontal midline (Fz, F3, F4) and the parietal midline (Pz, P3, P4) to capture activity from both the anterior and posterior parts of the scalp. Based on exploratory analysis from Chapter 4, we included the central midline (C3, Cz, C4) and the occipital midline (O1, Oz, O2), capturing activity from a broader array of scalp areas. Mean frequency band power for each participant was calculated by averaging the channels across time from each ROI, for each subject in each group. This procedure has been published (Thornberry et al., 2023) and is based on the restrictions placed on us by the experimental paradigm, and adapted versions of other researchers attempts to analyse behaviour-specific EEG during navigation (Nishiyama et al., 2002; Delaux et al., 2021; Jabès et al., 2021; Lin et al., 2022; Chrastil et al., 2022).

For analysis in Chater 4-6, we calculated the power of the frequency spectrum during recall trials using Welch's method to calculate Power Spectrum Densities (PSD). Unless otherwise stated, we chose a 2 second Hanning window with a 50% overlap between segments. This resulted in a frequency resolution of 0.5 Hz, calculated using the default MATLAB Fast Fourier Transform frequency definition. We utilised relative power as we are interested in the distribution of power within the frequency bands and the relationship between frequency bands, between the groups. Additionally, this calculation generated better between-group comparable data that is standardised and accounted for slow-drifts, artifacts and noise that may influence between-group analysis. The two groups may also have differing overall levels of absolute power and therefore relative power provides a correction for this (see Jabes et al., 2021, for

further information). Absolute power calculations also may give rise to inconsistencies across experiments compared to relative power calculations (Wang et al., 2013). Given the extremely large quantity of analysis expected, it was decided that relative power would be used throughout the thesis. Limitations that are caused by the implementation of this are discussed in Chapter 7. For the calculation of relative power (e.g., Chapter 4-6) we divided PSD output by the sum PSD from all bins for each frequency band within 0 and 40 Hz at each electrode (using the *spectrum correction* function within brainstorm). We were careful to define frequency bands at a frequency distribution to prevent overlap in our relativity calculation.

### *2.3.5 Statistical Analysis*

Statistical analyses & visualisation of the behavioural data were performed using a combination of JASP (version 0.15) and *R* software version 4.0.2 with the tidyverse and ggplot2 package (R Core Team, 2013). Statistical exploration of the EEG data was initially run using Brainstorm in MATLAB 2021b, comprising of two-tailed independent or paired parametric t-tests with a *p*-threshold of 0.05. We corrected for multiple comparisons in EEG data using an FDR correction. This was chosen as it is more detrimental to report an effect that is not there (type I error), as opposed to missing one that is (type II error; see Jabès et al. (2021) for similar EEG study with the similar statistical power to our experiments). However, statistics were typically performed again on mean power of oscillatory bands across time in JASP. The power of the time-frequency calculations was used (measured in $\mu V^2$). This amplitude (the real part of the complex values produced by EEG signals) is squared to convert magnitude into power and normalised using a *dB* (decibel) standardisation:

$$dB_f = 10 \times \log_{10}\left(\frac{signal\ power_f}{baseline\ power_f}\right)$$

Power values from the frequency ( *f* ) are then converted into decibels (*dB*) relative to baseline activity for visualizations purposes. Topographies and time-frequency plots are displayed as change of *dB* converted magnitude (or amplitude: √power) or for PSD/FFT work; as magnitude and relative power (% of overall spectrum). We use this throughout to provide clarity & more interpretable plots when using statistical comparisons, as has been encouraged by other researchers (Burgess, 2019). Unless otherwise stated, all data were combined for EEG analysis. When comparing data with *post-hoc* tests in JASP, Bonferroni is preferred for main effects to strictly control family-wise error when making all possible pairwise comparisons between marginal means. But Bonferroni can be overly conservative and increases the chances of false negatives for within-subjects factors with multiple levels. Therefore, for interactions, we use a Tukey correction, as we are making focused comparisons between subsets of means and want to balance type I and type II errors. Tukey corrected *p*-values are not appropriate for repeated measures post-hoc tests (Field, 2013). In most circumstances for descriptive statistics, we reported Mean Difference (MD), Mean (M) and Standard Error of the Mean (SEM).

### *2.3.6 Ethical Approval & Participant Recruitment*

Ethical approval was sought from the Maynooth University Biomedical & Life Sciences Research Ethics Subcommittee (BSRESC) which covers all aspects of biomedical/animal/life sciences research. The first phase of the project was approved under BSRESC-2020-2392604 (younger adults only). This was then subsequently updated due to the COVID-19 pandemic under the same approval: BSRESC-2020-2392604 with an additional approval under: SRESC-2020-2409892. This was to implement the COVID-19 pandemic standard operating procedures and risk assessment for data collection during reduced restrictions (see Appendix A). Finally, the two latter parts of the project (younger & older adults) was approved under: BSRESC-2021-2453422 which covered this research until 2024 (see individual chapters for details).

Participants outlined in this thesis were recruited from Maynooth University, the Greater Dublin Area and Kildare. Participants responded to posts on social media, through email or advertisements posted around Maynooth University campus. Some participants were recruited via the Department of Psychology Participant Pool (Module Codes: PS256, PS260, PS648, PS656). Participants were given course credit for participation, participants who did not complete participation or were not eligible to participate could submit a written assignment in lieu of participation.

For all experiments, participants were briefed on the nature of the experiment. They were told we were examining the brains electrical activity underlying learning and recall in humans using a task that depends on navigation and recall of a learned environment. They were given a full brief about the nature of EEG data collection (e.g., gel, washing facilities, non-invasive methodology) as well as instructions on the controls of NavWell. They were given an information sheet (see Appendix B) with more precise detail about the experimental paradigm. All participants were over the age of 18 and provided informed consent prior to participation. Participants were also informed that they could withdraw from the study at any time up to the point of data anonymisation. Any expression of concern about their performance of any behavioural tests or questionnaires, participants were advised to contact their general practitioner, or another medical professional. Participants were informed that none of the measures employed in this thesis were used for diagnostic purposes. Participants were fully debriefed following participation, and any questions were answered by the researcher. Further details are provided in each individual chapter.

# Chapter 3

# An investigation of theta & alpha dynamics underlying human spatial learning during navigation

**Publications Arising from this Chapter:**

The majority of the work described in this chapter has been published as:

Thornberry, C., Caffrey, M., & Commins, S. (2023). Theta oscillatory power decreases in humans are associated with spatial learning in a Virtual Water Maze task. *European Journal of Neuroscience*. 58 (8).

## Abstract

Theta (4–8 Hz) & Alpha (8–12 Hz) oscillations in humans play a role in navigation processes, including spatial encoding, retrieval, and sensorimotor integration. Increased power, particularly theta, at frontal and parietal midline regions is known to contribute to successful navigation. However, the dynamics of cortical theta & alpha and its role in spatial learning are not fully understood. This chapter aimed to investigate theta & alpha oscillations via EEG during spatial learning in a virtual water maze. Participants were separated into a learning group (n = 25) who learned the location of a hidden goal across twelve trials, or a time-matched non-learning group (n = 25) who were required to simply navigate the same arena, but without a goal. We compared both groups across all trials, at two phases of learning, the trial start, and the goal approach. We also compared the first six trials to the last six trials within-groups. The learning group showed reduced theta power at the parietal midline during the start phase, and greater reduced alpha, combined with a short but evident increase in theta at both midlines during the goal-approach phase. These patterns were not found in the non-learning group, who instead displayed greater theta & alpha power at both regions during the trial start, and at the parietal region during goal approach. We suggest our findings provide novel evidence for a link between efficient learning and theta/alpha oscillations in humans. Our theta results support the theory that this rhythm plays a crucial role in spatial encoding during exploration, as opposed to sensorimotor integration. Results found in alpha are discussed in terms of their contribution to spatial attention & sensorimotor planning during exploratory navigation.

## 3.1 Introduction

Navigation is an essential everyday skill that allows us to get to and from important locations. Spatial cognition involves combining acquired knowledge of our environment and its features, to help us plan and move through space with both ease and efficiency (Ekstrom et al., 2003; Epstein, 2008; Epstein et al., 2017). From our review in Chapter 1, theta oscillations (4-8 Hz) support successful spatial exploration but have also been argued to support sensorimotor integration during navigation (Burgess & O'Keefe, 2011; Colgin, 2020). For example, speed of travel and path distance have been shown to be related to increased theta power in both animals and humans (Bush et al., 2017; Kennedy et al., 2022; Yassa, 2018). Furthermore, bursts in theta power have been observed during navigational direction-changes (Do et al., 2021). According to Ekstrom et al. (2005) theta power changes observed in the human hippocampus are related to movement and not to learning. Theta oscillations have also been shown to have an important role in learning, particularly in spatial or episodic memory encoding and retrieval. This link has been found in several intracranial electroencephalogram (iEEG) and scalp electroencephalogram (EEG) studies with humans discussed in Chapter 1 (Bohbot et al., 2017; Buzsáki, 2005; Chrastil et al., 2022; Ekstrom et al., 2005; Kahana et al., 1999; Lega et al., 2012; Lin et al., 2017; Pastötter & Bäuml, 2014). For example, Kerrén et al. (2018); Lega et al. (2012); Vivekananda et al. (2021) all report increases in low-frequency theta power that are related to successful spatial memory encoding (but see Bohbot et al., 2017). Most recently, Chrastil et al. (2022) found theta power increases relate to encoding, specifically during a decision-making phase of active exploration.

In a recent review, Herweg, Solomon, et al. (2020) explored the dynamics of these theta changes, with iEEG studies reporting theta power reductions related to successful memory encoding, whereas scalp EEG studies demonstrated increases in theta power. EEG studies focusing on navigation have also reported increased theta power oscillations during active

learning, recall, and decision-making (Chrastil et al., 2022; Lin et al., 2022; Vivekananda et al., 2021). However, decreases in theta power have also been noted during associative learning and episodic recall (Greenberg et al., 2015). For example, decreases in human hippocampal theta power have been shown to be related to improved navigation performance and successful spatial encoding (Cornwell et al., 2012; Crespo-García et al., 2016). Spatial memory formation during real-world navigation has also recently been linked to theta power decreases in humans (Griffiths et al., 2016). As concluded from Chapter 1, the dynamics of these theta oscillations during navigation are highly debated (see section 1.4.2).

Connectivity models suggest that low-frequency oscillations from the hippocampus, retrosplenial cortex and posterior parietal cortex contribute to spatial navigation and may be reflected by cortical theta (Ekstrom et al., 2017; Ekstrom et al., 2003). Therefore, studies have generally focused on theta changes in two key cortical regions, the frontal and parietal midline (Chrastil et al., 2022; Kane et al., 2019; Kaplan et al., 2014; Lin et al., 2022; Meltzer et al., 2009). These areas are known to display synchrony during encoding and retrieval of information (Fell & Axmacher, 2011). There is also supporting evidence for communication between the two regions for spatial working memory and goal directed attention via the frontoparietal network (Fellrath et al., 2016; Sauseng, Klimesch, Schabus, et al., 2005). Frontal theta increases have also been observed during recall of successful spatial information (Kaplan et al., 2014; Roberts et al., 2013) and on approach to decision-points during active exploration at the frontal midline (Chrastil et al., 2022). Chrastil et al. also found increases at the parietal midline during spatial decision-making.

From our review in Chapter 1, navigation is dynamic and trying to capture sub-second neural changes during environment exploration and encoding is extremely difficult using classic EEG methodologies (also see section 2.3.2). As such, it is important to break navigation into its component parts and investigate each separately. One good place to start is the review

by Nyberg et al. (2022) which suggests evidence for three essential phases of navigation behaviour, (1) planning and route initiation, (2) travel and (3) goal approach. Importantly, each phase has evidence of related neural networks as well as behaviours which are relatively easy to identify. Using this approach, we focused on two phases, route initiation and goal approach, in an attempt to understand the role of frontal and parietal theta oscillations (specifically 4-8 Hz) in spatial learning (De Araújo et al., 2002; Kunz et al., 2019; Sosa & Giocomo, 2021) using a virtual navigation task. As noted in Chapter 1, there is evidence of theta changes in both encoding (e.g., associative learning, episodic memory retrieval) and searching behaviours (e.g., speed, sensorimotor integration) during navigation.

In an attempt to resolve the issues highlighted in our literature review in Chapter 1, we examined whether theta changes (across frontal and parietal sites) are specifically related to learning, by comparing the difference in theta between a group that was required to learn a specific target location to a non-learning control group. The control group was time-matched to each trial but simply had to navigate an arena without a goal present, i.e., this group was exposed to the same environment for the same number of trials and time but did not learn a specific location. Furthermore, we controlled for speed of movement in both learning and non-learning groups. In addition, both groups started in the same location of the arena for each trial in an attempt to control for directionality. As a second measure of learning, we did a within-group comparison and compared the first six trials to the last six of both groups – differences in the learning group should reflect learning changes, whereas any differences seen in the control group should reflect non-learning changes, such as exploratory behaviour or attentive searching.

Therefore, we hypothesised that if the contribution of theta power is related to learning during exploration, we should demonstrate theta power differences between the non-learning and learning groups following completion of the task. However, if it is related to active

sensorimotor integration, we should show no differences between the groups. Furthermore, we hypothesised that theta power would increase in the learning group and not in the non-learning group at both regions of interest (ROI), based on previous findings. We hypothesised this would also occur within-groups, as the task is eventually learned. Additionally, we decided to run this analysis focusing on the exact same ROIs within the Alpha band (8-12 Hz). Multiple studies discussed in Chapter 1 reported that much alpha activity relates to communication with the sensorimotor cortex (Babiloni et al., 2014; Hori et al., 2013; Vecchiato et al., 2015). Since the integration of information in this region plays a role in our hypothesis and alpha was another heavily debated rhythm found during human navigation (see section 1.4.3), we felt that some focus should be given towards it. As highlighted in Chapter 1, definition of the theta band can sometimes vary in animal and human studies with a large range between 1 – 12 Hz (Buzsáki, 2002; Buzsáki & Moser, 2013; Jacobs, 2014; Mao, 2023; O'Keefe & Recce, 1993; Yassa, 2018). We hope that including alpha will enhance broader translational value, enabling the application of our findings across both domains. Considering we did not control for motivation and frustration, we decided to include alpha for this reason also. We would expect to find increased alpha power in the learning group during active navigation. This prediction is based on the results and similarity to our protocol from Chrastil et al., 2022 – who recently reported strong evidence of increased alpha in active navigators during a virtual navigation task, with groups of active and passive navigators.

## 3.2 Methods

### *3.2.1 Participants*

Fifty young adults (34 females, 16 males) aged between 18 and 45 (M = 21.7, SEM = +/- 0.637) were recruited via Maynooth University Department of Psychology and externally using personal connections, flyers, and social media. The required sample size was estimated using the '*pwr*' package available in R (R Core Team, 2013). Based on typical sample sizes in similar EEG studies (Chrastil et al., 2022; Do et al., 2021) and general guidelines (Larson & Carbine, 2017), we calculated the minimum number of participants required with a Cohen's *d* of 0.8 and a power of 80% at an alpha level of 0.05. The sample size estimated for the non-learning and learning groups was 25.5/group (see Figure 3.1 below). All participants gave informed consent prior to starting the project and were given a full briefing of the experiment, along with the exclusion criteria. Some participants from Maynooth University received course credit.

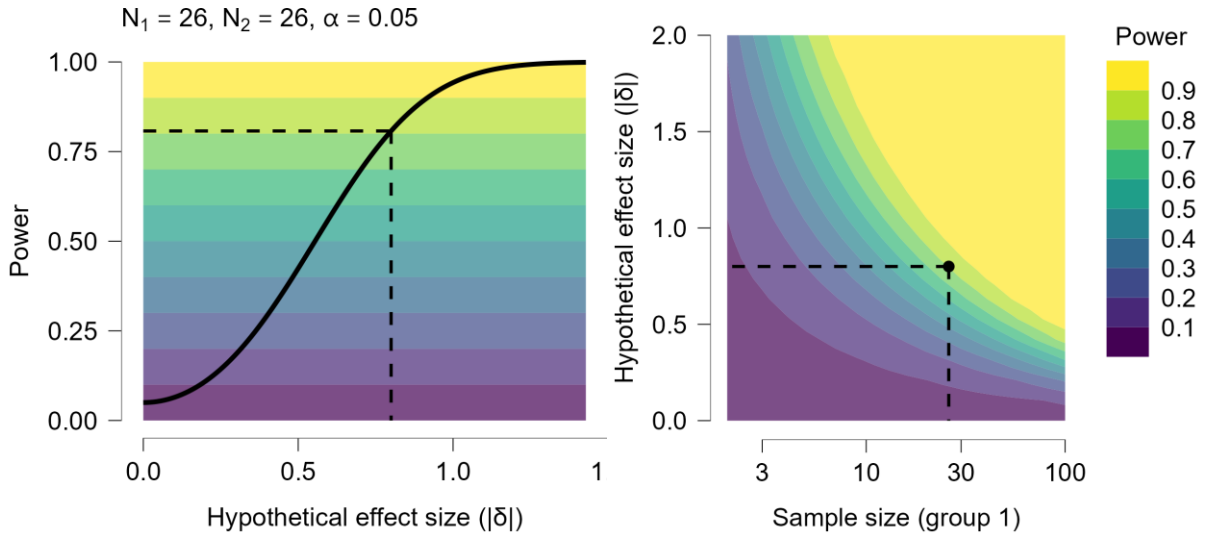


*Figure 3.1: A priori* power contour plot shows how the sensitivity of the test changes with the hypothetical effect size and the sample sizes in this design. As we increase the sample sizes, smaller effect sizes become reliably detectable (Left). A power curve displaying the sensitivity of the test, obtaining sample sizes of 26 in each group would be sufficiently sensitive (power >0.8) to effect sizes of |δ|>0.792 (Right).

Due to technical failure (2) or low recording quality resulting in excessive noise (1), the EEG epochs of 3 participants (learning group) were excluded from the associated analyses. This project and the use of human subjects with EEG was approved by the Maynooth University ethics committee (BSRESC-2021-2453422). A sample of participants (n = 32) were tested using several neuropsychological assessments to ensure that both learning (n = 7) and non-learning (n = 25) groups were cognitively matched (see section 2.1). Note the lower sample number in the learning group was due to Covid-19 restrictions at the time. Some learning participants had been tested in early 2020, from which neuropsychological assessment data was ascertained. Following the return of restricted testing, the urgent requirements to collect data, and the shorter exposure time to participants in the lab during early days, we could not facilitate these assessments for all participants. Non-learners were collected after the learning group during reduced periods of COVID restrictions. The tasks consisted of the National Adults Reading Test (NART; Nelson and Willison (1991); the Trail Making Test (TMT; Army Individual Test Battery, (1944); Reitan & Wolfson (1992) and The Montreal Cognitive Assessment (MoCA) to examine executive functioning, memory, and attention in one short sitting (see Chapter 2, section 2.1 for specific details).

### *3.2.2 Spatial Navigation Task*

After the electrophysiological preparation (see Chapter 2, section 2.3.4 for specific details), participants were seated 50 cm from the LCD computer screen on their own in a darkened, electrically shielded and sound-attenuated testing cubicle (150 cm × 180 cm) with access to a joystick for navigating. The spatial navigation task used was NavWell (see Commins *et al.* (2020) and Chapter 2, section 2.2 for in-depth details). In brief, the virtual maze consisted of a medium circular environment (taking 15.75s to traverse the arena, calculated at 22.05Vm). Two cues were used and were located on the wall of the arena: a yellow square (northeast

quadrant wall) and a light of 50% luminance (Figure 3.3a). A square goal was hidden in the middle of the northeast quadrant and was 15% of the total arena size and consisted of a bright blue square that only became visible when the participant crossed it (northwest quadrant wall, see Figure 3.3b).

All participants underwent 12 trials from pseudorandom starting positions around the arena (N, S, E & W), with a maximum of 60 seconds/trial to locate the goal. Participants were transported to the location of the goal if they failed to locate it. There was a 10s inter-trial interval between each trial. The goal remained in the same location throughout (centre of NE quadrant). Participants were randomly assigned to either a learning group (who were required to learn the location of a hidden target across 12 trials, n = 25), or a non-learning group (who were required to navigate around the same arena for 12 trials, but without the presence of a goal; each trial was time-matched to the group-mean latency of each trial reported by the learning group, n = 25). This meant that the learning group data were collected first and non-learning group trials ended after a set time, rather than 60 seconds. Latency (time taken to locate target or complete trial; measured in seconds), path length (distance travelled in virtual metres [Vm]) and percentage time spent in goal quadrant are typical measures of water maze performance (see Vorhees and Williams (2014a)). These were recorded for each participant during each trial by NavWell (see also Commins *et al.*, 2020; Chapter 2).

### *3.2.3 EEG Recording*

EEG data was acquired using a BioSemi ActiveTwo system (BioSemi B.V., Amsterdam, Netherlands) providing 32 Ag/AgCl electrodes positioned according to the 10/20 system during NavWell. Analogue event signals were sent during three time-points of each trial: (1) when participants began their trial, (2) when they reached the goal and (3) when their ITI (Inter Trial Interval) ended. BioSemi designed caps using the 32-electrode international 10-20 layout

were also used. The recording system was stored in the same room, and participants were seated during navigation and data were recorded continuously. A PC running the ActiView software (version 7.05) was positioned in the room adjacent to the experimental cubicle, for constant monitoring of the EEG recording. Participants were instructed to relax and move as little as possible. Four electrodes (EXG1 - EXG4) were positioned on the face to monitor eye movements and blinks. Raw EEG data were sampled at 1024Hz but were down-sampled offline to 512 Hz.

### *3.2.4 EEG Pre-Processing*

Continuously recorded EEG data were analysed offline in MATLAB R2021B using scripts within the Brainstorm package (Tadel et al., 2011). A 1 Hz high-pass filter and a 40 Hz low-pass filter was applied. Data were visually inspected for bad segments and bad electrodes, which were then removed. Independent Component Analysis (ICA) was performed to remove and correct artifacts, namely eye movements, blinks, and muscle artifacts. We used the EEGLAB infomax algorithm callable via brainstorm using the *runica* function. Bad electrodes that originated from pre-defined regions of interest were interpolated (1), if possible, using Brainstorm after ICA. EEG data were then referenced to the average of the 32 electrodes. For further information on EEG pre-processing see Chapter 2 section 2.3.4 for specific details.

### *3.2.5 EEG Frequency Band Analysis*

We investigated two frequency bands of interest: theta (defined as 4-8 Hz) and alpha (defined as 8-12 Hz). The frequency band definitions are based on previously discussed literature in the introduction and the rationale described in Chapter 2. Artefact-free data were then epoched around each analogue trigger for all 12 trials for all fifty participants. For analysis of the trial

start, we used -500ms and +2000ms. We then used -2000ms before and +500ms marker for the goal trigger. We chose these epoch times as we believe it was sufficient to perform a good estimation of the overall power spectrum and avoid edge-effect estimation contaminations near important behaviours. Additionally, we also used -1000ms to -500ms before the start of the trial as a baseline. During this time, all participants were sitting still waiting to start their next trial, irrespective of their group. To not contaminate our baseline with edge-effects, the full time epoched at the trial start was -1500ms to +2000ms. The initial 500ms was to adjust for edge-effect contamination (see Gyurkovics *et al.* (2021) for the importance of doing this), the baseline was then calculated for the following 500ms, then we examined the remaining -500ms before the trigger, which was *included* in the analysis to allow for some error/time-lag in the temporal accuracy for behaviours. This was a precautionary approach due to the relatively manual assignment of the event triggers for this experimental procedure. These data were included in the analysis to ensure possible behaviours of interest were not missed due to a delay in sending the tigger to the BioSemi system. The same baseline was used to standardise each participant's goal-approach epoch as well (see Figure 3.2).

Each participant's start epoch and goal approach epoch were extracted from all 12 trials in each condition. This provided a total of near 600 epochs per condition, 300 per phase. We used a Morlet wavelet time-frequency analysis, with a central frequency of 1 Hz & a full width half maximum time resolution of 3 seconds alongside a linear frequency definition from 1 to 30 Hz (1:1:30). A 1/f normalisation was not applied here. Instead, power was then standardised via baseline normalisation and converted to *dB* for each individual participant. This normalisation is done independently for each participant and electrode site. For statistical analysis outside of brainstorm, we averaged the power within each frequency band across time (using the underlying MATLAB Fast Fourier Transform defaults available via our linear frequency definition), then extracted these data for our regions of interest (ROIs) for each

individual participant. We examined the power at our ROIs, the frontal midline (Fz, F3, F4) and the parietal midline (Pz, P3, P4) to capture activity from both the anterior and posterior parts of the scalp. Mean theta & alpha power for each participant were calculated by averaging the channels across this time from each ROI, for each subject, in each group.

### *3.2.6 Statistical Analysis*

Statistical analyses & visualisation of the behavioural data were performed using a combination of JASP (version 0.15) and R software version 4.0.2 with the tidyverse and ggplot2 package. Statistical exploration of the EEG data was initially run using Brainstorm in MATLAB 2021b, comprising of two-tailed independent or paired parametric t-tests with a *p*-threshold of 0.05. We corrected for multiple comparisons in EEG data using an FDR correction. This was chosen as it is more detrimental to report an effect that is not there (type I error), as opposed to missing one that is (type II error; see Jabès et al. (2021) for similar EEG study with the same statistical power). However, statistics were then performed again on mean power of the oscillatory bands across time in JASP. For statistical analysis in JASP, the power of the time-frequency calculations was used ($\mu V^2$) and normalised using a *dB* (decibel) standardisation (10 * log10(x / μ). Topographies and time-frequency plots are displayed as change of *dB* converted magnitude (or amplitude: √power) in this chapter to provide clarity & more interpretable plots when using statistical comparisons (see Chapter 2). All data were combined for EEG analysis.

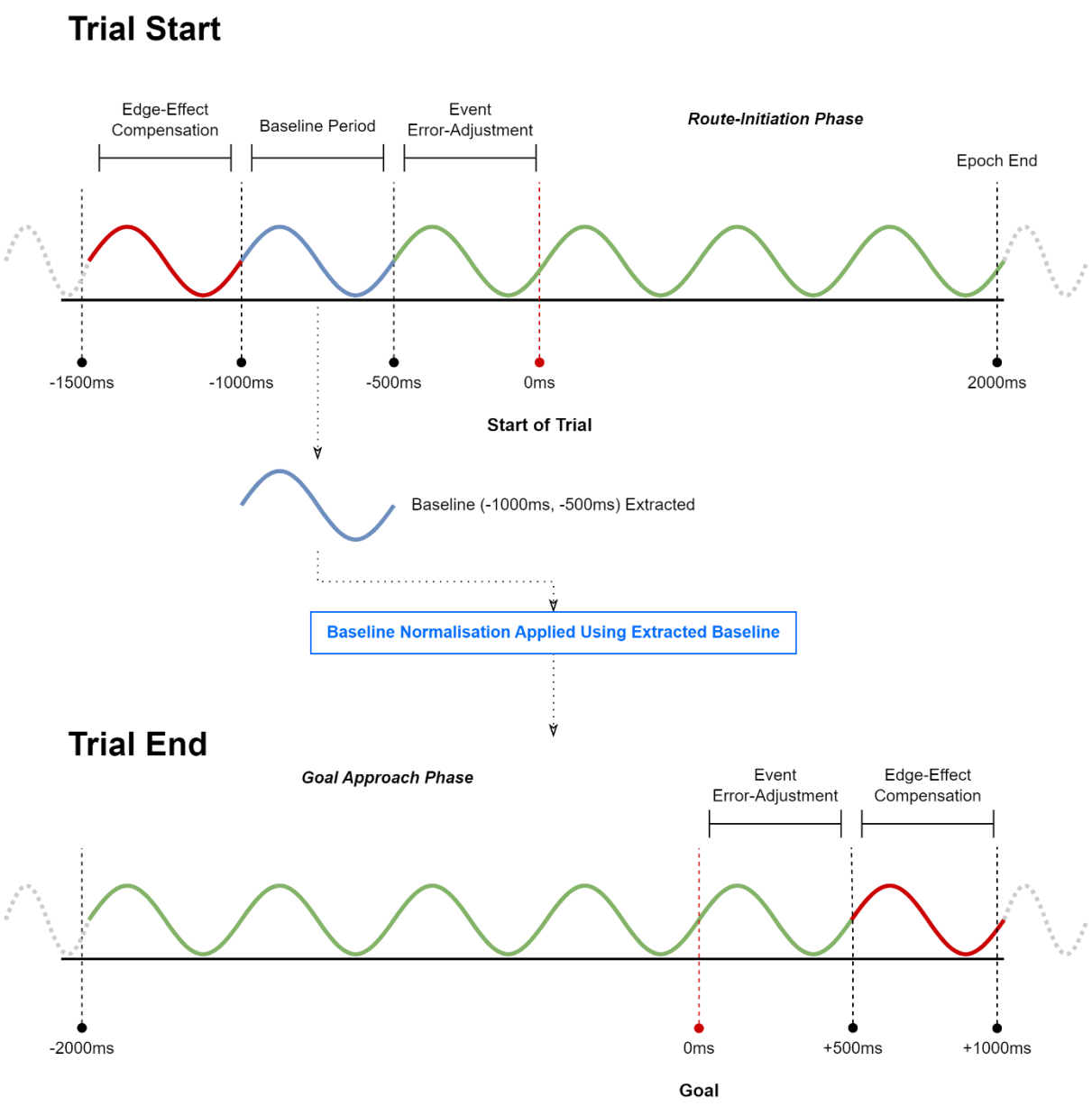


*Figure 3.2:* Diagram displaying the EEG data analysis and baseline normalisation process for each participant. The baseline was extracted from the start of the trial and normalised to the route-initiation phase data. This extraction was then used on the data at the end of a trial, to normalise the goal-approach phase data. Green is used to denote the analysed data, red is used to denote discarded data for edge-effect compensation, and blue is used to illustrate the baseline.

## 3.3. Results

### *3.3.1 Behavioural Results*

Initially, we compared both groups' scores on a variety of cognitive tests to ensure that both groups were generally cognitively matched. There were no significant differences between the two groups on the number of NART errors ($t(30) = 0.36, p = 0.721$), total time taken to complete the TMT ($t(30) = 0.448$, $p = 0.657$) and scores on the MOCA ($t(30) = -0.445$, $p = 0.659$). In addition both groups were well matched for age ($t(48) = -0.845, p = 0.402$). Gender differences were not the focus of this study, but there are some known gender differences in both navigation performance and theta power (Astur et al., 1998; Pu et al., 2020). Although the NavWell software seems to eliminate this effect (see Commins et al., 2020). However, just to confirm this, gender was included in the analysis of latency and EEG below.

We next analysed performance of the learning group on the virtual water maze task. The task latency of participants during the acquisition phase was analysed using a 2 (Gender) X 12 (Trials) mixed-factorial ANOVA. Mauchly's test of sphericity indicated that the assumption of sphericity was violated ($p < 0.05$) and a Greenhouse-Geisser sphericity correction was applied to the model. This was applied throughout this section where assumptions were violated. Latency was defined by the amount of time it takes a participant to find the target (with a maximum of sixty seconds). There was an overall significant decrease in latency across all participants for the 12 trials ($F_{(4.15, 48)} = 14.933$, $p < 0.001$, $\eta^2 = 0.338$). Tukey-corrected t-tests revealed that participants were significantly ($p < 0.001$) faster at locating the target on Trial 12 (M = 7.44s, SEM = +/- 0.96s) compared to Trial 1 (M = 36.88s, SEM = +/- 3.95s) and Trial 2 (M = 27.32s, SEM = +/- 4.22s). All participants in the learning group successfully learned the task, reducing their times across trials (see Figure 3.3c). There was no difference in latency between Gender ($F_{(1, 23)} = 1.78$, $p = 0.195$, $\eta^2 = 0.007$). Likewise, no Trial X Gender interaction effect ($F_{(4.15, 95.46)} = 1.98$, $p = 0.101$, $\eta^2 = 0.045$) was reported.

Latency was not analysed for the non-learning group, as they were time matched to the learning group in order to have comparable EEG trial lengths.

The percentage of time spent in the goal quadrant was used as a measure of spatial learning (Barnhart et al., 2015; Vorhees & Williams, 2006). We investigated differences from trial 1 to trial 12 across groups. Trial 1 should capture searching in both groups, and Trial 12 should capture goal-directed searching in our learning group. We ran a 2 (Group) X 2 (Trial) mixed-factorial ANOVA to investigate this. We report a main effect of Trial ($F_{(1, 48)} = 58.212$, $p < 0.001$, $\eta^2 = 0.272$). We report a significant between-groups difference in percentage time ($F_{(1, 48)} = 11.098$, $p < 0.002$, $\eta^2 = 0.062$). We also reported an interaction effect for Trial X Group ($F_{(1, 48)} = 36.933$, $p < 0.001$, $\eta^2 = 0.173$). Independent samples t-tests revealed that the learning group display significantly ($t(48) = 4.95$, $p < 0.001$) higher percentage time searching in the goal quadrant on Trial 12 (M = 79.2%, SEM +/- 0.31%) compared to the non-learning group (M = 38.1%, SEM +/- 0.77%, Figure 3.3d).

Although the non-learning group was matched to the learning group in terms of the number of trials and duration of each trial, path length may have differed between the two groups. Path length during learning was analysed using a 2 (Group) X 12 (Trials) mixed-factorial ANOVA. There was significant main effect for path length across all participants for the twelve trials ($F_{(3.3, 161.7)} = 86.33$, $p < 0.001$, $\eta^2 = 0.536$), with shorter path lengths on trial 12 compared to trial 1 ($p < 0.05$, Figure 3.3d). We also reported a significant difference between the two groups on path length ($F_{(1, 48)} = 86.932$, $p < 0.001$, $\eta^2 = 0.096$). Additionally, we reported a significant Trial X Group interaction effect ($F_{(3.3, 161.7)} = 86.33$, $p < 0.04$, $\eta^2 = 0.017$). Tukey-corrected t-tests reveal that the groups did not differ in path length at Trial 1 ($t = -1.769$, $p = 0.983$) but differed in later trials, e.g., Trial 6, Trial 9 & Trial 11 (all $p < 0.001$; MD = -54.329 Vm, -54.904 Vm & -54.848 Vm respectively). The non-learning group demonstrate longer path lengths than the learning group, possibly related to random searching behaviour.

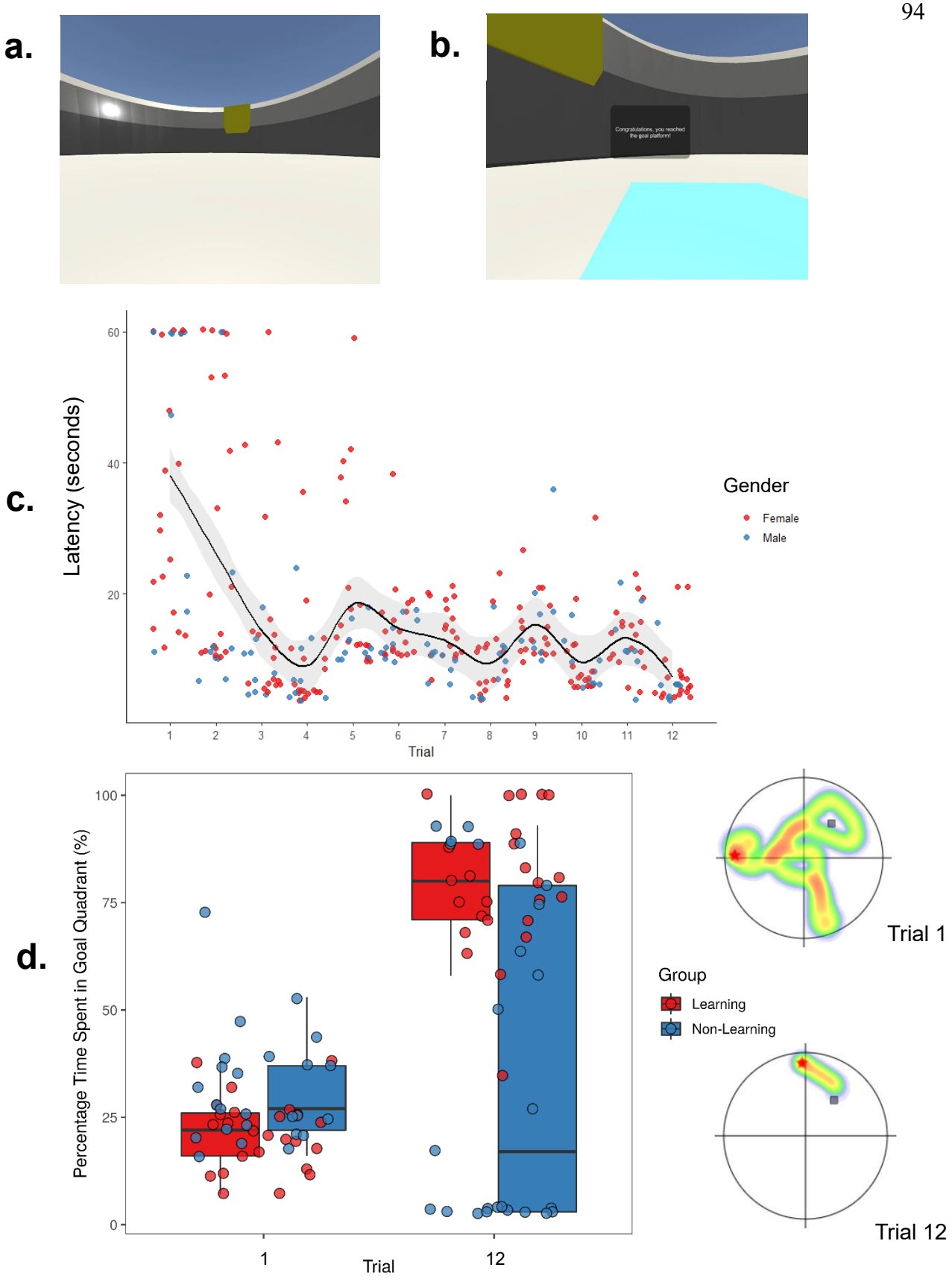


*Figure 3.3a:* Screenshot of the NavWell environment used in this experiment, with light & square cues on the wall of the environment. *Figure 3.3b:* NavWell goal becomes illuminated when a participant walks over it, "congratulations, you reached the goal platform!" message displayed. *Figure 3.3c:* Plot of task latencies (in seconds) across the twelve trials for learning group, split by gender. The mean time for each trial is denoted by the line along with standard error denoted by the shaded region around the line. *Figure 3.3d:* Box plots and individual data points for each groups participants percentage time spent searching in the target quadrant for trial 1 and trial 12. Diagrams of the water maze arena on the right side demonstrate heat maps of where learning participants spend most of their search time, during trial 1 and trial 12.

### *3.3.2 EEG Results*

#### *3.3.2.1 Trial Start/Route Initiation Phase*

We hypothesized that any changes in power related to spatial learning and our navigation task would occur at our ROIs, the frontal midline and parietal midline. However, we first carried out an exploratory analysis. We isolated our two frequency bands of interest, Theta (4-8 Hz) and Alpha (8-12 Hz). We investigated these frequency bands in each participant's trial epochs, one from each of the trial phases (as previously defined by Nyberg et al. 2022 – route initiation/trial start and goal approach/trail end). This resulted in twelve start epochs and twelve end epochs per participant which were averaged at the group-level for each phase. We then ran a parametric independent *t*-test between conditions (Learning/Non-Learning) with an alpha level of 0.05. We then corrected for multiple comparisons using an FDR correction across signals. Below, we see that the learning group show significantly less theta power at the Pz site during the task compared to the non-learning group. Additionally, the learning group demonstrate significantly reduced alpha power throughout the task at electrode sites PO3, PO4, O1, O2, Oz & AF4 (see Figure 3.4 below). Interestingly, it suggests that lower theta power at the parietal region (Pz) and lower alpha power at posterior parts of the scalp may be markers of spatial learning. However, the dynamics of these frequency bands are unclear. Additional analyses were required to investigate this further.

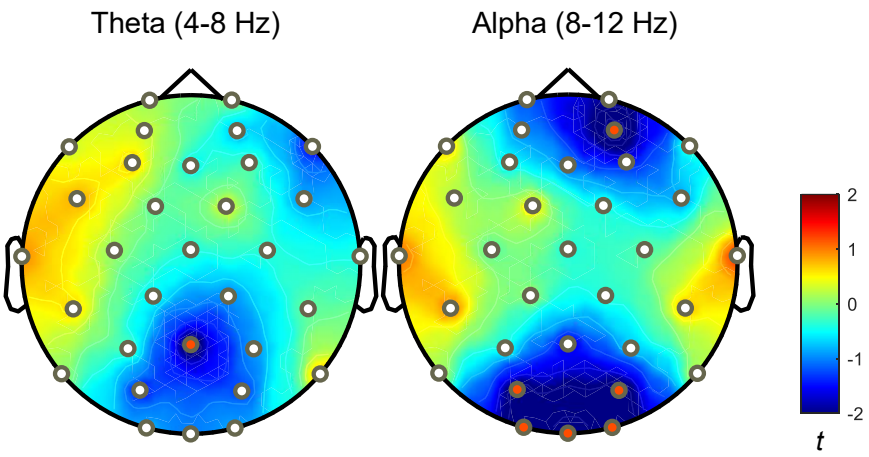


*Figure 3.4*: Topographical plots of activity from an FDR-corrected independent sample t-tests comparing the two conditions/groups Learning to the Non-Learning group. All significant electrodes at $p < 0.05$ are highlighted in red. The scale is presented in t-values.

Focusing on our two ROIs and mean theta power at each trial, we employed a 2 (Group) X 2 (Gender) X 12 (Trial) mixed-factorial ANOVA to compare theta between groups (Non-Learning and Learning) across the full epoch (-500ms before and 2000ms after participants started the trial) for each ROI. The data did not violate the assumptions of homogeneity, nor did they violate sphericity assumptions, therefore no correction was applied.

At the **frontal midline**, for theta power, there was no main effect for Trial ($F_{(11, 484)} = 1.005$, $p = 0.170$, $\eta^2 = 0.017$). There were no significant between-subjects effects for group or gender ($F_{(1, 44)} = 0.185$, $p = 0.669$, $F_{(1, 44)} = 0.612$, $p = 0.438$ respectively). However, there was a significant Trial X Group interaction effect ($F_{(11, 484)} = 2.086$, $p = 0.020$, $\eta^2 = 0.025$). Tukey corrected t-tests however revealed no group differences at any of the trials. There was also a significant Trial X Gender interaction effect ($F_{(11, 484)} = 2.636$, $p = 0.003$, $\eta^2 = 0.032$). Corrected *t*-tests did reveal that Males had significantly reduced theta power on Trial 12 compared to Trial 1 ($t = -2.001$, $p = 0.015$, MD = -0.056). For alpha, the data violated sphericity assumptions. Therefore, a Greenhouse-Geisser correction was applied to the model. We revealed no significant main effect of Trial ($F_{(7.4, 327.5)} = 1.041$, $p = 0.403$) nor any differences between

Genders or Groups ($F_{(1, 44)} = 0.134$, $p = 0.716$ & $F_{(1, 44)} = 0.559$, $p = 0.459$ respectively). We also reported no significant interaction effects ($F_{(7.4, 327.5)} = 1.157$, $p = 0.326$ & $F_{(7.4, 327.5)} = 1.143$, $p = 0.335$ respectively).

For **parietal midline** theta, there was no significant main effect of Trial ($F_{(11, 484)} = 0.998$, $p = 0.447$). There was also no significant difference in parietal midline theta between Genders ($F_{(1, 44)} = 3.890$, $p = 0.055$) nor Groups ($F_{(1, 44)} = 2.258$, $p = 0.140$). Additionally, there was no significant interaction effect for Trial X Group ($p = 0.457$) nor Trial X Gender ($p = 0.189$). For alpha, there was a significant main effect of Trial ($F_{(11, 484)} = 2.256$, $p = 0.011$, $\eta^2 = 0.023$). Tukey-corrected post-hoc t-tests revealed that there was a significant *increase* in alpha power across participants from Trial 1 & Trial 3 (M = 0.134, SEM = 0.009; M = 0.133, SEM = 0.011) to Trial 12 (M = 0.16, SEM = 0.011; $p = 0.013$). There were also no significant interaction effects for Trial X Gender ($F_{(11, 484)} = 1.373$, $p = 0.182$) nor Trial X Group ($F_{(11, 484)} = 0.626$, $p = 0.807$). There were also no significant differences between Genders ($F_{(1, 44)} = 0.385$, $p = 0.538$) or Groups ($F_{(1, 44)} = 1.603$, $p = 0.212$).

Further informed observations based on our time-frequency maps (Figure 3.5) and averaged frequency bands (Figure 3.6) to investigate the specificity of theta power, suggest that frontal midline theta decreases appear greater in the non-learning group than in the learning group, particularly at the lower frequencies (Figure 3.5, upper). The observed burst in theta power around the trial start (0ms – see Figure 3.6a & 3.6b) appears weaker in the learning compared to the non-learning group. A decrease can also be observed in parietal midline theta in the learning group compared to the non-learning group throughout this phase. This would be expected, as decreased theta reached statistical significance at the Pz site. We typically observe a reduction in theta at the parietal midline during spatial learning, with lesser reductions at the frontal midline.

Very little variation can be observed between the groups in the alpha frequency range at the frontal midline (Figure 3.5 lower). However, it is clear that the learning group have decreased alpha power at the parietal midline around the trial start (0ms – see Figure 3.6c). These observations are expected based on alpha differences reaching statistical significance at the Pz site. Interestingly, much of the posterior part of the scalp displays significantly decreased alpha power (see Figure 3.4). It is possible that further neural dynamics at play in the alpha band, perhaps not captured at the parietal midline.

# Route Initiation Phase

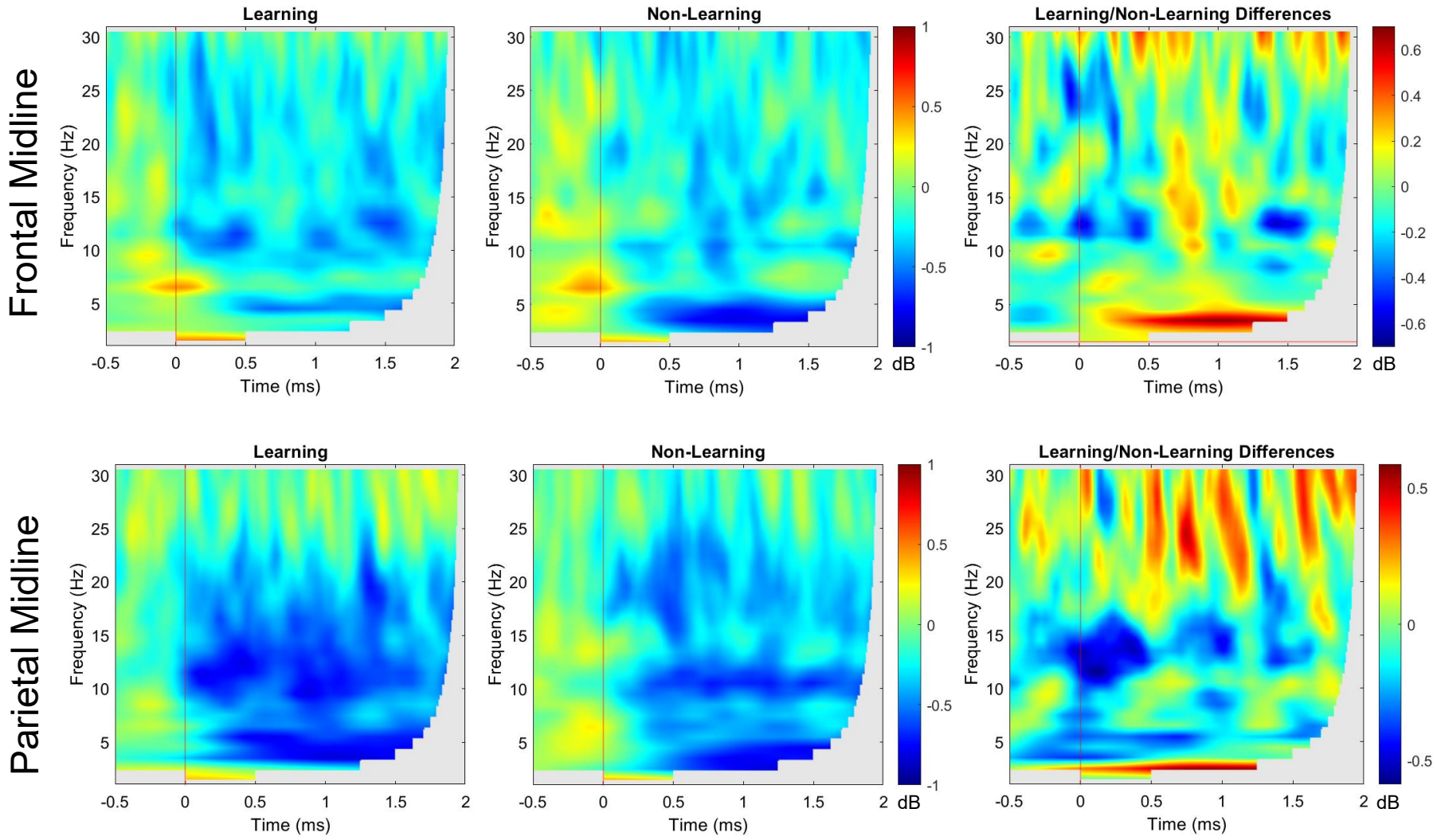


*Figure 3.5:* Time-frequency plots showing oscillatory power (1-30 Hz) differences between each group at each ROI. Displayed as baseline-normalized dB change. The line at 0ms marks when the trial started. The grey area after 1.5s is removed due to edge-effect contamination.

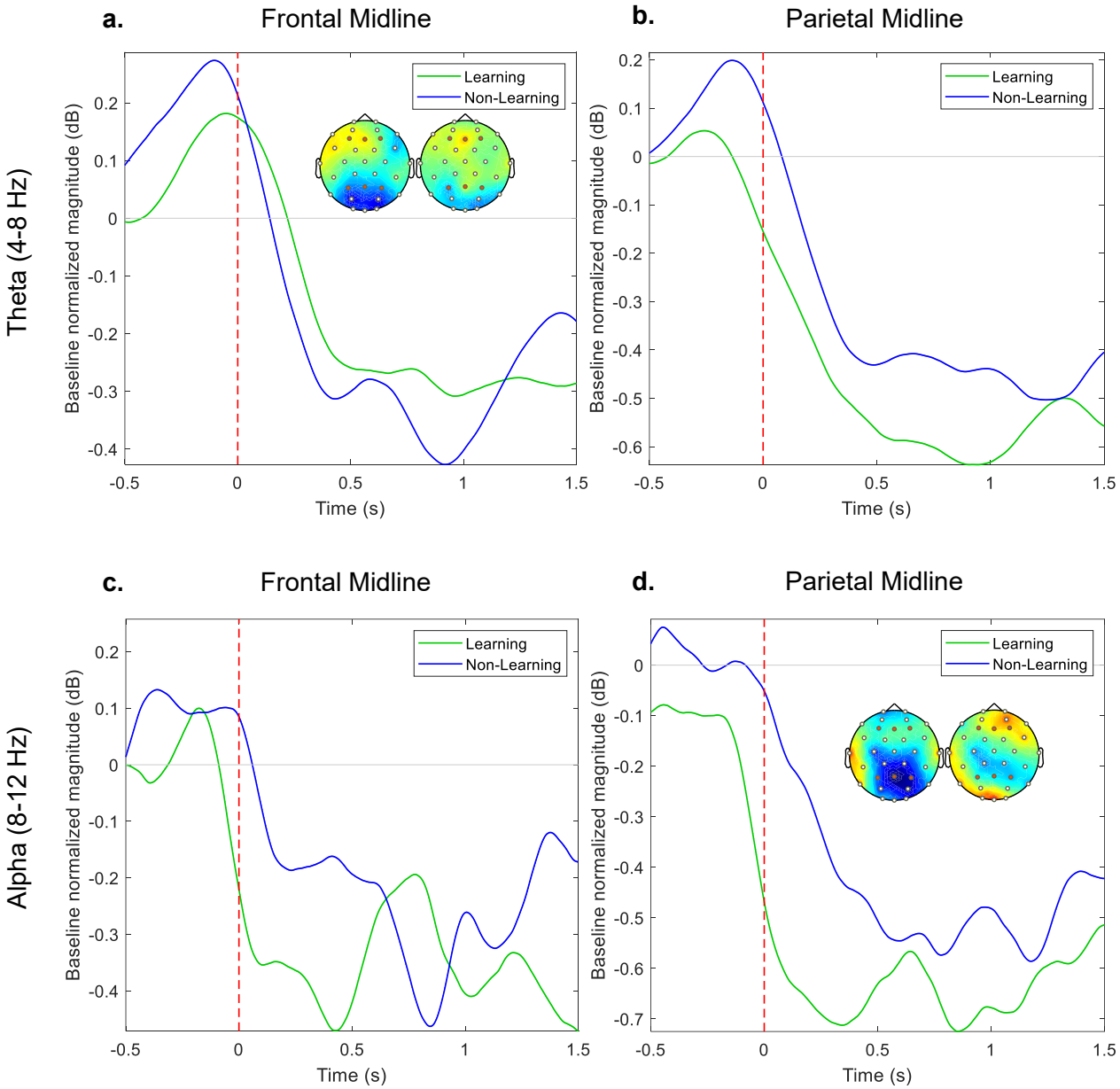


*Figure 3.6:* Time series plots of each epoch displaying normalized magnitude (dB) for both the learning and non-learning groups. Panels a and b represent average theta power changes across time, whereas panels c and d represent average alpha power across time. Topography maps (left: Learning, right: Non-Learning) display mean theta and alpha across the averaged time of the epoch and are scaled to the accompanying time-series. Both frontal and parietal midline ROIs are represented on these topographies and are highlighted in red.

### *3.3.2.2 Trial End/Goal Approach Phase*

We next investigated the parietal and frontal midlines again, but when participants approached the goal (learning group) and the equivalent trial end (for the non-learning group). We again ran an exploratory analysis using the same procedure as above, isolating our frequency bands of interest, Theta (4-8 Hz) and Alpha (8-12 Hz). We averaged across the mean epoch time and ran a parametric FDR-corrected independent *t*-test between conditions (Learning/Non-Learning) with an alpha level of 0.05. Below, we see that the learning group and non-learning group demonstrate no significant differences in theta power during the goal-approach phase at any point on the scalp. However, we see the same posterior signals as before showing significant differences in alpha between the two groups. The learning group display reduced alpha at posterior sites (PO3, PO4, O1, Oz, O2), but also at left-frontal (AF3, F3) sites upon approach to the goal location, compared to the non-learning group at the trial end (Figure 3.7). Therefore, it seems that theta may not be on average, involved in the learning process during goal-approach. However, lower alpha power at posterior parts of the scalp and left-frontal sites may be essential for recall and memory processing as participants navigated towards the goal.

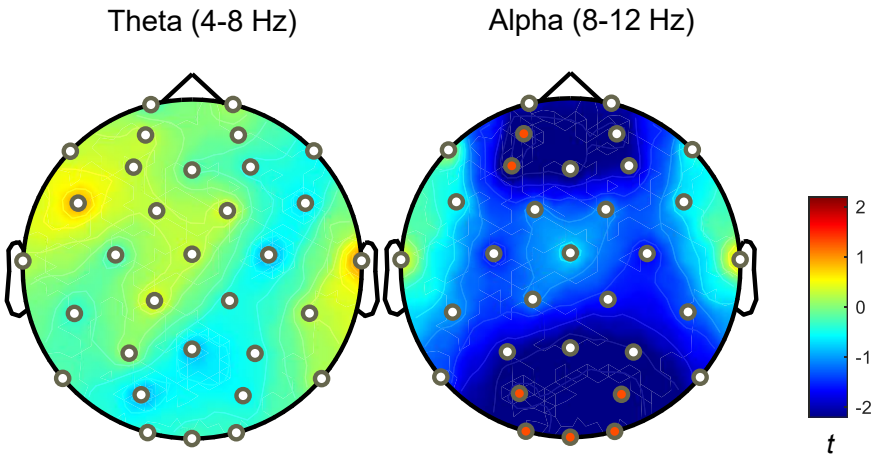


*Figure 3.7:* Topographical plots of activity from an FDR-corrected independent sample t-tests comparing the two conditions/groups Learning to the Non-Learning group. All significant electrodes at $p < 0.05$ are highlighted in red. The scale is presented in t-values.

Statistical analyses were run on our hypothesised ROIs, the frontal and parietal midline. A 2 X 2 X 12 mixed-factorial ANOVA was used to compare learning between groups (Non-Learning and Learning) across the full epoch (2000ms before and 500ms after participants reached the goal). The data did not violate the assumptions of homogeneity nor sphericity assumptions; therefore, no corrections were applied. Again, at the **frontal midline** for theta, there was no main effect of Trial ($F_{(11, 484)} = 1.162$, $p = 0.311$). There were no significant between-subjects differences reported for Gender ($F_{(1, 44)} = 0.001$, $p = 0.97$) nor Group ($F_{(1, 44)} = 0.019$, $p = 0.891$). There was also no significant interaction between Trial X Group ($F_{(11, 484)} = 0.404$, $p = 0.954$) nor Trial X Gender ($F_{(11, 484)} = 0.915$, $p = 0.525$). Nonetheless, there was a significant Trial X Group X Gender interaction effect ($F_{(11, 484)} = 2.214$, $p = 0.013$, $\eta^2 = 0.031$). However, *post-hoc* Tukey corrected t-tests revealed no significant differences at any measure (all $p > 0.9$). For alpha, we report no main effect for Trial ($F_{(8.4, 370.5)} = 0.986$, $p = 0.458$) nor any between-subjects effects for Gender ($F_{(1, 44)} = 0.263$, $p = 0.611$) nor Group ($F_{(1, 44)} = 0.011$, $p = 0.917$). There was also no significant interaction effect between Trial X Group ($F_{(8.4, 370.5)} = 0.588$, $p = 0.839$) nor Trial X Gender ($F_{(8.4, 370.5)} = 1.285$, $p = 0.238$).

At the **parietal midline** ROI, for theta, there was no main effect of Trial ($F_{(11, 484)} = 1.794$, $p = 0.052$, $\eta^2 = 0.025$). There were no significant between-subjects differences reported for Gender ($F_{(1, 44)} = 1.912$, $p = 0.174$) or Group ($F_{(1, 44)} = 0.974$, $p = 0.329$). Additionally, there was no Trial X Group ($F_{(11, 484)} = 1.101$, $p = 0.358$) nor Trial X Gender ($F_{(11, 484)} = 0.995$, $p = 0.449$) interaction effects. For alpha, we report no significant main effects for Trial ($F_{(8.3, 364)} = 0.675$, $p = 0.762$). We also reported no significant differences between Genders ($F_{(1, 44)} = 0.009$, $p = 0.926$) or Groups ($F_{(1, 44)} = 0.247$, $p = 0.622$). There were no reported significant interaction effects for Trial X Group ($F_{(8.3, 364)} = 1.152$, $p = 0.319$) nor Trial X Gender ($F_{(8.3, 364)} = 0.647$, $p = 0.788$). However, from our previous exploratory analysis, these results are not surprising, as much of the significant activity is not captured at sites belonging to our ROIs. Nevertheless,

further informed observation using our time-frequency maps (Figure 3.8) and averaged frequency bands across time (Figure 3.9) would suggest sustained decreases in both frontal and parietal midline theta as participants approached the goal location. This is followed by a burst of theta activity at the goal across a range of frequencies, especially at lower frequencies (4 Hz).

# Goal Approach/End Phase

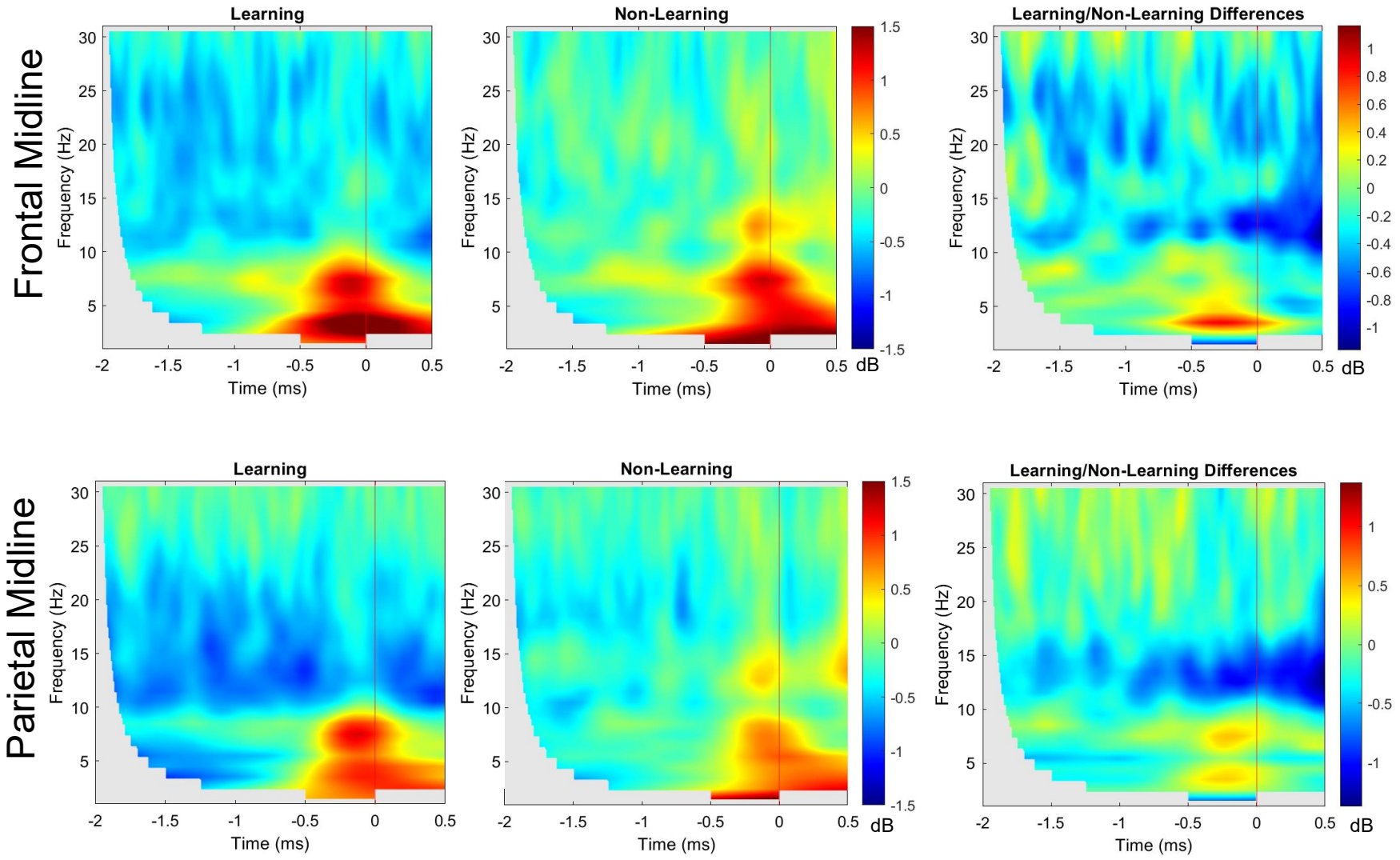


*Figure 3.8:* Time-frequency plots showing oscillatory power (1-30 Hz) differences between each group at each ROI. Displayed as baseline-normalized dB change. The line at 0ms marks when the trial ended, or the goal was found. The grey area before approx. -1.5s is removed due to edge-effect contamination.

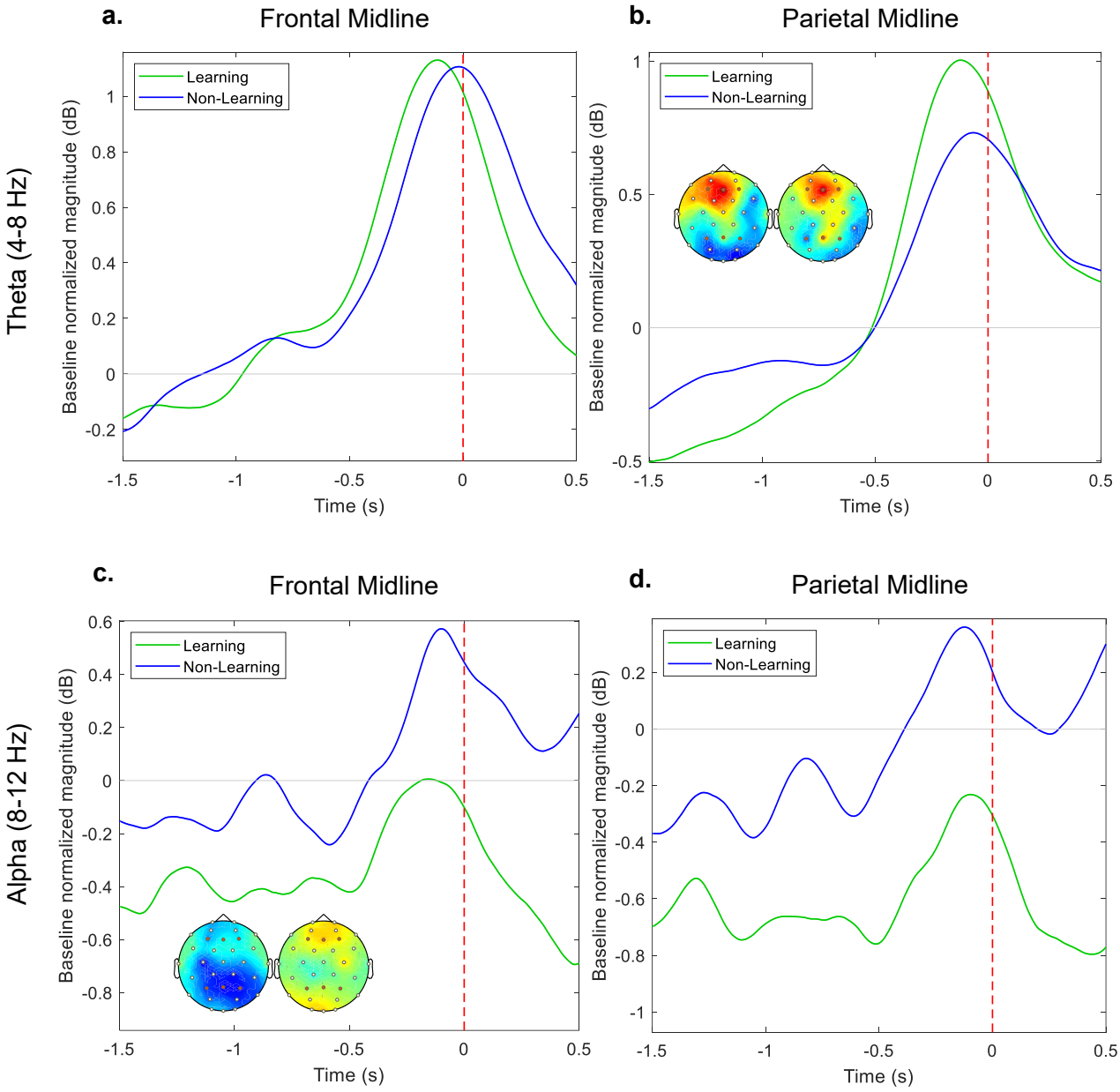


*Figure 3.9:* Time series plots of each epoch displaying normalized magnitude (*dB*) for both the learning and non-learning groups. Panels a and b represent average theta power changes across time, whereas panels c and d represent average alpha power across time. Topography maps (left: Learning, right: Non-Learning) display mean theta and alpha across the averaged time of the epoch and are scaled to the accompanying time-series. Both frontal and parietal midline ROIs are represented on these topographies and are highlighted in red.

*3.3.2.3 Exploratory within-groups learning dynamics*

Learning is a demanding and dynamic process; everyone does not learn at the same rate, this is particularly true for spatial cognition and navigation tasks (Commins et al., 2022). A second method was used, to capture learning, where we examined the within-groups differences [($T_{7-12}$) – ($T_{1-6}$)] from the first 6 and last 6 trials. Frequency estimation variance across time stabilises after approximately five trials on a memory task (Hanslmayr et al., 2009). This is also half-way through our task, in which almost all of those in the learning group, will have successfully learned and subsequently recalled the goal location, albeit at different rates (see Figure 3.3c). This analysis should provide further insight into the contributions of theta & alpha oscillations throughout the process of spatial learning. We examined the start (route initiation) and end (goal approach) phases again, averaging over the full epoch times, across 4 – 8 Hz & 8 – 12 Hz (see above). This equates to an approximate total of 598 trials, with approx. 150 per group, in each navigation phase. We used an FDR-corrected paired parametric *t*-test to evaluate the difference within each group. With the assumption that these changes occur after learning, and that our analysis is now performed within-groups, we anticipate a slight difference in the observed oscillatory dynamics from the between-conditions approach.

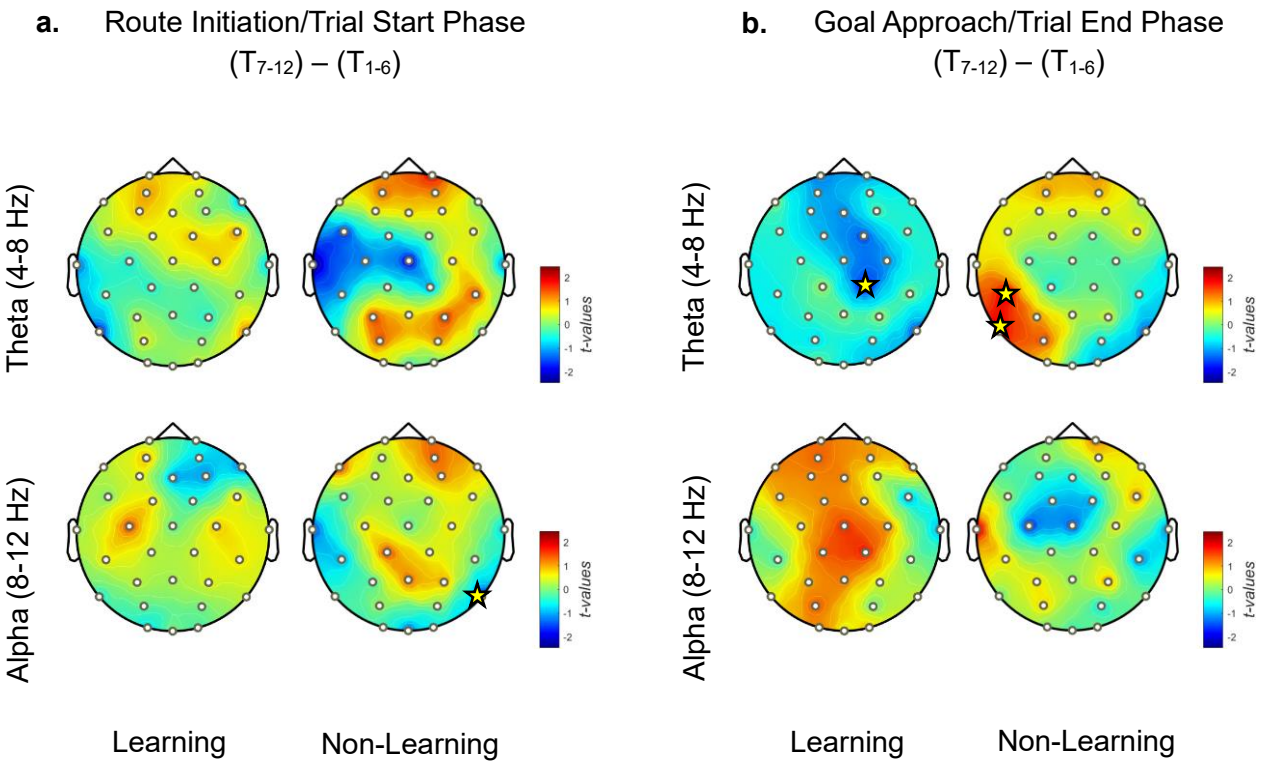


*Figure 3.10a:* Topography plots displaying within-group differences between the last and first 6 trials at the route initiation/trial start phase. Differences were calculated using a paired t-test for each group [$(T_{7\text{-}12}) - (T_{1\text{-}6})$]. Changes are displayed as t-values, averaged across time with an alpha level of 0.05, FDR-corrected across signal and frequency dimensions. Electrode sites with significant changes are denoted by a yellow star. *Figure 3.10b*: Topography plots displaying within-group differences between the last and first 6 trials at the goal approach/trial end phase. Differences were calculated using a paired t-test for each group [$(T_{7\text{-}12}) - (T_{1\text{-}6})$]. Changes are displayed as t-values, averaged across time with an alpha level of 0.05, FDR-corrected across signal and frequency dimensions.

*3.3.2.3.1 Theta Oscillations*

During route initiation, we demonstrate no significant changes within either group in the theta band (Figure 3.10a). Nevertheless, it is clear that there may be some learning-related changes; with the learning group showing low and stabilised theta in posterior parts of the scalp (reflecting our reported between-group changes; see Figure 3.5 and 3.6). However, these dynamics are not reflected in our non-learning group, who display increases at anterior and posterior parts of the scalp (possibly reflecting our between-group interaction effect reported at the frontal midline, and observations from Figure 3.5 and the group-differences displayed in Figure 3.6 upper). Though no site reaches significance, we do provide a general overview of how theta dynamics change as participants begin to navigate through the trials of the spatial task.

Interestingly, during the goal approach phase of navigation we demonstrate cross-scalp decreases (Figure 3.10b) in theta in our learning group (which we can see reflected in Figure 3.8a & 3.8b, as well as in Figure 3.7 upper). However, decreases in the learning group only reach statistical significance at site CP2. Whereas only site CP5 & P7 reach significance in the non-learning group, but as an increase in power. The similarity between the groups is reflected in the overall exploratory analysis conducted in Figure 3.7 and may explain why no statistical test on midline theta reported significance. However, it is clear that the learning group display more decreases with learning as they approach the goal, compared to the non-learning group who are still searching, but perhaps not encoding. We discuss this observation in-depth in the discussion.

*3.3.2.3.2 Alpha Oscillations*

During route initiation, we reported stabilised alpha power within the learning group and the non-learning group (Figure 3.10a). However, we also observed posterior *increases* in alpha power in the non-learning group (not significant at any site). These are interesting findings as they provide some interesting insights into the task-related dynamics of alpha oscillations. The learning group demonstrates lower alpha power compared to the non-learning group overall at parietal regions (see Figure 3.4 & 3.6). However, as the task progresses, some observed increases in alpha power within both groups may reflect mu oscillations (8 – 13 Hz) as both groups plan their actions or orientate themselves in relation to the goal location at the start of each trial.

At the goal approach phase, we report similar within-group alpha dynamics (also see Figure 3.9b). The learning group demonstrate that although overall alpha power is lower than the non-learning group, alpha during this phase increases with learning. On the other hand, alpha power in the non-learning group remains higher than the learning group but reduces as the task progresses. These reductions do not reach significance. Though we do not have sufficient spatial resolution with our EEG setup, these findings provide some good insights into alpha dynamics related to learning. Alpha power increases with learning as a function of trial progression across the scalp when the goal location is approached and may very well relate to the burst demonstrated in Figure 3.8 (upper). Some observed alpha suppression demonstrated in the non-learning group may be due to allocated spatial attention (particularly left frontal area) in order to improve search strategies for the goal. The lesser alpha power overall in the learning group may relate to fewer alpha-related neural resources being utilised to solve the task. This is discussed further below.

## 3.4 Discussion

### *3.4.1. Hypothesis-driven theta band analysis*

This study aimed to examine the changes in the brain's electrical activity during spatial learning in a virtual environment. We focused on two stages of learning: the route initiation phase and the goal-approaching phase. Firstly, we hypothesised that if theta power was related to learning, we should see theta power differences between the non-learning and learning groups following completion of the task. However, if theta power was related to active sensorimotor integration, we would find no differences between the groups. Having controlled for trial time, starting position, path length and speed, we observed changes in theta for our learning group at both start and goal phases that were different to the non-learning group, suggesting that theta is related to spatial learning rather than sensorimotor integration. The key difference between the two groups was that one group had learnt a specific goal location, while the other continued to navigate the environment.

Contrary to our hypothesis however, the learning group displayed significant *decreases* in oscillatory power overall. Reduced theta power was found at parietal electrodes (Pz) during route initiation compared to the non-learning group. Such decreases may indicate a more efficient use of neural resources. Once a task has been learned and the location is known, there may be little need for further exploration or encoding of the environment. As such, there may be no need to expend further neural energy on the task – both behaviour and neural activity have become efficient (see Commins, 2018b). Alternatively, low-frequency decreases have been associated with directed attention in both spatial memory and non-memory related tasks (Harris et al., 2017; Park et al., 2019). Decreases in theta power are also suggested to be responsible for the communication between areas involved in the successful formation of memories for spatial locations (Griffiths et al., 2016). As participants in the learning group

would have directed all attention to the goal location and/or an associated stimulus before setting off (e.g., landmarks – see Delaux et al. (2021)), theta decreases may be explained by a shift to a more efficient and direct spatial attention and memory formation process. Furthermore, these posterior decreases are also reflected in our within-groups analysis of the route initiation phase (Figure 3.10a), as the participants learn the task their theta power decreases, providing further support that these decreases are related to the task requiring less neural energy, successful spatial memory formation and by extension, spatial learning.

The non-learning group, which did not have a specific goal, showed *greater* theta during route initiation. Parietal theta power also seems to increase with progression of the task (see Figure 3.10a, though not significant) compared to the learning group. This is consistent with previous research indicating that the parietal cortex, which covers the parahippocampal and retrosplenial regions, is involved in the encoding of spatial information (Heimrath et al., 2012; Rodriguez, 2010; Sestieri et al., 2017). Greater theta power overall and the significant within-group increases may indicate that the non-learning group were attempting to encode their environment or recalling and combining features and/or previously explored places in order to develop new search strategies; which may place greater demand on theta rhythms (Caplan & Glaholt, 2007; Chrastil et al., 2022; Kahana et al., 1999; Kaplan et al., 2012). These findings align with previous research in the field that has linked theta *increases* to *exploratory* behaviour and suggests that theta may play a larger role in the encoding of spatial information, rather than movement speed or integration of sensory information, which we controlled for here (Buzsáki, 2005; Buzsáki & Moser, 2013; Goyal et al., 2020; Lega et al., 2012; Lin et al., 2017; Lin et al., 2022).

Another key finding was the similarity in theta dynamics between the groups during the goal approach phase of the task. Several studies have shown decreased theta oscillations relate to successful episodic (Guderian et al., 2009; Solomon et al., 2019) and associative

(Fellner et al., 2016; Michelmann et al., 2018) memory formation. These findings fit with the concept proposed by Herweg et al. (2020) in that decreased theta oscillations facilitate task-directed attention allowing neural representation of higher information content (perhaps a cognitive map). Overall, reduced theta power, and decreases related to the task may merely be a biomarker of the mechanisms required for task-engagement, one of which we isolate here: spatial learning. Importantly, differences in theta observed at the start of the task, but not at the goal suggest that these stages of navigation are different, and warrants analysing them separately based on Nyberg et al. (2022).

### 3.4.2 *Limitations of our theta hypothesis*

Firstly, It is important to note that we did not control for frustration or motivation in the non-learning group, which could be responsible for some of the EEG dynamics during the task. Therefore, the non-learning group may well have been engaged, as increased theta power has been shown to be related to increased cognitive load and attention (Chattopadhyay et al., 2021; Klimesch, 1999; Mussel et al., 2016). This needs to be further explored, perhaps using more electrode sites and/or frequency bands. Theta is the most important frequency band in the navigation literature, particularly due its relationship with the hippocampus and the firing of place cells (Bohbot et al., 2017; Buzsáki, 2002, 2005; Morris et al., 1982; O'Keefe, 1993; O'Keefe & Recce, 1993). Therefore, from a review of the literature we discovered that most activity reported is found near frontal and parietal midlines specifically, which is why we proposed these two regions of interest. Had we done an entirely exploratory analysis we may have found more significance across time-frequencies.

Besides, using 32-channel *scalp* EEG does place limits on the types of analysis we can run. Midlines are often different depending on the cap layout and number of electrodes available (For example, Liang et al. (2018) define the midline as AFz, AF3, AF4, F3, F1, F2,

F4, FC3, FC4, FC1, and FC2). We could also not perform accurate source analysis and reconstruction to explore possible communication or synchrony between the parietal cortex, hippocampus, retrosplenial cortex and frontal regions (Ekstrom et al., 2017). Most studies with humans use iEEG when examining virtual navigation, with some demonstrating sensorimotor-related increases in theta (Bohbot et al., 2017; Bush et al., 2017; Cornwell et al., 2012; Ekstrom et al., 2005; Epstein, 2008; Kunz et al., 2019; Lega et al., 2012; Miller et al., 2018). Virtual tasks, including NavWell, do not involve any physical traversal during navigation. The addition of this, alongside scalp EEG, may facilitate more accurate or ecologically valid sensorimotor integration, and should be considered in future research investigating theta dynamics (see Bohbot et al. (2017) but also see Griffiths et al. (2016)).

Focusing on only two of three phases of navigation suggested by Nyberg et al. (2022) may have limited our understanding of the complete dynamics of theta. However, there is a good reason for our selection, as the start and the end phases allowed us to have a standardised time epoch that was shared by all participants. Latencies would vary between individuals during travel, but every participant started and ended the task. This also provided confidence in the timestamp of events within out data whilst acknowledging some error (see Figure 3.2), as entirely automatic timestamping was not possible. Additionally, using the average trial time to time-match our non-learning group was perhaps not the most effective method. Instead, matching participants on an individual level as opposed to a group level, may have resulted in more accurate understanding of the non-learning groups searching behaviour (see Commins et al. (2022) for the advantages of this).

Furthermore, we did not accurately address individual differences in prior experience of virtual navigation/gaming, which has been shown to play an important role in learning accuracy of tasks such as NavWell (Murias et al., 2016; Yavuz et al., 2024). However, we did offer all participants practice trials to become familiar with the task controls (see Chapter 2).

We also verbally asked participants whether they were confident using the joystick or not for a task such as this. Upon reflection, it may have been more appropriate to assess the number of hours and categories of video games played or use a validated video-game-experience questionnaire (Unsworth et al., 2015).

### *3.4.3 Exploratory analysis of the alpha band*

Our main hypotheses focused on the involvement of theta dynamics in spatial learning. The alpha band (8-12 Hz) rests very close to the theta band on the frequency spectrum. Due to the underlying assumptions of calculating Morlet wavelets, it was very possible that some of theta's dynamics may have been reflected in the alpha band. Additionally, we wanted to be able to display the specificity of theta across the entire spectrum. Though not the primary focus of our study, it is known that alpha oscillations are heavily involved in attention, goal-directed movement and by extension, sensorimotor integration during spatial tasks (Ehinger et al., 2014; Hanslmayr et al., 2009; Harris et al., 2017; Liang et al., 2018; Liang et al., 2021). Therefore, we chose to explore this frequency band in addition to theta, but independent to our original hypotheses.

To our surprise, the dynamics within the alpha band generally reflected those seen in the theta band, with the learning group displaying less alpha power overall compared to the non-learning group, significantly at parieto-occipital sites (but generally reflected in the midline TF plots; see Figures 3.5 & 3.8). Therefore, we would propose that less alpha power is engaged overall when a task is learned, relating to "efficient" learning and the preservation of neural resources (Commins, 2018b). The opposite is seen within the non-learning group, who display higher alpha power than the learning group.

Alternatively, we propose that reduced alpha power in our learning group at route initiation relates to goal-directed orientation and motor-preparation towards the learned

location. Suppression within this range in goal-directed tasks tend to relate to mu oscillations, which are responsible for goal-directed motor movements (Pereira et al., 2017; Pineda, 2005). Interestingly, we see significantly lower alpha at right-frontal and parieto-occipital sites in the learning group during both phases. Suppression (desynchronisation) of alpha oscillations is typically related to goal-directed movement, with positive (synchronised) power relating to non-goal directed movements (this would explain the synchronisation observed at the trial end in the non-learning group in Figure 3.8). As all behaviour is non-goal directed in our non-learning group, this could explain the greater alpha power overall (Kock et al., 2023). It is also possible that these greater desynchronizations reflect learning participants monitoring their own actions for error, which has been demonstrated previously (van Schie et al., 2004). Additionally, at the trial start, significantly reduced alpha occurs at the side ipsilateral to the side of the body motor activity occurs on. Whereas at goal approach, it occurs contralaterally. Perhaps at the trial start, heading-error is assessed using these oscillations, whilst upon goal approach, these oscillations take on the role of goal-directed movements.

Secondly, based on our within-groups analysis, the gradual increases in alpha power could reflect attentional disengagement with the task (Ehinger et al., 2014; Klimesch, 2012; Peylo et al., 2021; Sauseng, Klimesch, Schabus, et al., 2005). Increases in alpha at parietal regions are also known to be related to decreased attention (Benedek et al., 2014; Foxe & Snyder, 2011). Our results are inconsistent with this explanation, demonstrating increases in alpha as a function of trial, particularly at goal approach (also reported by Chrastil *et al.* (2022) in a guided-navigation group). We further support the interpretation by Chrastil et al. (2022) of increased alpha activity in the parietal midline as trials progress in *all* participants. However, these within-subjects alpha increases as the task goes on, are most likely unrelated to learning. As previously observed, mental fatigue may cause alpha power to increase as a function of the duration of the experiment (Li et al., 2021). Occipital-only significant alpha reductions found

in the non-learning group may suggest increased visual-attention for searching (Li et al., 2021; Peylo et al., 2021); whilst in our learning group, encoding of spatial relationships may have disengaged attentional areas.

In summary, analysis of alpha has added additional support to our overall interpretation of efficient learning, in which the neural oscillatory energy required to complete a spatial task reduces with competent learning. However, the findings of increased alpha may relate to memory load or the engagement of internal rather than externally directed attention from our learning group (Cooper et al., 2003; Sauseng, Klimesch, Stadler, et al., 2005). Nonetheless, increasing alpha power may instead suggest fatigue or disengagement as the task progresses in both groups. Overall, our exploratory analysis of alpha supports the interpretation that our theta results likely reflect mnemonic processes specifically, rather than general attention or arousal. Therefore, future experiments should hypothesise the role of both theta and alpha involvement in spatial learning based on the above findings.

### *3.4.4 Conclusions*

Therefore, this chapter has uncovered that human theta (4-8 Hz), and alpha (8-12 Hz) oscillations are involved in spatial learning in a virtual environment. The non-learning group, who navigated without a goal, showed greater theta power in the route-initiation/start phase, indicating that increased theta oscillations play a larger role in exploratory behaviours. The learning group, who learned to navigate to a goal location, showed reduced theta power in the same phase. This suggests that as the spatial task is learned, the use of neural resources (particularly theta) becomes more efficient. Distinctly, reductions in parietal theta power (near the midline) may be a fundamental marker of spatial learning. Our findings also provide preliminary evidence of a human tendency towards learning efficiency, where the reduction in neural resources or shift in theta activity from an exploratory role to a more direct-attention

role occurs when efficient learning has taken place. This is particularly important during route-initiation, where we see greater theta power required if the route is exploratory in nature. Additionally, we have demonstrated that with spatial learning, comes lower overall alpha power. We suggest that route-planning and anticipatory goal-related motor responses at the trial start results in greater suppression of alpha oscillations. Whilst gradual increases in alpha power as a function of navigation relate to increased volitional attention. However, repeated exploration of the same environment results in some suppression of alpha oscillations in the visual areas, possibly related to the disengagement of visual spatial attention mechanisms. Overall, efficient spatial learning results in a reduction of overall oscillatory power, and by extension, the preservation of neural resources.

# Chapter 4

# An exploratory analysis of neural oscillations during immediate spatial recall.

**Abstract**

Various brain oscillations in humans play a role in a never-ending list of cognitive processes, including learning and memory. The oscillatory dynamics in humans contributing to successful spatial memory recall are not well understood. To investigate the involvement of particular oscillatory frequency bands in the recall process during navigation, we recorded the electroencephalographic (EEG) activity during an immediate recall trial in healthy young adults (n = 15) following the learning of a goal location in a Virtual Water Maze task. We compared this to the activity during the same trial length, in a group of participants who did not learn a target location and navigated freely but were time-matched to the learning group (non-learning, n = 15). We computed and compared relative power in all bands Delta (2-4 Hz), Theta (5-7 Hz), Alpha (8-12 Hz), Beta (15-29 Hz) & Gamma (30-40 Hz) across the scalp. We focused statistical analysis on regions of interest found to be important in our previous work, the frontal and parietal midline as well as the remaining midlines, central (C3, Cz, C4) and occipital (O1, Oz, O2). We found that delta and theta activity were greater during recall in our learning group, as opposed to our non-learning group. We also demonstrate clear suppression in the alpha band at posterior sites during memory-guided navigation compared to our non-learning group. We also reported that when goal-directed navigation (explicit navigation towards a previously learned goal) switches to focused searching behaviour (searching near a previously learned goal location), power becomes greater at the frontal midline; with increases in the delta and theta bands reflecting this strategy change. As the task progresses in our non-learning group, we report a significant increase in alpha power, significant at specific electrode sites. There is greater beta and gamma activity at posterior sites in our learning group, but overall, these two rhythms are suppressed in both groups during the recall trial. We discuss the results further in terms of the possible roles and functions of these oscillations and allow this exploratory analysis to guide our future work.

## 4.1 Introduction

Spatial memory is an important yet complex type of memory. Locations in space are encoded and stored in our different memory systems, much like other memories. Spatial memories not only prevent us from getting lost but can also provide context to autobiographical events. They may be complementary to episodic memory or may be an isolated semantic representation of an objects location in the environment. Though a large body of work has indicated the importance of slow-wave oscillations such as theta (4-8 Hz) to spatial encoding and retrieval in rodents and humans (see also Chapter 3). These cellular (Colgin, 2020; Eichenbaum et al., 1999; Moser et al., 2008; Ormond & O'Keefe, 2022) and oscillatory (Burgess & Gruzelier, 1997; Burgess & O'Keefe, 2011; Buzsáki, 2002, 2005; Buzsáki & Moser, 2013; O'Keefe & Recce, 1993) findings, typically derive from intracranial recordings with rodents. The cortical neurophysiology of spatial recall, including varying recall-based behaviours (such as directed, focused and exploratory navigation) in humans, has not been readily examined in the literature.

However, evidence relating to the function of these oscillations during spatial memory recall remains controversial. In a study by Watrous et al. (2013), researchers recorded low frequency oscillations in both rats and humans as they completed a Barnes maze and a virtual navigation task, respectively. They reported that human hippocampal rhythm centred around ~3 Hz, whilst the central frequency of the rats was centred around ~8 Hz. This suggests that low frequency oscillations from 1 Hz to 12 Hz may be important for memory-guided navigation (see Watrous et al., 2011). However, this is a very wide spectral range containing three of the traditional bands (Delta (1-4 Hz), Theta (4-8 Hz) and Alpha (8-12 Hz)), which have been linked to multiple other cognitive processes including episodic retrieval (Herweg, Sharan, et al., 2020; Vivekananda et al., 2021) and successful spatial working memory (Alekseichuk et al., 2016). Furthermore, the difference between humans and non-human animals questions the translatability of the role of specific frequency bands to spatial navigation and recall.

Despite this, there is good evidence that oscillations in the 1-12 Hz frequency range are involved in both navigation and the recall of spatial locations. For example, Bohbot et al. (2017) found hippocampal oscillations between 4-12 Hz during both searching and recall during real-world navigation, as well as 1-8 Hz oscillations during virtual navigation. It has been further suggested that the lack of physical locomotion and vestibular feedback in virtual navigation is responsible (Lin et al., 2022). Similarly, it has been shown that low-frequency delta-theta oscillations in the hippocampus are responsible for recall of distance information (Vass et al., 2016).

Therefore, it is essential to address the uncertainty of the role of oscillations in spatial memory and memory-driven navigation. Much of the literature reports scalp EEG recordings show prominent 1-12 Hz oscillations during spatial memory retrieval. For example, Jaiswal et al. (2010) showed theta oscillations lateralised to the right hemisphere during a virtual navigation task. Other researchers report oscillations around ~8 Hz being most prominent at the frontal and central midlines during spatial memory retrieval (Du et al., 2023; Liang et al., 2018). Moreover, Du et al. (2023) recently found that frontal midline theta (4-8 Hz) increases accompanied by posterior (occipital and parietal midline) alpha (8-12 Hz) suppression are involved in encoding early in learning and are related to memory performance during virtual navigation. Du et al. (2023) argued that multiple representations of the environment, essential to learning a path to the goal, compete until recall is required. In contrast, increased alpha prior to recall was also observed by Du et al. (2023), who suggest that this may reflect increased attention prior to deciding about a route or the presence of competing information during route learning.

Similarly, Chrastil et al. (2022) revealed increased alpha in active virtual navigation (where a decision about their next direction could be made at each maze intersection) but suppressed alpha at posterior sites during guided navigation (where participants are shown the

correct direction to choose at each decision point). It is possible that this may reflect increased attention related to active recall and decision-making. Alpha suppression may then reflect 'passive' navigation without active recall or decision-making (as suggested by Du et al., 2023 and Foxe & Snyder, 2011). Attentional demands during spatial memory recall have also been commonly characterised by the suppression of alpha-band at posterior parts of the scalp (Foxe & Snyder, 2011; Klimesch, 1999). Further research is required to fully understand this frequency bands contribution during memory-driven navigation.

Finally, Chrastil et al. (2022) reported that beta (12-20 Hz) & gamma (> 20 Hz) power was greater for correctly recalled decision-making and located at right frontal and left parietal channels. Furthermore, increases in beta and gamma (>30 Hz) power have been reported in those with high levels of unsuccessful recall in a memory task, located near the medial temporal lobe and parietal areas (Hanslmayr et al., 2016; Waldhauser et al., 2015; Waldhauser et al., 2012). Smyrnis et al. (2014) reported greater gamma oscillations during movement planning. However, beta power modulations were observed in sensorimotor areas during walking behaviour (Cevallos et al., 2015), with increased oscillations from 12 Hz to 30 Hz during movement adaptation (Seeber et al., 2014). These findings may also be relevant to our task despite constant movement speed (see Chapter 2 & 3). Nevertheless, it seems that increased high frequency oscillations are an indication of successful spatial memory formation.

In summary, frontal delta-theta (range from ~2-8 Hz) is involved in successful memory retrieval and execution of spatial recall. Parietal and occipital alpha suppression (ranging from ~8-12 Hz) may be vital for visual and memory attentional processing. Furthermore, high-frequency oscillatory decreases in the beta and gamma range (> 15 Hz) are involved with spatial memory retrieval but increases have been reported during successful spatial decision-making and working memory. Based on the above, we have performed an exploratory analysis of the oscillatory activity underlying immediate spatial memory during a recall trial in a virtual

water maze task. We will examine activity in Delta, Theta, Alpha, Beta & Gamma in participants who have successfully learned the task and are recalling the location of a goal in the environment following a short interval. We compared activity in these frequency bands to participants who did not learn a goal location (and therefore should not be using memory-driven navigation). This group freely navigated the arena for sixty seconds (see Chapter 3). We also compared this across four regions that have repeatedly found to be important in our previous work and the work discussed above: the frontal midline (F3, Fz, F4), parietal midline (P3, Pz, P4), central midline (C3, Cz, C4) and occipital midline (O1, Oz, O2). We predict greater delta-theta activity in our learning group compared to our non-learning group, reflecting successful spatial memory retrieval (Watrous et al., 2013; Jacobs, 2014). We also predict less alpha activity, allowing greater attention and prioritised processing of spatial information (Foxe & Snyder, 2011). Additionally, we expect to observe increased beta and gamma activity for successful binding spatial representations during recall for successful decision-making as suggested by Chrastil et al. (2022).

## 4.2 Methods

### *4.2.1 Participants*

The same fifty young adults (34 females, 16 males) aged between 18 and 45 (M = 21.7, SEM = +/- 0.637) from Chapter 3 were used for this chapter. All participants were right-handed. All participants were recruited via Maynooth University Department of Psychology and externally using personal connections, flyers, and social media (see section 3.2.1 in Chapter 3 for more details). However, due to the COVID-19 pandemic, only 30 of the original 50 participants completed a recall trial. These were then analysed and included a total of 30 young adults (19 females, 11 males) aged between 18 and 45 (M = 23.03, SEM = +/- 1.014). The recall phase of

this project and the use of human subjects with EEG was approved by the Maynooth University ethics committee (BSRESC-2021-2453422).

### *4.2.2 Spatial Navigation Task*

After the electrophysiological preparation (see Chapter 2 for details) and the completion of the learning phase (see Chapter 3), participants were seated 50 cm from the LCD computer screen on their own in a darkened, electrically shielded and sound-attenuated testing cubicle (150 cm × 180 cm) with access to a joystick for navigating. The spatial navigation task used was NavWell (see Commins et al. (2020) for in-depth details). The same virtual maze setup was used, which consisted of a medium circular environment (taking 15.75s to traverse the arena, calculated at 75 Vm). Two cues were used and were located on the wall of the arena (see section 3.2.2 for more details). A square goal was learned in the middle of the northeast quadrant and was 15% of the total arena size and consisted of a bright blue square that only became visible when the participant crossed it. Once the learning phase was completed (see Chapter 3) all participants took a 10–15-minute break. Following this, participants were given a single 60-second recall trial. Participants in the learning group (n = 15) were required to re-locate the target. However, for this trial, the target was removed from its location in the NE quadrant and did not illuminate blue nor display a message when walked on. During the recall trial all participants were presented with the same instructions that they were given during the learning trials, to locate the hidden goal (see Chapter 2 for details). The trial ended after 60 seconds. All participants started from the same novel south-west (SW) location. Those in the non-learning group (n = 15) had not learned about the target (see Chapter 2 for details).

To breakdown and analyse different elements of behaviour during the recall phase, we exported the x-y co-ordinates across time for each participant from NavWell. The x-y co-ordinates are recorded and stored in a *JSON* file for every 0.25s on average, as a participant

traverses the arena. Therefore, we first plotted the x-y co-ordinates in a plane that displayed the entire path trajectory. Based on these trajectories we derived a clear discrimination of behaviour, based on each quadrant and participants starting position. We plotted the x-y co-ordinates for each individual participant onto the same graph.

### *4.2.3 EEG Recording*

EEG data was acquired using a BioSemi ActiveTwo system (BioSemi B.V., Amsterdam, Netherlands) providing 32 Ag/AgCl electrodes positioned according to the 10/20 system that was used during the learning phase (see section 3.2.3 "*EEG Recording*"). Participants did not remove any equipment during the rest period. Electrode impedance was checked and adjusted to be below < 20Ω before recording began again. Analogue event signals were sent only once when participants began their trial. This was because all participant trial times were standardised. The recording system was stored in the same room, participants were seated, and data were recorded continuously. The four electrodes (EXG1 - EXG4) positioned on the face were checked and readjusted if necessary. Raw EEG data were again sampled at 1024Hz but down-sampled offline to 512 Hz (see Chapter 2 & 3 for details).

### *4.2.4 EEG Preprocessing*

Continuously recorded EEG data were analysed offline in MATLAB R2021B using scripts in combination with the Brainstorm package (Tadel et al., 2011). A 1 Hz high-pass filter and a 40 Hz low-pass filter were applied. Independent Component Analysis (ICA) was performed to remove and correct artifacts, namely eye movements, blinks, and muscle artifacts. We used the EEGLAB infomax algorithm callable via brainstorm using the *runica* function. For this analysis, the entire continuous recording was then epoched into 2-second epochs, producing 30

epochs per participant. These data were visually inspected for bad segments and bad electrodes, which were then removed. Bad electrodes that originated from pre-defined regions of interest were interpolated (n = 2), if possible, using Brainstorm after ICA. Epochs with voltage steps above 100 µV or peak-to-peak signal deflections exceeding 200 µV within 2-s intervals were automatically rejected. We had a rejection rate of approximately 8% of the total epochs produced. EEG data were then re-referenced to the average of the 32 electrodes. For further information on EEG pre-processing see Chapter 2.

### *4.2.5 EEG Spectral Analysis*

As this was an exploratory analysis, we investigated five frequency bands: delta (2-4 Hz), theta (5-7 Hz), alpha (8-12 Hz), beta (15-29 Hz) & gamma (30-40 Hz). The bands were defined using the default Brainstorm settings for the band for this chapter. This was to prevent adding overlapping frequency definitions into the relativity calculation twice. Power spectra were computed on artefact-free epochs for each participant. We used Hanning windows of 2-s with a 50% overlap using Welch's method for all electrodes. This resulted in a spectrum with frequency resolution of 0.5 Hz, and the power was computed using the underlying short Fast Fourier Transform (sFFT) with a linear frequency distribution of 1:1:40. This was then grouped into the previously defined bands using the *Frequency > Group in time or frequency bands* process. Relative power within these bands was then computed to reduce inter-subject variability in the power calculations.

We use relative power only for all group analyses. All raw Power Spectral Density (PSD) plots display the magnitude of power based on recommendations in the literature. We again focused our analysis on our pre-defined regions of interest, extracting these data for each individual participant. We examined the relative power at the frontal midline (Fz, F3, F4) and

the parietal midline (Pz, P3, P4) once again capturing activity from both the anterior and posterior parts of the scalp. As this analysis was exploratory, we investigated more regions that may be of interest, including the central midline (C3, Cz, C4) and the occipital midline (O1, Oz, O2). All epochs in each group and phase, were averaged together following computations.

For the behaviour-based EEG analysis, we split our EEG recording into relevant timestamps to examine EEG activity during these different navigational behaviours. We then divided artifact free 2-s epochs up into behavioural "phases" based on time from event trigger sent to the BioSemi system when participants started the trial. More detail is available in the relevant section (section 4.3.2.3).

### *4.2.6 Statistical Analysis*

Statistical analyses & visualisation of the behavioural data were performed using a combination of JASP (version 0.15) and R software version 4.0.2 with the tidyverse and ggplot2 package. Firstly, statistics were performed using extracted values from the power spectra via the *extract > values* process in Brainstorm. We extracted data from our ROIs and for differing time periods (see section 4.3.2.3 "*Behaviour-matched EEG dynamics*"). Statistical exploration of the EEG data across the scalp was performed using Brainstorm in MATLAB 2021b, comprising of two-tailed non-parametric independent or paired *t*-tests with 5000 permutations and a *p*-threshold of 0.05. We corrected for multiple comparisons in EEG data using an FDR (False Discovery Rate) correction. All data were combined for behaviour-matched EEG analysis, but gender was included as a factor in the overall behavioural analysis (based on its inclusion in Chapter 3 and Thornberry et al., 2023). Mixed-factorial ANOVAs were computed on the behavioural data comparing the two groups on time spent in each quadrant of the arena. Further mixed factorials were done for each frequency band, comparing the groups across the various ROIs. Bonferroni corrected t-tests were used to follow up within analysis, and independent sample t-tests were used to follow up group differences.

## 4.3 Results

### *4.3.1 Behavioural Results*

Firstly, we compared the learning group (n=15, 10 females) to the non-learning group (n=15, 9 females) on age to confirm the groups were matched for this variable (M = 23.6, SEM +/- 1.656 and M = 22.467, SEM +/- 1.214). We report no significant difference between the groups ($t(28) = 0.552$, $p = 0.585$, Cohen's $d = 0.202$). As previously mentioned, the NavWell software tends to eliminate gender effects in spatial navigation abilities (see Commins et al., 2020 & Thornberry et al., 2023). However, it was included in the analyses where possible (similar to Chapter 3). For all participants, percentage time spent searching in each quadrant of the pool (including the one containing the target, i.e., NE) were recorded. The data were analysed using a 2 (Group) X 2 (Gender) X 4 (Quadrant) repeated measures ANOVA. The data violated the assumption of sphericity, so therefore a Greenhouse-Geisser correction was applied to the model. We reported a significant main effect of Quadrant ($F_{(1.2, 30.2)} = 12.205$, $p < 0.001$, $\eta^2 = 0.193$). However, we reported no significant between subjects effects for neither Group ($F_{(1, 26)} = 1.500$, $p = 0.232$) or Gender ($F_{(1, 26)} = 1.501$, $p = 0.232$). We revealed a significant interaction effect for Quadrant X Group ($F_{(1.2, 30.2)} = 13.696$, $p < 0.001$, $\eta^2 = 0.216$) but found no significant interaction effect for Quadrant X Gender ($F_{(1.2, 30.2)} = 1.235$, $p = 0.283$) nor a significant three-way interaction effect ($p = 0.263$).

Focusing on the goal quadrant, we ran Tukey-corrected t-tests to investigate the reported interaction effects. The learning group's percentage of time spent in NE (M = 78.12%, SEM +/- 2.3%) was significantly greater (MD = 51.72%, $t = 4.837$, Cohen's $d = 1.838$, $p < 0.001$) compared to the time spent searching there by the non-learning group (M = 26.9%, SEM +/- 2.1%). Additionally, the learning group spent significantly more time searching in the goal quadrant (NE) than all other quadrants; NW (M = 7.97%, SEM +/- 1.8 %, $p < 0.001$), SW (M = 12.59%, SEM +/- 0.89%, $p < 0.001$) and SE (M = 1.32%, SEM +/- 1.14%, $p < 0.001$).

Importantly, time spent searching in the goal quadrant (NE) in the non-learning group, did not differ from any of the other quadrants: NW (M = 24.22%, SEM +/- 2.18%, $p < 0.999$), SW (M = 29.2%, SEM +/- 2.16%, $p < 0.999$), nor SE (M = 19.64%, SEM +/- 2.37%, $p < 0.758$). Therefore, all quadrants for the non-learning group were at near chance levels (25%) and did not differ from each other, compared to the directed searching displayed in the learning group (Figure 4.2), who spent a statistically significant amount of time searching there compared to other quadrants, and compared to the non-learning group.

Another interesting finding is that the learning group spend significantly less time searching in the quadrant containing the starting position (SW; MD = -36.47%, $t$ = -3.502, Cohen's $d$ = -1.279, $p$ = 0.015). Additionally, we examined any differences in average path lengths during the recall trial between the groups using an independent $t$-test. A significant difference in path length between the groups during recall ($t(28) = -4.296$, $p < 0.001$, Cohen's $d$ = -1.559) was noted, with the learning group having shorter search paths (M = 235.02 Vm, SEM +/- 12.378 Vm) compared to the non-learning group (M = 291.03 Vm, SEM +/- 4.35 Vm). The reduced time in the starting quadrant, along with shorter search paths would indicate goal directed-searching in the learning group, with longer and exploratory searching behaviour (see below Figure 4.1b) in the non-learning group.

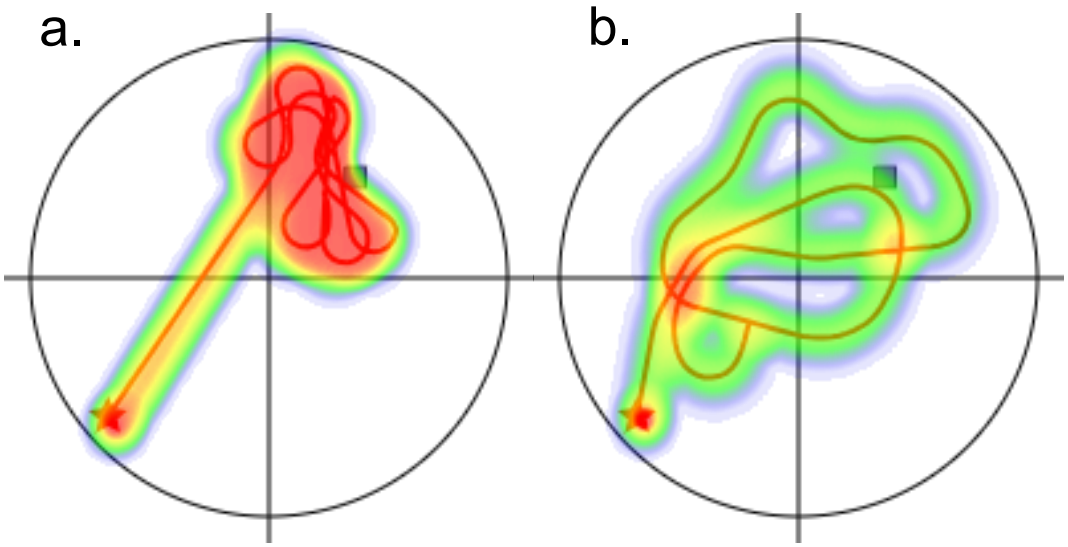


*Figure 4.1:* Maps of all four quadrants displaying sample paths and searching heatmaps from sample participants: a learning group participant (a) and a non-learning group participant (b). It is clear that 4.1a displays directed and persistent search patterns. Participant 4.1b displays random searching activity with no 'hot-spot'.

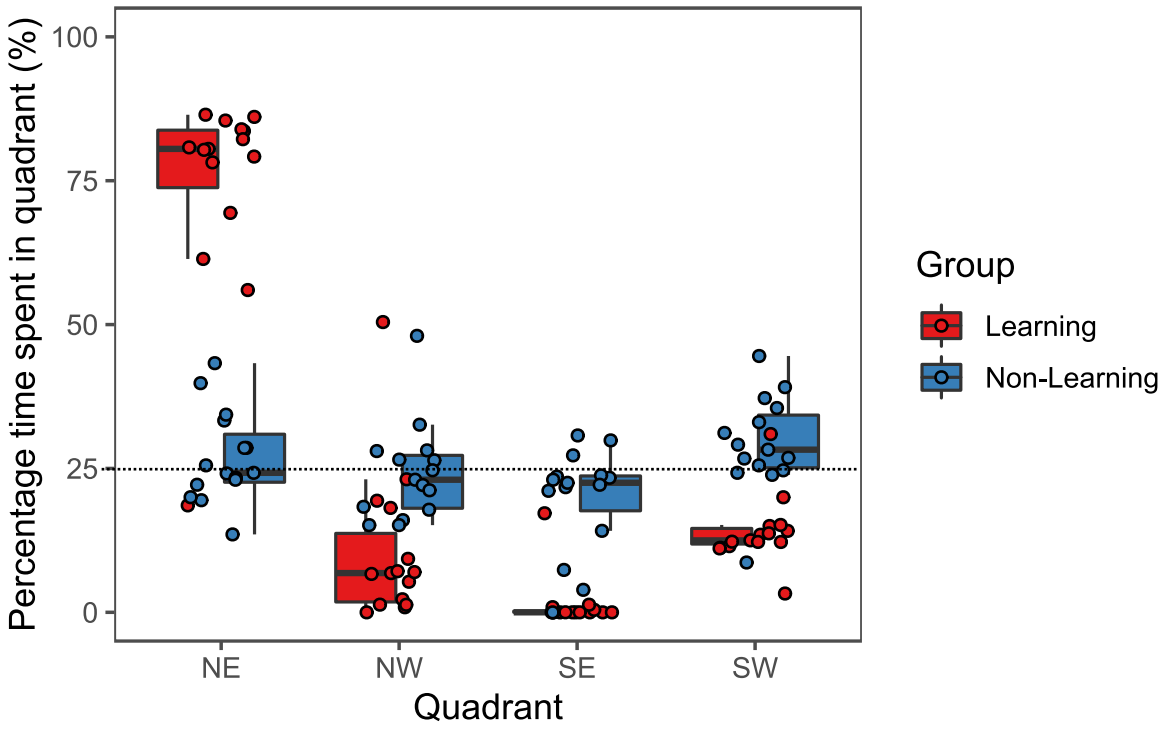


Figure 4.2: Boxplots with individual data points displaying mean search percentage times for each quadrant; Northwest, Northeast (goal quadrant in learning group), Southwest and Southeast. Black horizontal bar represents the mean.

### *4.3.2 EEG Results*

#### *4.3.2.1 Relative Frequency Band Power*

Power Spectral Density (PSD) using a Welch window (medium window length of 2s with an overlap ratio of 50%) was used to compute the power spectra ($\mu V^2/Hz$) based on a typical Fast-Fourier Transform (FFT) default frequency definition. Power spectra were computed for five bands: Delta (2-4 Hz), Theta (5-7 Hz), Alpha (8-12 Hz), Beta (15-29 Hz) & Gamma (30-40 Hz). The bands were defined as such for this chapter, to prevent adding overlapping frequency definitions into the relativity calculation twice (1 Hz was not included as it is too close to the band-pass filter limit). We then performed a spectrum normalisation to calculate relative power, for our four ROIs, the frontal (F3, Fz, F4), central (C3, Cz, C4), parietal (P3, Pz, P4) and occipital (O1, Oz, O2) midlines.

Figure 4.3 shows isolated PSDs with a linear frequency definition of 1:1:40 for the full scalp and our ROIs. This will allow us to see the specificity of dynamics within the bands. We report clear differences in alpha power (~ 10/11 Hz) at all sites (Figure 4.3b-e) and across the scalp (Figure 4.3a). We also report clear differences in delta power at the central region (Figure 4.3c), with the learning group having much greater power than the non-learning, particularly around ~2 Hz. Beta & gamma frequencies clearly differ between groups in the occipital area based on Figure 4.3e.

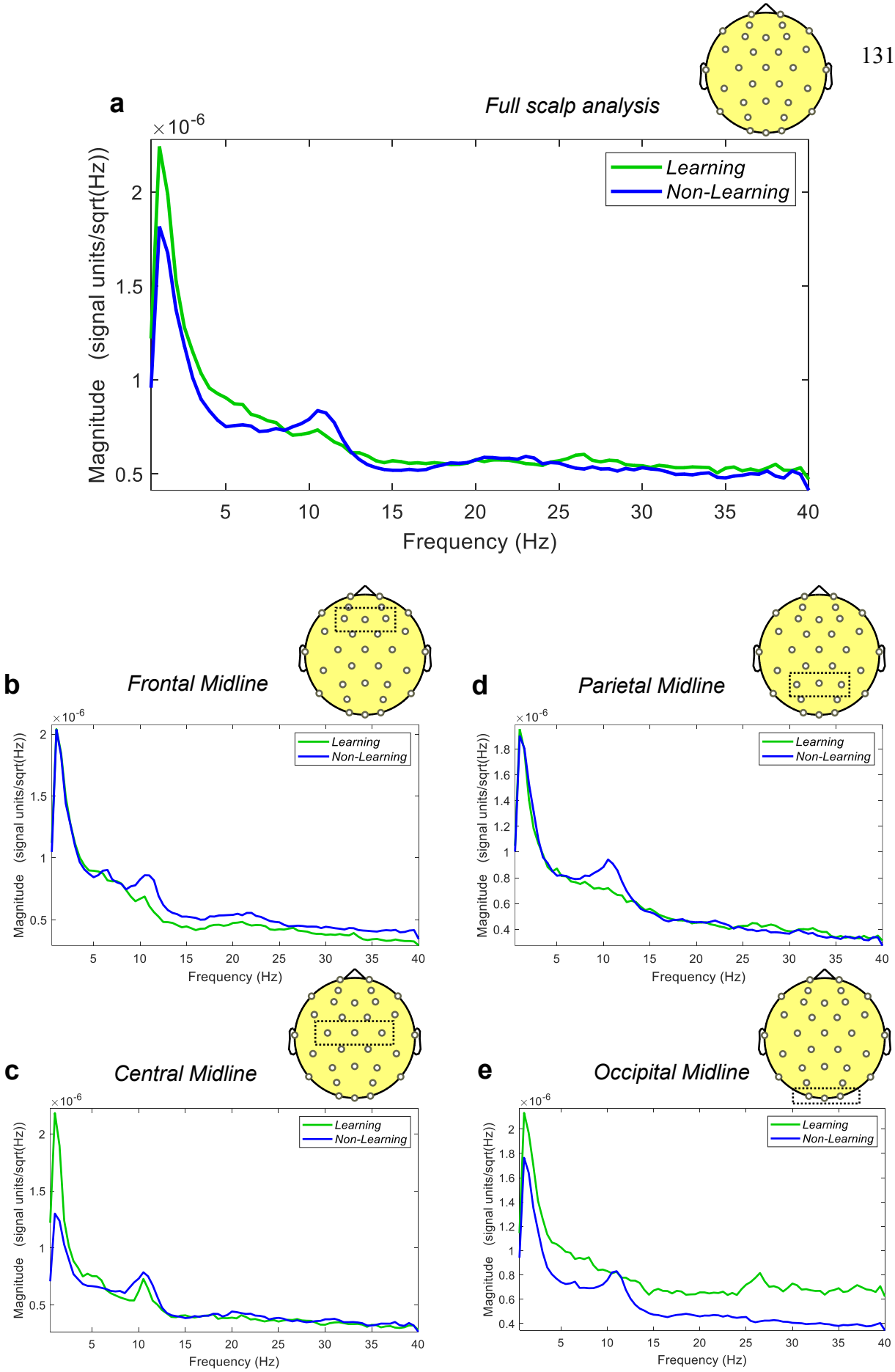


*Figure 4.3:* Power Spectral Density (PSD) plots calculated using underlying sFFT at a frequency resolution of 0.5Hz and a linear frequency definition of 1:1:40. We display mean power magnitude of each ROI (a=scalp, b=frontal midline, c=central midline, d=parietal midline and e=occipital midline) for both the learning and non-learning group. Some scales differ due the overall average power distribution.

Following the analysis approach of Du et al. (2023), power data were analysed using a 2 (Group) X 4 (ROI) mixed repeated measures ANOVA. The relative power data violated the assumption of sphericity in parts, so therefore a Greenhouse-Geisser correction was applied to the model where appropriate. All *post-hoc* analysis use Bonferroni corrected t-tests to examine a reported main within effect, and a Tukey correction to examine interaction effects (see Chapter 2 for rationale). For **Delta** (Figure 4.4a), we reported a significant main effect of region ($F_{(3, 84)} = 8.652$, $p < 0.001$, $\eta^2 = 0.097$). We reported no significant between-subjects effects for group ($F_{(1, 28)} = 0.736$, $p = 0.398$). However, we reported a significant interaction effect for Region X Group ($F_{(3, 84)} = 4.447$, $p = 0.006$, $\eta^2 = 0.05$). Using *post-hoc* t-tests we examined our main effect, revealing delta at the frontal midline was greater than at the central midline across the groups ($t = 3.236$, $p = 0.010$). Furthermore, delta power was greater at the parietal midline compared to the central ($t = 4.817$, $p < 0.001$) and occipital ($t = 3.240$, $p = 0.010$) but did not differ compared to the frontal midline ($t = 1.581$, $p = 0.706$). This illustrates that delta power is greater at the frontal and parietal regions of the scalp. Examining our interaction effects, corrected t-tests revealed that neither group had significant differences in delta at any midline (all $p > 0.23$). In the non-learning group, frontal, parietal & occipital midline delta was greater than central midline delta ($t = 3.185$, $p = 0.041$; $t = 5.090$, $p < 0.001$ and $t = 3.574$, $p = 0.013$). We reported no within-group differences for the learning group (all $p > 0.056$).

For **Theta** (Figure 4.4b), we reported a significant main effect of region ($F_{(3, 84)} = 10.857$, $p < 0.001$, $\eta^2 = 0.066$). We reported no significant between-subjects effect ($F_{(1, 28)} = 0.354$, $p = 0.556$). Furthermore, we reported no significant Region X Group interaction effect ($F_{(3, 84)} = 0.819$, $p = 0.487$). Interestingly, we reported that power at the frontal midline in both groups is significantly greater than at the parietal midline ($t = 3.300$, $p = 0.009$) and the occipital midline ($t = 5.653$, $p < 0.001$) and the central midline, though not significant ($t = 2.522$, $p =$

0.081). This may indicate that frontal midline theta is related to the navigation process itself during this phase.

For **Alpha** (Figure 4.4c), we reported a significant main effect for region ($F_{(1.87, 52.44)}$ = 6.183, $p$ = 0.005). However, we did not report a significant between-subjects effect for group ($F_{(1, 28)}$ = 1.351, $p$ = 0.255). Additionally, we reported no significant interaction effect between Region X Group ($F_{(1.87, 52.44)}$ = 0.637, $p$ = 0.523). Post-hoc tests of our main effect reveals that power is greater at the parietal midline ($t$ = 2.769, $p$ = 0.041) and the central midline ($t$ = 4.048, $p$ < 0.001), compared to the frontal midline across both groups. For **Beta** (Figure 4.4d), we reported a significant main effect of region ($F_{(3, 84)}$ = 7.034, $p$ < 0.001, $\eta^2$ = 0.058) but no significant difference between the groups ($F_{(1, 28)}$ < 0.001, $p$ = 0.984). Furthermore, we reported a significant interaction effect between Region X Group ($F_{(3, 84)}$ = 3.324, $p$ = 0.033, $\eta^2$ = 0.027). Using *post-hoc* Bonferroni corrected t-tests we revealed that across both groups, the power at the occipital area was significantly greater compared to the parietal midline ($t$ = 4.359, $p$ < 0.001), the central midline ($t$ = 3.133, $p$ = 0.014) and approaches significance for the frontal midline ($t$ = 2.633, $p$ = 0.06). We then ran *post-hoc* Tukey corrected t-tests to examine our interaction effect. We reported that for the learning group, power at the occipital midline was greater than at the parietal and frontal midlines ($t$ = 3.474, $p$ = 0.018 and $t$ = 3.595, $p$ = 0.012 respectively). These effects were not found in the non-learning group ($p$ > 0.14). The groups did not significantly differ between each other at any specific region of interest (all $p$ > 0.98).

Finally, for **Gamma** (Figure 4.4e), we reported a significant main effect of region ($F_{(3, 84)}$ = 14.506, $p$ < 0.001, $\eta^2$ = 0.095), but no significant difference between the groups ($F_{(1, 28)}$ < 0.001, $p$ = 0.995). We reported a significant interaction effect for Region X Group ($F_{(3, 84)}$ = 3.898, $p$ = 0.012, $\eta^2$ = 0.025). Our *post-hoc* Bonferroni corrected t-tests demonstrated a similar main effect to Beta. The occipital midline had greater power compared to the parietal midline ($t$ = 6.309, $p$ < 0.001) and frontal midline ($t$ = 4.175, $p$ < 0.001) across the groups but not the

central midline ($t = 2.248$, $p = 0.163$). Examining our interaction effect using Tukey corrected t-tests revealed that the groups do not differ at any region (all $p > 0.84$). Nevertheless, we found that in the learning group, occipital area gamma was greater than gamma power at the frontal midline ($t = 5.036$, $p < 0.001$), the parietal midline ($t = 5.719$, $p < 0.001$) and central midline ($t = 3.684$, $p = 0.009$). We reported no differences within the non-learning group (all $p > 0.19$). This may indicate that high-frequency oscillations, i.e., beta and gamma, may be involved in the navigation process primarily at the occipital area, but also primarily in the learning group.

However, calculating power in each band as a percentage of the summed power across all frequencies (i.e., relative power) indexes the distribution of power across bands, which inherently differs between frequency ranges across the spectrum. Investigating any cognitive event (such as a navigation phase for that matter) using relative averages from grouped ROIs, may be too coarse to reveal group-differences statistically (see Du et al., 2023). For this reason, we ran FDR-corrected permutation t-tests to reveal significant group level differences at all electrode sites and frequency bands (at an alpha level of 0.05 with 5000 permutations). In this randomisation procedure the 2 conditions are interchanged randomly for each subject in each run. The swapping of the conditions is done consistently across electrodes. This provides compensation for smaller sample sizes (Frossard & Renaud, 2021) and alleviates the impact of high signal to noise ratio (Mamashli et al., 2019). It is also recommended by the Brainstorm team (Pantazis et al., 2005) and has been used in the EEG/spatial navigation literature (Gehrke & Gramann, 2021).

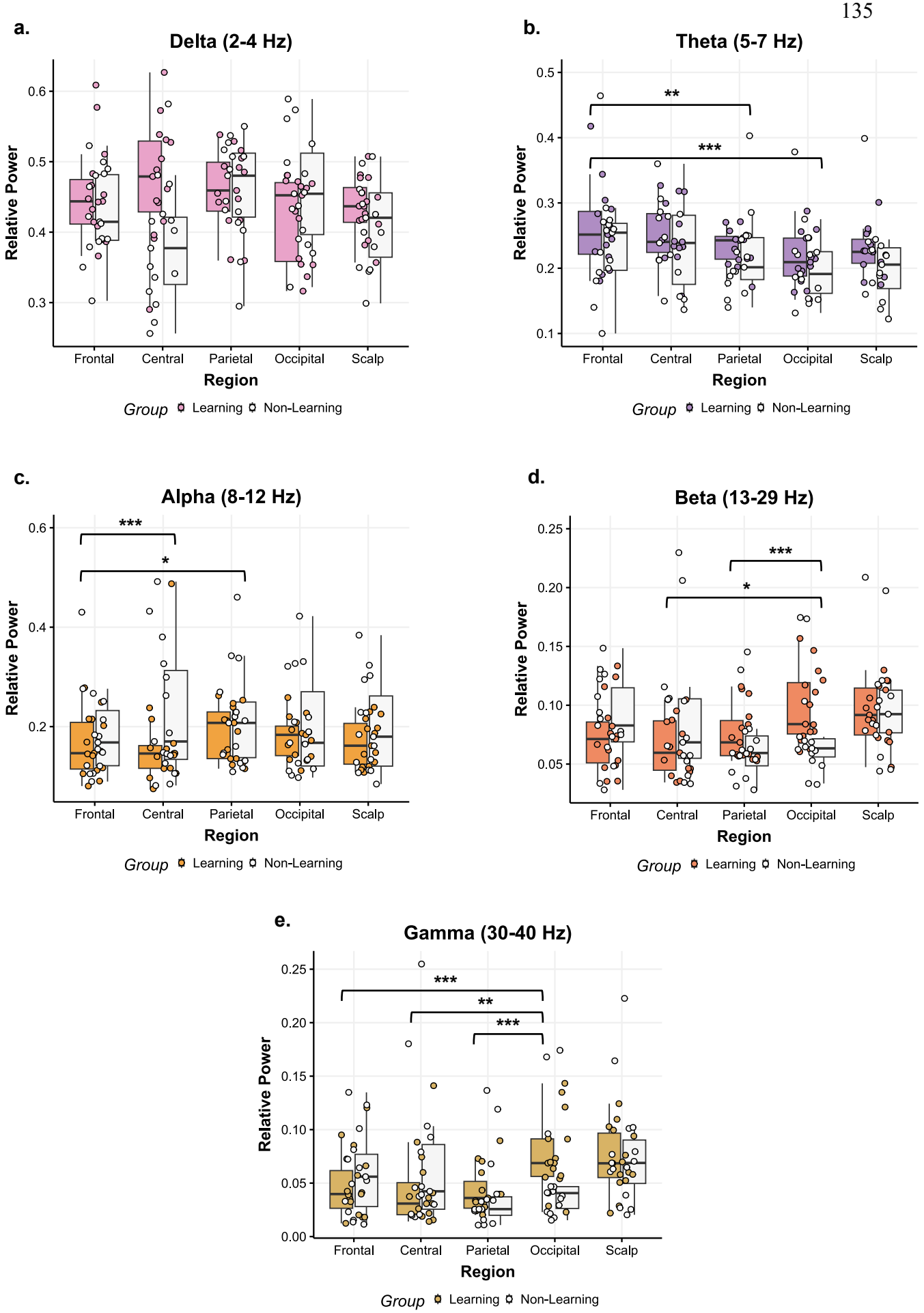


*Figure 4.4:* Boxplots displaying means as well as jittered data points of individuals from each group, and relative power for each frequency band at our four ROIs as well as the global scalp relative power. Each frequency band is represented by a different plot in different colours to help with visualisation. Any line demonstrating significance that goes from one group to the other demonstrates across-group effects. Any line going from one group to the same group implies a within difference. We reported no region-specific group differences so they are **not** displayed here. **NOTE:** * $p < 0.05$, ** $p < 0.01$, *** $p < 0.001$.

Examining the difference between the groups (i.e., Learning – Non-Learning), we reported that topographical distribution of power was significantly greater in the learning group in the delta band (2-4 Hz) at frontal and central sites including CP5, CP1, Cz, F8 and FC6 (Figure 4.5a). Similar significant increases in theta (5-7 Hz) are found at frontal and central sites for the learning group, with CP5 and FP2 as significant (see Figure 4.5b). Within the alpha range (8-12 Hz) we report no significant differences at any electrode site, but a large widespread activation over central and parietal sites are observed for the non-learning group in Figure 4.5c. This is also observed in the overall PSD (Figure 4.3d) and appears at 11 Hz, with most of the activation near the right motor areas (site C4) ipsilateral to the hand used for moving the joystick. Whilst a small activation is also seen in the learning group, it is not as prominent as the non-learning group. In beta (15-29 Hz) we demonstrate significantly greater power in the learning group compared to the non-learning group at occipital sites, with significance at sites PO3 and PO4 (Figure 4.5d), whilst reporting significantly isolated, but lower power at sites CP5 and F8. Finally, for gamma (30-40 Hz) we report very similar findings to beta, but not as marked, losing significance at sites PO3 & PO4, but retaining significance for CP5 & F8 (Figure 4.5e). Clearly there are some distinctive differences across all bands, that are not detected at our predefined ROIs, and our statistical analysis of mean relative power. Nevertheless, relative power provides us an insight into the typical dynamics of power distributions during spatial navigation and recall.

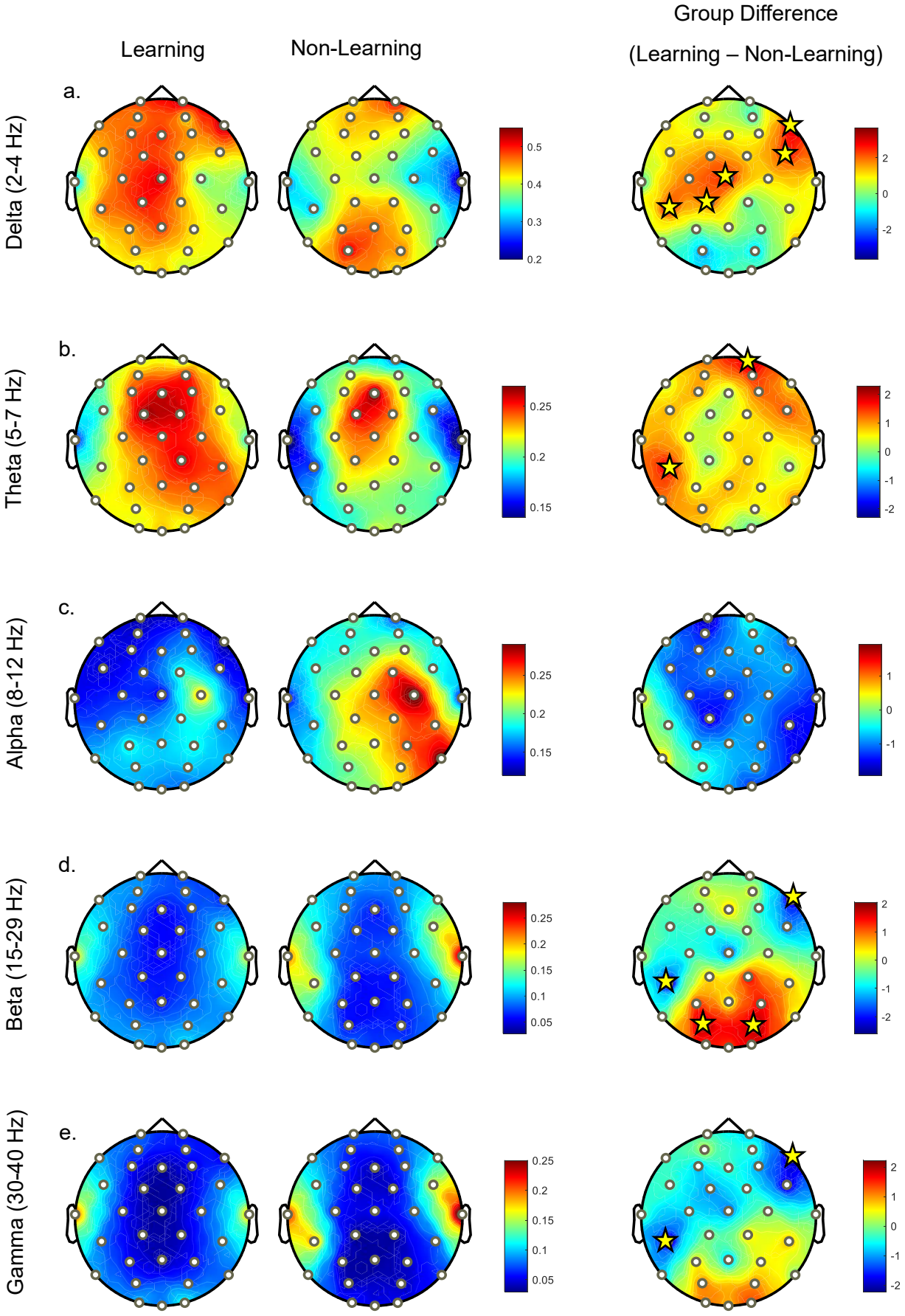


*Figure 4.5:* Topographical plots displaying each groups relative power distribution across the scalp at each frequency-band (a - e). Significant electrodes are displayed with yellow stars. The scale in relative power (%), whilst the scale for the differences is displayed in *t*-values.

*4.3.2.3 Behaviour-matched EEG dynamics*

Typically, in the classic MWM paradigm, during the probe trial of animals who have successfully learned the task, there is an initial goal-directed searching behaviour followed by focused searching behaviour within the same quadrant of the maze that contains the previously learned goal (Harvey et al., 2009; Nyberg et al., 2022; Rogers et al., 2017). We expected to see evidence of these two searching behaviours during our probe trial in our learning group: goal-directed navigation, followed by focused-searching. Furthermore, we would expect to see purely random searching behaviour in our non-learning group throughout the trial. Evidence of this can be seen in Figure 4.1. However, to capture the true dynamics of the search path across time, we exported the x-y coordinates from the NavWell system for each participant (see Figure 4.6 below).

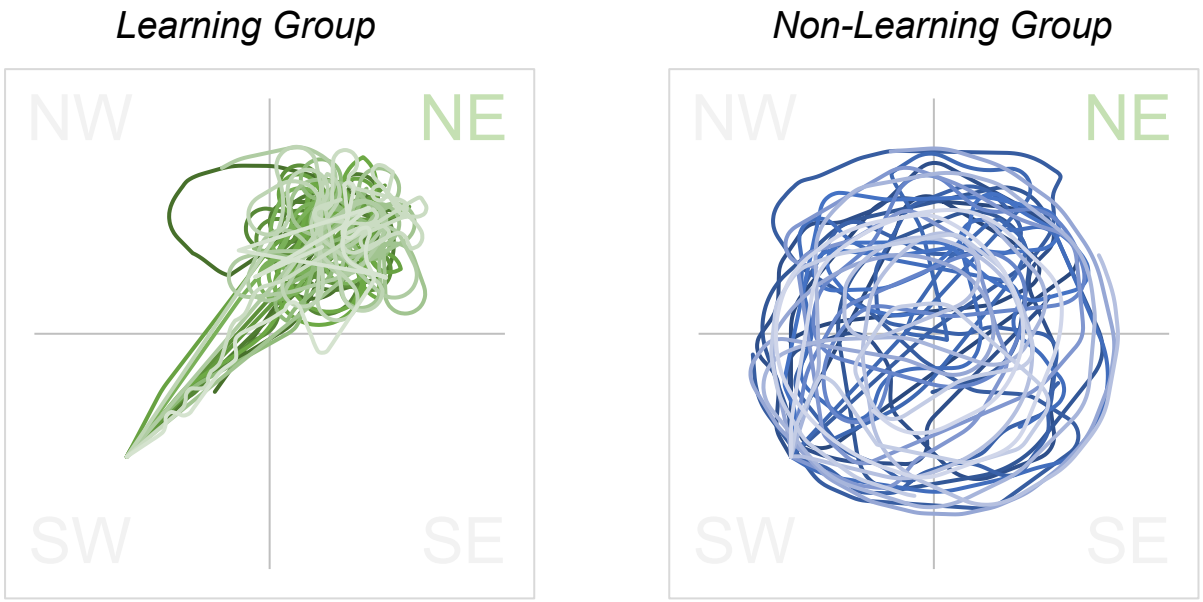


*Figure 4.6*: Full recall trial path trajectories plotted using x-y co-ordinate data for all participants in each group within the arena. They are scaled to fit a square (1,1) plane, with the centre point of the cross represented by (0,0).

Following this, based on the analysis of screen-recorded probe trials from participants, and the short latencies from the learning phase within the learning group, we split our trajectories into the first 10-seconds (which captured most of the goal-directed navigation, Figure 4.7 - green) and the final 50-seconds (which captured most of the focused searching behaviour in the NE quadrant, Figure 4.8 - green) for the learning group. For the non-learning group, the first 10-seconds showed that participants headed off in random directions (Figure 4.7 - blue) and then continued to move around the entire arena for the rest of the trial (Figure 4.8 - blue) in a random fashion.

#### *4.3.2.3.1 Goal-Directed vs Random Behaviour*

To examine difference between groups, we utilised a standard Welch's PSD with an underlying FFT linear function of 1:1:40. We present full-scalp power differences between the groups in Figure 4.7 (initial 10s) & Figure 4.8 (final 50s) below. For this phase, we compared relative frequency power differences between groups using an independent permutation *t*-test with 5000 permutations as implemented previously. We utilised relative power as we are interested in the distribution of power within the frequency bands between the groups. Additionally, this calculation generated better between-group comparable data that is standardised and accounted for slow-drifts, artifacts and noise that may influence between-group analysis. The two groups may also have differing overall levels of absolute power and therefore relative power provides a correction for this (see Jabes et al., 2021, for further information). Figure 4.7 shows that participants headed directly towards the goal (learning group), with increased delta and theta power, with significant increases in theta at the CP5 electrode, when compared to participants headed in a random direction. We reported less alpha power across central sites, but none reaching significance. We further reported greater beta and gamma power at anterior and

posterior sites, but significantly less power at sites CP5 and F8 for beta only. Figure 4.8 shows that participants that had searched with a focus on the NE quadrant showed even greater delta and theta power, with significant central (CP5, Cz, CP6) and frontal (FC6, F8) delta compared to the non-learning group. In addition, similar to reported above, this group showed higher frequency activity in the beta and gamma bands within the parietal and occipital regions (significant at PO3 and PO4 for beta only), compared to the non-learning group that moved randomly throughout the entire arena. We also reported significantly less beta in our learning group at sites CP5 and F8 again, with CP5 only becoming significant in the gamma band. Finally, the non-learning group showed greater alpha power (~11 Hz) during random movement, which was not observed in the learning group (see Figure 4.8).

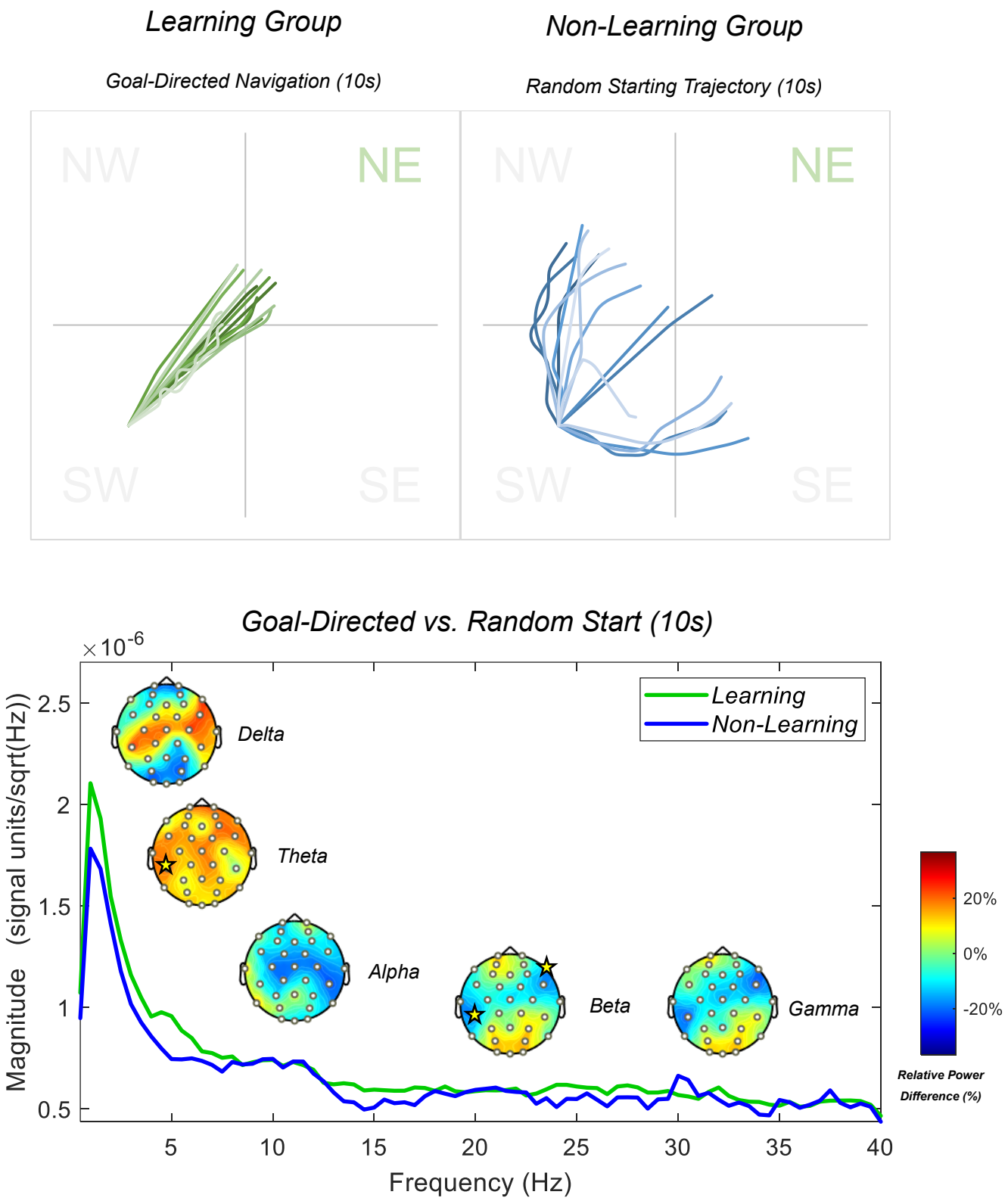


*Figure 4.7*: Learning & Non-Learning group paths generated via x-y co-ordinates from the first 10s of the recall trial are displayed above. Below these plots, we display the PSD spectrum from the comparison between the two groups in magnitude with a frequency resolution of 0.5 Hz during the first 10s of the recall trial. We then display corresponding topographies reflecting our frequency band definitions, which display the results of our between-subjects permutation t-tests. Yellow stars indicate electrode sites that have a significance level of 0.05 or less, following FDR-correction. Topographies are displayed in relative power differences, but PSD is plotted in magnitude based on guidelines from the literature.

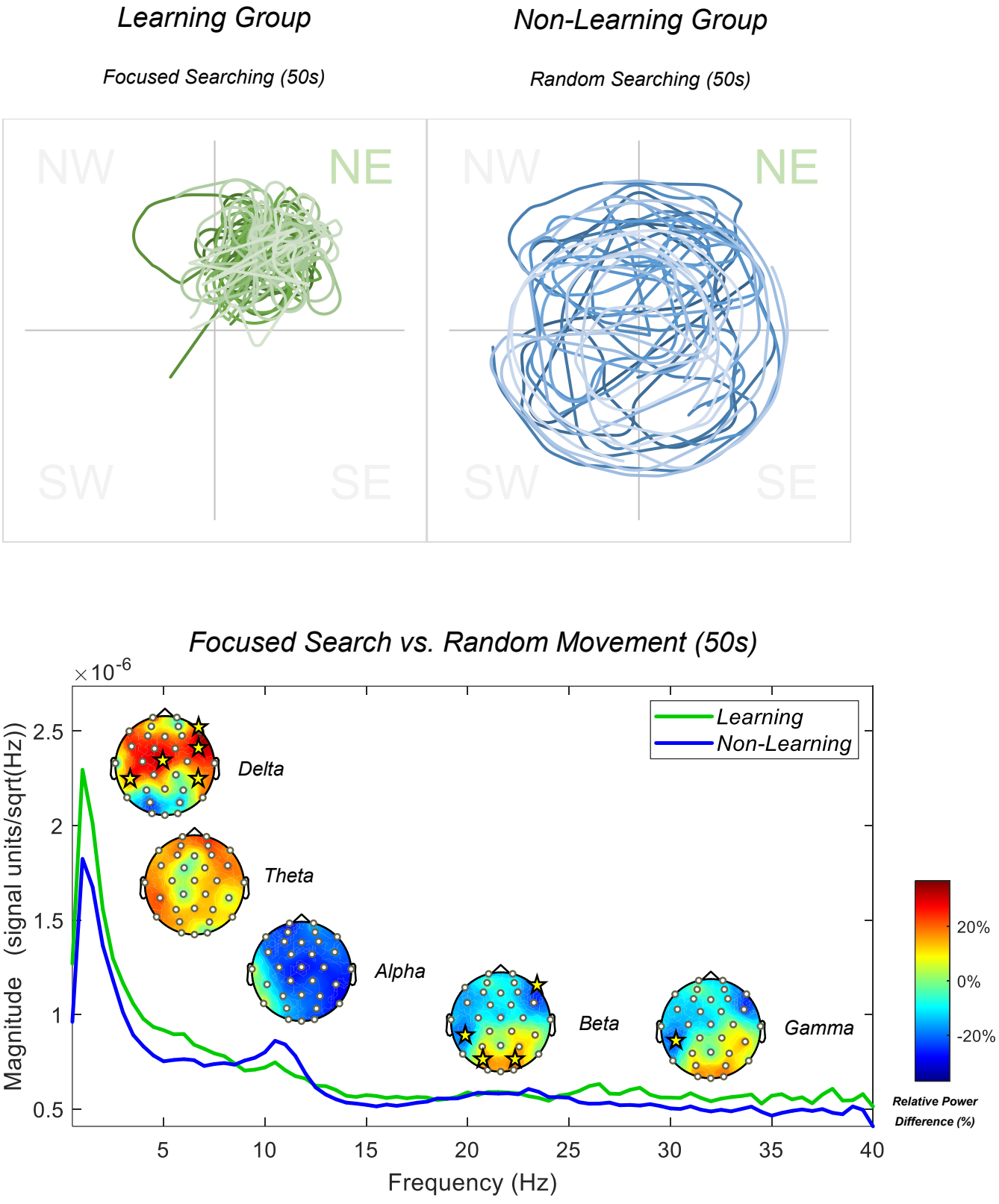


*Figure 4.8*: Learning & Non-Learning group paths generated via x-y co-ordinates from the last 50s of the recall trial are displayed above. Below these plots, we display the PSD spectrum from the comparison between the two groups in magnitude with a frequency resolution of 0.5 Hz during the last 50s of the recall trial. We then display corresponding topographies reflecting our frequency band definitions, which display the results of our between-subjects permutation t-tests. Yellow stars indicate electrode sites that have a significance level of 0.05 or less, following FDR-correction. Topographies are displayed in relative power differences, but PSD is plotted in magnitude based on guidelines from the literature.

*4.3.2.3.2 Switching Behaviour (Learning group)*

As mentioned previously, the learning group switched from goal-directed navigation to focused searching. This switch does not occur in the non-learning group, who searched randomly throughout the trial, as they had no location to learn. Therefore, we are interested to see if there is a difference in distribution of power within the two groups when this searching behaviour changes. Therefore, we examined relative power differences between the two phases [*First 10s vs Last 50s*] for each group using a paired permutation t-test with 5000 permutations, with an FDR-correction applied to the results. Here, we examined relative power as we are interested in the overall power increases/decreases that occur across frequency bands in response to the two observed changes in behaviour. We might expect that the searching would become more effortful during focused searching, as participants repeatedly attempted to recall the goal location. We would expect to find the opposite effect in the non-learning group, as continuously engaging in memory-driven recall is more challenging than free-navigation.

Figure 4.9 (top) shows that there is an increase in delta power across the frontal and central sites as the learning group focused their searching, but no electrode sites showed a significant change. Significant decreases were found primarily in the frontal (AF3, F3, FC1 and F8) and parietal (Pz and P4) sites in beta power. Similar decreases were found in gamma power, but to a lesser extent (significant at FC1 only). Figure 4.9 (bottom) shows that as the non-learning group progressed through the trial randomly, moving around the arena, there was a *significant* increase in alpha (primarily left hemisphere sites: AF3, F3 and P7). There was a notable difference at 11 Hz. In contrast to the learning group, there were significant widespread decreases in gamma (significant at sites FC1, FC2, Cz, CP1, CP5, P3, PO4). There was a similar decrease in beta but to a lesser extent (significant at FC1 only).

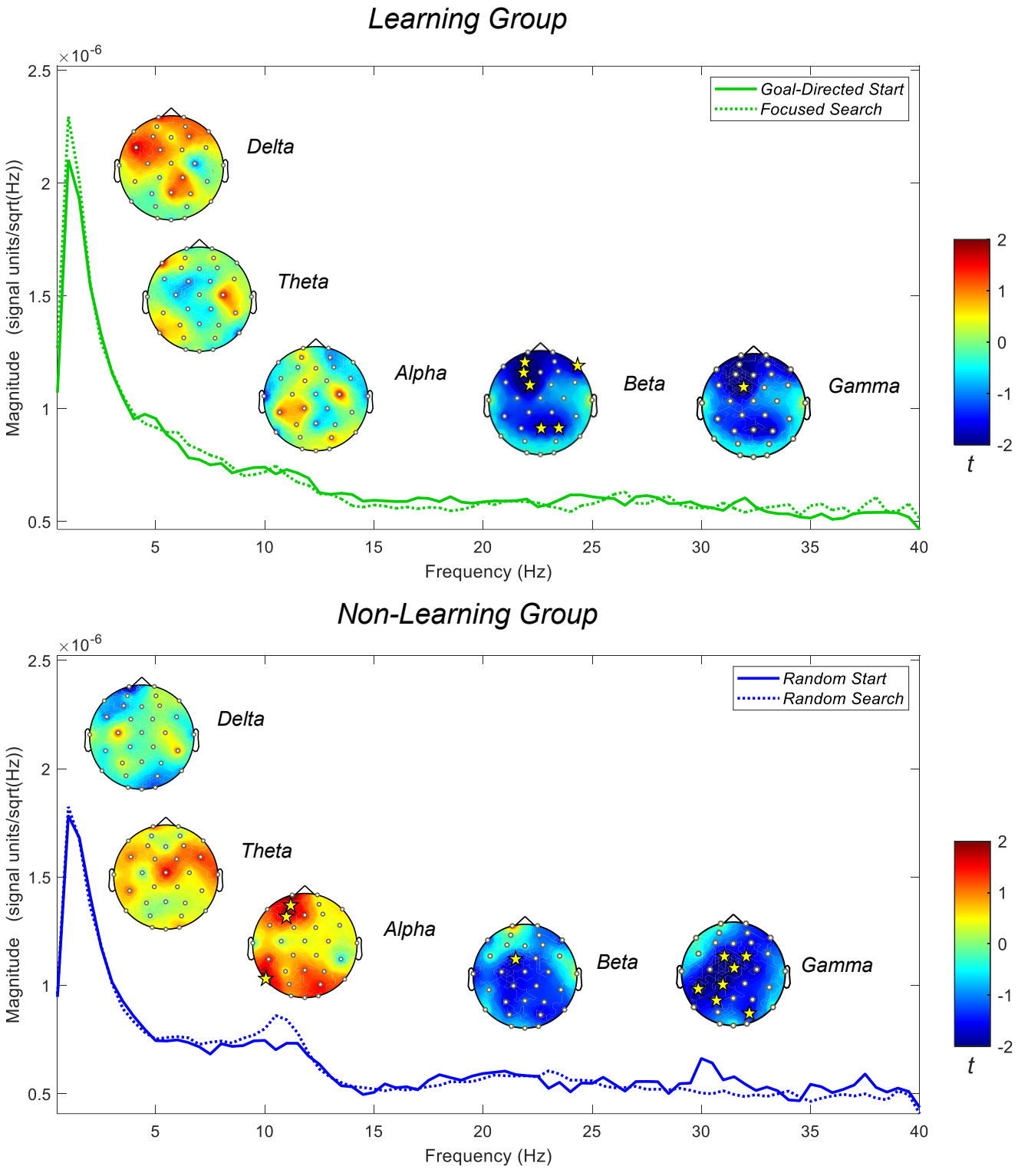


*Figure 4.9*: PSD plots for both groups display the within-group differences in power magnitude between the two phases of navigation behaviour. The solid line represents the first 10s of the recall trial and participants' start trajectory, and the dotted line represents the latter 50s of the recall trial and its relevant searching behaviour. Both PSDs are plotted on the same scale. Topographies display the results of the paired t-test within-groups on power changes within frequency bands. Topography is displayed in t-values and a small yellow star on an electrode

site represents significance at an alpha level of 0.05. T-test is permutation based with 5000 iterations and results are corrected for multiple comparisons using FDR-correction.

## 4.4 Discussion

The current chapter set out to perform an exploratory analysis of the oscillatory activity involved in immediate spatial recall of a goal location. We did not have any specific hypothesis for this chapter, though there were a couple of proposed events we expected to be observed, based on the human and animal literature. Firstly, we expected low-frequency oscillations (2-8 Hz) to play an important role in the recall process. Additionally, we expected alpha oscillations to be suppressed in the learning group, but not in the non-learning group. Furthermore, we expected to demonstrate some high frequency (> 15 Hz) differences between the groups. We discuss our findings based on different frequency bands.

### *4.4.1 Delta-Theta Oscillations*

We reported greater delta (2-4 Hz) and theta (5-7 Hz) power in our learning group compared to our non-learning group during the recall trial. Greater power was topographically located at frontal and central sites, though appears prevalent across the scalp. Though only select electrode sites show significance and not our frontal midline ROI, we suspect integrating more electrodes into our ROI as has been done previously (see Du et al., 2023) would reveal a significant interaction between group and region. Nevertheless, our results support the suggestion that low-frequency oscillations in humans (2-8 Hz) are involved in successful memory-guided navigation (Alekseichuk et al., 2016; Bohbot et al., 2017; Crespo-García et al., 2016; Greenberg et al., 2015; Liang et al., 2021; Vivekananda et al., 2021). The widespread activation of delta and theta in our learning group is contrasted with isolated or concentrated delta and theta activity in our non-learning group (see Figure 4.5). This idea is further supported by performing a behaviour-based analysis on our low-frequency oscillations. During goal-directed navigation at the start of the trial, we reported greater theta power across the scalp,

and greater delta power at central regions compared to our non-learning group's random starting trajectory. However, as participants switched to focused searching after realising that they had not successfully located the goal, we reported significantly greater frontal and central widespread delta power compared to the random searching of the non-learning group. Many of our significant electrodes were in the frontal right hemisphere of the scalp. Our results align with the previously discussed findings of the involvement of low-frequency oscillations within the range of 2-8 Hz being involved in successful spatial memory during navigation (Alekseichuk et al., 2016; Bohbot et al., 2017; Buzsáki & Moser, 2013; Chrastil et al., 2022; Delaux et al., 2021; Du et al., 2023; Greenberg et al., 2015; Liang et al., 2021; Lin et al., 2022; Miyakoshi et al., 2021; Watrous et al., 2013). Furthermore, our evidence suggests that theta supports the overall initial goal-directed retrieval and navigation, whereas delta (or lower frequency oscillations) become involved in subsequent focused searching, or when greater cognitive demand is placed on spatial memory systems.

These findings and interpretation map onto previously discussed intracranial data from humans, that illustrate successful associative retrieval results in increased low frequency oscillations (< 5 Hz), whereas low-frequency oscillations between 5-9 Hz seem to be increased during encoding (Bohbot et al., 2017; Kota et al., 2020; Lega et al., 2012). It could be argued here that the initial phase of goal-directed navigation does not require the recollection of learned associations (i.e., cue and goal) but instead incorporates retrieval of a place, using theta oscillations engaged during learning as found in our previous work (Thornberry et al., 2023). This information is retrieved from a cognitive map or a developed environmental schema (see General Introduction & General Discussion). When this retrieval strategy fails, low-frequency oscillations are further recruited to retrieve learned associations between the goal and other environmental stimuli (e.g., landmarks), to perform memory-dependent focused searching. Moreover, the involvement of the frontal midline during a virtual navigation task supports the

involvement of this region in active spatial navigation, reported by multiple other studies (Chrastil et al., 2022; Du et al., 2023; Liang et al., 2018; Liang et al., 2021; Lin et al., 2022; Mitchell et al., 2008). Nonetheless, it is difficult for us to report a *specific* role of increased frontal delta and theta in memory retrieval. However, it is clearly involved to a greater extent when a task has been learned, and delta in particular increases when applying memory based as opposed to random spatial search strategies.

### *4.4.2 Alpha Oscillations*

We reported a non-significant numerical trend toward less alpha (8-12 Hz) power in our learning group compared to our non-learning group across the entire duration of the recall trial. However no electrode site reached significance following correction of multiple comparisons. The non-learning group show distinctly heightened alpha (see Figure 4.5c) across the right hemisphere, with some concentration on central electrodes (C4 in particular, a sensorimotor electrode ipsilateral to the hand moving the joystick – all participants were right-handed). Some right-posterior electrodes also possess heightened alpha, with the learning group showing C4 activation, but not to the same extent. Furthermore, the non-learning group showed a non-significant trend increased alpha (centralised at ~11 Hz) during random searching, particularly as the trial progressed.

Our findings contradict the role proposed in Chapter 3 for the alpha rhythm (8-12 Hz). These are its involvement in attention, which is a robust finding reported throughout the literature (Foxe & Snyder, 2011; Händel et al., 2011; Harris et al., 2017; Klimesch, 2012; Klimesch et al., 1998). Firstly, the role of alpha in attention has been well documented. Decreases typically reflect an idle or focused state. Increases in this rhythm have been linked to difficulty focusing due to external, irrelevant or competing stimuli (Foxe & Snyder, 2011).

Our reported high-relative power in our non-learning group may indicate a lack of focus or attention during random exploration. As the trial progresses, this lack of focused or effortful attention increases. Alpha desynchronisation is typically associated with focused and controlled information processing (Klimesch, 2012). Our results from the learning group suggests that alpha may be supressed to a greater extent, and may index engaged memory-guided attentional mechanisms, facilitating focus and access to the memory of the goal. Lower alpha power has been reported during spatial attention tasks (Capotosto et al., 2009; Li et al., 2021; Thut et al., 2006). However, even with distractions, alpha power has recently been reported to decrease (Fodor et al., 2020). Nevertheless, we would argue that using memory-guided attention to navigate, suggests that this group have less effortful and more fixated attention – as their search strategy is memory-guided and place focused. Therefore, this interpretation would support the concept proposed by Du et al. (2023), that increased alpha reflects competing spatial cues. The non-learning group had more conflicting information processing and/or a lack of focused attention. It is possible that our results from Chapter 3 and those reported by Chrastil et al. (2022), could be explained by a disengagement of attention mechanisms following successful learning. However, we reported no significant electrodes sites within the learning group here. Further specific research on this topic is required.

Secondly, these alpha dynamics could also be explained by a dominant presence of the Mu rhythm (~ 10-12 Hz) within our alpha band. Mu is commonly found at the precentral motor cortex (C3, Cz, C4 electrodes: Garcia-Rill (2015)). Though it has been argued to be an idle rhythm, decreases in this rhythm can reflect goal-directed (Babiloni et al., 2014; Montirosso et al., 2019; Pineda, 2005) or cue-directed (Schneider et al., 2017) motor planning and execution. The significant increases (i.e., less suppression) in alpha (centred around 11 Hz) from the non-learning groups random start to random searching may reflect a lack of intentional sensorimotor engagement, hyperactivity or exploratory behaviour (Schneider et al., 2017). The mu

suppression in our learning group may then reflect memory-guided or cue-guided motor execution. Further research, with a focus on spatial attention would be required to confirm this. Therefore, considering our movement control and speed are kept constant between groups, we lean towards a spatial attention-related explanation of alpha activity. This would correspond to findings in Chapter 3, in which we reported less alpha in our learning group overall during learning (also see Thornberry et al., 2023) but gradually increasing alpha in both groups perhaps related to increased mind-wandering (Compton et al., 2019; Kam et al., 2022) or a reduction of focused-attention and motivation.

### *4.4.3 Beta-Gamma Oscillations*

We reported significantly elevated posterior beta (15-29 Hz) power in our learning group compared to our non-learning group across the entire trial at PO3 and PO4 electrodes, which are located around the occipital lobe. We reported similar trends for gamma (30-40 Hz) though no significant electrode sites were present at the posterior part of the scalp, though significant decreases were found at right frontal and left parietal sites as were found in beta. Significantly stronger posterior beta at the occipital regions in our learning group, was only found during the focused searching and not during the initial start trajectory. This may indicate that beta plays a role in more intense or directed visual scanning, as opposed to direct route following. Several studies also report enhanced beta and gamma power during visual and spatial working memory retention and maintenance (Park et al., 2011; Proskovec et al., 2018; Roux et al., 2012) particularly located at posterior parts of the scalp (Honkanen et al., 2015; Medendorp et al., 2007). Beta power at parieto-occipital regions has previously been reported to increase with memory load (Tuladhar et al., 2007). Roberts et al. (2013) found using scalp EEG that beta and gamma activity increased during the maintenance of spatial, but not temporal working memory.

Therefore, we suggest that greater beta power in our learning group at parieto-occipital sites may be related to memory maintenance or memory load, and possible memory-guided visual search – which is not used in the non-learning group.

Interestingly, we see significant suppression of beta in left frontal and right parietal regions as the learning group switch behaviour but report significant suppression of gamma at left-lateralised central regions in our non-learning group with time. Engel and Fries (2010) suggest that beta oscillations become suppressed when a novel or unexpected event occurs, forcing a change in the cognitive or perceptual status quo. Considering we see some significant suppression of beta within the learning group following a switch to focused searching, our results support this idea. Furthermore, considering they occur in frontal and parietal regions – we suggest this suppression is a cognitive or memory-related change rather than visual. Therefore, the gamma related suppression observed within our non-learning group, could be linked to increased alpha power, modulating visual attention processing of stimuli (Delaux et al., 2021), which is reported function of alpha–gamma networks, suggested to occur predominantly in the prefrontal cortex and parietal cortex (Roux & Uhlhaas, 2014). Bonnefond and Jensen (2012) reported weaker gamma activity during the processing of distractor stimuli compared to the processing of memory-related stimuli, suggesting lower gamma when presented stimuli are ignored. Considering there are no goal-related stimuli for this group, and that gamma power is greater in a group containing memory-related stimuli (e.g., learned place, landmarks or environmental features) our results may support this interpretation.

Nevertheless, we cannot conclude any clear role for these oscillations together and suggest that their suppression and greater powers are related to coupling with low-frequency oscillations between 2-8 Hz. Beta and gamma are incredibly broad bands and reflect multiple cognitive processes (see Herrmann et al. (2016)). As well as this, the actual functional roles of high frequency oscillations are still actively debated (Barone & Rossiter, 2021; Bragin et al.,

1995; Buzsáki & Wang, 2012; Engel & Fries, 2010). We did not measure eye movements, so cannot conclusively link occipital high frequencies to visual attentional processes. Yet, we believe the link between these high-frequency rhythms and activity at low-frequency are memory and attention related; and considering the constraints (but ecological validity) of our paradigm and the variables we control for (e.g., movement speed, time, landmarks etc.) more precise memory-focused experiments could help reveal the functions of these high-frequency oscillations.

### *4.4.4 Limitations and Future Directions*

We reported our findings in the context of relevant literature, and the current exploratory analysis is a follow-up from Chapter 3. The primary limitation is the use of a single recall trial. However, the design of the current study restricts direct comparison of findings between the two chapters. The analysis of the previous chapter differed greatly from the analysis approach of the current study. As we wanted to examine learning, we made use of the multiple trials carried out by participants, applying a Morlet wavelet analysis, and breaking down behaviour based on specific intra-trial events. Considering we are using the standard paradigm for the Morris water maze (Vorhees & Williams, 2006; Vorhees & Williams, 2014a) and the virtual water maze (Thornberry et al., 2021) we could only give participants a probe/recall trial once, as the goal location is removed. Since this is a novel environment again, giving any more trials would not actually examine memory. Furthermore, the nature of the VWM tasks means that memory-guided searching behaviour is elicited continuously. As a result, once a participant was engaged on their chosen path, there was no time window in between segments to serve as individual baselines to which the data could be normalized in the same way as in the previous chapter. As the data is continuously collected for the 60 second trial, statistical and oscillatory data only allowed for interpretations about the relative changes observed between the two

groups and behavioural conditions. The inclusion of individual baseline periods would have been required to compare effects within the spatial memory condition to the non-spatial memory condition individually, as opposed to each other. Future research should include a baseline data collection to facilitate changes from idle cognitive states to spatial memory "recall" states. We would recommend, and plan to implement a resting-state data collection for future chapters.

It should be noted that there are other limitations present in the current chapter. The sample of participants is much less than the previous chapter. At the time, participants could not stay for longer than one hour in the lab due to COVID-19 restrictions in place at the time. This meant that some participants could not perform their recall trial after learning the task. Data collection stopped entirely from 2020 to 2021 and eased back with looser restrictions then through 2022 in which participants from the learning phase, could participate in an immediate recall phase also. Therefore, the sample is smaller, and predominantly female; we did not include gender here due to the fact it had no influence on behaviour, no influence on any EEG learning measure (see Chapter 3) and due to the small sample size. Future studies should try to balance for gender, as some literature has illustrated behavioural and electrophysiological sex differences during spatial tasks (Astur et al., 1998; Astur et al., 2004; Kober & Neuper, 2011) and specifically during a virtual water maze task (Buckley & Bast, 2018). Previously discussed limitations are applicable here, such as low electrode numbers (32-channel cap), such low resolution prevents source analysis as it can lead to severe localisation errors (Michel & Brunet, 2019). Though more ecologically valid, our task does lack vestibular and sensorimotor feedback during the 2D navigation.

Though the use of the average reference is generally considered acceptable for continuous data (Li et al., 2020), this method of re-referencing should still be interpreted with caution. We plan to include mastoid electrodes in future chapters and assess if there are any

differences between average re-referencing and re-referencing to the mastoids. Furthermore, the assessment of navigation behaviour changes could be more precise, though we are limited by our software. We manually watched recordings of participants and analysed the x-y co-ordinates to assess the greatest angular shift visually and validated this across participants. We also considered the time-point based on the average latency in our learning group. However, though very much outside the scope of this thesis, machine learning algorithms or generalised mixed models could accurately extract significant angular shifts in traversed paths – which we have shown to be possible with NavWell (Commins et al., 2023; Palma et al., 2023).

### *4.4.5 Conclusion*

The current exploratory study provides support for particular oscillatory dynamics involved in spatial memory retrieval and memory-informed navigation behaviour. We have shown that these can be explored and evaluated using a virtual water maze task with non-invasive electrophysiological recording. In line with previous research, frontal and central cortical activity at lower frequencies such as delta (2-4 Hz) and theta (5-7 Hz) was associated with spatial memory retrieval, but particularly memory-informed focused searching. Theta power seems to support initial retrieval, whilst focused searching incorporates lower frequency oscillations. The power in these oscillatory bands was greater in our learning group, than the non-learning group. Our results suggest that lower alpha (8-12 Hz) power facilitates memory-guided attention, whereas greater power reflects a lack of focused attention. However, there are potential confounds of sensorimotor-related mu rhythms within this band. We suggest greater Beta (15-29 Hz) power at occipital sites may be involved in increased visual scanning during memory-guided searching or spatial memory maintenance during focused search behaviours. With a possible similar role for Gamma (30-40 Hz). Nevertheless, greater anterior low-

frequency oscillations and suppressed posterior alpha oscillations are associated with successful spatial memory retrieval and memory-guided navigation behaviour. This exploratory work is an essential step towards understanding the role and function of oscillation patterns in active virtual navigation.

# Chapter 5

# An investigation of oscillatory dynamics during recent and remote spatial memory

## Abstract

Brain oscillations are vital for several types of successful memory retrieval. Nevertheless, we typically allow a memory to consolidate prior to the need for recall. The dynamics of oscillatory activity in humans during successful spatial navigation following memory consolidation have not been addressed. Here, we recruited healthy young adults (n = 31). We recorded their electroencephalographic (EEG) activity during an immediate recall trial after they learned the location of a goal in a Virtual Water Maze task. Participants were then retested following a consolidation period of 24-hours or 1-month, producing either a recent (n = 16) or remote (n = 14) spatial memory. We computed and compared normalised power in all bands Delta (2-4 Hz), Theta (5-7 Hz), Alpha (8-12 Hz), Beta (15-29 Hz) & Gamma (30-40 Hz) across the scalp. We focused statistical analysis on regions of interest from Chapter 4, the frontal, parietal, central and occipital midlines. No performance differences were found behaviourally between the recall of spatial memories encoded 24-hours ago versus 1-month ago. However, we reported increased power in lower frequency bands delta (2-4 Hz) and theta (5-7 Hz) over frontal regions, during the consolidated recall trial compared to immediate recall. Additionally, frontal gamma increases were unique to remote retrieval. Delta/theta-gamma activity mirrors previous intracranial findings and provides further evidence that high-frequency oscillations support retrieval of cortically integrated remote memories. Overall, our results likely reflect greater cognitive demand and the requirement of a more controlled retrieval processes for consolidated memories.

## 5.1 Introduction

Spatial memory supports the encoding and retrieval of locations and objects in our environment, which are essential to understanding where we are and where we have been (Ekstrom et al., 2018). The memory for space is just one component of overall spatial cognition, which facilitates orientation, mental rotation, associative learning, path integration and cognitive mapping (see Chapter 1). Spatial memory, much like learning, is essential for navigating our environment, but also for adding context to our episodic memories (Ekstrom & Ranganath, 2018; Smith & Mizumori, 2006). The involvement of the medial temporal lobe, and in particular the hippocampus in spatial memories has been well supported (Maguire et al., 2003; O'Keefe & Dostrovsky, 1971; O'Keefe & Nadel, 1978; Schapiro et al., 2019; Spiers & Maguire, 2008; Stachenfeld et al., 2017). As previously discussed, research with rodents using the Morris water maze revealed that lesions to the hippocampus impair recall during probe trials (Barkas et al., 2010; Broadbent et al., 2006; de Bruin et al., 1994; Farina & Commins, 2016; Inostroza et al., 2011; Morris et al., 1982; O'Keefe, 1993). A single recall trial (see Chapter 2, section 2.2.1.2) is typically used as a measure of spatial memory; the platform is removed from the pool for the trial and the percentage of time spent searching in the correct quadrant of the environment where the goal once was is measured (Barnhart et al., 2015; Maei et al., 2009; Vorhees & Williams, 2006; Vorhees & Williams, 2014a).

Memories can have time-dependent differences in how they are retrieved. Recent spatial memories, formed within the last 24-hours for example, usually contain detailed and contextual episodic events – as they are thought to be dependent on the hippocampus (Ekstrom & Ranganath, 2018; Ekstrom et al., 2018; Nadel et al., 2000; Winocur et al., 2010). Remote spatial memories, formed longer ago can often be less detailed and more schematic in nature as they become hippocampus independent (Bolding & Rudy, 2006; Inostroza et al., 2011; Lifanov et al., 2021; Tse et al., 2007). However, human patients with hippocampal damage can

recall significant details about environments encoded remotely, such as the distance between landmarks (Daugherty & Raz, 2017; Luna & Martínez, 2015), but can struggle when locating a learned goal (Astur et al., 2002; Kim et al., 2013). Standard Consolidation Theory (Broadbent et al., 2006; Squire et al., 2015) suggests the hippocampus is responsible for the encoding and consolidation of memories. The memory trace is present in both the hippocampus and the cortex, with the cortex trained to hold all details of the memory following replay (Frankland & Bontempi, 2005; Marr et al., 1991). The theory predicts that the hippocampus is not required for the retrieval of remote memories, only recent ones that have not yet been fully consolidated (Squire et al., 2015). However, Multiple Trace Theory suggests that the hippocampus plays a role in episodic memory retrieval regardless of being recent or remote (Moscovitch et al., 2006; Nadel et al., 2000). Traces of the memory in the hippocampus are contextual and detailed in spatial information, whilst those traces in the cortex are mainly sematic (Moscovitch et al., 2006; Sutherland et al., 2020). The debate has multiple conflicting findings, and recently it is thought that cortical oscillations may instead reveal greater information about how spatial memories are stored and retrieved.

However, it is evident in humans that there exists a temporal gradient for spatial memory. Retrieval of spatial memory in a virtual navigation task is better for locations learned recently, as opposed to locations learned further in the past (Ekstrom & Bookheimer, 2007; Hirshhorn et al., 2012). Increased low-frequency power (1-8 Hz) during retrieval, has been demonstrated during episodic retrieval of remote memories (Nicolás et al., 2021). During spatial retrieval, numerous studies have reported increases in frontal midline delta and theta power (1-8 Hz). For example, Liu et al. (2022) reported increased frontal midline delta and theta (< 8 Hz) during a difficult variation of a wayfinding task compared to an assisted version. These increases may relate to increased memory load (Jensen & Tesche, 2002; Li et al., 2021), as alpha (8-12 Hz) suppression was greater during this phase at the parietal midline, possibly

related to heightened information processing or attentional demand (Benedek et al., 2014; Fodor et al., 2020; Foxe & Snyder, 2011; Li et al., 2021; Mitchell et al., 2008). However, most studies have linked increased delta and theta to decision-making points during navigation (Chrastil et al., 2022; Du et al., 2023; Lin et al., 2022). Frontal theta has been shown to be linked to hippocampal activation during spatial memory tasks (Epstein, 2008; Herweg, Sharan, et al., 2020; Herweg, Solomon, et al., 2020). Successful memory retrieval has also shown the involvement of beta and gamma oscillations, particularly at posterior parts of the scalp (Lundqvist et al., 2016).

Gamma oscillations (>30 Hz) have also shown increases during cued spatial retrieval tasks at the medial parietal cortex (Kaplan et al., 2014; Kaplan et al., 2012). The coupling between low-frequency theta and high-frequency gamma oscillations has been shown to be related to performance on a spatial delayed match-to-sample task (Park et al., 2011) and pictorial recognition task (Köster et al., 2014; Vivekananda et al., 2021). However, alpha (8-12 Hz) activity has previously been shown to decrease with the retrieval of spatial locations from working memory (Sutterer et al., 2019; Wolff et al., 2017). Hanslmayr et al. (2012) also claims that alpha (8-12 Hz) decreases were associated with retrieval of spatial locations from long-term memory, and accurately reflects the same patterns of activation seen during encoding (Griffiths et al., 2021).

However, in humans most work currently focuses on retrieval success and failure (Greenberg et al., 2015; Guderian et al., 2009; Herweg, Solomon, et al., 2020; Kota et al., 2020; Miyakoshi et al., 2021). There appears to be a gap in the EEG literature on spatial memory and oscillatory differences between recent and remote recall. Therefore, it is still an open question whether delta, theta, alpha, beta or gamma oscillations differ across consolidation time for spatial memories. Neural oscillations may hold the key to understanding and developing consolidation theories, and in particular, their relationship with the cognitive mapping theory.

Therefore, we have examined differences in oscillatory activity underlying recent (24 hours) and remote (1-month) spatial memory during a recall probe trial in a virtual water maze task. We will examine activity in delta, theta, alpha, beta & gamma in participants who have successfully learned the task and are recalling the location of a goal in the environment following their assigned interval. We compared activity in these frequency bands to each groups immediate probe trial, performed after their learning phase (e.g., Chapter 4) and then compared the differences between groups during their recent and remote probe trials. We compared this across four regions that were used in previous chapters: the frontal midline (F3, Fz, F4), parietal midline (P3, Pz, P4), central midline (C3, Cz, C4) and occipital midline (O1, Oz, O2).

We would hypothesise greater delta-theta activity in our remote group, possibly related to the retrieval of older, more semanticised spatial memories from the cortex (Frankland & Bontempi, 2005) which may require greater neural resources (Jaiswal et al., 2010). We also predict reduced alpha activity in our remote group compared to our recent group, as detailed spatial representations become more schema-like over time they may rely more on attention to the environment (Engel & Fries, 2010; Lundqvist et al., 2016; Robin & Moscovitch, 2017). Finally, we expect to see greater high frequency power in beta and gamma power at posterior sites in our remote group, related to the more effortful retrieval of complex visual and spatial information from long-term memory storage, as suggested by Crespo-Garcia et al. (2012) and Stutterer et al. (2019).

## 5.2 Methods

### *5.2.1 Participants*

Thirty-one new young adults (21 females, 10 males) aged between 18 and 40 (M = 21.7, SEM +/- 0.708) were recruited for this chapter. All participants were right-handed. All participants were recruited via Maynooth University Department of Psychology and externally using personal connections, flyers, and social media (see Chapter 2 for more details). This project and the use of human subjects with EEG was approved by the Maynooth University ethics committee (BSRESC-2021-2453422 & SRESC-2021-2453422).

### *5.2.2 Resting State Task*

Considering the lack of a standardised, non-task related baseline, we decided to implement the recording of resting state activity before running the spatial navigation task. The task was constructed using E-Prime Psychology Software Tools, version 3.0 (2022). The task was presented to participants seated 50 cm from a 15-inch standard 4:3 ratio computer screen, on their own in a darkened, electrically shielded and sound-attenuated testing cubicle (150 cm × 180 cm). The trial began with a fixation cross presented in the centre of the screen for the duration of three minutes (see Figure 5.1). The fixation-cross was displayed in black Courier New size 32 font on a silver background. Participants were asked to focus on the fixation cross with their eyes-open for the entire three minutes, which has been shown to be a useful timeframe acting well as a baseline for task-related activity (Chen et al., 2008; Chen et al., 2013; Huang, 2019). When the pre-test screen disappeared, and the fixation cross appeared on the screen (see Figure 5.1) an event trace, i.e., trigger, was automatically sent to the BioSemi system event (with < 10ms resolution). The eyes-open resting state lasted three minutes and participants were offered a rest period before they began the spatial navigation task.

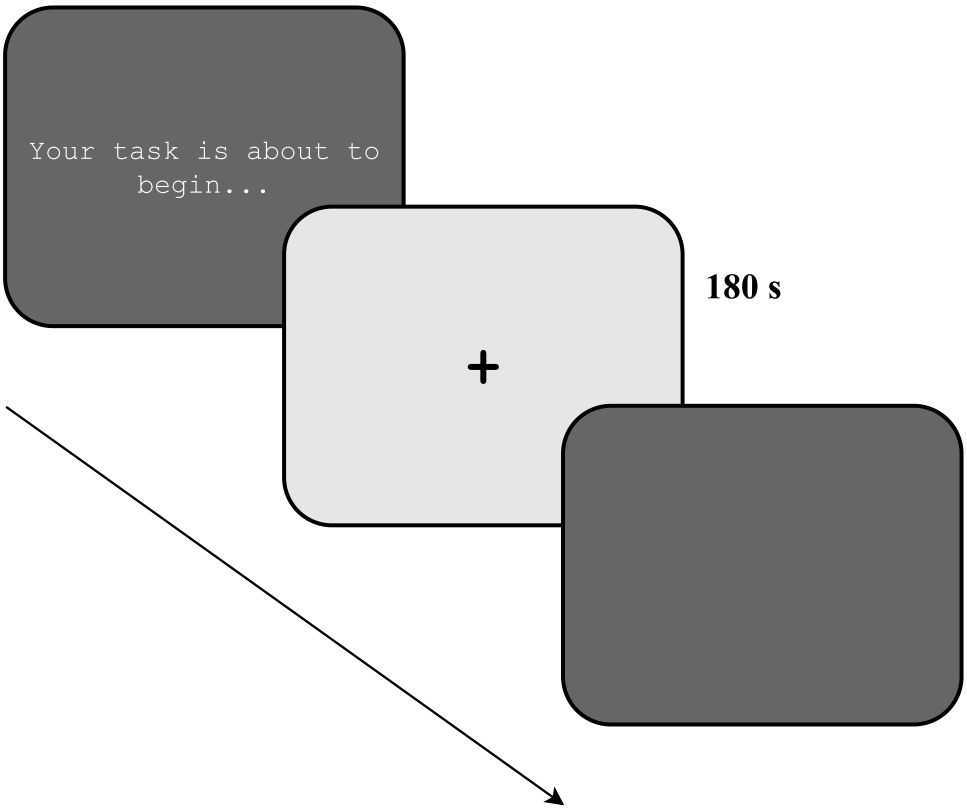


*Figure 5.1:* Example of resting state data collection trial. Participants were presented with the text "Your task is about to begin…" as they were seated in the experimental cubicle and electrodes were adjusted. The door was then closed and subsequently participants were asked if they were comfortable and ready to begin. Upon confirmation, the experimenter would start the task. A fixation cross would appear on the screen for 180 seconds. The screen would turn dark and display no text when the resting state trial was over.

### *5.2.3 Spatial Navigation Task*

After the electrophysiological preparation (see Chapter 2 for details), collection of resting state data and the completion of the learning phase (similar to that reported in Chapter 3), participants were seated as described previously with access to a joystick for navigating. The spatial navigation task used was NavWell (see Commins et al. (2020) for details). The same virtual maze setup used in the previous chapter was employed (see Chapter 2 for more details). A square goal was placed in the middle of the northeast quadrant and was 15% of the total

arena size and consisted of a bright blue square that only became visible when the participant crossed it. Once the learning phase was completed, all participants took a 10–15-minute break. During the break, participants completed a small battery of cognitive tasks as outlined in Chapter 2. Following this, participants were given a single 60-second recall trial, in which they were required to re-locate the target. However, for this trial, the target was removed from its location in the NE quadrant. All participants started from the same novel south-west (SW) location. Participants were then randomly allocated to either a recent condition (n = 16, 11 females) or remote condition (n = 15, 11 females). Following the immediate recall trial, participants in the recent condition were asked to come back 24-hours later, to perform another recall/probe trial as described above. Alternatively, those allocated to the remote group were asked to return in 1-month, to also perform another recall/probe trial.

### *5.2.4 EEG Recording*

EEG data was acquired using a BioSemi ActiveTwo system (BioSemi B.V., Amsterdam, Netherlands) providing 32 Ag/AgCl electrodes positioned according to the 10/20 system that was used during the learning phase (see section 3.2.3 "*EEG Recording*" or Chapter 2). Participants did not remove any equipment during the rest period. Electrode impedance was checked and adjusted to be below < 20Ω before recording began again. Analogue event signals were sent only once when participants began a trial recall. All participant trial times were 60 seconds in length. The recording system was stored in the same room, participants were seated, and data were recorded continuously. A PC running the ActiView software (version 7.05) was positioned in the room adjacent to the experimental cubicle, for constant monitoring of the EEG recording. Participants were asked to relax and move as little as possible. Six external electrodes (EXG1 – EXG6) were positioned on the face and under the ear. They were checked

and readjusted if necessary. Raw EEG data were again sampled at 1024Hz but down-sampled offline to 512 Hz (see Chapter 2 & 3 for details).

### *5.2.5 EEG Preprocessing*

Continuously recorded EEG data were analysed offline in MATLAB R2021B using scripts in combination with the Brainstorm package (Tadel et al., 2011). All previously used preprocessing steps remain the same as Chapter 4 (band-pass, ICA etc.). For the analysis of both recall trials, the entire continuous recording was then epoched into 2-second epochs, producing 30 epochs per participant for each probe trial, and 90 trials per participant for resting state. All of these data were visually inspected for bad segments and bad electrodes, which were then removed. Bad electrodes that originated from pre-defined regions of interest were interpolated (n = 1), if possible, using Brainstorm after ICA. Epochs with voltage steps above 100 µV or peak-to-peak signal deflections exceeding 200 µV within 2-s intervals were automatically rejected. We had a very low rejection rate of approximately 3% of the total epochs produced. EEG data were then re-referenced to two mastoid electrodes (EXG5 & EXG6) positioned behind the ears of the participant. For further information on EEG pre-processing see Chapter 2.

### *5.2.6 EEG Spectral Analysis*

Based on the protocol and our proposed research question, we investigated five frequency bands: delta (2-4 Hz), theta (5-7 Hz), alpha (8-12 Hz), beta (15-29 Hz) & gamma (30-40 Hz). The bands were defined using the default Brainstorm settings for the band for this chapter. Power spectra were computed on artefact-free epochs for each participant on both recall trials and resting state data. We used Hanning windows of 2-s with a 50% overlap using Welch's

method for all electrodes. This resulted in an averaged PSD spectrum with frequency resolution of 0.5 Hz, and the power was computed using the underlying short Fast Fourier Transform (sFFT) with a linear frequency distribution of 1:1:40. This was then grouped into the previously defined bands using the *Frequency > Group in time or frequency bands* process.

We then normalised the task-related PSD using a baseline correction method. Taking the non-task related resting state PSD, we baseline corrected each individual participants task-related data (i.e., immediate recall and recent/remote recall) using a decibel (*dB*) conversion:

$$dB_f = 10 \times \log_{10}\left(\frac{signal\ power_f}{baseline\ power_f}\right)$$

When we refer to relative power in this chapter, it is related to power (*dB*) with respect to the baseline. We did this by using the process: *Standardize > Baseline normalization (A=Baseline) > Scale with the mean (dB)*. We again focused our analysis on our pre-defined regions of interest, extracting these data for each individual participant. We examined the power relative to baseline at the frontal midline (Fz, F3, F4) and the parietal midline (Pz, P3, P4) once again capturing activity from both the anterior and posterior parts of the scalp. As this analysis was exploratory, we investigated more regions that may be of interest, including the central midline (C3, Cz, C4) and the occipital midline (O1, Oz, O2). All epochs in each group and phase, were averaged together following computations.

### *5.2.7 Statistical Analysis*

Statistical analyses & visualisation of the behavioural and EEG data were performed using a combination of JASP (version 0.15), MATLAB and R software version 4.0.2 with the tidyverse and ggplot2 package. First, statistics were performed using extracted values from the power

spectra via the *extract > values* process in Brainstorm. We then extracted mean power relative to baseline data from our ROIs. Statistical exploration of the EEG data across the scalp was performed using Brainstorm in MATLAB 2021b, comprising of two-tailed non-parametric independent or paired *t*-tests with 5000 permutations and a *p*-threshold of 0.05. We corrected for multiple comparisons in EEG data using an FDR (False Discovery Rate) correction. All data were combined for EEG analysis, but gender was included as a factor in the overall behavioural analysis (based on its inclusion in Chapter 3 and Thornberry et al. (2023)). Mixed-factorial ANOVAs were computed on the behavioural data comparing the two groups on time spent in each quadrant of the arena. Further mixed factorials were done for each frequency band, comparing the groups across the various ROIs. Bonferroni corrected *t*-tests were used to follow up within analysis, and independent sample *t*-tests were used to follow up any group differences.

## 5.3 Results

### *5.3.1 Behavioural Results*

Initially, we compared scores from both conditions on a variety of cognitive tests to ensure that both groups were generally cognitively matched. There were no significant differences between the two conditions on the number of NART errors ($t(29) = 1.214$, $p = 0.234$), total time to complete the TMTB - time to complete TMTA ($t(29) = 1.617$, $p = 0.117$) and scores on the MOCA ($t(29) = -0.182$, $p = 0.857$). In addition, both conditions were well matched for mean age ($t(29) = 1.086$, $p = 0.287$).

#### *5.3.1.1 Learning Phase*

We first analysed the learning performance of participants in both conditions *a priori*: recent (24-hours, n=16, 11 female) or remote (1-month, n=15, 10 female) to check that both groups had learned the task equally. One participant from the recent memory group had data synchronisation issues due to the network connection during the learning phase. However, their retention data synchronised successfully, so they were included in all analyses for which they had data. In order to remain consistent with Chapter 3, we ran a 2 (condition) X 2 (gender) X 12 (trial) repeated measures mixed factorial ANOVA to examine latency and path length across the trials.

For latency, we reported a main effect of trial ($F_{(4, 103.3)} = 27.323$, $p < 0.001$, $\eta^2 = 0.430$). But we reported no significant difference between the conditions ($F_{(1, 26)} = 0.023$, $p = 0.881$) nor gender ($F_{(1, 26)} = 0.012$, $p = 0.913$). We reported no significant interaction effect between trial X condition ($F_{(4, 103.3)} = 1.822$, $p = 0.131$) nor for trial X gender ($F_{(4, 103.3)} = 1.820$, $p = 0.131$) with no significant three-way interaction effect reported ($F_{(4, 103.3)} = 0.655$, $p = 0.623$). Using Bonferroni corrected t-tests we demonstrated that latency during Trial 12 was

significantly shorter than Trial 1 (MD = 34.79s, SEM +/- 2.47, $p < 0.001$, Cohen's $d = 3.758$) & Trial 2 (MD = 11.55s, SEM +/- 2.47, $p < 0.001$, Cohen's $d = 1.248$).

For path length, we reported a main effect of trial ($F_{(2.5, 65.9)} = 36.424$, $p < 0.001$, $\eta^2 = 0.504$). But we reported no significant difference between the conditions ($F_{(1, 26)} = 0.336$, $p = 0.567$) or genders ($F_{(1, 26)} = 0.211$, $p = 0.649$). We reported no significant interaction effect between trial X condition ($F_{(2.5, 65.9)} = 2.234$, $p = 0.102$) nor for trial X gender ($F_{(2.5, 65.9)} = 1.735$, $p = 0.176$) with no significant three-way interaction effect reported ($F_{(2.5, 65.9)} = 0.376$, $p = 0.737$). Using Bonferroni corrected t-tests we demonstrated that participants' path lengths during Trial 12 were significantly shorter than Trial 1 (MD = 149.98 Vm, SEM +/- 9.57 Vm, $p < 0.001$, Cohen's $d = 4.213$) & Trial 2 (MD = 70.28 Vm, SEM +/- 9.57, $p < 0.001$, Cohen's $d = 1.974$). All participants clearly successfully learned the task, reducing times and path lengths across trials (see Figure 5.2).

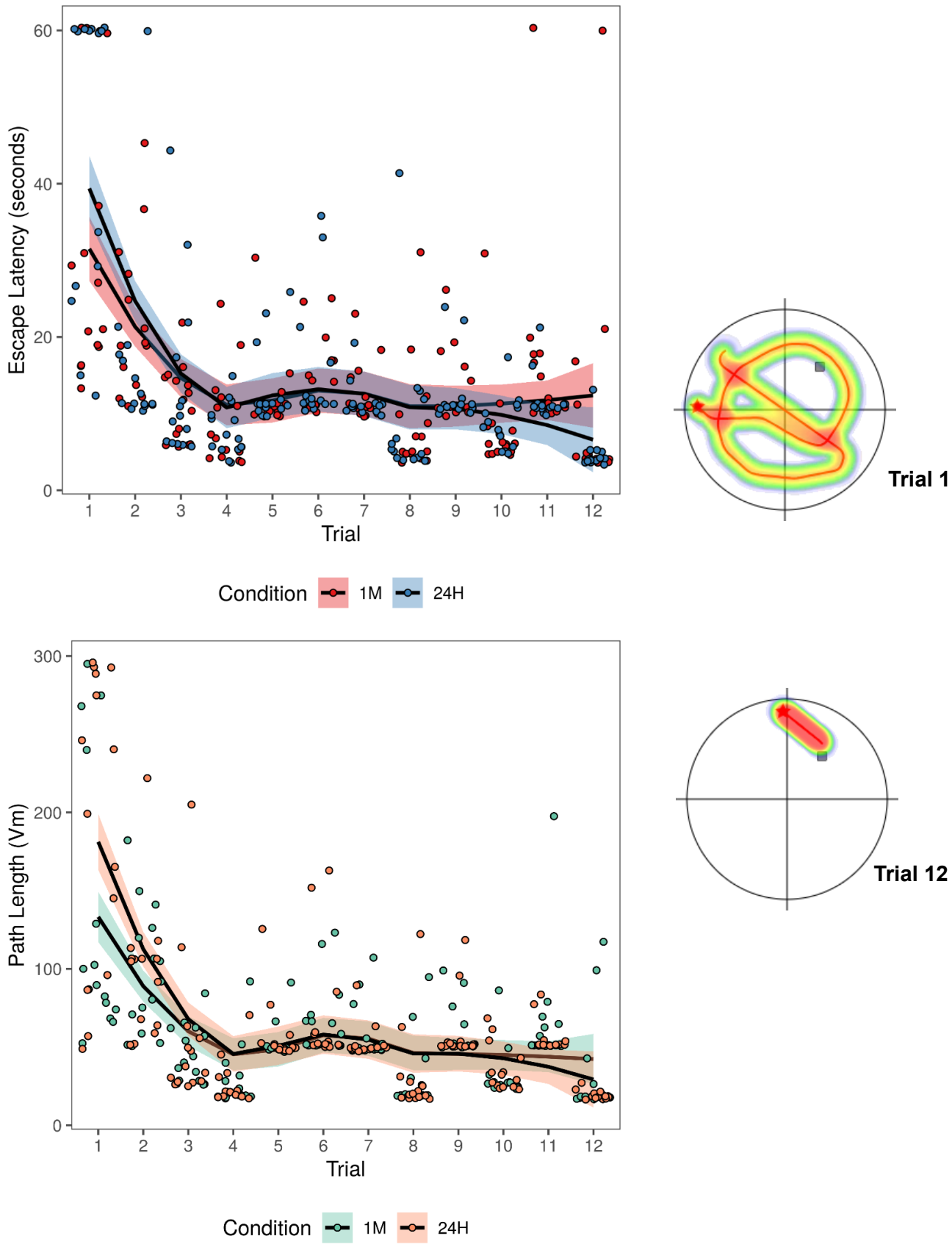


*Figure 5.2:* Line charts displaying individual data points and mean latency (top) and path length (bottom) across all participants and divided by condition (1M: remote and 24H: recent). Heatmaps of a sample participants path and search behaviour are displayed for trial 1 and trial 12.

*5.3.1.2 Recall*

Following the learning phase, all participants were given a probe trial (the target was removed from the arena) after a ten-minute interval. We termed this "immediate recall" as there is no real consolidation time, and it replicated the recall phase examined in Chapter 4. Since the probe trial for both groups are equivalent in length (60 seconds; see General Methods) we examined percentage time spent searching in the goal quadrant (Northeast), a typical measure in the animal and human versions of the water maze task (Vorhees & Williams, 2014; Thornberry et al., 2021). We again examined the two groups *a priori* on this trial as a check to make sure that the two groups could recall the location equally – and that any difference between the groups was due to the consolidation period rather than poor recall. For this we ran a 2 (condition) X 2 (gender) X 4 (quadrant) mixed factorial ANOVA.

For the immediate recall trial, we reported a main effect of quadrant ($F_{(1.5,\ 39.8)}$ = 231.250, $p < 0.001$, $\eta^2 = 0.882$). We did not report any differences between the conditions ($F_{(1,\ 27)}$ = 0.503, $p$ = 0.484) nor genders ($F_{(1,\ 27)}$ = 0.484, $p$ = 0.493). Additionally, we reported no significant interaction effect for condition X quadrant ($F_{(1.5,\ 39.8)}$ = 3.436, $p$ = 0.055), nor for gender X quadrant ($F_{(1.5,\ 39.8)}$ = 0.432, $p$ = 0.592) nor a three-way interaction effect ($F_{(1.5,\ 39.8)}$ = 0.146, $p$ = 0.799). Bonferroni-corrected *t*-tests revealed that (averaged over the levels of condition and gender), the percentage time spent searching in the NE (Goal) quadrant was significantly greater than all other quadrants, the NW ($t$ = 20.257, $p < 0.001$, MD = 57.61% +/- 2.84%, Cohen's $d$ = 6.356), SW ($t$ = 19.519, $p < 0.001$, MD = 55.51% +/- 2.84%, Cohen's $d$ = 6.125) and the SE ($t$ = 23.773, $p < 0.001$, MD = 67.61 % +/- 2.84%, Cohen's $d$ = 7.460). Therefore, all participants recalled the goal location, spending significantly more time in the NE quadrant than any other regardless of their assigned condition. All other quadrant searching percentages are below chance levels (see Figure 5.3).

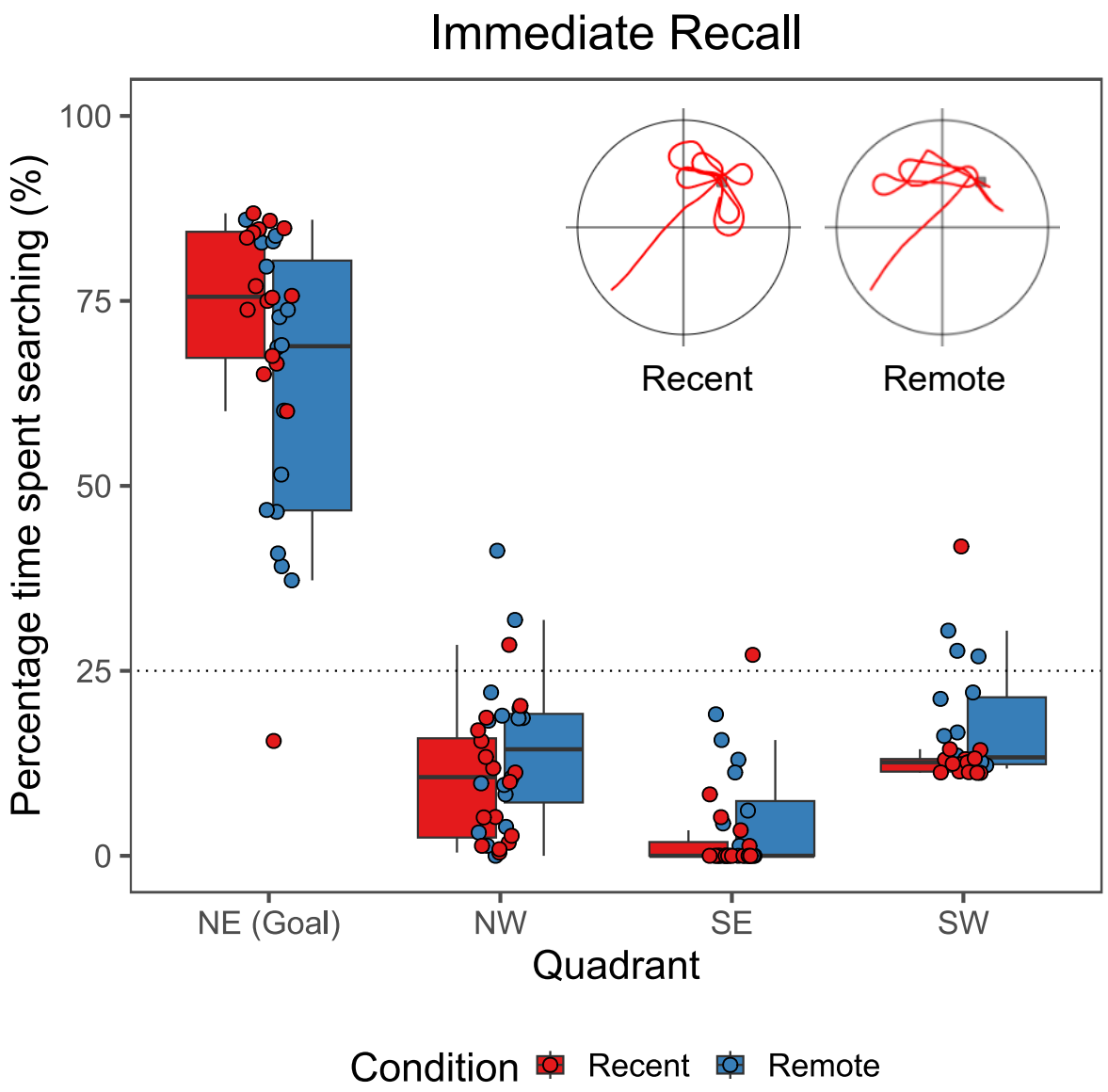


*Figure 5.3:* Boxplots with jittered individual datapoints showing the percentage time spent searching in each quadrant during the immediate probe trial, which was given approximately 10 minutes following learning. The group condition is displayed to demonstrate similarities between the two groups during immediate recall. The dotted line at 25% represents chance levels.

*5.3.1.3 Recent vs Remote Memory*

For the recent and remote conditions, we examined the corresponding follow-up probe trial for each group, given either 24-hours later or 1 month later. We ran the same 2 (condition) X 2 (gender) X 4 (quadrant) repeated-measures ANOVA on these data also. We reported a significant main effect of quadrant ($F_{(1.3, 34.9)} = 603.882$, $p < 0.001$, $\eta^2 = 0.954$). However, we reported no significant differences between the conditions ($F_{(1, 27)} = 0.175$, $p = 0.679$) or genders ($F_{(1, 27)} = 0.0003$, $p = 0.986$). Interestingly, we reported no significant interaction effects for condition X quadrant ($F_{(1.3, 34.9)} = 0.787$, $p = 0.412$), gender X quadrant ($F_{(1.3, 34.9)} = 0.071$, $p = 0.852$) nor a three-way interaction effect ($F_{(1.3, 34.9)} = 1.129$, $p = 0.312$). Once again, Bonferroni corrected t-tests revealed that the percentage time spent in the NE was significantly greater than time spent in the NW ($t = 34.691$, $p < 0.001$, MD = 70.2% +/- 2.02%, Cohen's $d = 10.887$), SW ($t = 31.950$, $p < 0.001$, MD = 64.65% +/- 2.02%, Cohen's $d = 10.027$) and SE ($t = 36.906$, $p < 0.001$, MD = 74.68% +/- 2.02%, Cohen's $d = 11.582$). Therefore, there was no difference between the conditions on recall ability. This suggests that even after a month, participants could recall the goal's location. No differentiation in memory was noted (Figure 5.4). Finally, to examine any changes between the immediate recall phase and participants' recall at a subsequent phase (either 24 hours or 1 month later) a 2 (phase) X 2 (group) mixed factorial ANOVA was conducted using the percentage time spent searching in the goal quadrant. We reported a significant main effect of phase ($F_{(1, 29)} = 11.450$, $p = 0.002$, $\eta^2 = 0.075$) but reported no significant difference between conditions ($F_{(1, 29)} = 3.111$, $p = 0.088$). But we reported a significant interaction effect between phase X condition ($F_{(1, 29)} = 4.315$, $p = 0.047$, $\eta^2 = 0.028$). Tukey-corrected *t*-tests revealed that the 1-month group seemed to *improve* their searching accuracy after 1-month ($t = 3.801$, $p = 0.004$, Cohen's $d = 0.940$, MD = 10.76% +/- 2.83%), whereas the 24-hour group did not ($t = 0.939$, $p = 0.784$, Cohen's $d = 0.225$, MD = 2.57% +/- 2.74%) improve on their immediate performance.

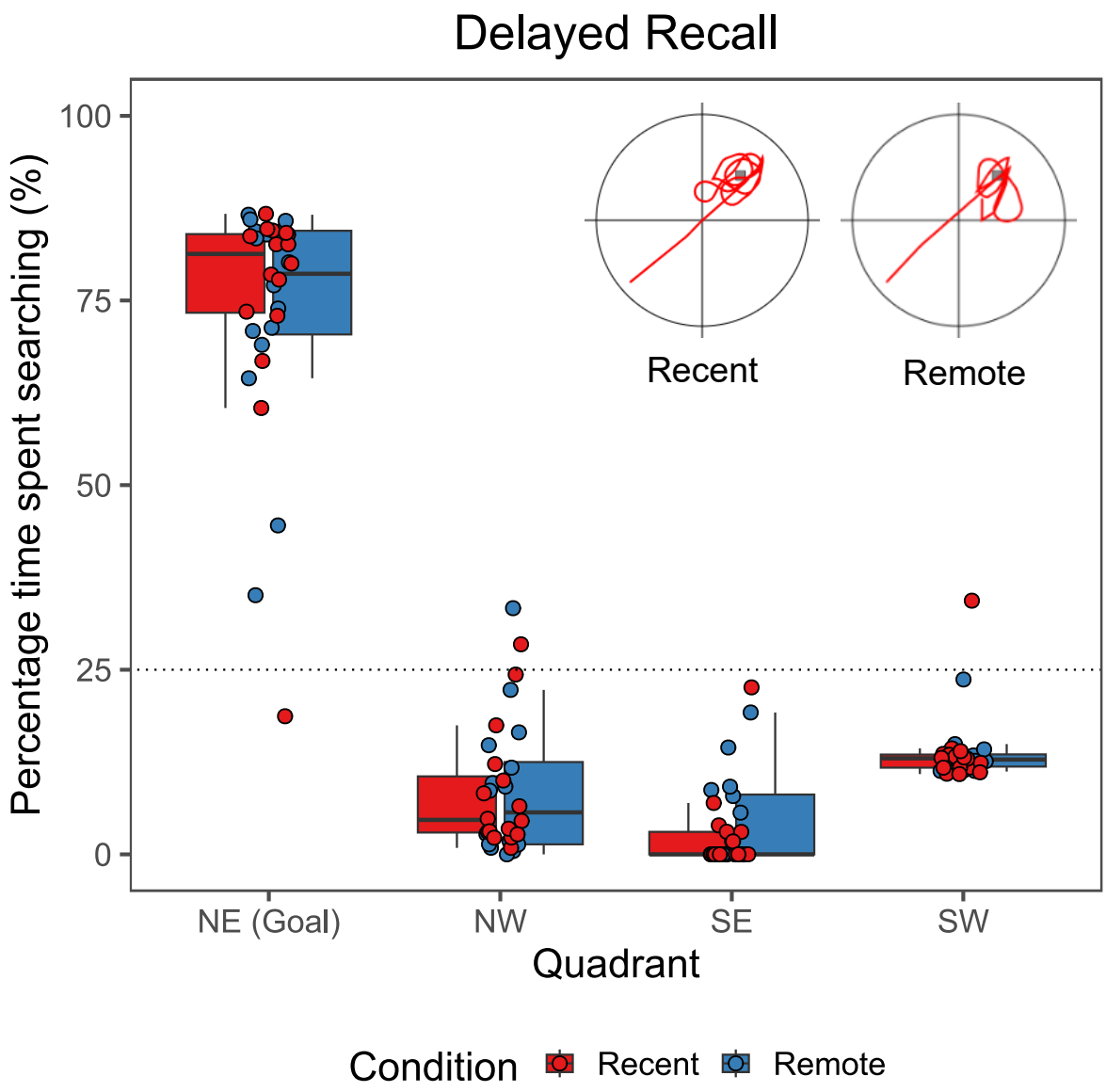


*Figure 5.4:* Boxplots with jittered individual datapoints showing the percentage time spent searching in each quadrant during the delayed probe trial, which was given either 24-hours (for the recent group) or 1 month (for the remote group) later. The dotted line at 25% represents chance levels.

### *5.3.2 EEG Results*

#### *5.3.2.1 Replication of immediate recall findings*

Initially, we thought it would be valuable to investigate whether our previous exploratory findings on immediate recall from Chapter 4 (n = 15, 10 female) would replicate to a larger sample size used in the current chapter (n = 31, 21 female). A total of n = 3 had incomplete immediate recall data and were excluded from the EEG analysis. However, to avoid mass univariate testing and comparison of results under two different recording and preprocessing conditions, we compared the two experimental groups on mean relative power (uncorrected) at our four ROIs using standard independent *t*-tests. Additionally, we compared the topographical power distribution visually to investigate if we would see similar spatial patterns during immediate spatial memory recall. Here, we ran a 4 (ROI) X 2 (Group, i.e., *Chapter 4 or Chapter 5*) for each frequency band separately, to report differences between groups or between the groups at certain ROIs (i.e., interaction effects). Should our exploratory findings from Chapter 4 replicate, we expected to report no differences between either of the groups at any ROI, as both experimental conditions involved the same immediate recall of a goal location.

First, to ensure that our groups were well-matched for age and cognitive ability we ran independent t-tests. We reported that there were no significant differences between the group from this chapter nor the Chapter 4 group on age ($t(44) = -1.214$, $p = 0.231$, Cohen's $d = -0.382$, M=21.7, SEM +/- 0.708 and M = 23.6, SEM +/- 1.656 respectively). We also reported no significant difference between groups for NART errors ($t(36) = 0.561$, $p = 0.578$, Cohen's $d = 0.235$), TMT B-A times ($t(36) = 0.469$, $p = 0.642$, Cohen's $d = 0.196$) and scores on the MOCA ($t(36) = 0.266$, $p = 0.792$, Cohen's $d = 0.111$). Therefore, both groups were well matched for

age and cognitive abilities. Furthermore, the gender distribution remained the same, with a double in the number of both males and females in the current chapters dataset.

For **Delta**, we reported a significant main effect of region ($F_{(3, 123)} = 3.223$, $p = 0.025$, $\eta^2 = 0.037$). Importantly, we reported no significant between-subjects effects for group ($F_{(1, 41)} = 0.590$, $p = 0.447$, MD = -0.019, Cohen's $d = -0.176$) and no significant interaction effect for Region X Group ($F_{(3, 123)} = 0.008$, $p = 0.999$). For **Theta**, we reported a main effect of region ($F_{(3, 123)} = 6.075$, $p < 0.001$, $\eta^2 = 0.065$). But again, we reported no significant between-subjects effects for group ($F_{(1, 41)} = 0.0003$, $p = 0.995$, MD = 0.0001, Cohen's $d = 0.001$) and no significant interaction effect for Region X Group ($F_{(3, 123)} = 0.067$, $p = 0.997$). For **Alpha,** we reported a main effect of region ($F_{(3, 123)} = 3.801$, $p = 0.012$, $\eta^2 = 0.035$). No significant between-subjects effects for group ($F_{(1, 41)} = 0.256$, $p = 0.616$, MD = 0.01, Cohen's $d = 0.126$) and no significant interaction effect for Region X Group ($F_{(3, 123)} = 0.770$, $p = 0.513$) was found. For **Beta,** we reported a main effect of region ($F_{(3, 123)} = 11.189$, $p < 0.001$, $\eta^2 = 0.095$). However, we reported no significant between-subjects effects for group ($F_{(1, 41)} = 0.904$, $p = 0.347$, MD = 0.01, Cohen's $d = 0.237$) and no significant interaction effect for Region X Group ($F_{(3, 123)} = 0.658$, $p = 0.579$). Finally, for **Gamma**, we reported a main effect of region ($F_{(3, 123)} = 14.208$, $p < 0.001$, $\eta^2 = 0.129$). Again, we reported no significant between-subjects effects for group ($F_{(1, 41)} = 0.185$, $p = 0.669$, MD = 0.005, Cohen's $d = 0.104$) and no significant interaction effect for Region X Group ($F_{(3, 123)} = 0.103$, $p = 0.958$). Considering the small mean differences (MD) between the groups (especially Theta) and the small effect sizes (Cohen's $d < 0.24$), we can further suggest that the EEG dynamics during immediate recall for the groups from Chapter 5 and Chapter 4 were similar. Visualisation of frequency band dynamics via topographies (Figure 5.5) helped to support these results.

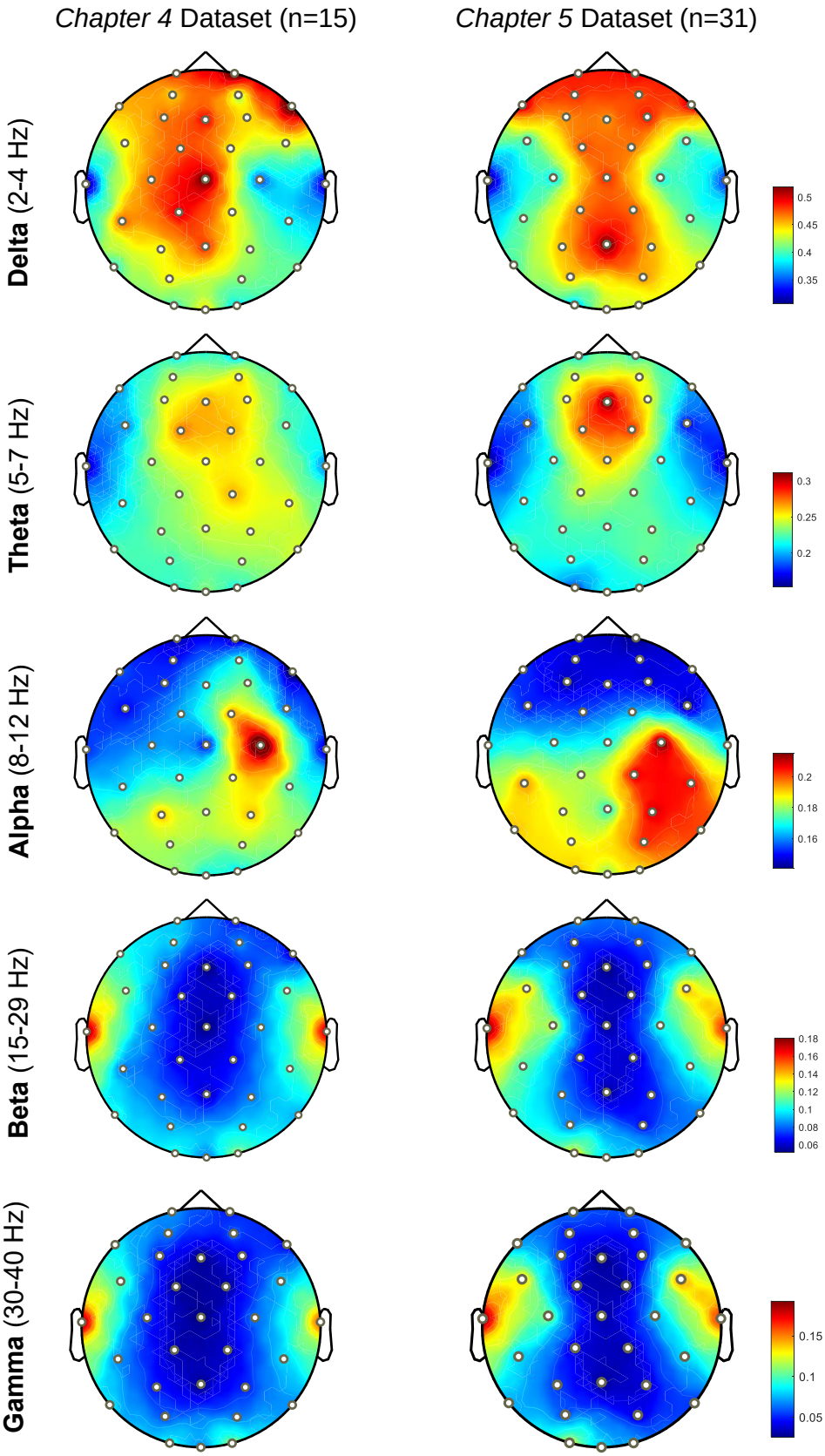


*Figure 5.5:* Topographical distribution of relative power (%) in each dataset group during immediate recall trial. Datasets are scaled to each other for meaningful visual comparison.

From a visual inspection of the topographical distribution of relative power, it is clear that the two groups are very similar. Much of the delta and theta activity is focused on the anterior part of the scalp with some activity in the central and parietal regions, whilst there is a right-lateralised focus, particularly around electrode C4 in the alpha rhythm. Higher frequency bands also seem to demonstrate similarities in the distribution of relative power, though these can be harder to compare visually.

#### *5.3.2.2 Task-related differences in recent and remote recall*

We calculated Power Spectral Density (PSD) using a Welch window (medium window length of 2s with an overlap ratio of 50%) to compute the power spectra ($\mu V^2/Hz$) based on a typical Fast-Fourier Transform (FFT) default frequency definition. Power spectra were computed for five bands: Delta (2-4 Hz), Theta (5-7 Hz), Alpha (8-12 Hz), Beta (15-29 Hz) & Gamma (30-40 Hz). The bands were defined as such for the same reasons outlined in Chapter 4. However, to examine task-related changes we utilised each participants resting state recording. We used the same PSD method on the epoched resting state data to produce a baseline spectrum for each participant. We then performed a baseline normalisation to calculate changes from baseline power (in decibels, *dB*). Each individual's immediate and recent or remote trials were then normalised to their own resting state. We then calculated a group average for visualisation purposes, though statistical tests were run using individual data. Similar to Chapter 4, we then isolated and extracted the mean power relative to baseline (*dB*) from each of our four ROIs, the frontal (F3, Fz, F4), central (C3, Cz, C4), parietal (P3, Pz, P4) and occipital (O1, Oz, O2) midlines. We then ran mixed-factorial repeated measures ANOVAs to assess differences between conditions and groups at ROIs that may not be captured by our cross-scalp analysis due to the FDR-correction for multiple signals and frequency bands.

*5.3.2.2.1 Immediate vs Recent Recall (24-Hour Group)*

We first incorporated the described epoch rejection criteria and visual inspection of participant data. Some participants did not have an immediate recall due to errors during the data collection phase (n = 1). For the recent recall group (24-hours) we compared two conditions, Immediate Recall (n = 15) and Recent Recall (n = 15) – a within-group comparison. These continuous recordings were then epoched and ran through our rejection criteria and visual inspection. This resulted in a total of approx. 1% of epochs being rejected. This left a total of 450 epochs in our immediate recall condition and 480 in our Recent Recall. Below, we compare the groups immediate and recent recall for each frequency band of interest. We first ran a 2 (Condition) X 4 (ROI) repeated-measures ANOVA to examine if there were any ROI-focused difference between the conditions on task-related changes in power.

For **Delta**, we reported no significant main effect of region ($F_{(2.1, 59.5)} = 0.979$, $p = 0.384$). We reported no significant effects for recall phase ($F_{(1, 29)} = 0.018$, $p = 0.447$) and no significant interaction effect for Region X Recall phase ($F_{(2.1, 59.5)} = 0.071$, $p = 0.935$). For **Theta**, we also reported no significant main effect of region ($F_{(2.2, 64.8)} = 0.996$, $p = 0.382$). We reported no significant effects for recall phase ($F_{(1, 29)} = 0.064$, $p = 0.801$) and no significant interaction effect for Region X Recall phase ($F_{(2.2, 64.8)} = 0.286$, $p = 0.776$). However, for **Alpha**, we reported a significant main effect of region ($F_{(2.4, 69.4)} = 5.123$, $p = 0.005$, $\eta^2 = 0.038$). We reported no significant effects for recall phase ($F_{(1, 29)} = 0.133$, $p = 0.718$) and no significant interaction effect for Region X Recall phase ($F_{(2.4, 69.4)} = 0.056$, $p = 0.966$). *Post-hoc* corrected t-tests revealed that alpha power at the frontal midline was significantly greater than the central ($t = 2.683$, $p = 0.035$, Cohen's $d = 0.372$) and parietal midlines ($t = 3.066$, $p = 0.017$, Cohen's $d = 0.425$, but not the occipital midline ($t = 0.242$, $p = 1$, Cohen's $d = 0.034$). Occipital alpha power was also shown to be greater than parietal alpha power ($t = 2.824$, $p = 0.035$, Cohen's $d$

= 0.391). Nevertheless, this is regardless of recall phase, and we expect the differences may not be reflected in the entire midline.

For **Beta**, we again reported a significant main effect of region ($F_{(3, 87)} = 2.774$, $p = 0.046$, $\eta^2 = 0.030$). However, we then reported no significant differences between recall phase ($F_{(1, 29)} = 0.451$, $p = 0.507$) and no significant interaction effect for Region X Recall phase ($F_{(3, 87)} = 1.393$, $p = 0.250$). Using *post-hoc* corrected *t*-tests to investigate our main effect we find no significant differences between any region of interest (all $p > 0.13$). Finally, for **Gamma**, we reported another significant main effect of region ($F_{(3, 87)} = 3.555$, $p = 0.018$, $\eta^2 = 0.039$). But then reported no significant effects for recall phase ($F_{(1, 29)} = 0.510$, $p = 0.481$) and no significant interaction effect for Region X Recall phase ($F_{(3, 87)} = 1.387$, $p = 0.252$). *Post-hoc* corrected t-tests revealed that gamma power at the central midline was significantly less than the gamma power at the parietal ($t = -2.856$, $p = 0.032$, Cohen's $d = -0.486$) and occipital ($t = -2.645$, $p = 0.49$, Cohen's $d = -0.450$). Again, this is averaged over both levels of recall phase but still reveals interesting dynamics.

As we expected that some changes between the recall phases are not focused on our predefined regions, we next reported the scalp topography task-related relative power compared to baseline (Resting State: n = 16, in decibels: *dB*) for each condition in isolation. We then demonstrate the condition differences (Recent – immediate recall), presenting them as *t*-values. To compare the within-group differences we ran a within-groups non-parametric paired permutation *t*-test with 5000 permutations. We then corrected for multiple comparisons using FDR-correction (see Chapter 3 and Thornberry et al., 2023). Any electrode site that reached significance at an alpha level of 0.05, was marked by a yellow star. Figure 5.6 below demonstrates the topographical distribution of task-related *dB* changes relative to baseline (rest) for each frequency band of interest.

Interestingly, power was generally greater (particularly gamma) during task performance compared to rest across bands (apart from alpha) and condition. However, we report no significant changes in any frequency band apart from Alpha (8-12 Hz). This showed significant increases at electrodes F3 and FC2. Furthermore, we can see from visual inspection that power increased across most bands following 24 hours and whatever pattern was observed during immediate recall, was slightly enhanced later. However, Beta (15-29 Hz) demonstrated a centralised decrease in power, but a right parietal-focused increase in power. Otherwise, there were very little changes across frequency dynamics from immediate to recent recall as might be expected. The greater alpha power at the frontal midline ROI (see above) compared to the central and parietal midlines, is well captured in Figure 5.6.

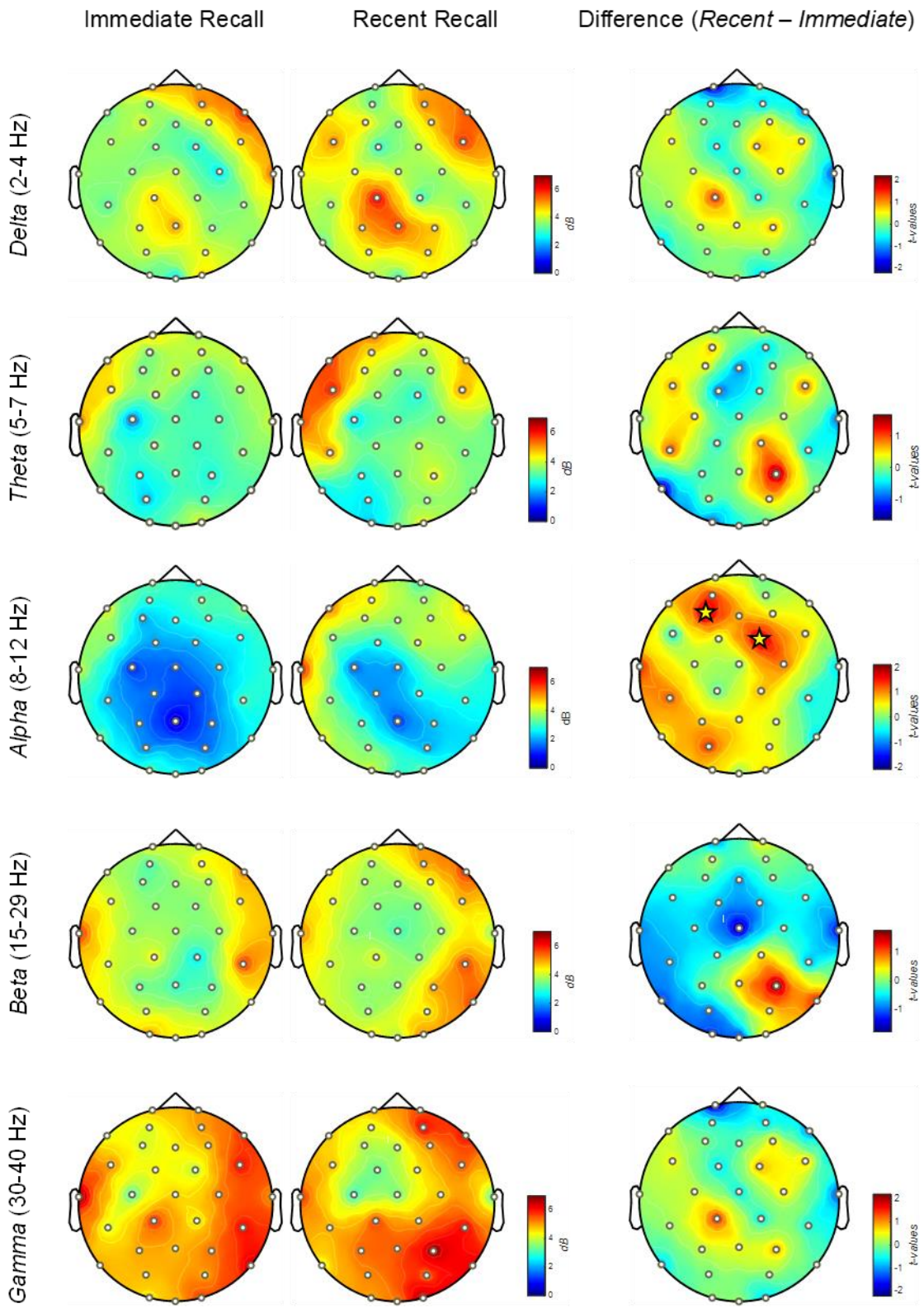


*Figure 5.6:* Topographical distribution of power during immediate and recent recall phases within the 24-hours group. Power in each frequency band is displayed as power relative to baseline (in decibels: *dB*, all positive). Both conditions are displayed on the same scale. Differences are displayed in *t*-values within their own local scale. Significant electrode sites ($p < 0.05$) are marked with a yellow star.

*5.3.2.2.2 Immediate vs Remote Recall (1-Month Group)*

Similar to the above group, we incorporated our described epoch rejection criteria and visual inspection of participant data. Participants were excluded due to incomplete recording data (n = 1) and insufficient event triggers (n = 2). For the remote recall group (1-month) we had two conditions, Immediate Recall (n = 13) and 1-Month Recall (n = 13). These continuous recordings were epoched and ran through our rejection criteria and further visual inspection. This resulted in a total of approx. 1.4% of epochs being rejected. This left a total of 389 epochs in our immediate recall condition and 390 in our 1-Month recall. Below, we compare the groups immediate and remote recall for each frequency band of interest. We first ran a 2 (Condition) X 4 (ROI) repeated-measures ANOVA to examine if there were any ROI-focused differences between the conditions on task-related changes in power.

Focusing on **Delta**, we reported no significant main effect of region ($F_{(3, 75)} = 0.929$, $p = 0.431$). Additionally, we reported no significant effects for recall phase ($F_{(1, 25)} = 0.705$, $p = 0.409$) and no significant interaction effect for Region X Recall phase ($F_{(3, 75)} = 0.333$, $p = 0.801$). For **Theta**, we reported a significant main effect of region ($F_{(3, 75)} = 2.986$, $p = 0.036$, $\eta^2 = 0.048$). We reported no significant effects for recall phase ($F_{(1, 25)} = 0.0005$, $p = 0.982$) as well as no significant interaction effect between Region X Recall phase ($F_{(3, 75)} = 1.004$, $p = 0.396$). However, we reported no significant differences between any region of interest using our *post-hoc* corrected *t*-tests (all $p > 0.08$). Interestingly, within the **Alpha** band, we reported a significant main effect of region ($F_{(2.2, 52.9)} = 5.627$, $p = 0.005$, $\eta^2 = 0.066$). We reported no significant effects for recall phase ($F_{(1, 25)} = 0.133$, $p = 0.718$) and no significant interaction effect for Region X Recall phase ($F_{(2.2, 52.9)} = 0.587$, $p = 0.569$). *Post-hoc* corrected *t*-tests revealed that alpha power at the occipital midline was significantly greater than the parietal and central midlines ($t = 2.587$, $p = 0.001$, Cohen's $d = 0.693$ and $t = 2947$, $p = 0.026$, Cohen's $d = 0.520$ respectively) but not the frontal midline ($t = 1.988$, $p = 0.302$, Cohen's $d = 0.351$).

Nevertheless, examining the descriptives, we see the largest difference in mean relative power is at the frontal midline (MD = 1.272 *dB*, +/- 1.44 *dB*). Considering we find no interaction effect here; we expect that the frontal differences are not contained entirely within the frontal midline.

For **Beta**, we again reported a significant main effect of region ($F_{(3, 75)} = 9.249$, $p < 0.001$, $\eta^2 = 0.121$). However, we reported no significant effects for recall phase ($F_{(1, 25)} = 0.544$, $p = 0.468$) and no significant interaction effect for Region X Recall phase ($F_{(3, 75)} = 0.100$, $p = 0.960$). Using *post-hoc* corrected *t*-tests to investigate our main effect we reported that power relative to baseline at the occipital midline was significantly greater than all other regions of interest (all $p < 0.001$): frontal ($t = 3.991$, Cohen's $d = 0.771$), parietal ($t = 4.264$, Cohen's $d = 0.823$) and central ($t = 4.570$, Cohen's $d = 0.882$). Though this is averaged across the recall phases, examining descriptives reveals that frontal beta power shows the largest increase from immediate to remote recall phases (*MD* = 0.833 *dB, SEM* = 0.914 *dB*). Finally, for **Gamma**, we reported another significant main effect of region ($F_{(3, 75)} = 11.306$, $p < 0.001$, $\eta^2 = 0.129$). But then reported no significant effects for recall phase ($F_{(1, 25)} = 0.164$, $p = 0.689$) and no significant interaction effect for Region X Recall phase ($F_{(3, 75)} = 0.367$, $p = 0.777$). *Post-hoc* corrected t-tests revealed that gamma power at the occipital midline was significantly greater than the gamma power at the parietal ($t = 4.885$, $p < 0.001$, Cohen's $d = 0.885$) and central ($t = 5.076$, $p < 0.001$, Cohen's $d = 0.920$) but not at the frontal midline ($t = 2.586$, Cohen's $d = 0.468$, $p = 0.07$).

Following our ROI analysis, we (as above) also reported the scalp topography task-related relative power compared to baseline (Resting State: n = 15, in decibels: *dB*) for each condition in isolation. We then demonstrate the condition differences, presenting them as *t*-values. To compare the within-group differences we ran a within-groups non-parametric paired permutation *t*-test with 5000 permutations. We then corrected for multiple comparisons using

FDR-correction (see Chapter 3 and Thornberry et al., 2023). As before, any electrode site that reached significance at an alpha level of 0.05, was marked by a yellow star. Figure 5.7 below demonstrates the topographical distribution of task-related *dB* changes relative to baseline (rest) for each frequency band of interest.

Once again, power was generally greater during task performance (especially for delta and gamma bands) than at rest with the exception of alpha. Specifically, we reported greater relative delta power at the frontal midline during the 1-month recall compared to the immediate recall (significant at sites F4 and FC2) and some minor increases at posterior sites. We also reported seemingly stabilised relative theta power, but with significantly decreased power at sites CP1 and FC6 from immediate to remote recall. Alpha power remains relatively low compared to other frequencies across the scalp in both recall trials. However, we report a clear and significant (at right-frontal midline site F4) attenuation in frontal alpha power from immediate to remote recall. This may explain our statistical reports above not showing interaction between region and recall phase, as significant increases appear to be right-lateralised.

In the Beta band (15-29 Hz) we demonstrate a stable level in power, but a seemingly cross-scalp increase in power (with a significant increase at P3). Interestingly, with Gamma (30-40 Hz) we can observe right-lateralised increases in power from immediate to remote recall, with increases in frontal and occipital sites (significant at AF4). Nevertheless, the clear lateralisation of power increases may explain the lack of reported significance between recall phases at the midlines above. Hence, there is clear recruitment of greater neural power for remote recall compared to immediate – apart from Theta, which tends to decrease or stay stable. Though, it is important to mention that multiple comparisons across signals and frequency bands within the same statistical comparison could lead to missed effects –it is better to control for this rather than report an effect that is not present (Jabes et al., 2021). Interestingly, alpha

power increases in this group also and is greater at the front of the cortex in the remote recall phase compared to the immediate – a finding we also reported in our recent recall group. Though not suppressed compared to baseline, alpha power in general is quite low compared to other frequencies – mapping on to a relative *frequency* suppression in relation to other bands (i.e., as found in Chapter 4).

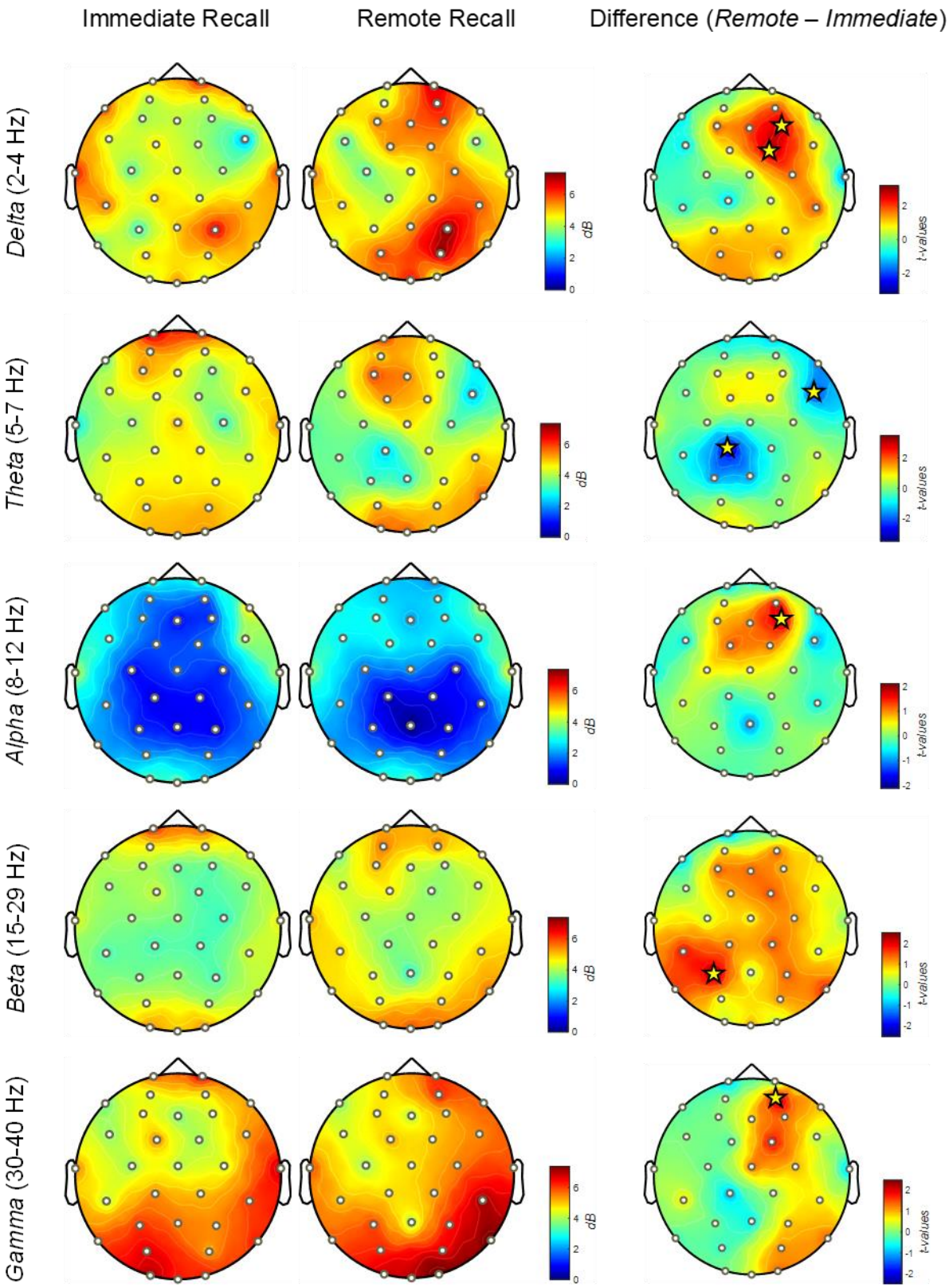


*Figure 5.7:* Topographical distribution of power during immediate and remote recall phases within the 1-month group. Power in each frequency band is displayed as power relative to baseline (in decibels: *dB*, all positive). Both conditions are displayed on the same scale. Differences are displayed in t-values within their own local scale. Significant electrode sites ($p < 0.05$) are marked with a yellow star.

*5.3.2.2.3 Recent vs. Remote memory*

Finally, we compare the power change from baseline (*dB*) between our two recall conditions: recent (n = 16) and remote (n = 14) at each ROI using a 4 (region) X 2 (condition) mixed factorial repeated-measures ANOVA. For **Delta**, we reported no significant main effect of region ($F_{(3, 84)} = 1.217$, $p = 0.309$). Additionally, we reported no significant effects between condition ($F_{(1, 28)} = 0.702$, $p = 0.409$) and no significant interaction effect for region X condition ($F_{(3, 84)} = 0.650$, $p = 0.585$). However, we did report greater relative power at the frontal and occipital midlines in the remote group, though not significant (see Figure 5.8). For **Theta**, we once again reported no significant main effect of region ($F_{(3, 84)} = 1.639$, $p = 0.186$). Additionally, we reported no significant differences for condition ($F_{(1, 28)} = 1.070$, $p = 0.310$) and no significant interaction effect for region X condition ($F_{(3, 84)} = 1.844$, $p = 0.145$). Once again, we observed higher means at the frontal and occipital regions for the remote in Figure 5.8, but none reached significance.

For **Alpha**, we instead reported a significant main effect of region ($F_{(3, 84)} = 5.732$, $p = 0.001$, $\eta^2 = 0.035$). However, we reported no significant effects for condition ($F_{(1, 28)} = 0.983$, $p = 0.330$) and no significant interaction effect for region X condition ($F_{(3, 84)} = 1.172$, $p = 0.326$). Corrected t-tests reveal that there was greater relative power at the frontal midline compared to the parietal when averaged over the levels of our conditions ($t = 3.424$, Cohen's $d = 0.437$, $p = 0.006$, MD = 1.905 *dB*, SEM +/- 0.57 *dB*) and the parietal midline relative power was significantly less than that at the occipital midline ($t = -3.738$, Cohen's $d = -0.477$, $p = 0.002$, MD = -2.079 *dB*, SEM +/- 0.57 *dB*). Though not significantly different, we observed much greater relative power at the parietal midline in our recent group, compared to our remote group (M = 2.01 *dB*, SEM +/- 1.2 *dB*; M = 0.434 *dB*, SEM +/- 1.01 *dB* respectively) which are reflected in Figure 5.8. For **Beta**, we again reported a significant main effect of region ($F_{(3, 84)} = 3.348$, $p = 0.023$, $\eta^2 = 0.047$). However, we reported no significant effects for condition ($F_{(1,}$

$_{28)}$ = 0.334, $p$ = 0.568) and no significant interaction effect for region X condition ($F_{(3, 84)}$ = 0.938, $p$ = 0.426). Corrected t-tests revealed significant differences averaged across the levels of our conditions between the occipital and central regions ($t$ = 2.839, Cohen's $d$ = 0.548, $p$ = 0.034, MD = 1.384 *dB*, SEM +/- 0.48 *dB*) with all other regions not reaching significance (all $p > 0.09$). Nevertheless, we see some non-significant differences between the recent and remote group in Figure 5.8.

Finally, for **Gamma**, we also reported a significant main effect of region ($F_{(3, 84)}$ = 7.238, $p < 0.001$, $\eta^2$ = 0.092). However, we reported no significant difference between conditions ($F_{(1, 28)}$ = 0.372, $p$ = 0.547) and no significant interaction effect for region X condition ($F_{(3, 84)}$ = 1.226, $p$ = 0.306). Once again, when averaged across levels of condition, corrected t-test revealed differences between relative power at the frontal and occipital midlines ($t$ = -3.868, Cohen's $d$ = -0.733, $p$ = 0.001, MD = -2.124 *dB*, SEM +/- 0.55 *dB*). However, all other regions were not significant ($p > 0.1$). Furthermore, we display greater, but not significantly greater, mean relative power at the occipital midline in our remote group compared to our recent group (M = 7.31 *dB*, SEM +/- 0.88 *dB*; M = 5.69 *dB*, SEM +/- 0.65 *dB* respectively) which is visible in Figure 5.8 and 5.9. Therefore, though we reported no interaction effects or difference in power across regions between groups, we predict that we should see some significant differences running a full-scalp permutation *t*-test to include all electrodes. It is possible that only some electrodes within predefined midlines are showing significance, and our permutation t-tests should capture these. We would also predict based on these results, that the electrodes appear within regions showing non-significant but large mean differences in power.

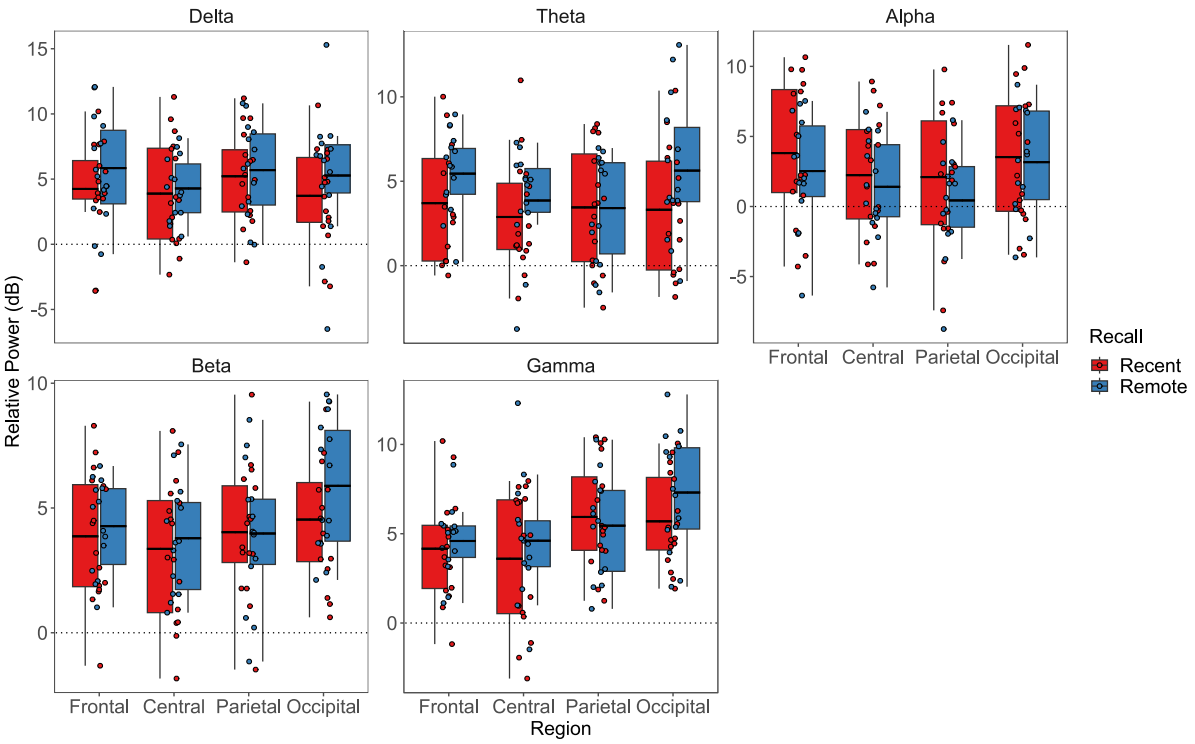


*Figure 5.8:* A boxplot displaying the mean relative power at each midline for each group across all five predefined frequency bands. The mean is depicted by the line in the boxplot, with individual datapoints jittered to help understand distribution.

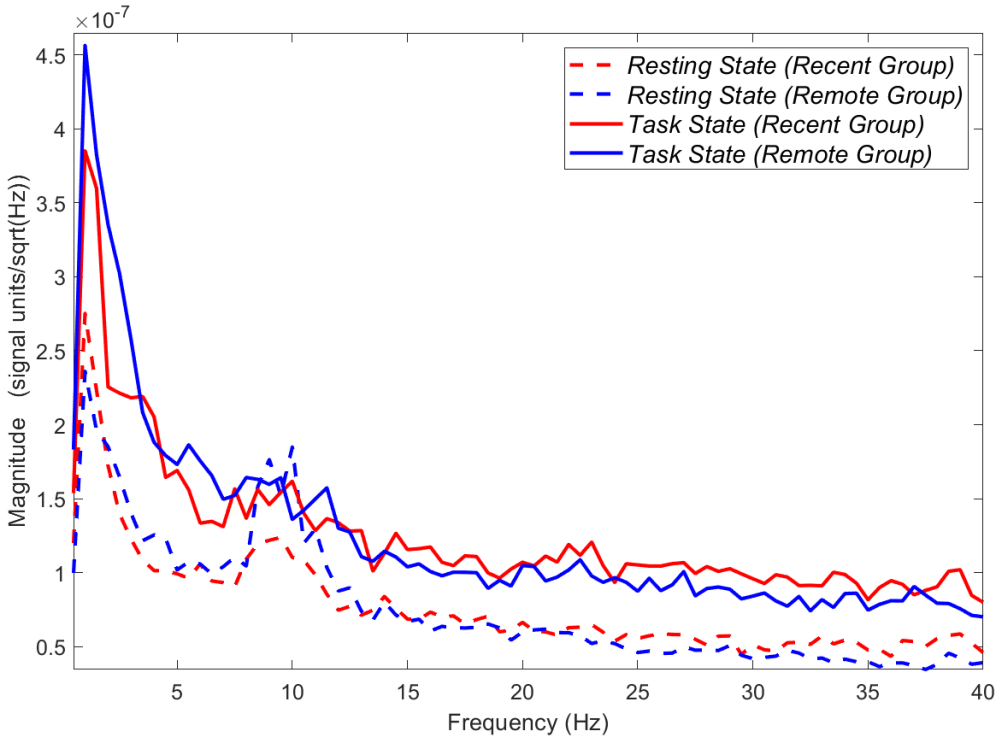


*Figure 5.9:* An FFT line graph displaying the non-normalised mean magnitude of power (μV²/Hz) across the scalp for each group during the recall trial following the relevant consolidation period. Power is displayed across the 1-40 Hz frequency range, with a frequency definition of 0.5 Hz. These are the uncorrected power spectrums.

Finally, we reported the scalp topography task-related relative power compared to baseline (in decibels: *dB*) for each recall condition, recent (n = 16) and remote (n = 14). For this analysis we included all participants who had these trials available. We then examined the condition differences (remote – recent), presenting them as *t*-values. To compare the between-group differences we ran a between-groups non-parametric permutation *t*-test with 5000 permutations. We then corrected for multiple comparisons using FDR-correction (see Chapter 3 and Thornberry et al., 2023). As before, any electrode site that reached significance at an alpha level of 0.05, was marked by a yellow star. Figure 5.10 below demonstrates the topographical distribution of task-related *dB* changes relative to baseline (rest) for each frequency band of interest, alongside the difference between these relative power changes between the groups.

We reported that power relative to baseline was mostly greater in the remote group compared to the recent group across bands, apart from alpha. Interestingly, we reported greater frontal and posterior delta (2-4 Hz) power in the remote group (significant at sites FC3 and Oz) with some greater right-lateralised power at parietal sites (with no site reaching significance). We reported greater relative theta (5-7 Hz) power in our remote group at frontal sites and some parieto-occipital sites (with O1 and PO3 reaching significance). Alpha power indicates trending decreases in the remote recall group, but we reported no site reaching significance. This may explain our statistical reports above not showing any between-groups nor any interaction effects between region and recall condition – as our Alpha band covers 8-12 Hz. In the Beta band (15-29 Hz) we demonstrate similar frontal and occipital increases in power, with significance at sites AF3 and Oz. Furthermore, with Gamma (30-40 Hz) we show trends towards greater power in the remote group, but none of the sites reach statistical significance. Nevertheless, it is clear that isolated and lateralised sites of greater power may explain the lack of reported significance between recall groups at the midlines. Hence, there is clear recruitment

of greater neural power for remote recall compared to recent – this time, apart from alpha power, which shows a reduction in power. The same limitations regarding missed effects mentioned above - comparison and correction for multiple comparisons apply here. Interestingly, all frequency bands apart from alpha show increased power during remote recall compared to recent recall in frontal and occipital regions.

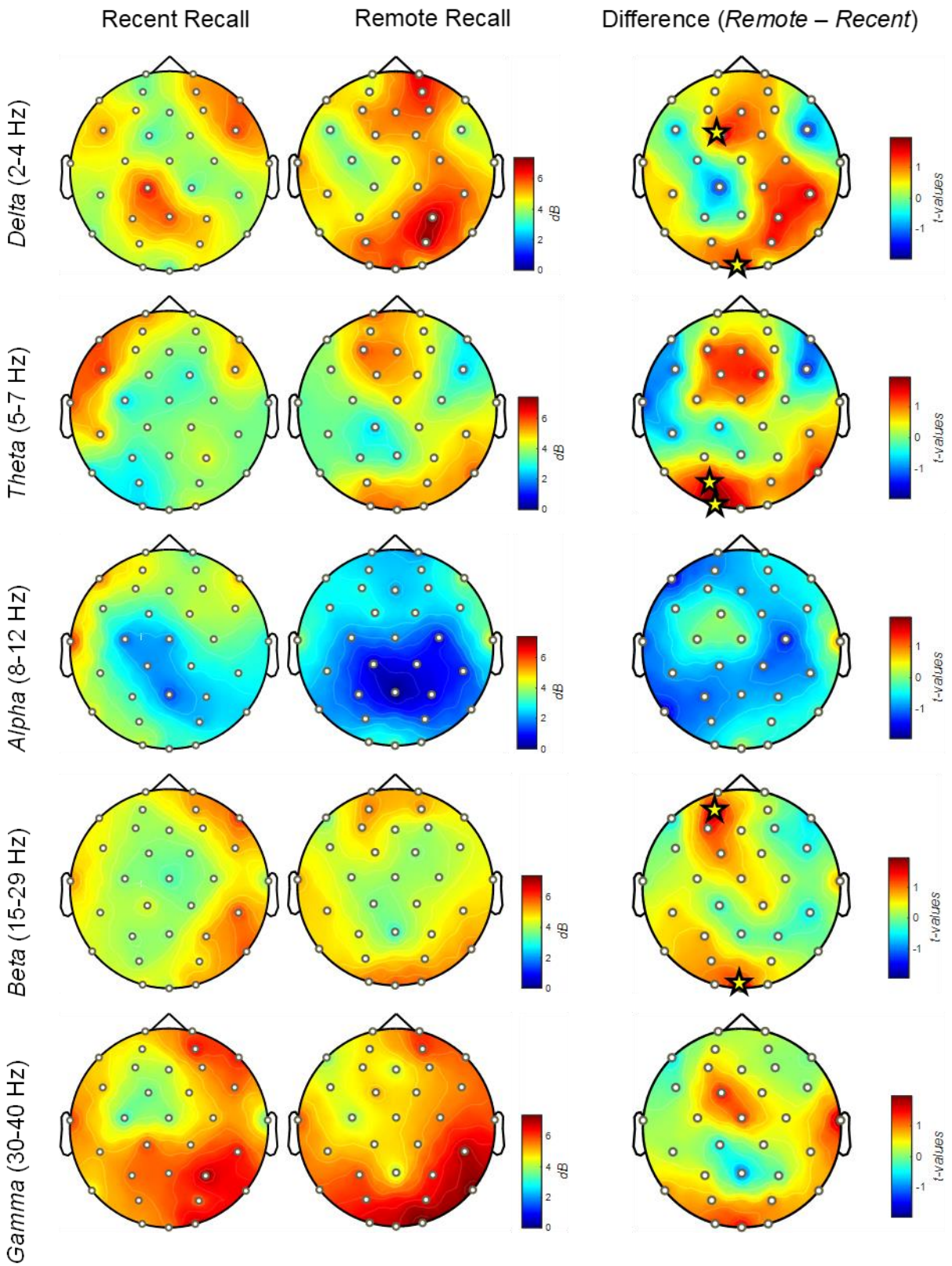


*Figure 5.10:* Topographical distribution of power during recent and remote recall phases compared between groups. Power in each frequency band is displayed as power relative to baseline (in decibels: dB, all positive). Both groups are displayed on the same scale. Differences are displayed in t-values within their own local scale. Significant electrode sites ($p < 0.05$) are marked with a yellow star.

## 5.4 Discussion

### *5.4.1 Memory performance*

Contrary to our original hypothesis, we did not find a significant difference in delayed recall performance between the recent and remote groups. Both groups demonstrated similar levels of performance in the immediate and delayed recall trials (Barry et al., 2016), regardless of whether the delay between the learning phase and recall phase was recent (24-hours) or remote (1 month). Interestingly, we actually observed an improvement in recall from the immediate to the delayed test in our remote group. These results suggest that time between spatial learning and recall up to 1 month does not impact spatial memory retrieval. If anything, there is evidence that a longer temporal gap may have helped additional consolidation processes to take place, strengthening memory traces and improving performance. It also supports some theoretical accounts that *spatial* memories are more stable across time than others (Kentros et al., 2004).

There are some potential explanations of the behavioural results from our task. Firstly, one could claim that the association formed between the landmarks and goal location has successfully strengthened following offline consolidation, with greater detail at remote recall, as opposed to recent (Alcalá et al., 2020; Shanks, Darby, et al., 1998). Considering the environment has not changed in any way, memory retrieval is helped by the matching context and environmental cues (Urcelay & Miller, 2014), which would explain the lack of differences between our two groups. Doeller and Burgess (2008) reported the importance of geometrical shapes in successful retrieval and contextual understanding during spatial learning. Considering the simplicity of the environment, and the saliency of one of our landmarks (Chamizo et al., 2006; Commins et al., 2020; Deery & Commins, 2023; Farina et al., 2015) recall should be relatively easy as the contextual aspects of the spatial memory can be easily retrieved and recalled – aided by the heavily geometric and minimalistic environment. Even

during remote recall, were the memory of the environment stored as a schema or a contextual "gist" – it can be retrieved with ease due to the minimalistic context and lack of complexity (Bestgen et al., 2017; Crespo-García et al., 2016; Herweg, Sharan, et al., 2020; Smith & Mizumori, 2006). Additionally, our learning phases facilitated active rather than passive navigation throughout, which has been shown to produce better spatial memory retrieval (Chrastil et al., 2022; Wallet et al., 2013). Nonetheless, based on our EEG results, we would argue that the way in which this information is retrieved by the brain is affected by the temporal delay between recall conditions, but not memory performance.

### *5.4.2 Relative dynamics of spatial recall remain similar*

We opted to examine all individuals immediate probe trial EEG data, due to its similarity to the data collected and analysed exploratorily in Chapter 4. Here we used the same signal processing method and relative power calculation that was used in the previous chapter, combining all participants from this chapter together to replicate the effects found in our last chapter with greater numbers (n = 31). We reported no differences between the sample from chapter 4 and the sample from chapter 5. Though this is not conclusive that neural activity is the same, it is certainly not much different. Visual inspection revealed a replication of two important characteristics of frequency power dynamics that we uncovered in chapter 4. We demonstrate low-frequency oscillations that show dominance in the frontal region of the scalp alongside increased alpha power activity across sensorimotor regions with alpha power suppression at the frontal regions.

The replication of EEG data is a major issue in the current literature, with low effect sizes, post-analysis selection of regions & time windows and failure to report preprocessing pipelines, which have all been shown to impact the data and its interpretation (Luck &

Gaspelin, 2017; Pavlov et al., 2021; Robbins et al., 2020). Here we provided an attempt to illustrate that our previously collected neural patterns can be (at least partially) replicated in different samples of greater numbers. These findings do provide confidence in our previous results, and also our use of the immediate probe trial data in this chapter, to examine the impact of recent and remote recall. It also highlights the usefulness of a relative power correction without a useful baseline.

### *5.4.3 Overall effort increases with retrieval demands*

In respect to our findings in Chapter 3 we reported inverse patterns to those demonstrated during learning, in which we see general decreases in power as the task becomes less effortful (Thornberry et al., 2023). In the current study, we reported clearly greater power in the delayed recall trial compared to the immediate recall trial within the two groups. Further examination reveals that in fact, the individual patterns within the groups are enhanced. For example, focusing on Theta (5-7 Hz) in Figure 5.6 demonstrates very unique patterns of power across the scalp, which become replicated but enhanced at the recent time-point. Similar patterns are revealed in Delta (2-4 Hz) in Figure 5.7 demonstrating enhancement of frontal and parietal power patterns on the scalp. We also reported greater power overall at certain electrodes sites when comparing recent recall to remote recall, though individual scalp patterns differ (see Figure 5.10). Increased low frequency (delta & theta) power has been reported mainly at frontal regions, as being related to the amount of cognitive processing required during a task, as well as memory retrieval and decision making (Jacobs et al., 2006; Jaiswal et al., 2010). For example, using a Sternberg Task, researchers have demonstrated that frontal theta power increased along with working memory capacity, but only in highly challenging versions of the task (Zakrzewska & Brzezicka, 2014). In more applied settings, theta power increased in chess

players during the game, but only when their opponents difficulty increased (Fuentes-García et al., 2020). In spatial navigation tasks, theta and alpha power have been correlated with memory performance, with increases in frontal theta related to active maintenance of information (Jensen & Tesche, 2002; Klimesch, 1999; Lithfous et al., 2015; Roberts et al., 2013), whereas alpha has been known to contribute indirectly by filtering irrelevant information from attention and predicting possible memory interference (Klimesch, 2012; Klimesch et al., 2007; Sauseng et al., 2009). Considering our results reflect within-group increases of overall power and topographical patterns in low-frequency oscillations, with resulting changes of alpha suppression within the two groups, we suggest it is related to overall effort required to retrieve spatial information.

### *5.4.4. Frontal regions are related to spatial memory retrieval*

Secondly, an interesting and consistent observation is the involvement of the frontal region during retrieval at the delayed recall trials. We reported some significant electrode sites in delta, but overall greater power at frontal sites in delta and theta in the remote compared to the recent group. Numerous scalp EEG studies have reported greater or higher low-frequency oscillations (1-8 Hz) at the anterior parts of the scalp during successful spatial recall, context-dependent recall, correct versus incorrect memory responses and long-term recall of objects (Alekseichuk et al., 2016; Düzel et al., 2003; Gruber et al., 2008; Herweg, Sharan, et al., 2020; Staudigl & Hanslmayr, 2013). Furthermore, gamma power (>30 Hz) has been shown to reflect associative processes of retrieval (i.e., familiarity) rather than episodic recollection (Gruber et al., 2008). During navigation, frontal midline theta oscillations specifically (loosely defined as 2-8 Hz in most EEG studies, which incorporates the traditional band definitions of delta and theta as we reported here) have been shown to be related to retrieval of spatial information during active

navigation (Chrastil et al., 2022; Du et al., 2023; Liang et al., 2018; Liang et al., 2021). However, we do report greater occipital low-frequency oscillations in our remote group also, which were reported by Chrastil et al. (2022) in their free (active) navigation group during correct navigational decisions and longer paths travelled. We would suspect these occipital increases are reflected in our remote group as there may be more visual scanning leading to longer or more complex paths travelled as they attempt to recall the target location. This may also explain the greater suppression of posterior and parietal alpha rhythms compared to rest, which have been shown to be related to increased attention prior to spatial decision-making (Chrastil et al., 2022; Du et al., 2023; Klimesch, 1999; Klimesch et al., 1997). Our remote group require more focused attention and inhibition of irrelevant sensory input (Bonnefond & Jensen, 2012; Foxe & Snyder, 2011; Hanslmayr et al., 2009; Khader et al., 2010) which have been demonstrated to accompany increased frontal theta power in a kind of inverse relationship, allowing spatial memory access via delta-theta ranges and attention with sensory inhibition via the alpha range (Du et al., 2023; Khader et al., 2010; Liang et al., 2018; Liang et al., 2021).

Additionally, we reported greater beta (15-29 Hz) power in the remote group in the same regions, with significance at AF3 and Oz. Chrastil et al. (2022) reported greater beta activity in an active virtual navigation group before they arrived at a familiar decision-making point, which coincided with theta during the decision-making process. Greater beta power has been linked to memory processing in controlled retrieval (Ketz et al., 2014) or even suppression of unwanted visual memories (Waldhauser et al., 2015; Waldhauser et al., 2012). Considering the topographical patterns and dynamics match that of our low-frequency oscillations which may be retrieving and utilising the spatial memory, beta oscillations could be controlling the retrieval process to allow successful recall. This may be required for remote memories as they are liable to interference (especially at 28 days, see Wichert et al. 2011) and are more likely to

contain misleading details (Wichert et al., 2011; Yassa & Reagh, 2013). Considering our recent memory group show different patterns with lesser beta power, and they had little likelihood of memory interference, we believe beta is responsible for a controlled spatial memory retrieval process for remote memories, which topographically mirrors delta and theta patterns.

### *5.4.5. Delta-Theta & Gamma support memory replay during remote retrieval*

Recent evidence suggests that although low frequency oscillations in the delta-theta range are vital for spatial memory retrieval (Jacobs et al., 2006), successful memory retrieval requires the coupling of gamma oscillations during particular theta rhythm phases (Alekseichuk et al., 2016; Greenberg et al., 2015; Lisman & Jensen, 2013). It is believed that these coupled oscillations support the exchange of mnemonic spatial information throughout the entorhinal–hippocampal network (Buzsáki & Moser, 2013; O'Keefe, 1993). Interestingly, we report greater delta and theta power in our remote group compared to our recent group, with greater beta/gamma power also. From our regression, we see that total scalp gamma power is a significant predictor of spatial task performance, with another significant coefficient being the remote memory condition. Interestingly, we just miss significance levels with beta and theta – which are two rhythms whose dynamics are primarily isolated to frontal midline areas. Increased frontal theta and posterior gamma have been reported to play an essential role during long-term spatial memory retrieval (Vivekananda et al., 2021). We see similar dynamics in our data, and considering these patterns are usually reflected on the cortex as coming from the hippocampus and surrounding areas (see Herweg et al., 2020 for a summary) we could suggest that there is greater hippocampal involvement during remote memory recall compared to recent. However, we are again limited by the inability to perform source reconstruction on our data.

Theoretically then, we would argue that when a memory has become remote, it requires more neural effort to retrieve it compared to a recent memory. The remote memory could be stored across the cortex and relies on the hippocampus and other regions to accurately retrieve it. However, because the memory may have become schematic in nature, performance and recall becomes more accurate. We believe that the reason for this is because the retrieval of remote spatial memories requires replay, and reactivation of the neural pathways utilised during encoding as found by Dupret et al. (2010). If we examine our remote group data (using Figure 5.7 and 5.9) we see very similar patterns reported in our sample for Chapter 3 (and see Thornberry et al., 2023). Reduced theta power from immediate to remote recall at posterior sites (near Pz) and some frontal sites along with suppression of alpha power at site Pz and parietal areas. These patterns are not reflected when our recent group perform the recall trial, but instead see an enhanced version of the neural dynamics of their immediate recall (see Figure 5.6). We also see that gamma power mirrors the delta activation also in our remote group only, with greater increase in delta and gamma power from immediate to remote recall, whilst staying stable between immediate and recent recall. Therefore, based on this we would suggest that remote spatial memories require replay of neural dynamics utilised during encoding.

We would further suggest that replay is required due to the fact that the remote memory has become more dispersed across the cortex. We are familiar with evidence that cortical and hippocampal replay allows for consolidation and retrieval of long-term spatial memories (Michelmann et al., 2018) with theta and alpha rhythms showing significant involvement during recall-related replay at hippocampal and prefrontal areas (Sutterer et al., 2019; Zielinski et al., 2020). These replay events are known to occur during active navigation (Ólafsdóttir et al., 2018) which is also evoked by our task paradigm. Therefore, we believe that this replay is reflected on the cortex during remote retrieval in a virtual water maze task in rhythms closely related to those found in the replay literature (Herweg, Sharan, et al., 2020; Köster et al., 2014;

Pu et al., 2020; Staudigl & Hanslmayr, 2013; Sutterer et al., 2019; Vivekananda et al., 2021) and also expected to derive from the parahippocampal cortex and hippocampus (delta-theta and gamma: see Lisman and Jensen (2013); Nyhus and Curran (2010)). This would support and be accounted for through Multiple Trace Theory (MTT) in which the hippocampus stores a distributed pattern of cortical activity related to the memory (Nadel et al., 2000). Hippocampal replay then facilitates retrieval of the memory traces, which leads to remote spatial memories being stored as gist-like representations. Our data supports this concept, but that replay is not required for recent memories, as the schematic of the environment has not been fully consolidated, and the required traces do not yet exist. Evidence that the disruption of awake hippocampal replay in rats does not affect recent (short-term) recall ability in a spatial task been shown for the first time by Deceuninck and Kloosterman (2022). However, it is entirely possible that our findings may relate to standard consolidation theory, and that replay for remote memories occurs at cortical level independent of the hippocampus. Nevertheless, without in-depth detailed source reconstruction we cannot verify these observations. Therefore, though there are some limitations of our work, we believe these aspects require further investigation in future work to demonstrate possible support for multiple trace theory.

### *5.5 Conclusions*

In short, this study did not find any significant differences in spatial memory performance between recent and remote recall groups. However, our EEG data suggests that more neural effort is required to accurately retrieve remote spatial memories compared to more recent ones. We observed increased power in lower frequency bands delta (2-4 Hz) and theta (5-7 Hz), especially over frontal regions, during the delayed recall trial compared to immediate recall. This likely reflects greater cognitive demand and a more controlled retrieval process for

accessing consolidated remote memories. Additionally, the remote group showed stronger gamma power. We suggest that these rhythms could be related to cortical (or perhaps hippocampal) replay, which may be required for retrieval of remote spatial memories. In contrast, the recent group displayed an intensified version of their immediate recall's neural dynamics during delayed recall, suggesting that consolidated schematic representations have not yet formed after 24 hours. Overall, these findings provide some novel evidence about the time course of consolidation for spatial memories. The results also provide an insight into how the nature of spatial memory retrieval for navigation may change after encoding. Further investigation into replay phenomena during remote spatial recall could provide more evidence for theoretical models of consolidation.

# Chapter 6

# Age-related differences in resting-state and task-related EEG during recent & remote spatial recall

## Abstract

The concept of healthy ageing and its impact on spatial navigation and memory ability is well-established in the literature. However, the neural basis of these age-related changes is not well understood. In particular, there is limited research that examines the impact of healthy ageing on the neural mechanisms underlying spatial memory retrieval for memories encoded recently (24-hours ago) compared to those encoded remotely (1-month ago). This study attempted to explore the neural basis of recent and remote spatial memory retrieval during navigation in older adults (n = 21) using EEG and a virtual water maze. Our results suggest that recent memories tend to be better preserved than remote memories for retrieval during navigation in older adults. Compared to younger adults (n = 31), our older adults showed differences in both resting state and task-related oscillatory activity. We reported reduced high-frequency oscillations in both conditions compared to younger adults. Older adults also demonstrated reduced high-frequency oscillations at recent recall, but increased delta with reduced theta during remote recall compared to their immediate recall. We suggest that these differences could relate to the storage of the memories and the regions required for retrieval. The results are discussed in terms of age-related compensation for spatial navigation skills in healthy ageing.

## 6.1 Introduction

According to the World Health Organization, the number of people aged over 60 is set to rise to two billion by 2050. Age-related decline in cognition is widely reported to impact a variety of processes, including decision making (Cauffman et al., 2010; Harty et al., 2017; Peters et al., 2007), working memory (Jost et al., 2011; Salthouse & Babcock, 1991) and long-term memory (Caffrey & Commins, 2023; Smith, 2014; Werkle-Bergner et al., 2006). Spatial navigation ability is considered to be one of the first cognitive functions to decline with age, and some of the first early pre-clinical signs of mild cognitive impairment and Alzheimer's disease (Coughlan et al., 2018; Coughlan et al., 2020). Spatial navigation is a combination of multiple different processes combined, mainly for learning a route to the goal, travelling it and then remembering both the route and the goal location.

Older adults show impairment on virtual water maze tasks (Moffat, 2009; Moffat & Resnick, 2002; Moffat et al., 2001). Worsening performance has been reported across a two-year longitudinal study (Daugherty & Raz, 2017), with repeated training required to improve cognitive mapping skills and episodic memory. In a review, Lester et al. (2017) explain that because navigation is such a complex behaviour, deficits can occur at any stage of the process, including spatial information processing (vestibular feedback, sensorimotor integration) or spatial learning and memory processes (episodic memory, associative learning). Focusing on the use of a virtual water maze, older adults are known to have slower reaction time and orientation during navigation (Moffat, 2009; Zhong et al., 2017). They are also known to make more errors in a VWM task (Moffat et al., 2001; Schoenfeld et al., 2014). Older adults tend to have more complex routes which impacts their performance (Daugherty et al., 2015). For example, Yu et al. (2021) reported older adults made fewer shortcuts compared to younger adults (see Chapter 1 for the importance of this). However, older adults lack of exposure to virtual reality and desktop navigation tasks could influence their performance (McGee et al.,

2000). Recent work by Hill et al. (2023) described that older adults perform worse in a VWM desktop task, but age-differences significantly reduced when examined using an immersive virtual reality environment. In NavWell, we reported that older adults could recall the goal location well above chance levels during a recall trial but performed worse compared to younger adults (Commins et al., 2020). Additionally, remote spatial memory retrieval was better and less prone to the impairment in older adults compared to recent memories, but both were impaired compared to younger adults (Lopez et al., 2019). Therefore, age-related navigation decline is a complex phenomenon. General spatial navigation ability assessed across the world population by a virtual task does decline as a function of age with increased individual variability (Coughlan et al., 2018). However, the specific processes that are involved in this decline are still unknown, though many studies point to issues with memory.

Ageing also impacts the neural systems involved in spatial cognition. For example, the spatial specificity of place cells has been shown to decline in ageing animals (Lithfous et al., 2013). Older adults have shown a loss of grey matter in the medial temporal lobe (mainly at the amygdala, anterior hippocampus and entorhinal cortex) – but tend to display marginal alterations outside of the MTL (Chan et al., 2021; Zúñiga et al., 2023). It is thought that our underlying brain oscillations attempt to adjust to the age-related changes in physiology (Zúñiga et al., 2023). This results in decreased specialised processing and greater recruitment of multiple brain regions for compensation, particularly in high performing older adults (Cabeza et al., 2002; Stern et al., 2005). During rest, there is typically reduction in alpha activity in older adults, and a general increase in delta and theta power (Ishii et al., 2018). Greater theta power at rest is associated with healthy ageing and better cognitive function (Finnigan & Robertson, 2011; Fleck et al., 2017). Recently, Jabès et al. (2021) reported reduced low frequency power (1-7 Hz), but equal levels of alpha (8-12 Hz) power in older compared to younger adults. Beta (15-29 Hz) and gamma (30-47 Hz) powers were found to be greater in older compared to

younger adults during rest. Following the resting state recording participants performed a virtual spatial navigation working memory task. Theta, alpha and beta were linked to spatial working memory performance in older adults (Jabès et al., 2021). Similarly, brain connectivity during rest recorded by fMRI facilitates predicted activation of the specific brain circuit engagement needed to perform a working memory task (Zou et al., 2013). Recent analysis of a large EEG dataset from older adults (n = 1703, mean age = 70) revealed that increased peak alpha frequency is associated with working memory performance. Typically reported age-related decline in alpha power at rest is due to the activity at other frequencies, and mainly increased alpha at frontal regions was associated with slower processing speed (Cesnaite et al., 2023). The authors proposed functional reorganisation of brain networks in older age with a reliance on frontal brain regions for complex cognition. This would further support the idea that neural oscillatory networks already exist, and become enhanced for cognition but altered with age and disease (Buzsaki, 2006).

Fewer studies have examined oscillations during spatial navigation. Decreased theta oscillations have been observed in older adults during retrieval of spatial memories (Rondina Ii et al., 2019). Differences in age related to VWM performance in older adults have been typically reported in frontal regions, with decreased theta and alpha power (Lithfous et al., 2018; Lithfous et al., 2015). Recent work by Durteste et al. (2023) revealed differences between age groups during scene-recognition phases of spatial navigation. They reported similar findings to others, with enhanced delta-theta power and reduced beta-gamma power in older adults using scalp EEG (Park et al., 2012). During a spatial memory task, younger adults show greater alpha desynchronisation compared to older adults (Marshall et al., 2018). The authors also reported increased alpha during memory maintenance and higher theta power was associated with better memory performance. However, to our knowledge there exists very little research based on age-related differences in oscillatory activity *during* spatial navigation.

Furthermore, to our knowledge there is no research examining oscillations during recent and remote aspects of spatial memory in relation to age, considering the dominant theories suggest that spatial memory in age leads to navigational decline.

Therefore, this chapter will attempt to investigate age differences in healthy older and younger adults during a spatial recall phase of navigation in a virtual water maze task. Similar to Chapter 5, we examined age-differences in oscillatory activity underlying immediate (10 minutes), recent (24 hours) and remote (1-month) spatial recall. We will examine activity in delta, theta, alpha, beta & gamma. Based on the above, we also decided to explore the resting state activity of older and younger adults. Therefore, behaviourally we would hypothesise that our healthy older adults should perform poorer than our younger adults but should not be impaired. For resting state oscillatory activity, we would anticipate to report similar findings to Jabès et al. (2021): increased delta-theta oscillations, decreased beta-gamma oscillations with similar alpha activity across age groups. We would then expect theta, alpha and/or beta to correlate with spatial memory performance. For task-related oscillatory activity, we would hypothesise to report differences between younger and older adults. We would expect differences in alpha power in older adults with enhanced delta-theta activity and reduced beta-gamma activity. We should also report alternative differences between younger and older adults during immediate, recent and remote recall phases.

## 6.2 Methods

### *6.2.1 Participants*

Twenty-two older adult participants (16 female, 6 male) aged between 60 and 76 (M = 64.7, SEM +/- 1.118) were recruited for this chapter. Originally, recruitment of twenty-four adults was anticipated. However, one older adult dropped out before experimentation, and another had no data recorded due to a power cut on the day. Older adults were recruited from Maynooth University and the wider Maynooth Community, as well as through personal or participant-driven connections from the Greater Dublin Area (see Chapter 2). Thirty-one young adults (21 female, 10 male) from Chapter 5 aged between 18 and 40 (M = 21.7, SEM +/- 0.708) were also used in the analysis for this chapter. This project, the use of human subjects with EEG and the recruitment of older adults was approved by the Maynooth University ethics committee (BSRESC-2021-2453422 & SRESC-2021-2453422). The below sections will focus only on our older adult sample and will refer to relevant sections of Chapter 5 where appropriate.

### *6.2.2 Resting State Task*

Participants underwent electrophysiological preparation (see Chapter 2 for details) before starting any task. We then implemented the recording of resting state activity using the same task as Chapter 5 (section 5.2.2) before running the spatial navigation task. This was constructed in E-Prime version 3.0 (2022) and presented to participants seated 50 cm from a 15-inch standard 4:3 ratio computer screen, on their own in a darkened, electrically shielded and sound-attenuated testing cubicle (150 cm × 180 cm). Participants were required to focus on a fixation cross in the centre of the screen for three minutes (see Chapter 5, Figure 5.1). The eyes-open resting state lasted three minutes and older participants were encouraged to take a

rest period before they began the spatial navigation task. Almost all older adults took a rest period before commencing.

### *6.2.3 Spatial Navigation Task: Practice Trials*

Based on our work from Commins et al. (2020), we implemented a phase of practice trials for our older adult sample. The spatial navigation task was NavWell, described in Chapter 2 and used in all experimental chapters. Older adult participants completed a series of four training trials before commencing their experimental phases (Figure 6.1). This was to help them familiarise themselves with the controls, the nature of the task and allowed them to get comfortable with the EEG equipment. During these practice trials, the goal remained visible (blue square), and older participants simply had to move towards it. The goal moved location for each of the 4 trials. The practice trials were also used to control for potential motor, visual or motivational issues. The training maze contained no landmarks, and the participants started each trial from the north, south, east and west positions respectively. The arena was a medium circular pool, as explained above. Each trial was 60 seconds in length or ended when the goal had been reached. Older adults were supervised during this phase by the researcher. They typically explained the nature of the task and answered any questions about the task, equipment or the joystick controls. All older adults successfully carried out these practice trials. Data from these trials was not reported and EEG was not recorded during them, in order to facilitate researcher presence in the Faraday cage. Typical participant paths of the routes from each of the starting locations are displayed in Figure 6.1.

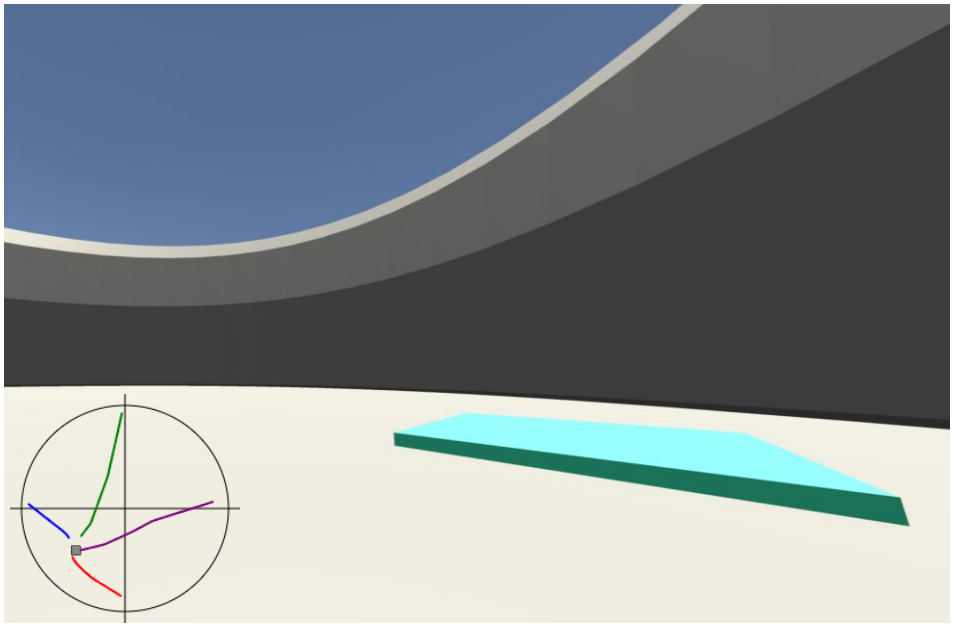

*Figure 6.1:* Screenshot of the NavWell software at the start of a practice trial in older adults. The blue square to the right of this is the visible target/goal. Path data is presented in the bottom left from a sample participant of typical paths taken during each practice trial by older adults (each trial is displayed in a separate colour and starts from each cardinal point).

### *6.2.4 Spatial Navigation Task: Experimental Trials*

Older adults underwent the exact same experimental paradigm as our younger adults in Chapter 5. Older adult participants underwent events in the following order: electrophysiological preparation, resting state data collection, practice phase, learning phase (described in previous chapters and Thornberry et al., 2023), cognitive assessment and immediate recall (see Chapter 2 for specific details). Participants were seated 50 cm from a computer screen in a quiet, darkened testing cubicle with a joystick. They used the same circular virtual environment used previously (taking 15.75s to traverse the arena, calculated at 75 Vm), which had two cues on the walls and a hidden blue square goal in the northeast quadrant. After finishing the learning phase, participants took a 10–15-minute break. They were then given a 60-second recall trial,

in which they had to navigate back to the goal location, starting from a new southwest location. The goal was removed for this trial (see Chapter 2). Older adult participants were then randomly allocated to either a recent condition (n = 11, 9 females) or remote condition (n = 11, 7 females). Following the immediate recall trial, participants in the recent condition were asked to come back 24-hours later, to perform another recall/probe trial as described above. Alternatively, those allocated to the remote group were asked to return in 1-month, to also perform another recall/probe trial.

### *6.2.5 EEG Recording*

EEG data was acquired using a BioSemi ActiveTwo system (BioSemi B.V., Amsterdam, Netherlands) with 32 Ag/AgCl electrodes positioned according to the 10/20 system that had been used throughout this thesis (see section 3.2.3 "*EEG Recording*" or Chapter 2). Older adults were given a longer duration to undergo this stage compared to younger adults but underwent the same procedure (see Chapter 5 for details).

### *6.2.6 EEG Preprocessing*

Continuously recorded EEG data were analysed offline in MATLAB R2021B using scripts in combination with the Brainstorm package (Tadel et al., 2011). The same preprocessing steps from Chapter 5 were used here. For the analysis of both recall trials, the entire continuous recording was then epoched into 2-second epochs, producing 30 epochs per participant for each probe trial, and 90 trials per participant for resting state. All of these data were visually inspected for bad segments and bad electrodes, which were then removed. No bad electrodes were found. Epochs with voltage steps above 100 μV or peak-to-peak signal deflections exceeding 200 μV within 2-s intervals were automatically rejected. We had an average rejection

rate in our older adults of approximately 4% of the total epochs produced. EEG data were then re-referenced to two mastoid electrodes (EXG5 & EXG6). For further information on EEG pre-processing see Chapter 2.

### *6.2.7 EEG Spectral Analysis*

Once more, based on our task and experimental paradigm, we used spectral analysis to investigate five frequency bands: delta (2-4 Hz), theta (5-7 Hz), alpha (8-12 Hz), beta (15-29 Hz) & gamma (30-40 Hz). Power spectra were computed on artefact-free epochs for each participant on both recall trials using the same procedure as Chapter 5. For analysis of the resting state data, we computed relative power in each group based on the processes used in Chapter 4. We then normalised the task-related power using a baseline correction method (see Chapter 5). Taking the non-task related resting state PSD, we baseline corrected each individual participants task-related data (i.e., immediate recall and recent/remote recall) using a decibel (*dB*) conversion. We did *not* focus on any particular region of interest for this chapter (see below). All epochs in each group and condition, were averaged together following computations. We chose to baseline correct and analyse relative power based on previously described rationale in Chapter 2, because we are interested in the distribution of power within the frequency bands and needed a more robust measure with low participant numbers that accounted for slow-drifts, artifacts and noise that may influence between-group analysis.

### *6.2.8 Statistical Analysis*

Statistical analyses & visualisation of the behavioural and EEG data were performed using a combination of JASP (version 0.15), MATLAB and R software version 4.0.2 with the tidyverse and ggplot2 package. First, statistics were performed using extracted values from the power

spectra via the *extract* > *values* process in Brainstorm. We then extracted mean relative power (%) for resting state analyses and mean normalised power (*dB*) for experimental trial analyses. Mixed-factorial ANOVAs were computed on the behavioural data comparing the two groups on several behavioural and electrophysiological measures. Bonferroni corrected *t*-tests were used to follow up within analysis, and independent sample *t*-tests were used to follow up any group differences. Based on several null findings previously, we did not extract power at any region of interest. Instead, we extracted global scalp power in each frequency band. We facilitated site-specific effects to be explored by using Brainstorm in MATLAB 2021b. This comprised of two-tailed non-parametric independent or paired *t*-tests with 5000 permutations and a *p*-threshold of 0.05 across all 32 electrode sites. All statistical tests corrected for multiple comparisons in EEG data using an FDR (False Discovery Rate) correction across signals. All data were combined for EEG analysis, but gender was included as a factor in the overall behavioural analysis (Thornberry et al., 2023) and in non-resting state age-group EEG analyses as a control measure.

## 6.3 Behavioural Results

### *6.3.1 Cognitive Tasks*

All younger participants (n = 31) and older participants (n = 22) were given the TMT, NART, & MOCA after resting-state data were collected and the learning phase of the virtual navigation task was completed. This was to allow for a break in between spatial learning & recall phases, but also to allow for time between resting state data acquisition and the cognitive tasks. Here we reported no significant differences between the groups on NART errors ($t(51) = -1.806$, $p = 0.077$, Cohen's $d = -0.503$) nor on the TMT using the typically calculated overall score of TMTB-A ($t(51) = 1.585$, $p = 0.119$, Cohen's $d = 0.442$). To further confirm this, we also

reported no difference between the groups on individual sections of the test, TMTA ($p = 0.304$) & TMTB ($p = 0.062$). However, we reported significant differences in performance on the MOCA ($t(51) = -2.878$, $p = 0.006$, Cohen's $d = -0.802$) with older adults scoring significantly less (M = 25.41, SEM = +/- 0.491) compared to younger adults (M = 27.1, SEM = +/- 0.337).

### *6.3.2 Young vs. Old: Learning Phase*

We first compared younger (n = 30) and older (n = 22) adults on their performance during the learning phase of the NavWell task. One younger adult had data synchronisation issues due to loss of network connection during testing. They were included in all analysis for which they possess data (see Chapter 5, section 5.3.1.1). We used a 2 (group) X 2 (gender) X 12 (trial) repeated measures mixed factorial ANOVA to examine differences between the groups on latency and path length across the trials.

For latency, we reported a main effect of trial ($F_{(11, 528)} = 8.833$, $p < 0.001$, $\eta^2 = 0.072$). We also reported a significant difference between the groups ($F_{(1, 48)} = 98.482$, $p < 0.001$, $\eta^2 = 0.323$) but not for gender ($F_{(1, 48)} = 1.401$, $p = 0.213$). We also reported a significant interaction effect between trial X group ($F_{(11, 528)} = 4.006$, $p < 0.001$) but not for trial X gender ($F_{(11, 528)} = 0.897$, $p = 0.543$). Using Bonferroni corrected t-tests we reported that latency during Trial 12 was significantly shorter than Trial 1 across all participants (MD = 17.8s, SEM +/- 2.94, $t = 6.051$, $p < 0.001$, Cohen's $d = 1.174$). However, using Tukey corrected t-test to examine our trial X group interaction effect, we reported that there were no significant differences in performance time between younger and older adults on Trial 1 (MD = 17.8s, SEM +/- 4.72, $t = 0.812$, $p = 0.997$, Cohen's $d = 0.253$). However, younger adults were significantly quicker on Trial 12 compared to older adults (MD = 37.1s, SEM +/- 4.72, $t = 7.857$, $p < 0.001$, Cohen's $d = 2.447$). Therefore, though both groups learned the task, the younger adults could perform it with greater speed and efficiency (Figure 6.2a and 6.2b).

For path length, we reported a main effect of trial ($F_{(11, 528)} = 16.016$, $p < 0.001$, $\eta^2 = 0.163$). We also reported a significant difference between the groups ($F_{(1, 48)} = 44.481$, $p < 0.001$, $\eta^2 = 0.136$), with older adults producing longer paths compared to younger adults (MD = 52.5 Vm, SEM +/- 7.8 Vm, $t = 6.696$, $p < 0.001$, Cohen's d = 0.999). No gender effect was reported ($F_{(1, 48)} = 0.349$, $p = 0.558$). We again reported a significant interaction effect for trial X group ($F_{(11, 528)} = 4.830$, $p < 0.001$, $\eta^2 = 0.049$) but no interaction for trial X gender ($F_{(11, 528)} = 1.190$, $p = 0.291$) with no significant three-way or between-subjects interaction effects reported (all $p > 0.7$). Bonferroni corrected t-tests demonstrated that participants' path lengths during Trial 12 were significantly shorter than Trial 1 (MD = 102.327 Vm, SEM +/- 10.61 Vm, $t = 9.644$, $p < 0.001$, Cohen's $d = 1.95$) & Trial 2 (MD = 77.523 Vm, SEM +/- 10.61, $t = 7.306$, $p < 0.001$, Cohen's $d = 1.475$). Interestingly, using Tukey-corrected test to examine our interaction effect, there was no difference between the younger and older adults on path length for Trial 1 (MD = 45.25 Vm, SEM +/- 16.37, $t = 2.765$, $p = 0.467$, Cohen's $d = 0.861$) nor on Trial 12 (MD = 47.5 Vm, SEM +/- 16.37, $t = 2.902$, $p = 0.365$, Cohen's $d = 0.904$). Therefore, the groups did not differ on path length on essential trials, but overall show a significant difference in path length – with older adults displaying slightly longer paths compared to younger adults overall (see Figure 6.2c and 6.2d). Therefore, older adults were not as efficient at locating the hidden target as the younger adults.

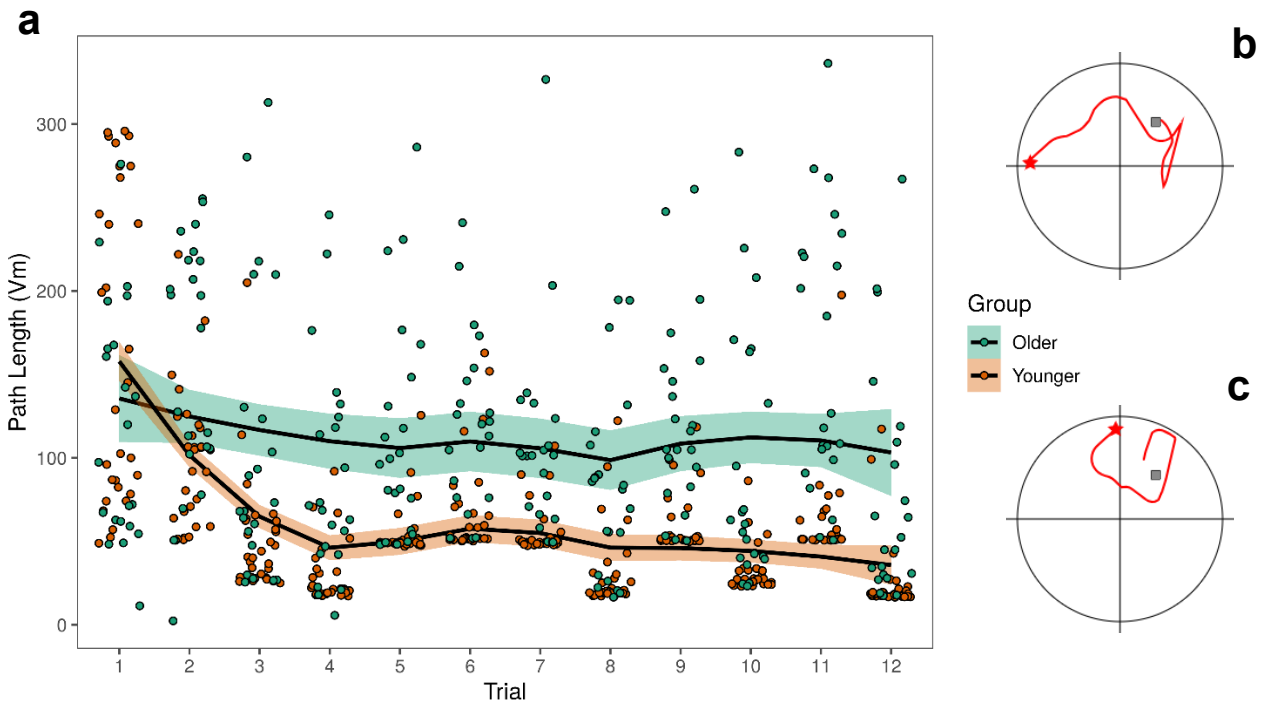


*Figure 6.2:* (a) Line graph and jittered individual data points for older and younger adult path length. Standard error is represented by the shaded outline. (b) Sample path from NavWell of an older adult participant Trial 1 with a complex undirected path. (c) Sample path of an older adult from NavWell of a participants Trial 12 with a more direct route.

### *6.3.3 Older Adults: Learning Phase*

Based on our previous reports and the above findings, we incorporated a further measure for older adults. Older adults seem to be significantly slower at performing the task and locating the target, with slightly lengthier routes. Therefore, we have extracted and reported the percentage of time spent searching in the target quadrant during each trial to ensure our older adults learned the task. This measure is typically used during recall trials (see Chapter 4 & Chapter 5) but can give an indication of task performance during learning (Vorhees & Williams, 2006; Vorhees & Williams, 2014a, 2014b). For quadrant percentage (see Figure 6.3a), we reported a significant main effect of Trial ($F_{(11, 198)} = 9.684$, $p < 0.001$, $\eta 2 = 0.280$). We found no significant differences between conditions ($F_{(1, 18)} = 1.428$, $p = 0.248$) nor genders ($F_{(1, 18)} = 1.586$, $p = 0.224$). We also reported no significant interaction effects for trial X condition ($F_{(11,}$

$_{198)}$ = 0.996, $p$ = 0.451) nor trial X gender ($F_{(11, 198)}$ = 0.681, $p$ = 0.755). Furthermore, we did not report any three-way interaction, nor a gender X condition interaction (all p > 0.27). Using Bonferroni-corrected t-tests we reported that percentage time spent searching the goal quadrant was significantly greater on Trial 12 compared to Trial 1 (MD = -42.1%, SEM +/- 9.23%, $t$ = -4.559, $p$ < 0.001, Cohen's $d$ = -1.54) and Trial 2 (MD = -30.7%, SEM +/- 9.23%, $t$ = -3.324, $p$ = 0.46, Cohen's $d$ = -1.22). Therefore, though not quicker nor more efficient at locating the target – our older adults learned the location of the goal during their learning phase as they increased their searching behaviour above chance level (see Figure 6.3b-c).

As with Chapter 5, we *a priori* analysed the learning performance of participants in both conditions: recent (24-hours, n = 11, 9 female) or remote (1-month, n = 11, 7 female) to check that both conditions for recall had learned the task equally. In order to remain consistent with Chapter 5, we ran a 2 (condition) X 2 (gender) X 12 (trial) repeated measures mixed factorial ANOVA to examine latency and path length across the trials within our older adults. For latency, we reported no significant main effect of trial ($F_{(11, 198)}$ = 1.105, $p$ = 0.359, $\eta^2$ = 0.034). Importantly, we reported no significant difference between recent and remote conditions ($F_{(1, 18)}$ = 3.373, $p$ = 0.083) nor gender ($F_{(1, 18)}$ = 2.622, $p$ = 0.123). We also reported no significant interaction effect between trial X condition ($F_{(11, 198)}$ = 0.709, $p$ = 0.821) nor trial X gender ($F_{(11, 198)}$ = 0.608, $p$ = 0.821). We did not report any three-way interaction, nor a gender X condition between-subjects interaction (all $p$ > 0.3). For path length, we reported a significant main effect for Trial ($F_{(6.1, 110.7)}$ = 2.238, $p$ = 0.043, $\eta^2$ = 0.075). However, we again reported no differences between conditions ($F_{(1, 18)}$ = 4.225, $p$ = 0.053; see Figure 6.3d) nor genders ($F_{(1, 18)}$ = 0.043, $p$ = 0.837). We again reported no significant interaction effect between trial X condition ($F_{(6.1, 110.7)}$ = 0.457, $p$ = 0.843) nor trial X gender ($F_{(6.1, 110.7)}$ = 0.595, $p$ = 0.738). We did not report any three-way interaction, nor did we report a gender X condition between-subjects interaction (all $p$ > 0.3).

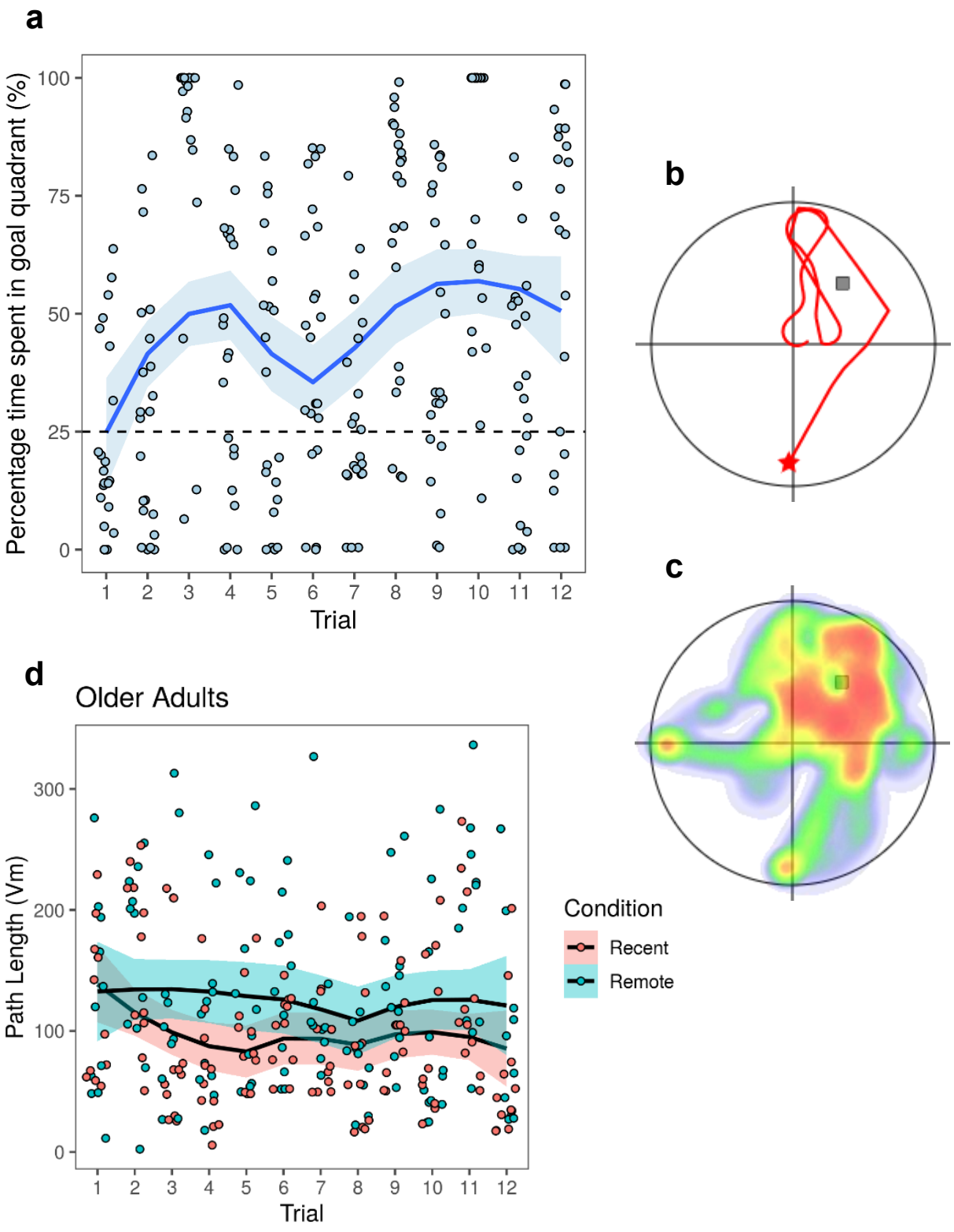


*Figure 6.3:* (a) Line graph and jittered individual data points for older adult quadrant percentage search times across trials. Data is above the chance line (25%) from Trial 2 onwards. (b) Sample path from older adult participant with 85% goal quadrant search time but an unsuccessful trial. (c) Average learning heatmap from an older adult participant with several unsuccessful trials. (d) Older Adults path length for recent and remote conditions.

*6.3.4 Young v Old: Immediate Recall Trial*

As per the protocol in Chapter 5, all participants were given a probe trial (the target was removed from the arena) after a ten-minute interval. We termed this "immediate recall" as there is no real consolidation time, and it replicates the recall phase examined in Chapter 4 & 5. We examined percentage time spent searching in the goal quadrant (Northeast). As in Chapter 5, as a check to make sure that the two groups could recall the location during this trial, and that difference between the groups may be due to age rather than poor task performance, we ran a 2 (group) X 2 (gender) X 4 (quadrant) mixed factorial ANOVA.

We reported a main effect of quadrant ($F_{(1.5,\ 72.3)} = 191.9$, $p < 0.001$, $\eta^2 = 0.743$). Interestingly, we did not report any differences between the groups ($F_{(1,\ 49)} = 0.084$, $p = 0.773$) nor genders ($F_{(1,\ 49)} = 0.551$, $p = 0.461$). However, we reported a significant interaction effect for quadrant X group ($F_{(1.5,\ 72.3)} = 10.858$, $p < 0.001$, $\eta^2 = 0.042$). But we did not report an interaction for quadrant X gender ($F_{(1.5,\ 72.3)} = 0.525$, $p = 0.539$), nor a three-way interaction effect or any between-subject interaction effects (all $p > 0.17$). Bonferroni-corrected t-tests revealed (averaged across group) that the percentage time spent searching in the NE (Goal) quadrant was significantly greater than all other quadrants, the NW ($t = 17.474$, $p < 0.001$, MD = 45.6% +/- 2.6%, Cohen's $d = 3.798$), SW ($t = 16.77$, $p < 0.001$, MD = 43.8% +/- 2.6%, Cohen's $d = 3.817$) and the SE ($t = 22.502$, $p < 0.001$, MD = 58.7 % +/- 2.6%, Cohen's $d = 5.123$). We used Tukey corrected t-tests to explore our quadrant X group interaction effect reporting that our older adults spent significantly less time in the NE (Goal) quadrant compared to our younger adults ($t = -3.882$, $p = 0.004$, MD = -14.18% +/- 3.65%, Cohen's $d = -1.191$; see Figure 6.4). We reported no other differences between the groups at any other quadrant (all $p > 0.6$) but both groups demonstrated greater preference for the NE quadrant, searching significantly more here than any other quadrant.

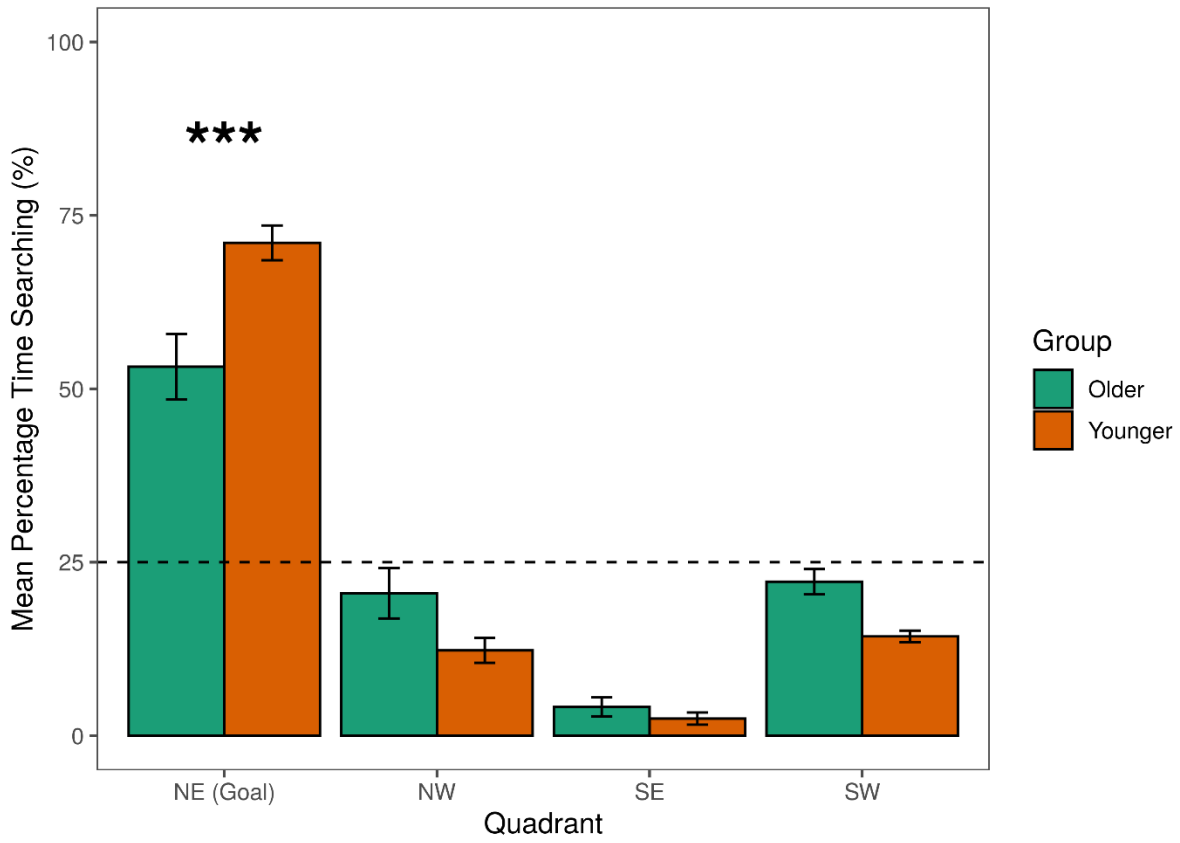


*Figure 6.4:* Standard bar chart of quadrant search percentages (%) for each quadrant during immediate recall trials for older and younger adults. The chance line (25%) is displayed showing all other quadrants below this regardless of group.

### *6.3.5 Recent & Remote Recall*

#### *6.3.5.1 Older Adults*

After our older adults participants were randomly assigned their condition: recent/24-hours (n = 11, 9 female) or remote/1-month (n = 11, 7 female) they were then retested after the corresponding consolidation period. However, to ensure that the two groups could recall the location equally – and that any difference between the groups was due to the consolidation period rather than poor recall, we ran a 2 (condition – recent v remote) X 2 (gender) X 4 (quadrant) mixed factorial ANOVA. Similar to Chapter 5, we reported a main effect of quadrant ($F_{(2.1,\ 38.7)} = 11.683$, $p < 0.001$, $\eta^2 = 0.363$). Importantly, we did not report any

differences between the conditions ($F_{(1, 18)} = 0.024$, $p = 0.878$) nor genders ($F_{(1, 18)} = 1.550$, $p = 0.229$). We reported no significant interaction effect for quadrant X condition ($F_{(2.1, 38.7)} = 1.181$, $p = 0.320$) nor for quadrant X gender ($F_{(2.1, 38.7)} = 0.814$, $p = 0.458$), nor a three-way interaction effect or any between-subject interaction effects (all $p > 0.6$). Using Bonferroni corrected *t*-tests, we reported that regardless of condition, our older adults spent significantly more time in the NE (Goal) quadrant, compared to the NW ($t = 4.095$, $p < 0.001$, MD = 33.4% +/- 8.2%, Cohen's $d = 1.675$), SW ($t = 3.510$, $p = 0.005$, MD = 28.7% +/- 8.2%, Cohen's $d = 1.436$) and the SE quadrants ($t = 5.742$, $p < 0.001$, MD = 46.9% +/- 8.2%, Cohen's $d = 2.349$). Therefore, regardless of consolidation time, both groups recalled the goal location particularly well (see Figure 6.5).

#### *6.3.5.2 Younger vs. Older Adults*

To investigate the differences between younger [n = 31; 24-hours/recent (n=16, 11 female) or 1-month/remote (n=15, 10 female)] and older adults [n = 22; recent/24-hours (n = 11, 9 female) or remote/1-month (n = 11, 7 female)] at two different consolidation periods, we ran a 2 (condition – recent v remote) X 2 (group – younger v older) X 4 (quadrant) mixed factorial ANOVA. We removed gender as it has had no reported impact throughout this chapter and did not contribute to any findings in our ANOVA models from Chapter 5 using our younger adults. We reported a main effect of quadrant ($F_{(2.2, 105.4)} = 143.795$, $p < 0.001$, $\eta^2 = 0.659$). We also reported a significant difference between the groups ($F_{(1, 49)} = 9.310$, $p = 0.004$) but not conditions ($F_{(1, 49)} = 0.465$, $p = 0.499$). Furthermore, we reported a significant interaction effect for quadrant X group ($F_{(2.2, 105.4)} = 22.079$, $p < 0.001$, $\eta^2 = 0.101$). We did not report a significant interaction for quadrant X condition ($F_{(2.2, 105.4)} = 1.948$, $p = 0.144$), nor a three-way interaction effect or any between-subject interaction effects (all $p > 0.2$). Firstly, we investigated our main

effect using a Bonferroni corrected t-test. We revealed that our participants search in the NE (Goal) quadrant more than any other quadrant (all $p < 0.001$) as reported above and in Chapter 5. Secondly, we used a Tukey corrected t-test to explore our quadrant X group interaction effect. We reported that regardless of condition, our younger group searched for a longer time in the NE (Goal) quadrant compared to our older group ($t = 7.923$, $p < 0.001$, MD = 29.5% +/- 3.7%, Cohen's $d = 2.209$). We also reported that our older group spent significantly longer searching in the adjacent NW quadrant compared to our younger group ($t = 3.933$, $p = 0.003$, MD = 14.6% +/- 3.7%, Cohen's $d = 1.097$).

To explore this further, we ran a 2 (group) X 2 (condition) ANOVA to investigate our between-subject group effect, focusing only on percentage time spent searching in the NE (Goal) quadrant. We reported no significant differences between conditions ($F_{(1, 49)} = 1.102$, $p = 0.299$) but reported a significant difference between groups ($F_{(1, 49)} = 1.102$, $p < 0.001$, $\eta^2 = 0.414$). Notably, we reported no significant interaction effect for group X condition ($F_{(1, 49)} = 0.349$, $p = 0.558$). Therefore, averaged across conditions, our younger adults (M = 77.5%, SEM +/- 5.4%) spent significantly more time searching here compared to our older adults (M = 47.97%, SEM +/- 1.69%). From an examination of the descriptive statistics, we reported greater time spent searching in the NE for the older adults recent group (M = 52.03%, SEM +/- 6.2%) compared to the remote group (M = 43.9%, SEM +/- 8.89%), with contrasting results reported for the younger group in Chapter 5 (see Figure 6.5 also).

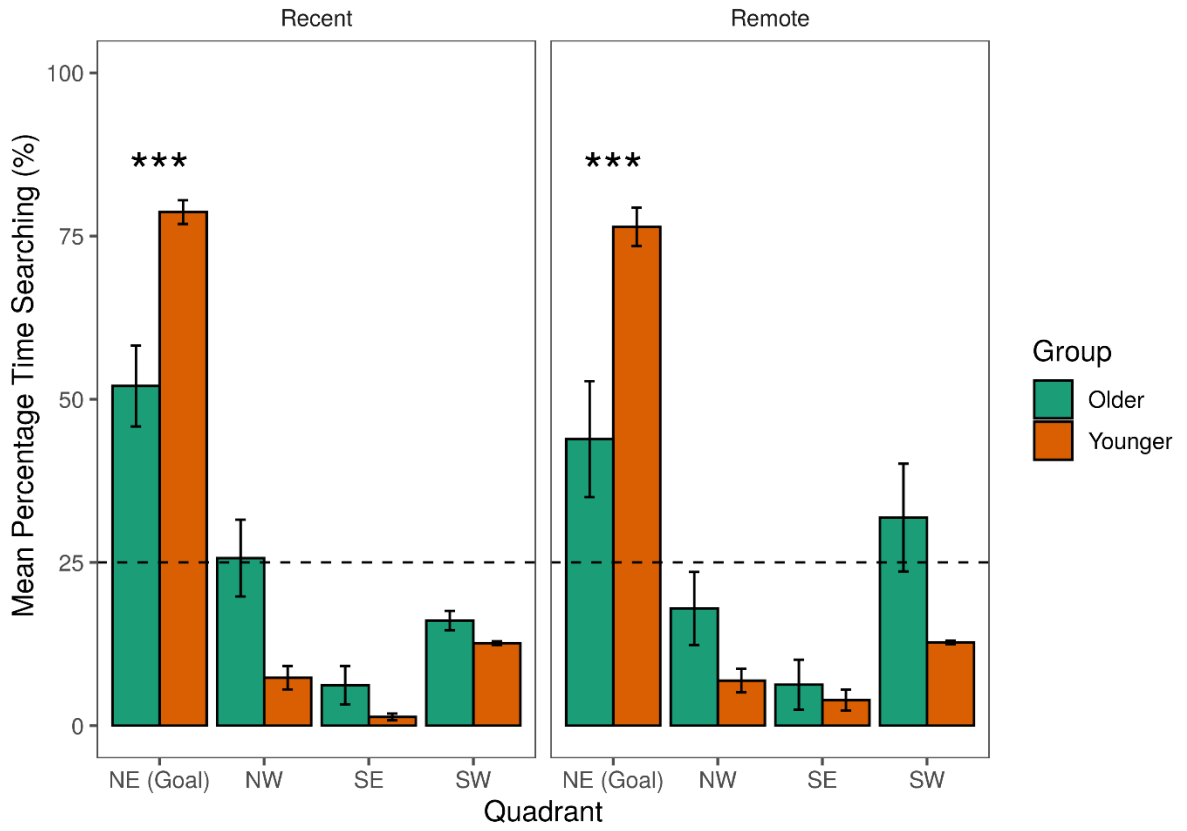


*Figure 6.5:* Standard bar chart of quadrant search percentages (%) for each quadrant during Recent and Remote recall trials for older and younger adults. The chance line (25%) is displayed showing most other quadrants below this regardless of group or recall phase.

### *6.3.5.3 Performance Change in Older Adults*

In order to determine if performance declines from immediate to recent/remote, we ran a non-parametric alternative to the paired t-test. Due to our small sample size, it is not possible to assume normality with the data. A Wilcoxon signed-rank test was conducted to evaluate whether there was a statistically significant change in percentage time spent searching the goal quadrant from immediate recall trial to the recent/24-hour recall trial in the older adult group. Results showed that time searching in the goal quadrant increased from immediate recall (M = 45.45%, SEM +/- 6.9%) to 24-hour recall (M = 52.03%, SEM +/- 6.2%), but was not

statistically significant ($Z$ = -1.156, $p$ = 0.278; see Figure 6.6a). We also examined this change from immediate recall trial to the remote/1-month recall trial. We reported that time searching in the NE quadrant decreased from immediate (M = 60.9%, SEM +/- 5.84%) to remote recall (M = 43.9%, SEM +/- 8.9%). This decrease in performance was statistically significant ($Z$ = 2.134, $p$ = 0.032, effect size = 0.727; see Figure 6.6b). These results reflect our observation in the descriptive data, but are contrasted to our findings from Chapter 5, in which our younger remote group actually significantly improved their performance.

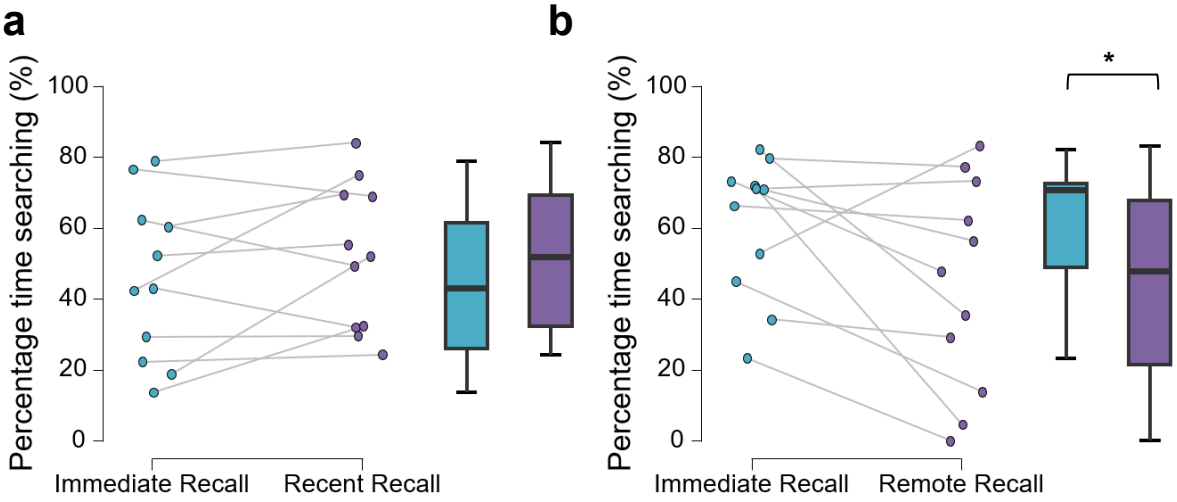


*Figure 6.6:* (a) Boxplot representing recent condition older adults' percentage time in NE quadrant change from immediate to delayed (recent) trial. (b) Remote condition older adults percentage time in NE quadrant change from immediate to delayed (remote) trial.

## 6.4 EEG Results

### *6.4.1 Age-Related Differences in Eyes-Open Resting State*

As discussed above, recent work by Jabès et al. (2021) revealed significant differences in resting state frequency power between younger and older adults, with their data containing a similar sample size to ours. Here, we calculated Power Spectral Density (PSD) using a Welch window (medium window length of 2s with an overlap ratio of 50%) to compute the power spectra ($\mu V^2/Hz$) based on a typical Fast-Fourier Transform (FFT) default linear frequency definition (1:1:40). Power spectra were computed for five bands: Delta (2-4 Hz), Theta (5-7 Hz), Alpha (8-12 Hz), Beta (15-29 Hz) & Gamma (30-40 Hz). The bands were defined based on previous chapters. The data was pre-processed and epoched as described.

We incorporated the described epoch rejection criteria and visual inspection of participant data. These continuous recordings were then epoched and ran through our rejection criteria and visual inspection. This resulted in a total of approx. 5.6% of epochs being rejected. A participant from the younger adult group without sufficient data to facilitate analysis were excluded (n = 1). This left a total of 1870 epochs for older adults (n = 22) and a total of 2619 epochs for younger adults (n = 30). We first extracted the mean relative resting state power for each frequency band at a global scalp level. Following this, we ran a 2 (group) X 2 (condition) X 5 (Frequency Band) mixed factorial ANOVA to investigate group differences in mean resting state data, and to ensure that there were no differences at rest between assigned memory conditions. We reported a main effect of frequency ($F_{(4, 188)} = 100.140$, $p < 0.001$, $\eta^2 = 0.667$). However, we reported a significant difference between groups ($F_{(1, 48)} = 5.822$, $p = 0.020$, $\eta^2 = 0.110$) but not between conditions ($F_{(1, 48)} = 0.034$, $p = 0.854$). We reported no interaction effects for frequency X group ($F_{(4, 188)} = 1.722$, $p = 0.147$) nor frequency X condition ($F_{(4, 188)} = 0.455$, $p = 0.769$). We also reported no three-way interaction effect, nor any between-subjects group X condition interaction (all $p > 0.5$). Therefore, across all frequency bands, our older adults

had significantly greater relative power compared to younger adults (MD = 0.1%, $t = 2.413$, $p = 0.02$, Cohen's $d = 0.019$). However, we decided to investigate each frequency band individually using independent *t*-tests – considering the mean difference reported above is so low – and due to the fact that power relativity corrections induce a main effect between the frequencies (see Chapter 4 & 5). Therefore, we reported no significant difference between younger and older adults on relative delta ($t(50) = -0.919$, $p = 0.363$, Cohen's $d = -0.262$), theta ($t(50) = -1.024$, $p = 0.311$, Cohen's $d = -0.291$) nor alpha ($t(50) = -0.556$, $p = 0.581$, Cohen's $d = -0.158$). However, for beta we reported that older adults (M = 0.134, SEM +/- 0.009) compared to younger adults (M = 0.087, SEM +/- 0.007) had significantly greater beta power ($t(50) = 3.992$, $p < 0.001$, Cohen's $d = 1.136$). Furthermore, we also reported that older adults (M = 0.072, SEM +/- 0.007) compared to younger adults (M = 0.053, SEM +/- 0.007) had significantly greater gamma power at rest ($t(50) = 2.007$, $p = 0.05$, Cohen's $d = 0.571$). These data are plotted in Figure 6.7a. Following this, we plotted isolated PSDs with a linear frequency definition of 1:1:40 for the full scalp providing a frequency resolution of 0.5 Hz. This allowed us to see the specificity (and magnitude) of the reported relative dynamics within the bands (Figure 6.7b) between younger and older adults.

To compare the group differences more accurately across individual sites, we ran a within-groups non-parametric permutation *t*-test with 5000 permutations. We then corrected for multiple comparisons using FDR-correction (see Chapter 3 and Thornberry et al., 2023). As in previous chapters, any electrode site that reached significance at an alpha level of 0.05, was marked by a yellow star. Figure 6.8a below demonstrates the topographical distribution of resting state relative power for each frequency band of interest in each group, with the results of permutation t-test below (Figure 6.8b).

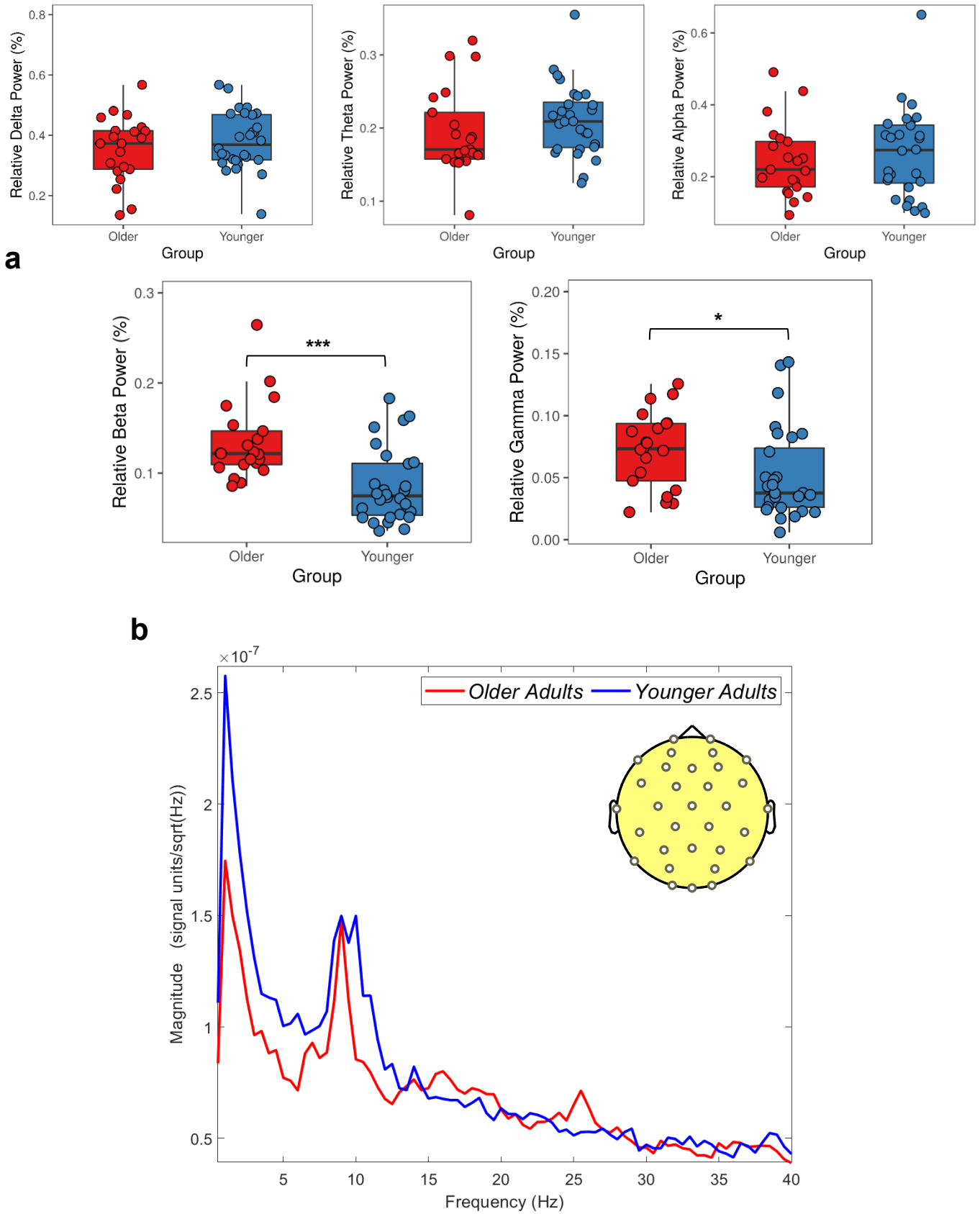


*Figure 6.7:* (a) Relative power boxplot displaying each frequency and older and younger adult groups. Significance is denoted *$p < 0.05$ and ***$p < 0.001$. (b) An FFT line graph displaying the non-normalised mean magnitude of power (μV²/Hz) across the scalp for each group during resting state. Power is displayed across the 1-40 Hz frequency range, with a frequency definition of 0.5 Hz.

For our FDR-corrected permutation *t*-tests, we reported some interesting differences in relative power between the groups (Figure 6.8). We first reported significantly greater frontal delta power in our younger participants compared to our older group, significant ($p < 0.05$) at sites F3 and AF3 (see Figure 6.8b). We also reported greater posterior theta power in our younger group, concentrated at the left-parietal area, significant ($p < 0.05$) at sites P3 and CP1 (see Figure 6.8b). We reported no significant differences between our younger and older adults for alpha power, however, there is greater alpha power in our younger adults (which should be the case – see Tröndle et al. (2023)). This greater relative power is also better dispersed in our younger adults across the posterior scalp sites (see Figure 6.8a). For beta power, we reported a clear and significant difference (see Figure 6.8b) between our younger and older adults, with older adults having significantly greater beta power across the scalp, significant at sites F3, Fz, FC1, C3, Cz, C4, CP1, CP2, CP6 ($p < 0.01$) and also F4, AF3, AF4, CP5, CP6 & Pz ($p < 0.05$). Additionally, similar patterns were reported for gamma power (Figure 6.8b), with older adults having greater right-lateralised gamma power significant at sites AF4, F4, Cz, C4, CP2, CP6, P4, P8 ($p < 0.05$). These results are almost identical to Jabès et al. (2021), who reported lower theta and alpha power alongside greater beta and gamma power in older adults compared to younger adults, with a similar sample size.

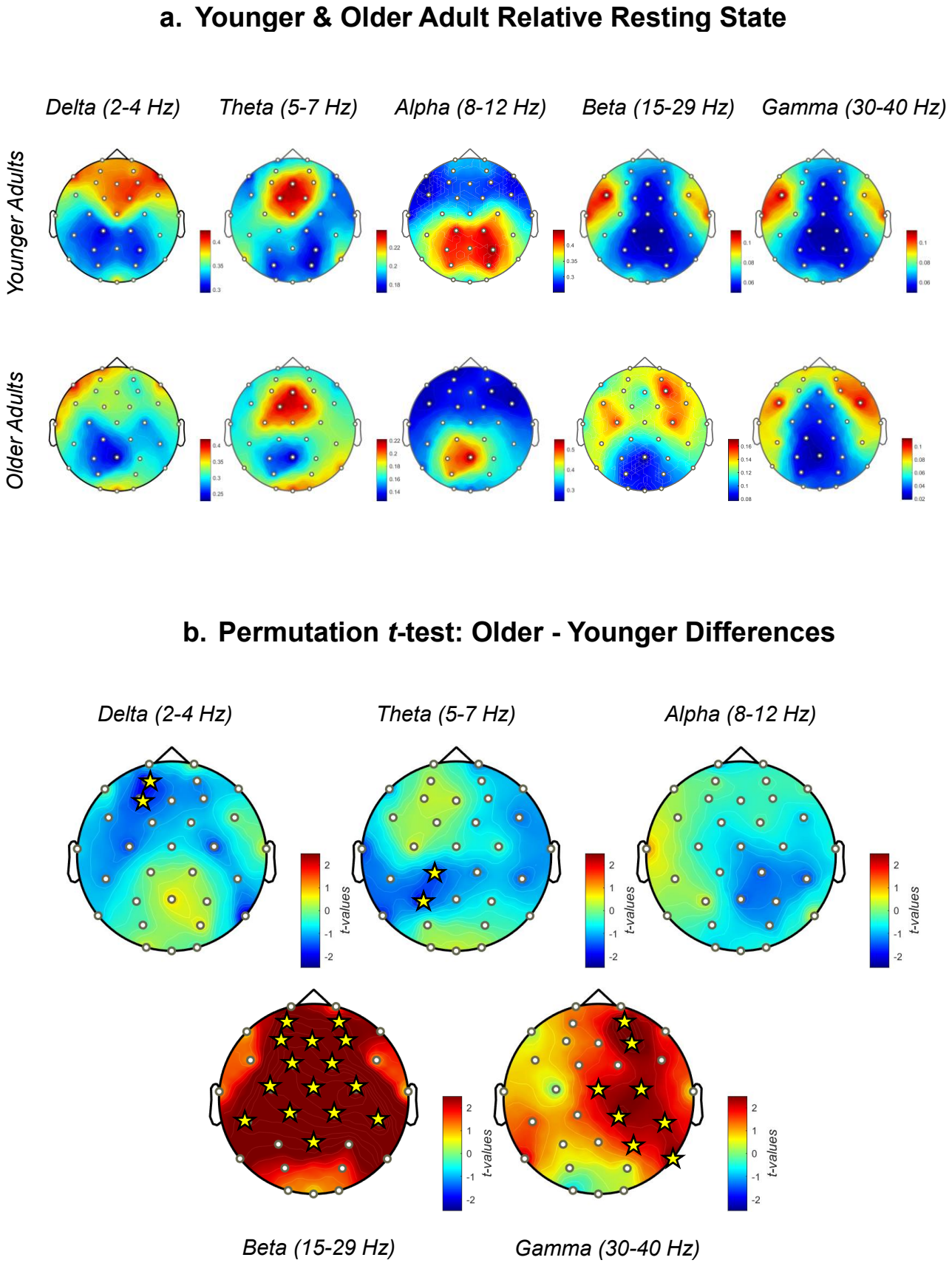


*Figure 6.8:* (a) Topographical plots of younger and older adult resting state topographies for each frequency band. Each are displayed on a local scale in relative power units (%). (b) Results from a permutation t-test examining differences between older and younger adults. Values are scaled at min/max globally in t-values. Stars mark significant electrode sites at $p < 0.05$.

### *6.4.2 Resting State Correlates of Spatial Navigation & Cognition*

We investigated whether the relative power of our chosen frequency bands during rest, related to any key measures of spatial learning as reported by Jabès et al. (2021). We also examined whether performance on cognitive tasks, which examine learning and memory abilities, are also related to the relative power in our frequency bands as reported by Finnigan and Robertson (2011). Not all measures from EEG, spatial learning and cognitive tasks were found to be normally distributed for both groups (via Q-Q plots & multivariate normality tests). Therefore, Spearman's correlation co-efficient was used. Correlations were run on all participants and then for both groups independently to provide an entire overview. We included the following variables: MOCA scores, TMTB-A scores, NART errors, average path length (Vm) and average latency (seconds) during learning and time spent (%) in the target quadrant during immediate [Immediate NE (Goal)] and time spent (%) in the target quadrant during the delayed recall (24 hours or 1 month: [Recall NE (Goal)]). We then included mean relative power across the scalp for delta, theta, alpha, beta and gamma.

#### *6.4.2.1 All participants*

Initially, we will ignore correlations found between EEG bands. Some of these correlations would be expected, including any relationship between latency and path length, as both are measures of performance on the virtual water maze. Firstly, we reported no correlations with the TMTB-A scores (all $p > 0.14$) nor NART errors and any other variable (all $p > 0.054$). Interestingly, we reported a significant positive correlation between performance on the MOCA and percentage time spent searching in the NE (Goal) quadrant at both recall phases (Immediate: $r(50) = 0.312$, $p = 0.023$; see Figure 6.9a and Delayed: $r(50) = 0.397$, $p = 0.003$; not displayed). Furthermore, we reported a significant positive correlation between resting state

beta power and average latency ($r(50) = 0.476$, $p < 0.001$) and path length ($r(50) = 0.474$, $p < 0.001$) during learning (see Figure 6.9b). We reported a similar but weaker significant positive correlation between resting state gamma power and average latency ($r(50) = 0.288$, $p = 0.043$; see Figure 6.9c) and path length ($r(50) = 0.318$, $p = 0.025$). We also reported a significant negative correlation between resting state beta power and performance during delayed recall ($r(50) = -0.438$, $p = 0.001$; Figure 6.9d). We reported no correlations between any other variables. All significant correlations are reported in Table 6.1.

#### *6.4.2.2 Group-specific Correlations*

For younger adults, we reported no significant correlations between mean relative power at any frequency and any cognitive task (all $p > 0.35$) nor any spatial task performance measure (all $p > 0.06$). Only relative gamma power and average path length ($r(30) = 0.354$, $p = 0.060$) & relative alpha power and average latency ($r(30) = -0.351$, $p = 0.062$) *approached* significance. For older adults, we also reported no significant correlations between mean relative power at any frequency and any cognitive task score (all $p > 0.11$) nor any spatial task performance measure (all $p > 0.17$).

*Table 6.1:* Significant Spearman's correlations for all participants

| | | Spearman's rho | *p* |
|---|---|---|---|
| Average Path | - Immediate NE (Goal) | -0.291 * | 0.036 |
| Average Path | - Recall NE (Goal) | -0.459 *** | < .001 |
| Average Path | - beta | 0.474 *** | < .001 |
| Average Path | - gamma | 0.318 * | 0.025 |
| Average Latency | - Recall NE (Goal) | -0.421 ** | 0.002 |
| **Average Latency** | **- beta** | **0.476 *** ** | **< .001** |
| **Average Latency** | **- gamma** | **0.288 *** | **0.043** |
| Immediate NE (Goal) | - Recall NE (Goal) | 0.614 *** | < .001 |
| **Recall NE (Goal)** | **- beta** | **-0.438 ** ** | **0.001** |
| **MOCA scores** | **- Immediate NE (Goal)** | **0.312 *** | **0.023** |
| MOCA scores | - Recall NE (Goal) | 0.397 ** | 0.003 |

* p < .05, ** p < .01, *** p < .001

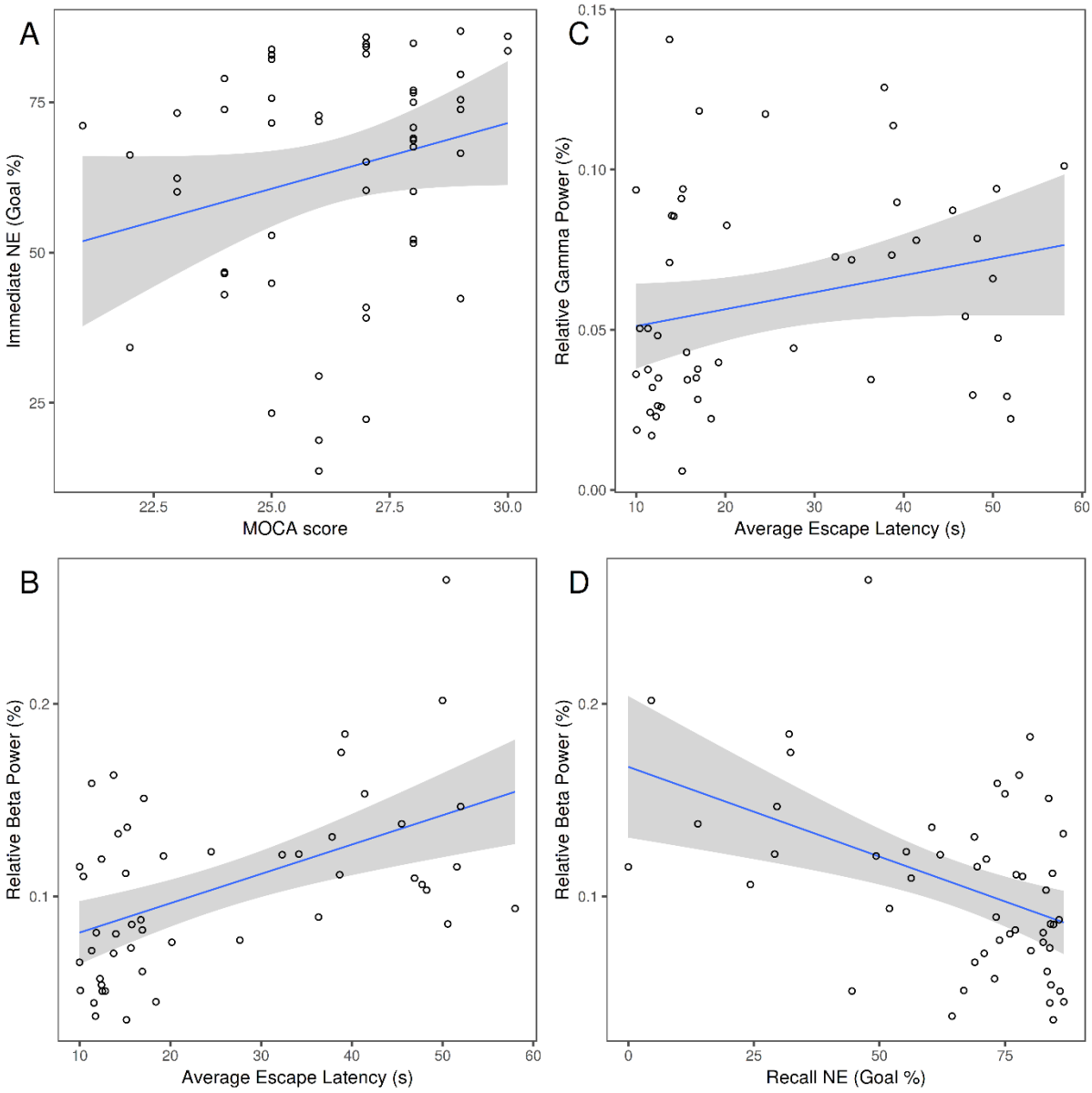


*Figure 6.9:* Sample of Spearman's rho correlation plots and respective confidence intervals for significant correlations reported in section 6.4.2 (A-D). Displayed plots are bolded in Table 6.1 and were chosen based on typical reported measurements in the virtual water maze (Latency, Goal Quadrant %).

*6.4.3 Immediate Recall: Young vs Old*

In order to examine any age differences in immediate recall (following an interval of approximately 10-15 minutes, see Chapter 2) we computed power spectra ($\mu V^2/Hz$) for each frequency band for each group. We computed Power Spectral Density (PSD) using a Welch window (window length of 2s with an overlap ratio of 50%) based on a typical Fast-Fourier Transform (FFT) default frequency definition. Power spectra were computed for five bands: Delta (2-4 Hz), Theta (5-7 Hz), Alpha (8-12 Hz), Beta (15-29 Hz) & Gamma (30-40 Hz). Following this, we normalised the task-related PSD using a baseline correction method (see Chapter 2 & 5). Taking the resting state PSD, we baseline corrected each individual participants data using a decibel (*dB*) conversion:

$$dB_f = 10 \times \log_{10}\left(\frac{signal\ power_f}{baseline\ power_f}\right)$$

Relative power is now relative to a corrected baseline and expressed in decibels (*dB*). We did this by using the same process used in Chapter 5: *Standardize > Baseline normalization (A=Baseline) > Scale with the mean (dB)*. We decided not to focus our analysis on pre-defined regions of interest used in Chapter 4 & Chapter 5. Due to the large amount of processing required, as well as the last two studies reporting no significance at ROIs – we decided not to look at specific ROIs, but instead extract the scalp mean power (*dB*) for each participant. Our permutation *t*-tests examined differences at each individual electrode site, providing the same value whilst correcting for multiple comparisons. We excluded younger adults with incomplete immediate recall trial data (n = 3) and one older adult with no trigger in the data. Following our epoch rejection phase, this left us with 628 epochs in our older adults group (n = 21) and 840 epochs in our younger adult group (n = 28). We first ran a 2 (group) X 2 (gender) X 5 (frequency) mixed-factorial ANOVA to examine if there were any differences between the age

groups on mean global scalp power, and whether gender could have had an impact on these differences.

Firstly, we reported a significant main effect for frequency ($F_{(4, 180)} = 12.240$, $p < 0.001$, $\eta^2 = 0.108$). We did not report any significant differences between group ($F_{(1, 45)} = 0.033$, $p = 0.856$) nor gender ($F_{(1, 45)} = 2.750$, $p = 0.104$). Furthermore, we did not report any significant interactions between frequency X group ($F_{(4, 188)} = 0.867$, $p = 0.485$) nor frequency X gender ($F_{(4, 188)} = 1.846$, $p = 0.122$). We also reported no significant between subjects interactions nor three-way interaction effects (all $p > 0.23$). To investigate our main frequency effect, we used Bonferroni corrected *t*-tests averaged over levels of group and gender. We reported that during immediate recall, delta ($t = 3.755$, $p = 0.002$, Cohen's $d = 0.658$), theta ($t = 3.898$, $p = 0.001$, Cohen's $d = 0.683$) and gamma powers ($t = 4.866$, $p < 0.001$, Cohen's $d = 0.853$) showed significantly greater increases from baseline compared to alpha power (MD = 1.7 *dB*, SEM +/- 0.45 *dB;* MD = 1.76 *dB*, SEM +/- 0.45 *dB* and MD = 2.2 *dB*, SEM +/- 0.45 *dB* respectively). This supports our previous findings, suggesting that delta-theta and gamma increases accompanying alpha suppression may support immediate spatial memory processing – seemingly regardless of age.

To further examine the dynamics of these frequency bands between groups, we ran a non-parametric permutation *t*-test using (see Thornberry et al., 2023). We reported a baseline-corrected scalp topography for each group, followed by group differences presented in *t*-values (Figure 6.10). From this analysis, we observed heightened power at posterior parts of the scalp, with less frontal and central power in our older adults compared to younger adults for delta, theta and alpha. No site reached significance. We reported less overall beta power in older adults with significance at the right centro-parietal electrode CP6. We reported significantly less right-posterior gamma (significant at sites Pz, P4, CP6, P8) but overall similar activation to our younger adults across the scalp.

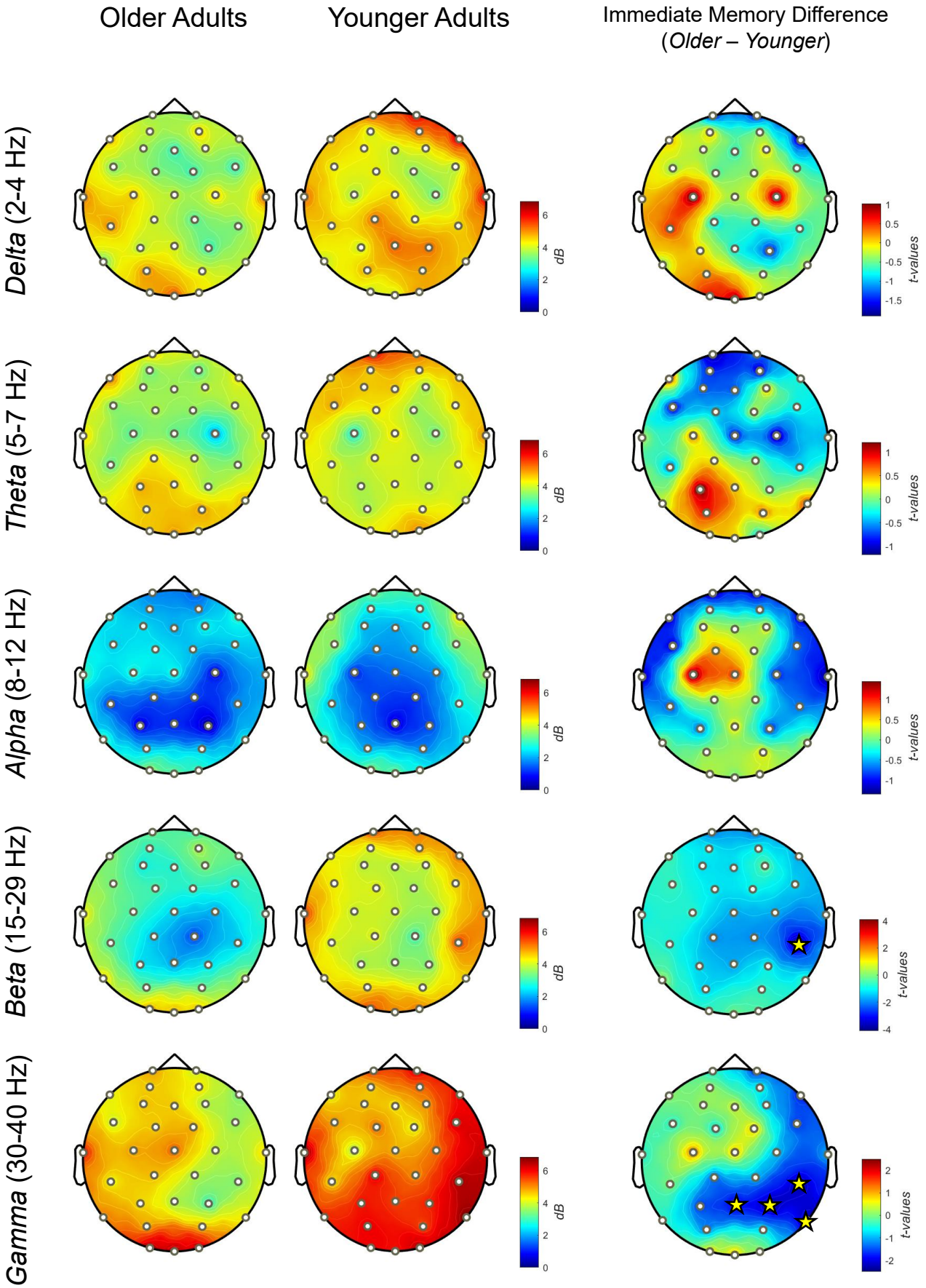


*Figure 6.10:* Topographical distribution of power during immediate recall phase within the older and younger adult groups. Power in each frequency band is displayed as power relative to baseline (in decibels: *dB*, all positive). Both groups are displayed on the same scale. Differences are displayed in t-values within their own local scale. Significant electrode sites ($p < 0.05$) are marked with a yellow star.

*6.4.5 Recent Memory (24-hours): Young vs Old*

We then chose to examine age-related differences in spatial memory recall during navigation after 24-hours, alternatively proposed as "recent" spatial memory. We computed PSDs for the relevant recall trials for younger adults (n = 16) and older adults (n = 11) using the methodology outlined previously. Our older adults had a very low epoch rejection rate (0.3%) leaving 329 epochs for our older adult group and 480 epochs for our younger adult group. We then performed the previously discussed baseline correction for each individual participant. Firstly, we ran a 2 (group) X 2 (gender) X 5 (frequency) mixed-factorial ANOVA to examine if there were any differences during recent spatial memory recall between the age groups on mean global scalp power, and whether gender had any impact on these differences.

We reported no significant main effect of frequency ($F_{(4, 92)} = 2.283$, $p = 0.066$), nor did we report any significant difference between groups ($F_{(1, 23)} = 1.031$, $p = 0.320$) nor genders ($F_{(1, 23)} = 2.599$, $p = 0.121$). We reported no significant interaction effect for frequency X group ($F_{(4, 92)} = 1.257$, $p = 0.292$) nor any significant interaction for frequency X gender either ($F_{(4, 92)} = 2.013$, $p = 0.099$). We reported no significant three-way interaction effects nor any interaction effect between group X gender (all $p > 0.8$). Rather than exploring cross-scalp descriptives, we instead further investigated the group dynamics of these frequency bands using a non-parametric permutation *t*-test with the same criteria reported previously. We reported baseline-corrected scalp topography for each group below, followed by group differences presented in *t*-values (see Figure 6.11). It is important to note that group-level mean task-related activity for individual groups are displayed on a global scale, whilst group differences are displayed on frequency-specific *t*-scales from minimum to maximum t-value for the corresponding frequency.

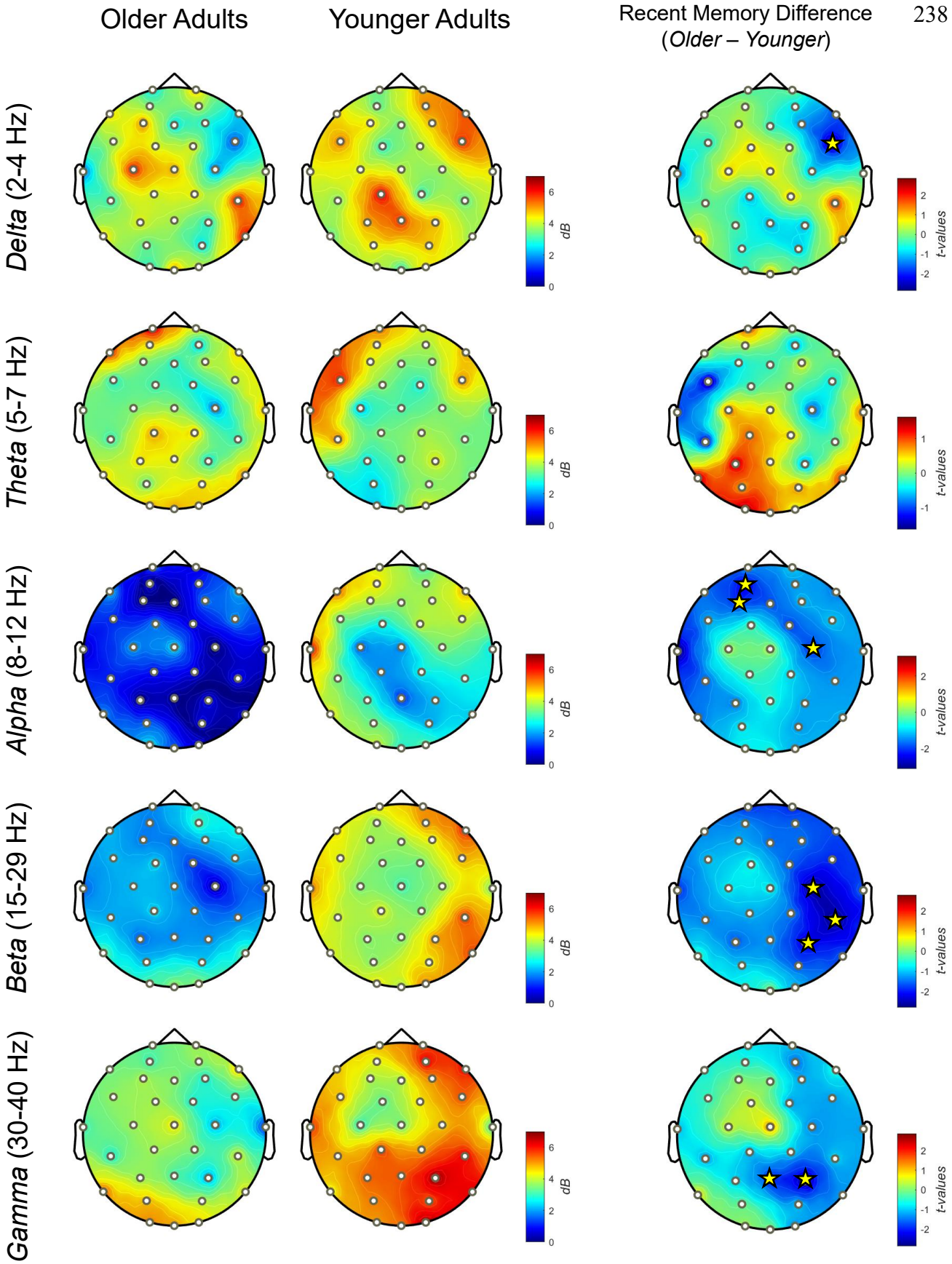


*Figure 6.11:* Topographical distribution of power during recent (24-hour) recall phase within the older and younger adult groups. Power in each frequency band is displayed as power relative to baseline (in decibels: *dB*, all positive). Both groups are displayed on the same scale. Differences are displayed in t-values within their own local scale. Significant electrode sites ($p < 0.05$) are marked with a yellow star.

The results of our permutation *t*-tests revealed significantly less right-lateralised frontal delta power in our older adults compared to our younger adults (significant at site FC6) with some generally similar synchronisation across the scalp. Our younger adults showed greater activation of the parietal area compared to older adults, but we did not report significance here. For theta power, we reported lesser left frontal and central activation compared to younger adults. However, older adults displayed greater theta activation at posterior areas, namely the parietal and central regions. Nevertheless, we reported no significance at any site. In alpha power, we reported much lesser activation across all areas of the scalp in our older adults. reduced alpha activation during spatial memory recall reflects greater alpha suppression in older adults. We reported significance at left frontal sites AF3 & F3 as well as at electrode C4. Interestingly, for beta power we report cross-scalp differences again between groups, with older adults showing lesser power compared to younger adults, demonstrating greater increases in beta activity. We report significantly less beta power at right-central and parietal sites C4, CP6 & P4. Finally, for gamma we reported much greater increases in gamma power during recent memory retrieval in our younger adults compared to our older adults, significant at parietal midline sites Pz & P4. As might be expected, the activations for recent memory show a very similar pattern to those of immediate memory. Older adults show greater activation of theta posterior sites, activation of alpha central sites surrounded by general suppression of surrounding areas and a general suppression of beta and gamma, that tend to be posterior and right lateralised. The suppression of power is visible across the scalp average of non-normalised data presented in Figure 6.13.

*6.4.6 Remote Memory (1-month): Young vs Old*

We then investigated age-related differences in spatial memory recall during navigation after 1-month, i.e. remote spatial memory. We computed PSDs for the relevant recall trials for younger adults (n = 14) and older adults (n = 10) using the methodology outlined previously (1 older adult was removed from the analysis as they had too many missing epochs). Here, our older adults had no epochs rejected leaving 300 epochs for our older adult group and 417 epochs for our younger adult group. We again performed the previously discussed baseline correction for each individual participant. Firstly, we ran a 2 (group) X 2 (gender) X 5 (frequency) mixed-factorial ANOVA to examine if there were any differences in mean scalp power during remote spatial memory recall between the age groups, and whether gender had any impact on these differences.

This time, we reported a significant main effect of frequency ($F_{(4, 80)} = 7.189$, $p < 0.001$, $\eta^2 = 0.123$). Nonetheless, we reported no significant difference between the groups ($F_{(1, 20)} = 0.996$, $p = 0.330$) nor between the genders ($F_{(1, 20)} = 0.059$, $p = 0.811$). We reported no significant interaction effect for frequency X group ($F_{(4, 80)} = 0.913$, $p = 0.460$) nor any significant interaction for frequency X gender either ($F_{(4, 80)} = 0.380$, $p = 0.823$). We also reported no significant three-way interaction effects nor any interaction effect between group X gender (all $p > 0.54$). Using Bonferroni corrected *t*-tests we explored our main effect, revealing that across both groups, delta ($t = 4.503$, $p < 0.001$, Cohen's $d = 1.022$), theta ($t = 2.902$, $p = 0.048$, Cohen's $d = 0.658$) and gamma powers ($t = 4.633$, $p < 0.001$, Cohen's $d = 1.051$) were all significantly greater than alpha, reporting no significant difference between alpha and beta power ($t = 2.265$, $p = 0.262$, Cohen's $d = 0.514$). Interestingly, this reflects our main effect reported during the immediate recall. We reported permutation t-test results on topographies for each group below, followed by group differences presented in *t*-values (Figure 6.12). We note again that individual groups are plotted on a global scale (*dB*).

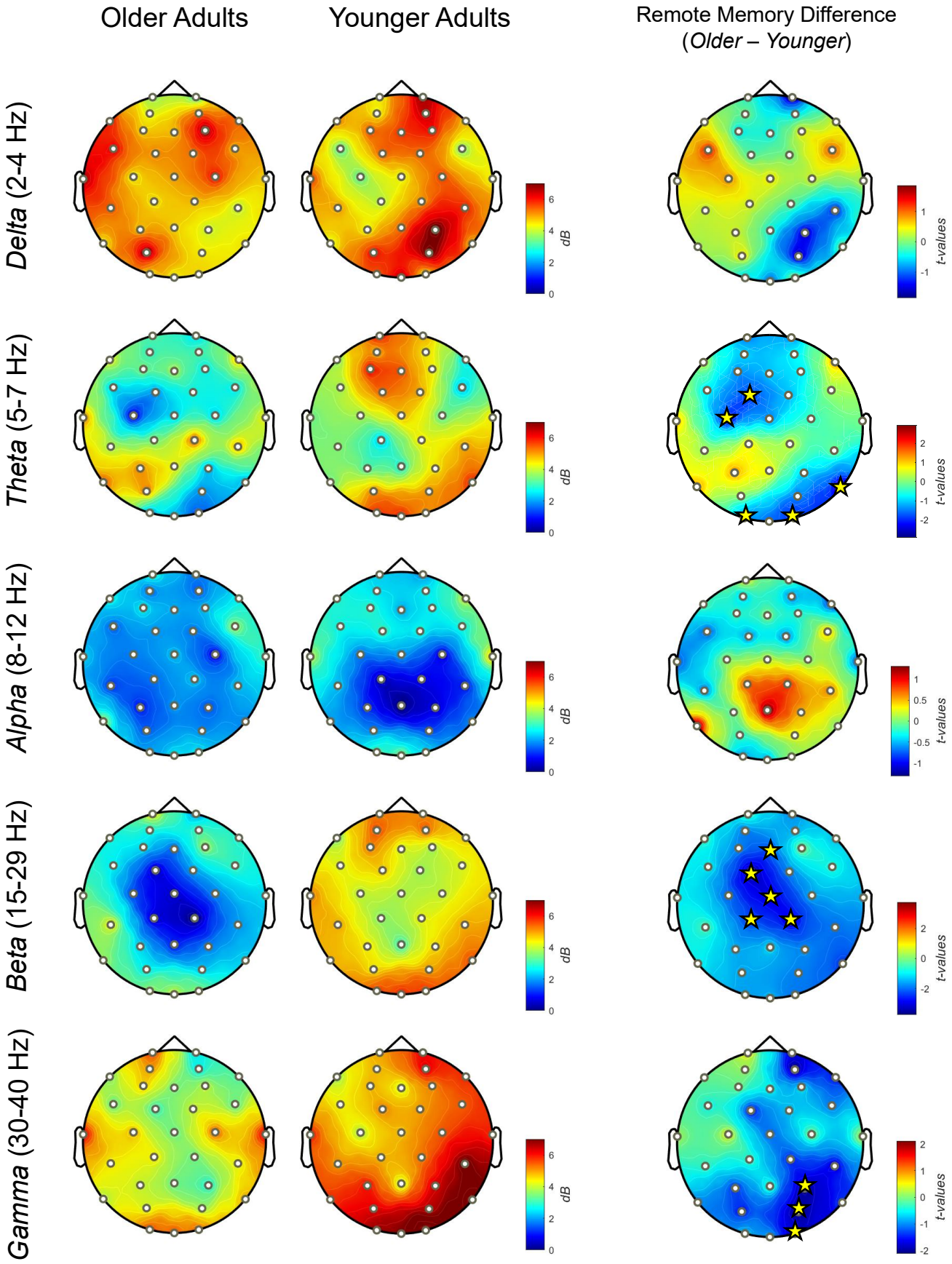


*Figure 6.12:* Topographical distribution of power during remote (1 month) recall phase within the older and younger adult groups. Power in each frequency band is displayed as power relative to baseline (in decibels: *dB*, all positive). Both groups are displayed on the same scale. Differences are displayed in t-values within their own local scale. Significant electrode sites ($p < 0.05$) are marked with a yellow star.

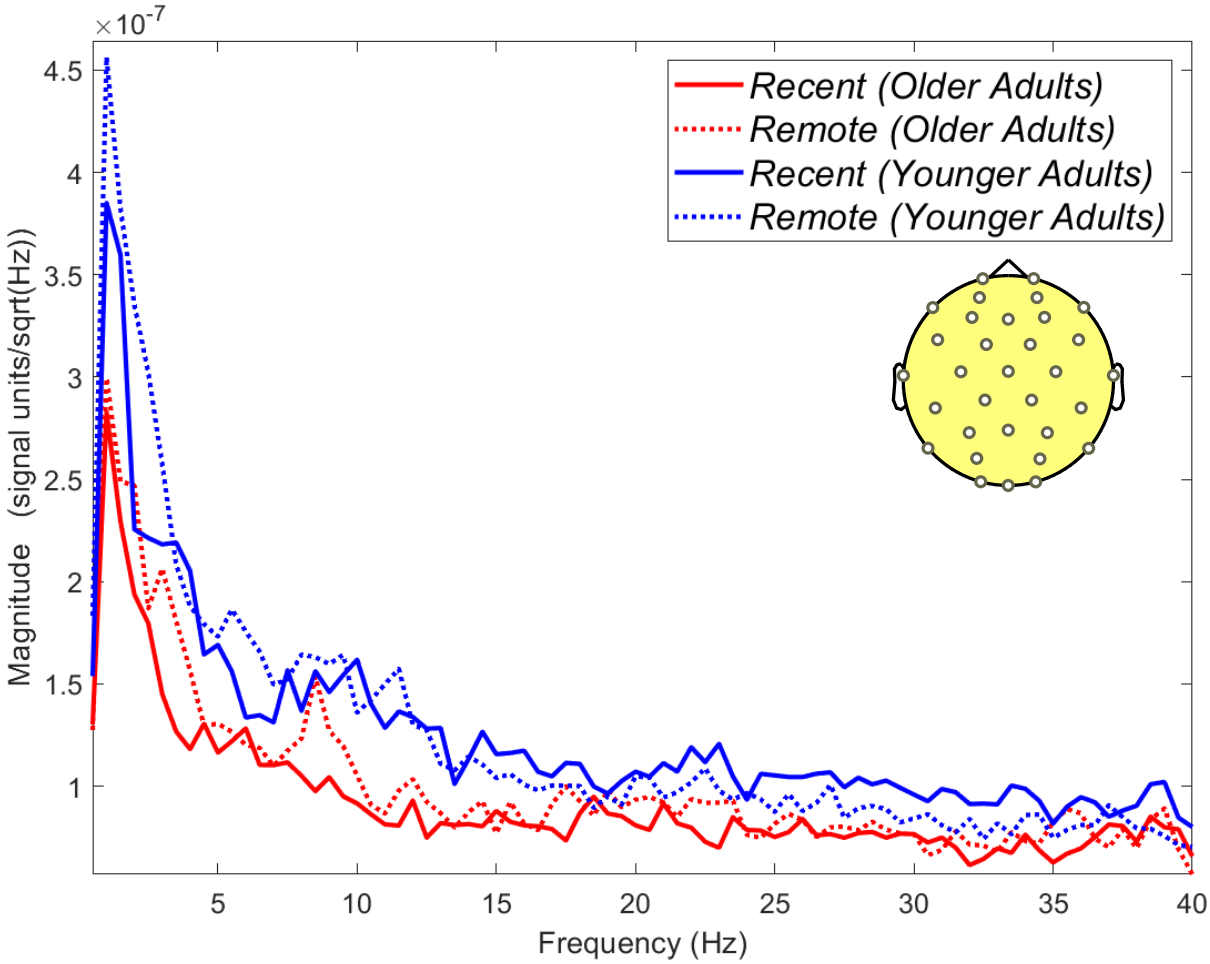


*Figure 6.13:* (a) An FFT line graph displaying the non-normalised mean magnitude of power (μV²/Hz) across the scalp for the older and younger adult groups during recent and remote. Power is displayed across the 1-40 Hz frequency range, with a frequency definition of 0.5 Hz.

### *6.4.7 Recent vs. Remote Memory in Older Adults*

Finally, we wanted to examine the difference within the older adult group, between recent (n = 11) and remote (n = 10) spatial recall. We extracted mean scalp power for each of our memory consolidation groups in each of the five frequency bands of interest. We then also ran a permutation *t*-test to compare activity across 32-sites between the groups in each frequency band using the aforementioned test criteria and correction method. Individual group topographies are not displayed here, as they are already available in Figure 6.11 and 6.12.

However, we also plotted a PSD graph the non-normalised mean magnitude of power ($\mu V^2/Hz$) for each group (Older: recent/remote & Younger: recent/remote) with a frequency definition of 0.5 Hz produced from a linear 1:1:40 FFT (brainstorm default). This provides an insight into the frequency dynamics across the full spectrum and away from baseline correction – which can also provide useful extra information.

Focusing on just our older adults (red lines in Figure 6.13), we ran a permutation *t*-test with the same parameters and corrections as before. We report group difference topographies (Remote – Recent) in Figure 6.14 below. We reported significantly increased delta power in our remote condition at right frontal and central sites (F4, FC6 & C4) as well as increased delta at posterior occipital site PO3. Overall delta power is enhanced in our remote memory condition (see Figure 6.13 and 6.14). Data trended towards reduced theta power in our remote condition, but we reported no significance at any specific electrode site. Interestingly, alpha power trended towards being greater in our remote memory compared to our recent memory condition, but no site reached statistical significance. We suspect that this is driven by an increase within alpha at a particular range within alpha (approx. 8 – 10 Hz, also shown with less enhancement in our younger group – see Figure 6.13). No other significant differences were noted. These are interesting findings as our early work illustrated the importance of delta power during remote memory recall (see Chapter 5 section 5.3.2.2). This may suggest a low-frequency age-specific deficit, accompanied by an age-dependent reduction in theta power (reported in section 6.4.6).

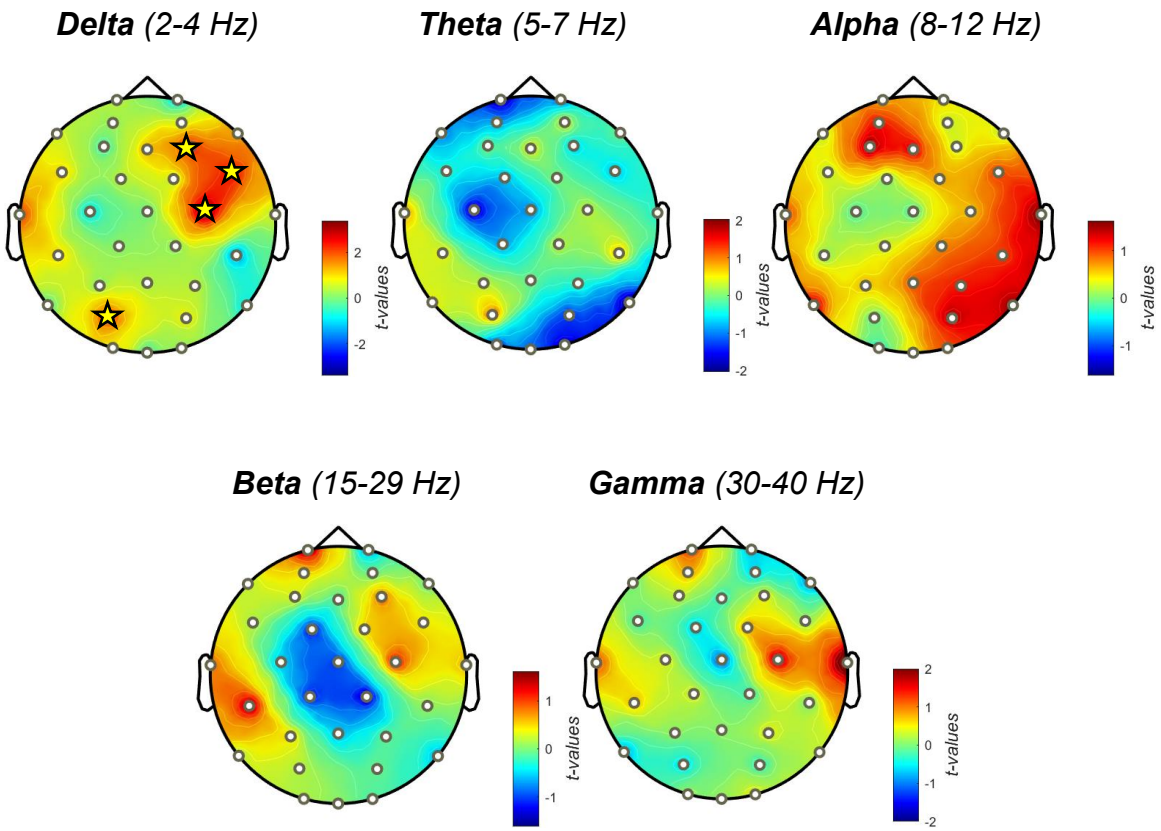


*Figure 6.14:* Topographical difference plots showing results from a permutation *t*-test examining differences between older adult delayed recall conditions (Remote – Recent). Values are scaled at min/max globally in t-values. Stars mark significant electrode sites at $p < 0.05$.

### *6.4.8 Within-group explorative analysis of age-specific performance change*

Previously, we reported a behavioural condition-specific within-group effect in our remote condition, with a reduction in time spent searching in the target quadrant significantly reduced from immediate to remote memory trials. We also reported a neural difference, with reduced theta power compared to our remote condition younger adults and a delta power increase compared to our recent older adults – accompanied by various shifts in alpha power. To explore this, we decided to perform an exploratory within-groups comparison, similar to the analyses completed in Chapter 5. However, we only reported the phase (immediate and recent/remote) differences rather than including isolated group topographies, to ensure we only report

corrected and statistically relevant information. We used a non-parametric permutation within-subjects t-test. We performed two of these *t*-tests one for recent versus immediate (n = 11 per phase) and one for remote versus immediate (n = 10 per phase). Both topographies are displayed on a global scale (*dB*) comparing the delayed recall phase to the immediate recall phase, meaning positive *t*-values represent greater activity in the delayed phase compared to immediate, and vice-versa (Figure 6.15a). We also reported the non-normalised mean magnitude of power ($\mu V^2/Hz$) as a PSD (with the same criteria as section 6.4.7 above) for each phase and condition – to further investigate differences across the full power spectrum (Figure 6.15b).

We reported interesting remote *and* recent recall specific changes at different ends of the frequency spectrum. It is important to note that our t-tests are run with individually normalised signal (*dB*) which do not necessarily reflect the patterns seen in non-normalised signal. We revealed significant increases in frontal delta power (significant: Fz and FC1) from immediate to remote. We also reported cross-scalp decreases in theta power from immediate to remote (significant: FC6). Delta & theta power in our recent memory group appear stabilised reporting no significance at any site. For alpha, we reported decreases from immediate to delayed recall in both recent and remote condition but no significance at any site. Similar beta dynamics were reported, showing decreased central beta power from immediate to delayed recall in both conditions. These decreases are significant from immediate to recent recall (at sites FC1, FC2, and C3). Finally, we reported stabilised gamma from immediate to remote recall, with no significant changes. However, we showed significant fronto-central, central and parieto-central decreases in gamma power from immediate to recent (significant: FC2, Cz and CP1). The non-normalised PSD shows these patterns but are difficult to interpret across trials and within-groups with no correction to individual baselines.

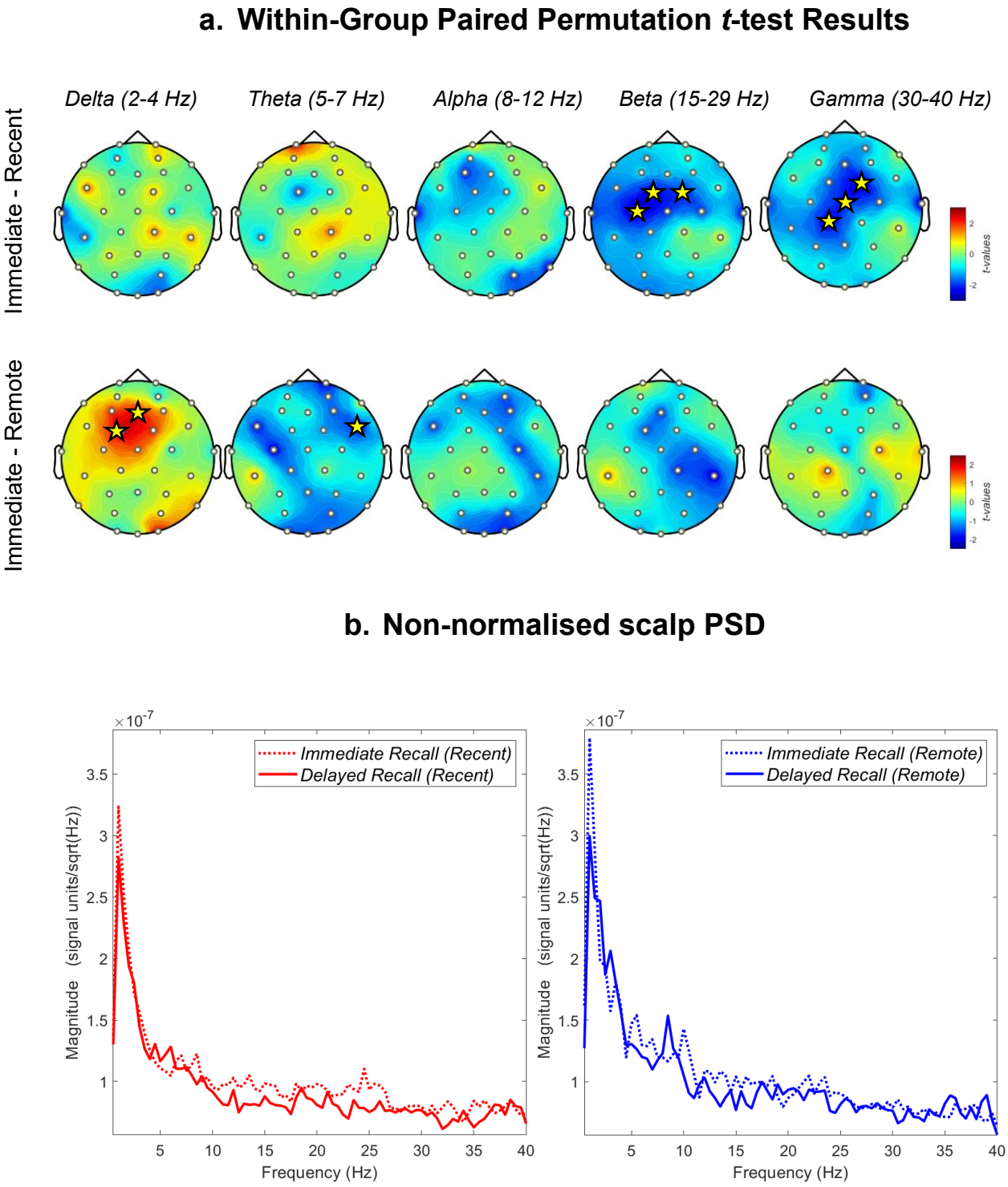


*Figure 6.15:* (a) Topographical difference plots showing results from a within-groups paired permutation t-test examining differences between older adults immediate and delayed recall conditions (Remote & Recent). Values are scaled at min/max globally in t-values. Stars mark significant electrode sites at $p < 0.05$. (b) An FFT line graph displaying the non-normalised mean magnitude of power ($\mu V^2/Hz$) across the scalp for the older adult groups. Both the immediate and recent trial of the recent condition (Left) and immediate and remote trial of the remote condition (Right) are reported. Power is displayed in both across the 1-40 Hz frequency range, with a frequency definition of 0.5 Hz.

## 6.5 Discussion

### *6.5.1 Behavioural Results*

Consistent with our hypothesis, we found that healthy older adults performed worse on a virtual water maze task in both learning and memory phases compared to younger adults. Our older adults had longer path lengths and were slower to locate the target during learning. During immediate, recent and remote recall, older adults also searched less in the target quadrant compared to younger adults. Older adults still successfully learned the task, as they reduced their path lengths from initial trials to later trials. This was further supported by an increase in target quadrant search time, above chance levels, from initial trials to later trials. Nonetheless, we reported a decrease in accuracy from immediate to remote recall in older adults which we did not report in our younger adults. However, they still searched well above chance regardless of consolidation time.

This would suggest older adults have intact, but poorer spatial learning and memory abilities compared to younger adults. We do not believe that it is related to issues with technology or familiarity with the task. It may also suggest that recent spatial memories are better preserved than remote memories in older adults. Our behavioural findings would support most virtual water maze literature (Antonova et al., 2011; Daugherty et al., 2015; Moffat et al., 2006; Reynolds et al., 2019) – which illustrate that older adults learn the task but execute behaviours slower and create more complex routes, with greater differences in memory performance. One explanation (Rodgers et al., 2012) is that older adults tend to prefer response strategies (e.g., learning a series of movements). This strategy does not require knowledge of the relationships between goals and landmarks which slows performance (Konishi et al., 2017). The water maze promotes the use of these strategies, which could explain why older adults perform slower and are less accurate than younger adults. Neuroimaging studies also show

support for this, with heavy reliance from older adults on the frontal cortex and extrahippocampal regions during successful navigation (Korthauer et al., 2016; Reynolds et al., 2019). This may be compensation for deterioration of the MTL and anterior hippocampus due to ageing (Berron et al., 2018; Gallagher et al., 2006; Ward et al., 2015).

### *6.5.2 Resting State Activity*

Once again, consistent with our proposed hypothesis we reported that healthy older adults showed differences in resting state EEG compared to younger adults. We replicated recent findings from Jabès et al. (2021) reporting lesser/suppressed low-frequency oscillations in frontal delta (2-4 Hz) and parietal theta (5-7 Hz) alongside greater centralised beta (15-29 Hz) and gamma (30-40 Hz) in older adults. Interestingly, we also found no difference in alpha power between younger and older adults. Though we observed more alpha power in younger adults replicating typically reported effects (Ishii et al., 2018) – they are not significant, which has been explained and reported using larger datasets (Cesnaite et al., 2023). Therefore, we were also satisfied that this resting state could act as a non-task related baseline for our data, as it matches typical dynamics reported in the literature. Uniquely, our study design allows us to report location-specific differences within our resting state. Reduced frontal low-frequency oscillations (1-7 Hz) have been associated with poorer executive function and spatial task performance in older adults (Mathewson et al., 2012; Vlahou et al., 2014). Excess activity in these oscillations during rest has been shown to predict onset of cognitive impairment (Prichep et al., 2006) – but increased low-frequency power has also been shown to result in improved performance on memory tasks (Finnigan & Robertson, 2011; Fleck et al., 2017). Posterior decreases in theta power are associated with poorer memory capacity and performance (Fleck

et al., 2017), reflected with corresponding reduced theta during memory tasks in older adults (Cummins & Finnigan, 2007). This may possibly be explained by deficits in MTL connectivity.

Additionally, increased high-frequency (beta and gamma) oscillations have also been reported in older adults at rest (Jabès et al., 2021; Vysata et al., 2014). Increased high-frequency power at rest is associated with better cognitive performance in older adults (Alexander et al., 2006). Oscillatory slowing (reduced high-frequency oscillations) has been shown to be predictive of cognitive performance, and a relative biomarker for cognitive decline (Dauwels et al., 2010; Jeong, 2004; Knott et al., 2000; Laptinskaya et al., 2020). It is possible that older adults use high-frequency oscillations as a compensatory mechanism for reduced low-frequency oscillatory networks (typically associated with hippocampal communication and spatial cognition). Considering we also reported (similarly reported by Jabès et al., 2021) a negative correlation between beta power and memory performance following consolidation – this may be a plausible explanation. Further research would be needed to confirm this.

### *6.5.3 Age-related differences across memory phases*

During the immediate recall, we reported relatively similar delta power with decreased frontal theta power and greater parietal theta power in our older adult group. There was less frontal alpha power in our older adults with some central increases – but not significant. Interestingly, we reported decreased beta power in older adults, with the opposite in younger adults, who showed increased beta. We also reported significantly less gamma power in older adults during their immediate spatial recall trial. Though there are no behavioural differences, our results align with some literature relating to memory and reduced gamma oscillations. For example, gamma power was reduced during successful short-term memory recall in healthy older adults compared to patients with MCI (Park et al., 2012). As suggested previously (see Chapter 5) -

gamma oscillations are likely involved in the memory retrieval process, specifically the comparison of retrieved information to environmental information (Herrmann et al., 2004). Reduction of gamma power in our older adults may reflect the strategy used to learn the task having no contextual or spatial framework. In other words, associative spatial relationships nor a schematic of the environment were encoded by older adults – who instead encoded egocentrically-driven movement knowledge leading to difficulty facilitating recall (Boone et al., 2018; Moffat et al., 2001; Wiener et al., 2020). Furthermore, gamma-theta coupling has been shown to be more variable in the older adults, resulting in poorer associative memory performance (Karlsson et al., 2022; Reinhart & Nguyen, 2019). Considering we see reduced theta power at frontal areas, which are known to be involved with working memory (Owen et al., 1990; Prabhakaran et al., 2000) - it is possible our older adults show a deficit in associative or working memory during immediate recall required for efficient and successful spatial navigation. Interestingly, these findings reflect results from Chapter 5. We reported increased gamma power accompanied by greater delta (both at frontal regions). In older adults, we report the opposite but with theta and gamma power (which could be explained by the reported age-related shifts in peak frequencies - Cesnaite et al. (2023)). Though these rhythms are clearly involved in spatial memory retrieval, we cannot determine whether it is strategy choice or decline in memory network efficiency that results in our older adults' poorer performance.

During recent retrieval we reported that older adults had significantly less frontal delta and alpha along with significantly less beta and gamma activity at parietal sites. We also reported reduced alpha power in our younger adults during their recent memory phase of navigation (also see Chapter 5) – which we attributed to greater task-related attention and inhibition of irrelevant stimuli (Foxe & Snyder, 2011; Händel et al., 2011; Hanslmayr et al., 2009; Waldhauser et al., 2012). Therefore, it is entirely likely to report largely and significantly more alpha suppression in older adults. Researchers suggest this is related to greater task-

related attention (Nguyen et al., 2020) or perhaps greater demand on inhibitory networks due to inefficient cognitive mapping (Lithfous et al., 2015). Alternatively, as we suggested before it could also be related to inefficient strategy choice during encoding or non-spatial features available during retrieval, having greater impact on recall after 24 hours. However, Strunk et al. (2017) reported alpha and beta desynchronisation in older adults during a contextual-retrieval task, suggesting it is linked to the fact that they require episodic reconstruction to successfully recall. The authors argue that this is a compensatory mechanism caused by poor recall of information, due to deficits at encoding (James et al., 2016). This may explain our findings and that they operate at higher frequencies, as we reported no behavioural difference between our younger and older recent memory groups, just slower performance. We were pleased to have reported similar patterns of activation between immediate and recent conditions.

During remote recall, we reported significant reductions in theta power at various sites across the scalp in older adults – a sign of healthy ageing (Cummins & Finnigan, 2007). However, we also reported centralised beta suppression compared to our younger adults who demonstrated beta increases (see Chapter 5). We further reported a reduction in parietal gamma power compared to recent recall. We would suggest that since the memory has become consolidated in long-term memory, recruitment of theta and gamma power is required to retrieve it. Recall in older adults, particularly for remote memories, may be subject to the anterior-posterior shift. This is an age-related reduction in posterior activity alongside increases in frontal activity (Zhang et al., 2017). Decreases in gamma have been reported during episodic memory encoding (Després et al., 2017) leading to issues at retrieval. Nevertheless, spatial memory retrieval in older adults results in significant reduction in high-frequency (beta and gamma) power, with frontal delta and theta increases. During remote memory retrieval, theta power is significantly less compared to younger adults – with other frequency bands displaying

the same characteristics. We believe that theta suppression is responsible for remote memory retrieval in older adults compared to younger adults – whereas greater alpha suppression is required for accurate recall of recent memories. Reduced beta and gamma power with age may be signatures of compensatory functions to facilitate spatial navigation. These networks are enhanced compared to younger adults at rest – should they need to be recruited. It would be interesting to focus on good and poor performing older adults to confirm this (see Chapter 7). Nevertheless, the lack of similar studies makes our results difficult to interpret with regards to the literature.

### *6.5.4 Anterior-posterior shift evident within older-adult memory conditions*

Finally, we reported some interesting dynamics within our older adult groups, that are reflective of the aforementioned anterior-posterior hypothesis of ageing (Ansado et al., 2012; Zhang et al., 2017). We reported recruitment of low-frequency oscillations from immediate to remote memory, resulting in significantly increased *frontal* delta power and reduced theta power – with the standard decreased beta and gamma levels from immediate to remote. Furthermore, older adults performed worse in their remote trial compared to their immediate. Alternatively, we reported recruitment of higher-frequency oscillations from immediate to recent recall, resulting in significant decreases in beta and gamma activity – with no behavioural performance change. There is a decreased but stable level of alpha power in both groups from immediate to delayed. Taken together, these findings would suggest that high-frequency oscillations are required to recall recent memory, as beta and gamma suppression acts as a compensatory mechanism for higher level cognition – facilitating recent spatial memory retrieval. These differences are observed between ages at posterior sites but are found within older adults more centrally. During remote memory, older adults depend on low-frequency frontal oscillations, increasing

delta and suppressing theta power – with theta in older adults reflecting gamma behaviour via desynchronisation whereas in younger adults, theta and gamma increase in power.

# Chapter 7

# General Discussion

### 7.1 Overview of thesis findings

The main aim of this thesis has been to investigate the neural oscillations in humans in a virtual water maze task – through experimental paradigms that would examine learning and memory during spatial navigation. Very little is known about the cortical oscillations responsible for these two essential processes as humans navigate. Furthermore, the role and dynamics of different frequency bands throughout the navigation process are not well understood. Current theories surrounding the role and dynamics of oscillations derive from intracranial electrophysiology of the hippocampus (see Ekstrom et al., 2017 for a review), with some scalp studies not assessing navigation as a complex behaviour and instead recording cortical EEG at different processes throughout, such as decision-making (Chrastil et al., 2022; Lin et al., 2022) or scene-recognition (Durteste et al., 2023; Nicolás et al., 2021; Strunk et al., 2017). There are a small number of studies that address the impact of ageing on these oscillations during spatial cognition (Ekstrom & Hill, 2023). To our knowledge, no research has been carried out to date on these oscillations during recent and remote memory-driven spatial navigation.

Chapter 3 attempted to examine the learning or encoding process during spatial navigation in healthy younger adults using a virtual water maze task. Though this is an essential part of successful spatial navigation, it has only been studied at a behavioural level (Chrastil & Warren, 2013; Deery & Commins, 2023; Hamilton et al., 2002; Kelly & Gibson, 2007; Newhouse et al., 2007; Redhead & Hamilton, 2009; Schoenfeld et al., 2014; Schoenfeld et al., 2010). Empirical examination of neural oscillations during spatial learning has been limited, with memory recall being the main focus of much human intracranial work (Aguilera et al., 2022; Colgin et al., 2009; Goyal et al., 2020; Herweg, Sharan, et al., 2020; Kota et al., 2020; Nyhus & Curran, 2010; Vivekananda et al., 2021). In virtual navigation work, there are *some* papers that address the encoding process. For example, Bischof and Boulanger (2003) reported greater theta power in participants during virtual navigation when new spatial information was

being encoded, and when participants made a mistake and needed to revise their route. However, the authors suggest this increased theta is related to retrieval of stored views to aid their navigation. Chrastil et al. (2022) reported increased theta and alpha power in midfrontal and parietal channels respectively during learning in active navigation. They suggest a plausible link between these oscillations and memory encoding and retrieval (Hsieh & Ranganath, 2014). Participants undergoing guided navigation displayed suppressed parietal theta power. Considering the authors reported these dynamics before a decision-making point in their navigation task – we would argue that the flexibility of spatial behaviour is not considered. Therefore, our work in Chapter 3 aimed to control for all other aspects of behaviour during spatial navigation known to influence theta and alpha oscillations, including speed, orientation and movement (Babiloni et al., 2014; Bush et al., 2017; Caplan et al., 2003; Hori et al., 2013; Kaplan et al., 2012; Kropff et al., 2021; Yassa, 2018) and examine differences in these rhythms during important phases of natural navigation (Nyberg et al., 2022). To do so, we used a control (non-learning) and a learning group. Furthermore, we wanted to investigate the dynamics of these rhythms as there has been mixed reporting of increases and decreases within the literature (Herweg, Solomon, et al., 2020).

In Chapter 3 participants carried out twelve trials in our virtual water maze task NavWell (Commins et al., 2020; Thornberry et al., 2023) and were randomly assigned to either a learning group (who were required to learn the location of a hidden target across 12 trials) or a non-learning group (who were required to move around the same arena for 12 trials, but without the presence of a goal; each trial was time-matched to the average latency of the learning group). The results of our experiment revealed that theta power increased in an explorative condition (non-learning) but was decreased in our learning condition, with parietal midline theta a marker of successful spatial encoding. We also reported decreased alpha power with learning at frontal and parietal regions, with similar suppression in our non-learning group.

We initially hypothesised that if the contribution of theta and alpha power is related to learning, we should report differences between the groups. If it is related to active sensorimotor integration, we should report no group differences. We found support for the theory that theta plays a crucial role in spatial encoding during exploration, as opposed to sensorimotor integration (Alekseichuk et al., 2016; Buzsáki, 2005; Chrastil et al., 2022; Du et al., 2023; Greenberg et al., 2015; Herweg, Solomon, et al., 2020; Klimesch et al., 1997; Lithfous et al., 2015; O'Keefe, 1993). Furthermore, we reported reduced theta related to successful encoding, typically found in associative learning tasks (Fellner et al., 2016; Greenberg et al., 2015; Kota et al., 2020; Michelmann et al., 2018). We interpreted our results as support for the neural efficiency hypothesis – which claims that greater neural effort is recruited when learning a task, compared to when a task has been learned – as task completion now relies on the retrieval of encoded information (Commins, 2018b; Jaiswal et al., 2010; Thornberry et al., 2023). With focus on studies that attempted to investigate spatial learning during navigation, we reported similar attention-modulation interpretations of decreased parietal alpha power, as reported by Gehrke and Gramann (2021).

Chapter 4 examined the oscillations underlying performance in the immediate recall trial of participants from Chapter 3. In the standard Morris Water Maze procedure, a “retention” or “probe” trial is carried out following the learning trials to verify learning and examine spatial recall (Morris, 1984; Morris, 1981; Nunez, 2008; Vorhees & Williams, 2014a). Typically, this test can be used to examine hippocampal-dependent spatial memory (Astur et al., 2002; Barnhart et al., 2015; Morris et al., 1982). Our participants had to recall the targets’ location during a single trial, however, the target was removed. Our learning group demonstrated greater delta and theta activity during memory recall, as well as alpha suppression at posterior sites. Delta and theta power also increased when searching behaviour shifted. Our non-learning group showed significant alpha power increases over time suggestive of attentional

disengagement. We suggest that our alpha findings relate to memory-guided attention with a lack of competing associations and an ability to inhibit attention to interfering or unwanted visual stimuli (Du et al., 2023; Foxe & Snyder, 2011; Händel et al., 2011; Klimesch, 2012; Klimesch et al., 1998; Sutterer et al., 2019; Waldhauser et al., 2012). Low-frequency oscillations are involved to greater extent during spatial retrieval, with delta & theta power increasing when applying memory based spatial search strategies. These results align with previous studies reporting low-frequency oscillation increases during spatial memory retrieval (Bohbot et al., 2017; Buzsáki, 2005; Chrastil et al., 2022; Du et al., 2023; Greenberg et al., 2015; Liang et al., 2018; Lin et al., 2017; Nishiyama et al., 2002; Park et al., 2014). We found it difficult to align our high-frequency findings with the literature, though would suggest they are involved in memory and attention maintenance during navigation (Alekseichuk et al., 2016) – reflected in enhanced beta and gamma oscillations in our learning group.

Chapter 5 sought to build on some of the limitations from the previous chapter (such as a lack of baseline, COVID-19 precautions, etc.) and to examine the impact of consolidation time on spatial memory retrieval. This would also expand our oscillatory findings to address theoretical questions regarding memory consolidation. To our knowledge, this is the first attempt to study retrieval of recent (encoded 24-hours ago) and remote memories (encoded 1-month ago) during human spatial navigation. We recruited thirty-one new healthy younger adults who underwent twelve learning trials, an immediate recall trial and then another delayed recall trial (either 24-hours or 1-month later). Here, we found that there was no difference in performance between our recent and remote recall participants. All participants learned and recalled the target location at a similar level. Interestingly, our remote condition actually improved performance from their immediate recall trial. Of most interest were our neural findings. We replicated relative power dynamics from Chapter 4 using a new set of participants. We also reported more support for an efficiency hypothesis, as low-frequency oscillations and

alpha suppression were greater from immediate to recent and from recent to remote retrieval. We suggest it is related to overall effort required to retrieve spatial information (Jaiswal et al., 2010) which has been shown to produce greater (delta-theta) and less (alpha) power relative to task and cognitive demands (Grabner et al., 2004; Riečanský & Katina, 2010). For example, Maurer et al. (2015) reported that increased frontal theta power (5–7 Hz) was linked to variations in task difficulty and cognitive effort. Therefore, greater task demands may lead to greater delta-theta and suppression of alpha.

Additionally, we reported supporting roles of gamma oscillations (30-40 Hz) in retrieval of cortically distributed memories, i.e. remote (Alekseichuk et al., 2016; Colgin et al., 2009; Herrmann et al., 2004; Honkanen et al., 2015; Lundqvist et al., 2016; Pu et al., 2018; Roux et al., 2012). We found that gamma power mirrors the delta activation in our remote condition only, with greater increases in delta-theta and gamma power from immediate to remote retrieval. Similar dynamics were also reported in the human hippocampus during long-term memory retrieval in a virtual navigation task by Vivekananda et al. (2021). A possible explanation of these findings from consolidation theories is discussed later.

Finally, Chapter 6 aimed to explore age-differences related to spatial memory retrieval, as well as the impact of age on recent and remote spatial recall. We recruited twenty-one older adults and compared them to our younger adults from Chapter 5 using the same experimental procedure. As we had collected resting state data, we also attempted to examine the relationship between resting-state dynamics and spatial navigation performance (Cesnaite et al., 2023; Finnigan & Robertson, 2011; Fleck et al., 2017; Jabès et al., 2021; Laptinskaya et al., 2020; Scally et al., 2018; Vlahou et al., 2014; Zou et al., 2013). This would also support proposals by Buzsaki (2006) that oscillatory patterns are pre-established and become enhanced during engagement for cognition. We hypothesised that our older adults should perform worse than our younger adults. We also hypothesised that older adults performance would decline as a

function of consolidation time. Behaviourally we reported that healthy older adults had worse, but not impaired spatial learning and memory performance compared to younger adults (Commins et al., 2020). Our findings also suggest that recent spatial memories are better preserved than remote memories in older adults as we reported a significant decline in performance within the older adults from immediate to remote memory condition. Much of our behavioural findings align with the virtual water maze literature (Daugherty & Raz, 2017; Daugherty et al., 2015; Dobbels et al., 2020; Reynolds et al., 2019; Zhong et al., 2017). We also replicated resting state EEG age-differences reported by Jabès et al. (2021) – reporting a correlation between high-frequency oscillatory power in gamma and task performance. We also replicated a negative correlation between beta power and memory performance – but only after a consolidation period (i.e., delayed recall performance).

Older adults show reduced frontal theta, beta and significantly reduced parietal gamma during immediate spatial recall. Frontal theta and gamma suppression may indicate impairments in working or associative memory abilities (Barr et al., 2014; Basu et al., 2021; Dimitrov et al., 1999; Hanninen et al., 1997). These impairments may be explained by encoding strategy choice during learning (Lithfous et al., 2015). For recent memory performance, older adults displayed greater alpha suppression with less delta, beta and gamma power compared to younger adults. Alpha may relate to enhanced cognitive effort or spatial attention (Cesnaite et al., 2023; Nguyen et al., 2020; Rondina Ii et al., 2019), whereas the reduced power in rhythms we have previously reported as important for successful retrieval may explain slower navigational performance (Després et al., 2017; Karlsson et al., 2022). In remote recall, older adults displayed significant theta power reductions, central beta suppression and less parietal gamma power compared to younger adults. We suggest that this may indicate compromised retrieval (linked to theta and gamma: (Kardos et al., 2014; van de Vijver et al., 2014)) and the need for compensation after long-term consolidation (previously reported for beta: Winterling

et al. (2019)). Within our older adults, results suggested reduction in posterior high-frequency oscillations during recent memory but increases in frontal delta and reduced theta oscillations during remote retrieval. We suspect that these differences could relate to the storage of the memory and the cortical regions required for retrieval.

### 7.2 Potential implications and future directions

Our findings from Chapter 3 have some important implications for our understanding of spatial learning during navigation (Thornberry et al., 2023). For example, our results provide supporting evidence for an associative encoding model of learning during human spatial navigation. Firstly, explorative navigation and the route initiation phase demonstrate increased theta power at frontal sites. It is possible this reflects the binding of various sensory cues (e.g., the light or the square) into associative representations within the hippocampal-entorhinal circuit (Horner & Burgess, 2013; Horner et al., 2012). Delaux et al. (2021) reported sustained theta increases prior to the start and towards the end of a mobile virtual navigation task. The authors suggest that increases may relate to decision-making (reported by Chrastil et al., 2022) and/or preparation to encode information (reported by Kline et al., 2014).

These oscillations remain relatively heightened in our non-learning group, whilst we report typical decreases in power observed following successful encoding in our learning group (Crespo-García et al., 2016; Greenberg et al., 2015; Miyakoshi et al., 2021; Park et al., 2014). These theta decreases may represent efficient encoding and on-demand retrieval of goal-related stimuli. Furthermore, several spatial and non-spatial experiments report reduced theta following successful associative learning (Crespo-García et al., 2016; Fellner et al., 2016; Greenberg et al., 2015; Herweg, Solomon, et al., 2020; Karlsson et al., 2022; Lithfous et al., 2015; Michelmann et al., 2018) as opposed to increases in theta during decision-making, exploration or memory retrieval (Chrastil et al., 2022; Delaux et al., 2021; Herweg, Sharan, et

al., 2020; Herweg, Solomon, et al., 2020; Jensen & Tesche, 2002; Khader et al., 2010; Liang et al., 2021). Furthermore, theta decreases alongside greater alpha suppression likely represent focused attention towards spatial features and goal associations – as well as controlled information encoding and retrieval (Foxe & Snyder, 2011; Klimesch, 2012). The dynamics of these bands most likely support an associative model of spatial learning, and the uptake of efficient, energy-saving associative retrieval strategies; which is strongly supported behaviourally (Commins & Fey, 2019; Pearce, 2009; Shanks, Charles, et al., 1998; Shanks, Darby, et al., 1998; Tse et al., 2007; Urcelay & Miller, 2014). Future studies should investigate if similar dynamics exist within theta and alpha bands during encoding using more precisely timed associative learning tasks such as the face-name pairs task (Caffrey & Commins, 2023). This would provide great insight into the contribution of neural oscillations and general associative learning to the development of spatial schemas (Tse et al., 2007) and cognitive maps (O'Keefe & Nadel, 1978; Tolman, 1948).

Nevertheless, only using a 32-channel scalp EEG placed limits on the types of analysis we can run. We could not perform accurate source analysis and reconstruction to explore this proposed communication between the parietal and entorhinal cortex and the hippocampus (Ekstrom et al., 2017). Future studies should attempt source analysis during these navigation phases using higher-density EEG or Magnetoencephalography (MEG) systems to examine our proposed hippocampal associative integration hypothesis. The low number of trials used to estimate oscillatory activity may have reduced the quality of data used to draw some of the above suggestions. Human navigation is a fast and fluid process, but we did our best to control for these limitations as much as possible. We used averaged time-frequency plots for each participant to improve the signal-to-noise ratio and stability (Cohen, 2014) - fewer trials are required to produce reliable and less variable oscillatory estimates than would be for ERPs (Boudewyn et al., 2018; Morales & Bowers, 2022). This is not the first attempt to capture the

spatial learning and navigation process using few trials combined with EEG (e.g., 3 trials per environment in the *Audiomaze*: Miyakoshi et al., 2021). We also performed an a priori power calculation (rarely done in EEG studies; of 100 reviewed, not a single study reported a sample size calculation; see Larson & Carbine, 2017). Furthermore, we corrected for multiple comparisons using FDR correction, utilised non-parametric permutation t-tests and only reported findings we previously hypothesised (see Thornberry et al., 2023). Future studies will also need to address the travel phase of spatial navigation, during which sensorimotor and environmental information is integrated (Nyberg et al., 2022). We do not report this phase due to the complexity of the data and the differences between individuals learning rates (Commins et al., 2023) which results in timing differences between every trial for every participant. In a recent study, we have attempted to address these issues by applying Hidden Markov Models on full trial data to uncover discrete oscillatory 'states' rather than oscillatory timings (Palma et al., 2023).

On the face of it, our studies from Chapter 4 and Chapter 5 seem to align better with the EEG literature surrounding spatial memory retrieval. However, many previous studies did not record oscillatory activity of spatial memory retrieval *during* active navigation – but instead using controlled experimental paradigms to assess one cognitive domain (Alekseichuk et al., 2016; Foster et al., 2016; Jones & Wilson, 2005; Kaplan et al., 2012; Li et al., 2021; Proskovec et al., 2018; Pu et al., 2018; Sutterer et al., 2019). Though these studies are designed better to investigate spatial memory – it is difficult to apply the work to the complete process of navigation. Chapter 4 examined recall after a very short timeframe, almost immediately after the learning phase. Chapter 5 built on this in an attempt to replicate our findings from immediate recall and to examine delayed recall, after recent (24-hours) and remote (1-month) recall. We propose that successful retrieval of recently encoded spatial information relies on increased delta and theta oscillations (2-7 Hz). These replicate much of the literature on scalp

and intracranial EEG and memory retrieval (Addante et al., 2011; Alekseichuk et al., 2016; Burgess & Gruzelier, 1997; Buzsáki, 2005; Du et al., 2023; Herweg, Sharan, et al., 2020; Hsieh & Ranganath, 2014; Kaplan et al., 2014; Klimesch et al., 1997; Osipova et al., 2006; Vivekananda et al., 2021). Therefore, it is entirely possible that low-frequency oscillations on the scalp reflect frontal cortex communication with the MTL (Bohbot et al., 2017; Ekstrom et al., 2005; Herweg, Sharan, et al., 2020; Kaplan et al., 2014; Mitchell et al., 2008). Du et al. (2023) recently claimed that their observed frontal midline theta increases during virtual navigation most likely relates to decision-making (also see Chrastil et al., 2022) and mnemonic processes. In a virtual water maze, Cornwell et al. (2008) reported hippocampal theta was also associated with successful spatial memory retrieval, further replicated using MEG showing coupling between theta at the frontal cortex and the hippocampus for memory-based decision-making (Backus et al., 2016; Soltani Zangbar et al., 2020).

Considering in Chapter 4, we also reported further increased low-frequency oscillations when searching strategy required changing – we would suggest that this was an attempt to utilise more complex and more demanding (Jensen & Tesche, 2002) memory-based decision-making. These networks are supported by suppressed alpha oscillations to facilitate focused attention and limited competing processing (Klimesch, 2012; Klimesch et al., 2007; Morrow et al., 2023; Roux & Uhlhaas, 2014; Waldhauser et al., 2012). Future work would again require higher-density EEG or MEG systems to examine if the proposed subcortical regions are the source of the signals during recall. Furthermore, connectivity analysis would facilitate whether the increased low-frequency oscillations are synchronised with our observed suppression of high-frequency beta and gamma (>15 Hz) as they may be controlling active retrieval from more detailed memory traces (such as visual memories – we reported beta increases at occipital areas) as has been suggested by some work (Aguilera et al., 2022; Herweg, Sharan, et al., 2020; Köster et al., 2014; Nyhus & Curran, 2010; Pu et al., 2018; Vivekananda et al., 2021).

In Section 7.1, we discussed the involvement of more neural effort possibly explained by a greater memory load retrieving remote compared to recent memories reported in Chapter 5 (Jaiswal et al., 2010; Jensen & Tesche, 2002). However, aside from the similar low-frequency oscillations during retrieval increasing, we reported a remote-specific gamma dynamic, showing frontal gamma power increasing from immediate to remote retrieval. However, we do not report any difference between recent and remote recall phases. Therefore, fast rhythms such as gamma may coordinate recall of cortically consolidated remote memories in combination with delta-theta in frontal regions. This has been reported during remote memory retrieval (Steinvorth et al., 2010; Yaffe et al., 2017) and has been suggested to be used to recruit hippocampus-dependent contextual information (Hebscher et al., 2019; Nyhus & Curran, 2010).

Future studies should attempt to further investigate this effect, perhaps by changing the difficulty or contextual cueing of remote memories. For example, using a modified hippocampal-dependent Face-Name Pairs retrieval task in which only some facial features are presented (Commins et al., 2023), this could then be compared to NavWell or a navigational decision-making task (Chrastil & Warren, 2013) in which landmark positions and appearance are manipulated. Any modulation of gamma power using these manipulations may provide further support for its possible functional role in remote memory. Furthermore, recording longer periods of navigation would be useful here (Daugherty & Raz, 2017), as well as longitudinal connectivity models (Laptinskaya et al., 2020; Park et al., 2011) to facilitate whether the greater the remote period (e.g. 6 months), the weaker or stronger these gamma oscillations become. Connectivity models with higher-density EEG may link both gamma and delta-theta oscillations to the hippocampus (shown during VWM probe trials by Bauer et al. (2021). Nevertheless, the preserved accuracy but changing oscillatory activity with

consolidation suggests some type of network reorganisation to preserve (and perhaps improve) memory traces.

Finally, in Chapter 6 we reported that ageing has an impact on spatial navigation ability as expected (Bécu et al., 2020; Daugherty & Raz, 2017; Hill et al., 2023; Moffat & Resnick, 2002; Moffat et al., 2001). However, not on learning ability but mainly on performance, with deficits in spatial memory only evident over longer consolidation periods (i.e. after 1 month). We also reported typical age-dependent resting state differences between younger and older adults (Cesnaite et al., 2023; Finnigan & Robertson, 2011; Fleck et al., 2017; Jabès et al., 2021). Our correlation results suggest that performance issues may represent underlying high-frequency network constraints (particularly beta oscillations). Future research should focus on high-frequency network changes during ageing. Some current, high-density EEG studies with a large dataset of older adults has reported a shift in beta burst sources from age 60 onwards (Power & Bardouille, 2021). Interestingly, task-related beta decreases in older adults were reported during selective motor memory retrieval task with distractors (Proskovec et al., 2018; Steiger et al., 2022; Tempel et al., 2020; Winterling et al., 2019). These and several other researchers (Kober et al., 2016; Sauseng et al., 2009; Steiger et al., 2022) suggest that beta in older adults is responsible for inhibitory mechanisms associated with memory retrieval. This would align with our suggestion that their strategy choice may be route-knowledge driven (Lithfous et al., 2015), as opposed to associative. Some future suggestions beyond the scope of this thesis would be to analyse the EEG of spatial learning trials with older adults and contrast it to their performance during an associative task (e.g. Face-Name Pairs) and younger adults (Thornberry et al., 2023).

Furthermore, our observed decreases in beta and gamma oscillations during all recall phases fits very well with the well supported compensation hypothesis of neurocognitive ageing, which suggests that older adults engage additional or different brain mechanisms when

performing the same cognitive task as younger adults, to compensate for declining brain functions (Azami et al., 2023; Brookes et al., 2011; Cabeza et al., 2002; Cabeza et al., 2004; Proskovec et al., 2018). The compensation hypothesis is further supported by the fact that we observed no difference in behavioural performance, but a clear difference in neural dynamics between younger and older adults (Cabeza et al., 2018; Grady, 2012). Less beta and gamma power are evident at both recent and remote time-points but become suppressed from immediate to recent retrieval. However, when navigation performance declines at remote intervals, we see recruitment of lower frequency oscillations (delta: 2-4 Hz). Therefore, our data may also suggest that suppressed beta and gamma oscillations are required to facilitate accurate spatial memory and navigation performance in healthy ageing. Future research on ageing in spatial navigation should investigate compensatory neural networks that may be involved in better performing older adults. Researchers should also focus on the recruitment of low-frequency oscillations for retrieval of remote memories in older adults, using a less dynamic and more direct memory task to examine whether our observed shift to frontal delta oscillations are navigation-specific.

### 7.3 Potential applications

We hope that our research has provided a possible suggested methodology to examine continuous EEG during fluid and active cognitive tasks such as spatial navigation. It has built on similar proposed methods used during 3D virtual navigation with physical locomotion (Delaux et al., 2021; Jabès et al., 2021; Miyakoshi et al., 2021) in which frequency oscillations were recorded across a continuous period of navigation and then epoched to events and behaviours of interest. Although we acknowledge that this method has its limitations (see Section 7.4 and also Thornberry et al., 2023) it does facilitate the capture of complex and changing behaviour, even changes occurring within the behaviour itself (e.g., search strategy

changes in Chapter 4). The literature on spatial navigation and oscillatory dynamics is incredibly novel and still evolving with the development of mobile EEG systems and more immersive VR applications. Nevertheless, we hope that our methodology can be built upon and developed to further research in this area.

Secondly, regardless of methodological approaches, we believe that we have uncovered some interesting findings regarding the dynamics of oscillatory bands during human spatial navigation. From this, we propose a summary of our observations that should hopefully generate hypotheses for future navigation and oscillation studies (Tables 7.1, 7.2 and 7.3).

*Table 7.1:* Younger Adults within-group frequency band dynamics

| *Frequency Band* | Spatial **Learning** | **Recent compared to Immediate** | **Remote compared to Immediate** | **Remote compared to Recent** |
|---|---|---|---|---|
| Delta (2-4 Hz) | 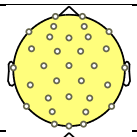 | 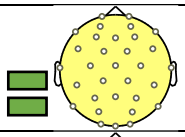 | 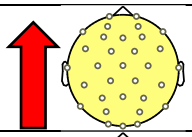 | 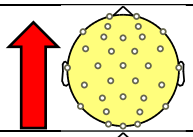 |
| Theta (5-7 Hz) | 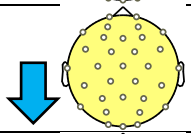 | 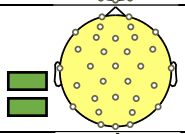 | 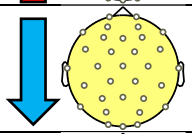 | 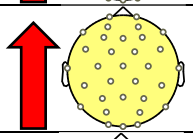 |
| Alpha (8-12 Hz) | 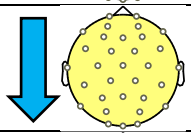 | 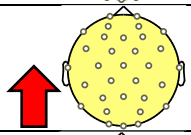 | 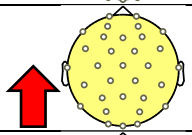 | 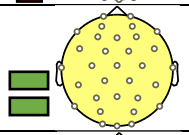 |
| Beta (15-29 Hz) | 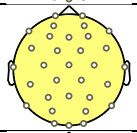 | 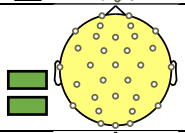 | 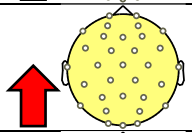 | 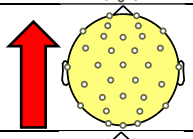 |
| Gamma (30-40 Hz) | 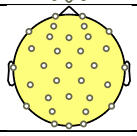 | 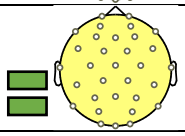 | 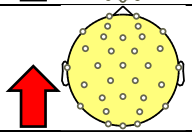 | 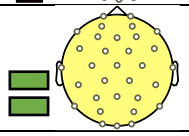 |

**Note**: Arrow direction and colour represents increases (upwards and red) or decreases (downwards and blue). Equal signs in green represent no significant changes in activation. Short arrows represent only a single significant site. Longer arrow represents two or more significant sites. The differences refer to A ≷ B if the top columns are read in terms of "condition A compared to condition B".

*Table 7.2:* Older Adult within-group differences in frequency dynamics at various recall phases

| *Frequency Band* | **Recent compared to Immediate** | **Remote compared to Immediate** | **Remote compared to Recent** |
|---|---|---|---|
| Delta (2-4 Hz) | 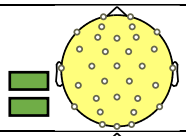 | 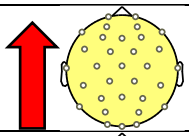 | 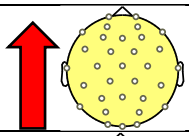 |
| Theta (5-7 Hz) | 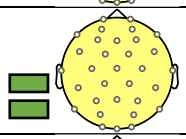 | 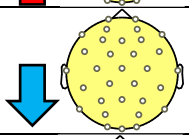 | 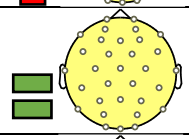 |
| Alpha (8-12 Hz) | 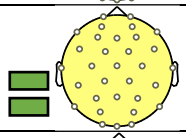 | 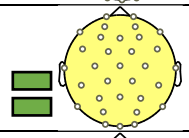 | 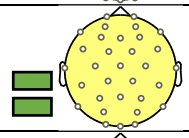 |
| Beta (15-29 Hz) | 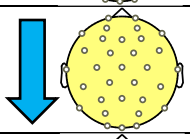 | 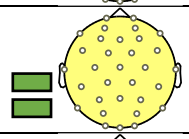 | 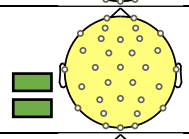 |
| Gamma (30-40 Hz) | 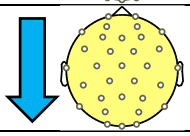 | 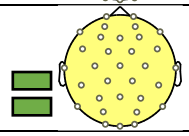 | 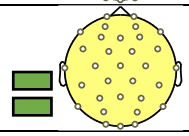 |

**Note**: Arrow direction and colour represents increases (upwards and red) or decreases (downwards and blue). Equal signs in green represent no significant changes in activation. Short arrows represent only a single significant site. Longer arrow represents two or more significant sites.

*Table 7.3:* Older-Younger differences in frequency dynamics at various recall phases

| *Frequency Band* | **Older compared to Younger Immediate** | **Older compared to Younger Recent** | **Older compared to Younger Remote** |
|---|---|---|---|
| Delta (2-4 Hz) | 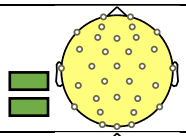 | 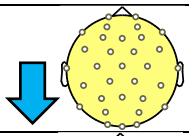 | 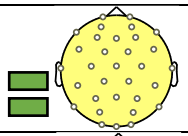 |
| Theta (5-7 Hz) | 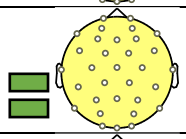 | 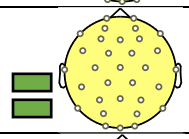 | 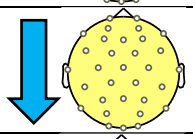 |
| Alpha (8-12 Hz) | 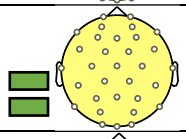 | 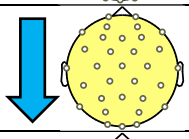 | 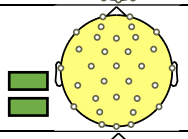 |
| Beta (15-29 Hz) | 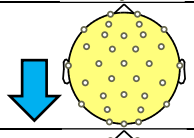 | 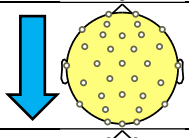 | 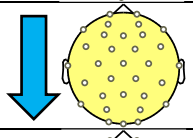 |
| Gamma (30-40 Hz) | 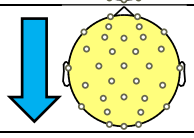 | 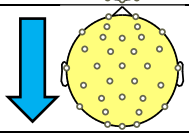 | 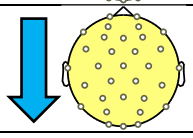 |

**Note**: Arrow direction and colour represents increases (upwards and red) or decreases (downwards and blue). Equal signs in green represent no significant changes in activation. Short arrows represent only a single significant site. Longer arrow represents two or more significant sites. The differences refer to A ≷ B if the top columns are read in terms of "condition A compared to condition B".

In the above summary, we only report *significant* dynamics, though overall dynamics that were not significant should be, and are acknowledged in their corresponding chapters. Furthermore, considering our EEG system is relatively low-resolution, we have excluded the location of these significant observations, as it is unlikely that we have a truly accurate and replicable source localisation for these using 32-channel cap (Yao & Dewald, 2005).

There are many potential applications of our findings from the current thesis. For example, our findings from Chapter 3 may be used to understand individual learning differences in spatial cognition. Though not examined for the current thesis, some participants are known to perform spatial navigation tasks more effectively than others, whilst some individuals may be slower or take longer to construct and apply a useful navigation strategy (Cheng et al., 2022; Commins et al., 2023; Coughlan et al., 2018; Coutrot et al., 2019; Hegarty et al., 2023). A reduction in parietal theta at the beginning of a spatial task may be a neural marker for learning and may be used to distinguish good from bad spatial learners. Using this, researchers could design interventions to train and improve spatial performance using applied rhythmic transcranial magnetic stimulation (TMS) in the theta rhythm. Previous TMS studies have shown to improve working memory performance through theta-burst stimulation (Hoy et al., 2016; Riddle et al., 2020). This may be useful for MCI or dementia patients suffering from early deficits in spatial cognition and may even act as a preventative or "decelerative" intervention – as the link between spatial deficits and these disorders has been reported numerous times (Coughlan et al., 2018; Coughlan et al., 2020).

Our findings from Chapter 4 and Chapter 5 may also have some interesting applications. For example, memory driven spatial navigation is an essential skill for successful cognition. If we can further standardise oscillatory dynamics during spatial navigation, researchers could produce standardised EEG-based assessments for deficits. Recently, disrupted theta rhythms were linked to poor spatial navigation in schizophrenic patients, with

theta thought to be responsible for deficits in grid cell firing patterns (Convertino et al., 2023). Furthermore, impairments in spatial cognition, mainly spatial memory in depressed and schizophrenic patients have been found to be modulated by theta and gamma oscillations (Adams et al., 2020; Cornwell et al., 2010; Lynn & Sponheim, 2016). A standardised assessment procedure (Thornberry et al., 2021) accompanied by a standardised EEG metric of successful spatial memory retrieval may facilitate easier diagnosis of deficits and symptomology. These, combined with newly developed at-home dry EEG wearables for electrophysiological monitoring and early detection of cognitive deficits (Barbey et al., 2022; Mathewson et al., 2017; Whelan et al., 2022) could prove vital for the monitoring and detection of deficits in spatial cognition across a wide range of disorders.

Additionally, our age-related oscillatory findings from Chater 6 replicated typical EEG resting state age differences reported in the literature. These differences fit well with findings from the Default Mode Network model of EEG activity. This is a resting state network, deemed essential for assessing and understanding age differences and brain responses during cognition (Scheeringa et al., 2008; Ward et al., 2015). Dysfunction in this network has consequences for cognitive performance and has been cited as an excellent baseline condition to evaluate changes due to task demands (Chen et al., 2008; Smallwood et al., 2021). For task-related EEG, we reported consistently less power at each of the memory retrieval phases. A decrease in beta and gamma power after 24-hours, but identical behavioural performance to our younger adults on the task suggests possible high-frequency compensatory mechanisms, which help to maintain behavioural performance. This could have many wide-ranging applications should it be investigated further. For example, gamma activity has been shown to vary with the memory ability of older adults (Park et al., 2012). Staufenbiel et al. (2014) demonstrated beta and gamma neurofeedback (NFB; continuous, real-time feedback of brain activity patterns to allow self-modulation of oscillations in a desired direction) enhances beta oscillations but with no

impact on cognitive ability. Nevertheless, some other studies reported success using beta and gamma NFB, with improved episodic memory performance in both healthy older adults and MCI-patients (Becerra et al., 2012; Keizer et al., 2010; Lin et al., 2023). Therefore, it is possible that the compensatory nature of high-frequency oscillations may just be a natural part of ageing (Staufenbiel et al., 2014) or that possibly reversing the decrease in these rhythms through NFB could improve short-term (recent) spatial memory in older adults. Furthermore, as the memory becomes consolidated in a more long-term situation (i.e., remote) different, low-frequency oscillations change during recall. Delta power increases with a decrease in theta power. Decreases in theta power and a decline in memory retention are natural with age (Cummins & Finnigan, 2007) – with theta shown to decrease in older adults during cognitive mapping tasks and spatial memory retrieval (Ferreira et al., 2019; Lithfous et al., 2015). Stimulating and by result increasing delta-theta and synchronising these oscillations with gamma in older adults has been recently shown to improve memory performance (Reinhart & Nguyen, 2019) with theta neurofeedback showing similar improvements (Reis et al., 2016). Therefore, focusing on low-frequency stimulation or neurofeedback may help with long-term spatial memory retention. However, our remote group's behavioural performance was poorer, but still significantly above chance levels.

All of our memory results from Chapter 4-6 may be applied to the current theoretical debate regarding consolidation (Nadel & Moscovitch, 1997; Squire et al., 2015; Tse et al., 2007). We reported low-frequency delta-theta increases across retrieval phases, which may suggest reliance on hippocampus for spatial memory retrieval – which aligns with multiple trace theory. However, we reported increased frontal alpha power with increased retrieval periods (immediate < recent < remote). As discussed throughout the current thesis, alpha increases is thought to represent effortful engagement of the cortex resulting in successful memory retrieval, aligning with standard consolidation theory. Therefore, it is possible our

results could be applied to a dual-consolidation approach in which when retrieval is not successful through cortical networks (i.e., in older adults at remote recall) hippocampal-dependent networks are recruited (Robin & Moscovitch, 2017), and its recruitment is altered by memory workload. This would need to be much more strongly investigated to propose such a concept, using high-density source analysis amongst other methodologies. The ability to integrate information into an overall schematic of spatial memory traces, has been proposed previously (Farzanfar et al., 2023; Robin & Moscovitch, 2017; Tse et al., 2007), which may align with the above interpretation. Specific/detailed and gist-like/schematic representations can co-exist with different subregions responsible for their retrieval (Audrain & McAndrews, 2022; McCormick et al., 2020). How they are recruited may not be determined by the age of the memory, but by the task demands (Robin & Moscovitch, 2017). This leaves some open questions for future research:

- Does the reduced theta power in spatial learning reflect the similar dynamics reported during associative learning tasks? How does it interact with other frequency bands?
- Do oscillatory dynamics during spatial recall change with spatial navigation deficits?
- What subcortical EEG sources are responsible for recent and remote recall, and do they both involve the hippocampus?
- Are neural dynamics different for good and poor performing older adults?

### 7.4 Thesis Difficulties, Limitations and Strengths

One major limitation of the current thesis was the COVID-19 pandemic, and the restrictions in Ireland. In March 2020, the Irish government announced the closure of all higher education facilities and the introduction of physical distancing measures. Government plans were made to reopen university settings at various stages throughout the pandemic, but the spread of COVID-19 in Ireland was constantly fluctuating, with universities not returning in-person until

September 2021. All in-person research had stopped during this period, and further distancing and safety measures were still in place until 22nd January 2022, with mask wearing still in effect until the 28th of February 2022. Contingency plans for the current thesis were put in place, but all research was placed on hold, as it required in-person close contact.

The original project proposal was to involve more older adult data collection, but such a vulnerable population was difficult to access in the months following the lifting of restrictions. We had some data (n = 3) from before March 2020 from Experiment 3 which was then placed on hold. The remaining participants were not tested until after November 2021, following completion of COVID-19 safety training, a new standard operating procedure and a renewal of ethics approval. The time was used to learn how to analyse the EEG data collected prior to the pandemic, but all planned experiments incurred a delay of up to 2 years. The older adult experiment was moved to much later in thesis timeline, to allow for older adults to feel comfortable and safe coming to the lab and in close contact with the researcher. Data from younger adults was collected once feasible, but several participants dropped out due to COVID-19 infection or being a COVID-19 close-contact (as per restriction criteria). This caused significant delays to data collection for Chapter 3 as well as data quality issues due to the wearing of masks, gloves and lab time-constraints with the new COVID-19 safety precautions. Data from Chapter 4 was also impacted by this, and some participants did not complete a recall trial, as some did not feel well during testing or exceeded their permitted timeslot, which caused further significant delays. This had a knock-on delay to data collection for Chapter 5 which only began in late 2022/early 2023. Simultaneous recruitment of older adults during this time also proved difficult but eased into late 2023.

Further specific limitations of particular studies are addressed in their corresponding chapters throughout the thesis. However, in Chapter 4-6 we examined EEG data during spatial recall trials in NavWell. To our knowledge, no other studies had attempted to examine this

within the same restrictions of our paradigm. Relying on clean and useable data from a single recording session was an incredibly large risk. Particularly for Chapters 5 and 6, some participants may have completed a learning phase and immediate recall phase, returned after one month and produced unusable data during the remote phase. Which essentially removes that participant from majority of the analysis. A small amount of participant data was lost due to this (as well as some participants only revealing they do not meet inclusion criteria on their re-test). Careful testing protocols and data quality assurance were carried out during all recording sessions, which caused even further delays. This is where retaining the typical protocol of the Morris water maze was challenging. We would strongly encourage future researchers to design spatial memory consolidation and electrophysiology paradigms with this in mind.

Aside from time-constraints, convenience sampling and the use of the Department of Psychology Participation Pool resulted in population samples for most studies being predominantly female. Due to the restrictions and time-constraints mentioned above, we could not afford to be demanding or selective with participant recruitment. Though many of our studies report little to no influence of gender (but see Buckley & Bast, 2018), and even though NavWell is known to eliminate this bias (Commins et al., 2020) – the results are not as generalisable as originally intended.

Furthermore, much of our research was exploratory due to the lack of supporting literature and the novelty of our research paradigm and protocols. Where possible, we tried to remain hypothesis-driven in our approach, but this proved difficult, due to the incredibly problematic differences in the literature in *behavioural procedures* (Alcalá et al., 2020; D'Hooge & De Deyn, 2001; Padilla et al., 2017; Thornberry et al., 2021; Vorhees & Williams, 2024), *EEG analysis methods* (Cohen, 1995; Cohen, 2014; Cohen, 2017, 2019; Cohen et al., 2013; Delaux et al., 2021; Delorme, 2023; Morales & Bowers, 2022), and even *relevant*

*research findings* (Chrastil et al., 2022; Delaux et al., 2021; Du et al., 2023; Herweg, Solomon, et al., 2020; Jones & Wilson, 2005; Kaplan et al., 2014; Liang et al., 2021; Lin et al., 2015; Lithfous et al., 2015; Miyakoshi et al., 2021; Thornberry et al., 2023; Vivekananda et al., 2021). There are even disputes over the definition of frequency bands, with no definitive division of the human EEG frequency range (Chen et al., 2008; Herrmann et al., 1979; Herweg, Solomon, et al., 2020; Jaušovec & Jaušovec, 2010), and more than 20 arbitrary frequency boundaries reported in the literature for alpha alone (Bazanova & Vernon, 2014). Therefore, it was incredibly difficult to obtain guidance on procedure, protocol or signal-processing and analysis techniques. Despite these difficulties, we remained as controlled as we could. We performed *a priori* power calculations and remained hypothesis driven where possible (see Larson & Carbine, 2017). Furthermore, all statistics were corrected for multiple comparisons using FDR correction, utilised non-parametric permutation *t*-tests and only reported findings if they were previously hypothesised. For exploratory analyses and our novel paradigms, we predefined any regions of interests, used very strict analysis methods and utilised control groups where possible. We ensured all participants were cognitively matched before experimentation and kept signal processing procedures the exact same throughout, based on key research papers (see above).

Finally, prior to the beginning of the outlined series of experiments, we made the active decision to use relative power as opposed to absolute power throughout out analyses. Considering the large number of analyses that were planned to be conducted, it would have been impossible to analyse both power outputs. Since relative power values are interdependent, changes in one frequency band will affect the values of other frequency bands (Cohen, 1995; Cohen, 2014). This made the interpretation of some of our relative power changes more challenging (for example, see Figure 6.7 – in which higher delta/theta in younger adults results in lower beta/gamma power). Furthermore, Relative power measures can be influenced by

individual differences in total power, which may be related to factors such as skull thickness or electrode impedance, introducing unwanted noise. Nevertheless, we gain reduced sensitivity to artefacts, a normalisation for some individual differences and is probably a better choice for examining task-related changes in power distribution (Fernández et al., 1993). Based on the methodology of previous EEG and navigation studies (Jabès et al., 2021; Lin et al., 2015; Lin et al., 2017), we opted for relative power despite these limitations. However, future research should analyse and report both absolute and relative power outputs to provide a more comprehensive understanding of neural dynamics during spatial navigation tasks.

## 7.5 Conclusions

In conclusion, the current thesis presents a series of experiments which examined both learning (Chapter 3) and memory (Chapter 4) during human spatial navigation in a virtual water maze task. We further investigated the dynamics of brain oscillations using EEG during these cognitive processes, and how they are influenced by consolidation time (Chapter 5) and age (Chapter 6). Results suggest that successful and efficient spatial encoding results in the reduction of posterior theta (4-8 Hz) accompanied by continuous alpha (8-12 Hz) suppression. During spatial memory retrieval, increased low-frequency oscillations in delta (2-4 Hz) and theta (5-7 Hz) are related to successful navigation. When search strategies are unsuccessful, frontal midline power within these bands increases. During remote spatial memory retrieval, we found increases in all bands apart from theta, suggested to relate to active retrieval and memory load. Recent spatial memory retrieval requires greater oscillatory recruitment, but no change in dynamics. Older adults show reduced power throughout most frequency bands compared to younger adults. Within older adults, delta power increases and theta power decreases are also observed during remote memory retrieval, with beta (15-29 Hz) and gamma

(30-40 Hz) decreases during recent memory retrieval. Results suggest that increased low-frequency oscillations are associated with spatial memory retrieval for demanding tasks or remote memories. These dynamics do not change with healthy ageing but may become less efficient resulting in poorer spatial performance. Many of these findings contribute to existing literature, whilst introducing novel findings to hopefully generate new hypotheses. They also possess some theoretical and practical implications for spatial learning and memory research.

# References


Adams, R. A., Bush, D., Zheng, F., Meyer, S. S., Kaplan, R., Orfanos, S., Marques, T. R., Howes, O. D., & Burgess, N. (2020). Impaired theta phase coupling underlies frontotemporal dysconnectivity in schizophrenia. *Brain*, *143*(4), 1261-1277.

Addante, R. J., Watrous, A. J., Yonelinas, A. P., Ekstrom, A. D., & Ranganath, C. (2011). Prestimulus theta activity predicts correct source memory retrieval. *Proceedings of the National Academy of Sciences*, *108*(26), 10702-10707.

Aghajan, Z. M., Schuette, P., Fields, T. A., Tran, M. E., Siddiqui, S. M., Hasulak, N. R., Tcheng, T. K., Eliashiv, D., Mankin, E. A., & Stern, J. (2017). Theta oscillations in the human medial temporal lobe during real-world ambulatory movement. *Current Biology*, *27*(24), 3743-3751. e3743.

Aguilera, M., Douchamps, V., Battaglia, D., & Goutagny, R. (2022). How Many Gammas? Redefining Hippocampal Theta-Gamma Dynamic During Spatial Learning [Mini Review]. *Frontiers in Behavioral Neuroscience*, *16*.

Aida, J., Chau, B., & Dunn, J. (2018). Immersive virtual reality in traumatic brain injury rehabilitation: a literature review. *NeuroRehabilitation*, *42*(4), 441-448.

Alcalá, J. A., Callejas-Aguilera, J. E., Nelson, J. B., & Rosas, J. M. (2020). Reversal training facilitates acquisition of new learning in a Morris water maze. *Learning & Behavior*, *48*(2), 208-220.

Alekseichuk, I., Turi, Z., De Lara, G. A., Antal, A., & Paulus, W. (2016). Spatial working memory in humans depends on theta and high gamma synchronization in the prefrontal cortex. *Current Biology*, *26*(12), 1513-1521.

Alexander, D. M., Arns, M. W., Paul, R. H., Rowe, D. L., Cooper, N., Esser, A. H., Fallahpour, K., Stephan, B. C., Heesen, E., & Breteler, R. (2006). EEG markers for cognitive decline in elderly subjects with subjective memory complaints. *Journal of Integrative Neuroscience*, *5*(01), 49-74.

Andersen, R. A., & Cui, H. (2009). Intention, action planning, and decision making in parietal-frontal circuits. *Neuron*, *63*(5), 568-583.

Ansado, J., Monchi, O., Ennabil, N., Faure, S., & Joanette, Y. (2012). Load-dependent posterior–anterior shift in aging in complex visual selective attention situations. *Brain research*, *1454*, 14-22.

Antonova, E., Parslow, D., Brammer, M., Simmons, A., Williams, S., Dawson, G. R., & Morris, R. (2011). Scopolamine disrupts hippocampal activity during allocentric spatial memory in humans: an fMRI study using a virtual reality analogue of the Morris Water Maze. *Journal of Psychopharmacology*, *25*(9), 1256-1265.

Astur, R. S., Ortiz, M. L., & Sutherland, R. J. (1998). A characterization of performance by men and women in a virtual Morris water task: A large and reliable sex difference. *Behavioural Brain Research*, *93*(1-2), 185-190.

Astur, R. S., Taylor, L. B., Mamelak, A. N., Philpott, L., & Sutherland, R. J. (2002). Humans with hippocampus damage display severe spatial memory impairments in a virtual Morris water task. *Behavioural Brain Research*, *132*(1), 77-84.

Astur, R. S., Tropp, J., Sava, S., Constable, R. T., & Markus, E. J. (2004). Sex differences and correlations in a virtual Morris water task, a virtual radial arm maze, and mental rotation. *Behavioural Brain Research*, *151*(1-2), 103-115.

Audrain, S., & McAndrews, M. P. (2022). Schemas provide a scaffold for neocortical integration of new memories over time. *Nature Communications*, *13*(1), 5795.

Azami, H., Zrenner, C., Brooks, H., Zomorrodi, R., Blumberger, D. M., Fischer, C. E., Flint, A., Herrmann, N., Kumar, S., Lanctôt, K., Mah, L., Mulsant, B. H., Pollock, B. G., Rajji, T. K., & on behalf of the, P.-M. D. S. G. (2023). Beta to theta power ratio in EEG periodic components as a potential biomarker in mild cognitive impairment and Alzheimer's dementia. *Alzheimer's Research & Therapy*, *15*(1), 133.

Babiloni, C., Binetti, G., Cassarino, A., Dal Forno, G., Del Percio, C., Ferreri, F., Ferri, R., Frisoni, G., Galderisi, S., & Hirata, K. (2006). Sources of cortical rhythms in adults during physiological aging: a multicentric EEG study. *Human brain mapping*, *27*(2), 162-172.

Babiloni, C., Del Percio, C., Arendt-Nielsen, L., Soricelli, A., Romani, G. L., Rossini, P. M., & Capotosto, P. (2014). Cortical EEG alpha rhythms reflect task-specific somatosensory and motor interactions in humans. *Clinical Neurophysiology*, *125*(10), 1936-1945.

Babiloni, C., Frisoni, G. B., Vecchio, F., Lizio, R., Pievani, M., Cristina, G., Fracassi, C., Vernieri, F., Rodriguez, G., & Nobili, F. (2011). Stability of clinical condition in mild cognitive impairment is related to cortical sources of alpha rhythms: an electroencephalographic study. *Human brain mapping*, *32*(11), 1916-1931.

Babiloni, C., Lizio, R., Marzano, N., Capotosto, P., Soricelli, A., Triggiani, A. I., Cordone, S., Gesualdo, L., & Del Percio, C. (2016). Brain neural synchronization and functional coupling in Alzheimer's disease as revealed by resting state EEG rhythms. *International Journal of Psychophysiology*, *103*, 88-102.

Backus, A. R., Schoffelen, J.-M., Szebényi, S., Hanslmayr, S., & Doeller, C. F. (2016). Hippocampal-prefrontal theta oscillations support memory integration. *Current Biology*, *26*(4), 450-457.

Barbey, F. M., Farina, F. R., Buick, A. R., Danyeli, L., Dyer, J. F., Islam, M. N., Krylova, M., Murphy, B., Nolan, H., & Rueda-Delgado, L. M. (2022). Neuroscience from the comfort of your home: Repeated, self-administered wireless dry EEG measures brain function with high fidelity. *Frontiers in Digital Health*, *4*, 944753.

Barkas, L. J., Henderson, J. L., Hamilton, D. A., Redhead, E. S., & Gray, W. P. (2010). Selective temporal resections and spatial memory impairment: Cue dependent lateralization effects. *Behavioural Brain Research*, *208*(2), 535-544.

Barnes, C. A. (1979). Memory deficits associated with senescence: a neurophysiological and behavioral study in the rat. *Journal of comparative and physiological psychology*, *93*(1), 74.

Barnhart, C. D., Yang, D., & Lein, P. J. (2015). Using the Morris Water Maze to Assess Spatial Learning and Memory in Weanling Mice. *PLOS ONE*, *10*(4), e0124521.

Barone, J., & Rossiter, H. E. (2021). Understanding the role of sensorimotor beta oscillations. *Frontiers in systems neuroscience*, *15*, 655886.

Barr, M. S., Radhu, N., Guglietti, C. L., Zomorrodi, R., Rajji, T. K., Ritvo, P., & Daskalakis, Z. J. (2014). Age-related differences in working memory evoked gamma oscillations. *Brain research*, *1576*, 43-51.

Barry, C., Lever, C., Hayman, R., Hartley, T., Burton, S., O'Keefe, J., Jeffery, K., & Burgess, N. (2006). The boundary vector cell model of place cell firing and spatial memory. *Reviews in the Neurosciences*, *17*(1-2), 71-98.

Barry, D. N., & Commins, S. (2019). A novel control condition for spatial learning in the Morris water maze. *J Neurosci Methods*, *318*, 1-5.

Barry, D. N., Coogan, A. N., & Commins, S. (2016). The time course of systems consolidation of spatial memory from recent to remote retention: A comparison of the Immediate Early Genes Zif268, c-Fos and Arc. *Neurobiology of Learning and Memory*, *128*, 46-55.

Barry, D. N., & Maguire, E. A. (2019). Remote Memory and the Hippocampus: A Constructive Critique. *Trends in Cognitive Sciences*, *23*(2), 128-142.

Basu, R., Gebauer, R., Herfurth, T., Kolb, S., Golipour, Z., Tchumatchenko, T., & Ito, H. T. (2021). The orbitofrontal cortex maps future navigational goals. *Nature*, *599*(7885), 449-452.

Bauer, M., Buckley, M. G., & Bast, T. (2021). Individual differences in theta-band oscillations in a spatial memory network revealed by electroencephalography predict rapid place learning. *Brain Neurosci Adv*, *5*, 23982128211002725. https://doi.org/10.1177/23982128211002725

Bauer, M., Oostenveld, R., Peeters, M., & Fries, P. (2006). Tactile spatial attention enhances gamma-band activity in somatosensory cortex and reduces low-frequency activity in parieto-occipital areas. *Journal of Neuroscience*, *26*(2), 490-501.

Bazanova, O. M., & Vernon, D. (2014). Interpreting EEG alpha activity. *Neuroscience & Biobehavioral Reviews*, *44*, 94-110.

Becerra, J., Fernández, T., Roca-Stappung, M., Díaz-Comas, L., Galán, L., Bosch, J., Espino, M., Moreno, A. J., & Harmony, T. (2012). Neurofeedback in healthy elderly human subjects with electroencephalographic risk for cognitive disorder. *Journal of Alzheimer's Disease*, *28*(2), 357-367.

Bécu, M., Sheynikhovich, D., Tatur, G., Agathos, C. P., Bologna, L. L., Sahel, J.-A., & Arleo, A. (2020). Age-related preference for geometric spatial cues during real-world navigation. *Nature Human Behaviour*, *4*(1), 88-99.

Bell, A. J., & Sejnowski, T. J. (1995). An information-maximization approach to blind separation and blind deconvolution. *Neural computation*, *7*(6), 1129-1159.

Benedek, M., Schickel, R. J., Jauk, E., Fink, A., & Neubauer, A. C. (2014). Alpha power increases in right parietal cortex reflects focused internal attention. *Neuropsychologia*, *56*, 393-400.

Berron, D., Neumann, K., Maass, A., Schütze, H., Fliessbach, K., Kiven, V., Jessen, F., Sauvage, M., Kumaran, D., & Düzel, E. (2018). Age-related functional changes in domain-specific medial temporal lobe pathways. *Neurobiology of aging*, *65*, 86-97.

Bestgen, A.-K., Edler, D., Müller, C., Schulze, P., Dickmann, F., & Kuchinke, L. (2017). Where is it (in the map)? Recall and recognition of spatial information. *Cartographica: The International Journal for Geographic Information and Geovisualization*, *52*(1), 80-97.

Bischof, W. F., & Boulanger, P. (2003). Spatial navigation in virtual reality environments: an EEG analysis. *Cyberpsychology & Behavior*, *6*(5), 487-495.

Bjerknes, T. L., Moser, E. I., & Moser, M.-B. (2014). Representation of geometric borders in the developing rat. *Neuron*, *82*(1), 71-78.

Bohbot, V. D., Copara, M. S., Gotman, J., & Ekstrom, A. D. (2017). Low-frequency theta oscillations in the human hippocampus during real-world and virtual navigation. *Nature Communications*, *8*(1), 1-7.

Bohbot, V. D., Kalina, M., Stepankova, K., Spackova, N., Petrides, M., & Nadel, L. (1998). Spatial memory deficits in patients with lesions to the right hippocampus and to the right parahippocampal cortex. *Neuropsychologia*, *36*(11), 1217-1238.

Bolding, K., & Rudy, J. W. (2006). Place learning in the Morris water task: Making the memory stick. *Learning & Memory*, *13*(3), 278-286.

Bolhuis, J. J., Bijlsma, S., & Ansmink, P. (1986). Exponential decay of spatial memory of rats in a radial maze. *Behavioral and neural biology*, *46*(2), 115-122.

Bonnefond, M., & Jensen, O. (2012). Alpha oscillations serve to protect working memory maintenance against anticipated distracters. *Current Biology*, *22*(20), 1969-1974.

Boone, A. P., Gong, X., & Hegarty, M. (2018). Sex differences in navigation strategy and efficiency. *Memory & Cognition*, *46*(6), 909-922.

Bostock, E., Muller, R. U., & Kubie, J. L. (1991). Experience-dependent modifications of hippocampal place cell firing. *Hippocampus*, *1*(2), 193-205.

Boudewyn, M. A., Luck, S. J., Farrens, J. L., & Kappenman, E. S. (2018). How many trials does it take to get a significant ERP effect? It depends. *Psychophysiology*, *55*(6), e13049.

Bragin, A., Jando, G., Nadasdy, Z., Van Landeghem, M., & Buzsáki, G. (1995). Dentate EEG spikes and associated interneuronal population bursts in the hippocampal hilar region of the rat. *Journal of neurophysiology*, *73*(4), 1691-1705.

Bright, P., Jaldow, E., & Kopelman, M. D. (2002). The National Adult Reading Test as a measure of premorbid intelligence: a comparison with estimates derived from demographic variables. *Journal of the International Neuropsychological Society*, *8*(6), 847-854.

Broadbent, N. J., Squire, L. R., & Clark, R. E. (2006). Reversible hippocampal lesions disrupt water maze performance during both recent and remote memory tests. *Learning & Memory*, *13*(2), 187-191.

Bromley-Brits, K., Deng, Y., & Song, W. (2011). Morris water maze test for learning and memory deficits in Alzheimer's disease model mice. *JoVE (Journal of Visualized Experiments)*(53), e2920.

Brookes, M. J., Wood, J. R., Stevenson, C. M., Zumer, J. M., White, T. P., Liddle, P. F., & Morris, P. G. (2011). Changes in brain network activity during working memory tasks: a magnetoencephalography study. *NeuroImage*, *55*(4), 1804-1815.

Buckley, M. G., & Bast, T. (2018). A new human delayed-matching-to-place test in a virtual environment reverse-translated from the rodent watermaze paradigm: Characterization of performance measures and sex differences. *Hippocampus*, *28*(11), 796-812. https://doi.org/10.1002/hipo.22992

Bures, J., & Fenton, A. A. (2000). Neurophysiology of spatial cognition. *Physiology*, *15*(5), 233-240.

Burgess, A. P. (2019). How Conventional Visual Representations of Time-Frequency Analyses Bias Our Perception of EEG/MEG Signals and What to Do About It [Opinion]. *Frontiers in Human Neuroscience*, *13*.

Burgess, A. P., & Gruzelier, J. H. (1997). Short duration synchronization of human theta rhythm during recognition memory. *Neuroreport*, *8*(4), 1039-1042.

Burgess, N., & O'Keefe, J. (2011). Models of place and grid cell firing and theta rhythmicity. *Current Opinion in Neurobiology*, *21*(5), 734-744.

Burgess, N., Trinkler, I., King, J., Kennedy, A., & Cipolotti, L. (2006). Impaired Allocentric Spatial Memory Underlying Topographical Disorientation. *17*(1-2), 239-252. (Reviews in the Neurosciences)

Bush, D., Bisby, J. A., Bird, C. M., Gollwitzer, S., Rodionov, R., Diehl, B., McEvoy, A. W., Walker, M. C., & Burgess, N. (2017). Human hippocampal theta power indicates movement onset and distance travelled. *Proceedings of the National Academy of Sciences*, *114*(46), 12297-12302.

Buzsaki, G. (2006). *Rhythms of the Brain*. Oxford university press.

Buzsáki, G. (2002). Theta Oscillations in the Hippocampus. *Neuron*, *33*(3), 325-340.

Buzsáki, G. (2005). Theta rhythm of navigation: link between path integration and landmark navigation, episodic and semantic memory. *Hippocampus*, *15*(7), 827-840.

Buzsáki, G., Anastassiou, C. A., & Koch, C. (2012). The origin of extracellular fields and currents--EEG, ECoG, LFP and spikes. *Nat Rev Neurosci*, *13*(6), 407-420.

Buzsáki, G., & Moser, E. I. (2013). Memory, navigation and theta rhythm in the hippocampal-entorhinal system. *Nature Neuroscience*, *16*(2), 130-138.

Buzsáki, G., & Vanderwolf, C. H. (1983). Cellular bases of hippocampal EEG in the behaving rat. *Brain Research Reviews*, *6*(2), 139-171.

Buzsáki, G., & Wang, X.-J. (2012). Mechanisms of gamma oscillations. *Annual review of neuroscience*, *35*, 203-225.

Cabeza, R., Albert, M., Belleville, S., Craik, F. I., Duarte, A., Grady, C. L., Lindenberger, U., Nyberg, L., Park, D. C., & Reuter-Lorenz, P. A. (2018). Maintenance, reserve and compensation: the cognitive neuroscience of healthy ageing. *Nature Reviews Neuroscience*, *19*(11), 701-710.

Cabeza, R., Anderson, N. D., Locantore, J. K., & McIntosh, A. R. (2002). Aging gracefully: compensatory brain activity in high-performing older adults. *NeuroImage*, *17*(3), 1394-1402.

Cabeza, R., Daselaar, S. M., Dolcos, F., Prince, S. E., Budde, M., & Nyberg, L. (2004). Task-independent and task-specific age effects on brain activity during working memory, visual attention and episodic retrieval. *Cerebral Cortex*, *14*(4), 364-375.

Caffrey, M., & Commins, S. (2023). Preservation of long-term memory in older adults using a spaced learning paradigm. *European Journal of Ageing*, *20*(1), 2.

Cao, X., Huang, S., & Ruan, D. (2008). Enriched environment restores impaired hippocampal long-term potentiation and water maze performance induced by developmental lead exposure in rats. *Developmental Psychobiology: The Journal of the International Society for Developmental Psychobiology*, *50*(3), 307-313.

Caplan, J. B., & Glaholt, M. G. (2007). The roles of EEG oscillations in learning relational information. *NeuroImage*, *38*(3), 604-616.

Caplan, J. B., Madsen, J. R., Schulze-Bonhage, A., Aschenbrenner-Scheibe, R., Newman, E. L., & Kahana, M. J. (2003). Human θ Oscillations Related to Sensorimotor Integration and Spatial Learning. *The Journal of Neuroscience*, *23*(11), 4726-4736.

Capotosto, P., Babiloni, C., Romani, G. L., & Corbetta, M. (2009). Frontoparietal cortex controls spatial attention through modulation of anticipatory alpha rhythms. *J Neurosci*, *29*(18), 5863-5872.

Carr, M. F., Jadhav, S. P., & Frank, L. M. (2011). Hippocampal replay in the awake state: a potential substrate for memory consolidation and retrieval. *Nature Neuroscience*, *14*(2), 147-153.

Carson, N., Leach, L., & Murphy, K. J. (2018). A re-examination of Montreal Cognitive Assessment (MoCA) cutoff scores. *International journal of geriatric psychiatry*, *33*(2), 379-388.

Cauffman, E., Shulman, E. P., Steinberg, L., Claus, E., Banich, M. T., Graham, S., & Woolard, J. (2010). Age differences in affective decision making as indexed by performance on the Iowa Gambling Task. *Developmental psychology*, *46*(1), 193.

Cave, C. B., & Squire, L. R. (1991). Equivalent impairment of spatial and nonspatial memory following damage to the human hippocampus. *Hippocampus*, *1*(3), 329-340.

Cesnaite, E., Steinfath, P., Jamshidi Idaji, M., Stephani, T., Kumral, D., Haufe, S., Sander, C., Hensch, T., Hegerl, U., Riedel-Heller, S., Röhr, S., Schroeter, M. L., Witte, A. V., Villringer, A., & Nikulin, V. V. (2023). Alterations in rhythmic and non-rhythmic resting-state EEG activity and their link to cognition in older age. *NeuroImage*, *268*, 119810.

Cevallos, C., Zarka, D., Hoellinger, T., Leroy, A., Dan, B., & Chéron, G. (2015). Oscillations in the human brain during walking execution, imagination and observation. *Neuropsychologia*, *79*, 223-232.

Chamizo, V. D., Rodrigo, T., Peris, J. M., & Grau, M. (2006). The influence of landmark salience in a navigation task: An additive effect between its components. *Journal of Experimental Psychology: Animal Behavior Processes*, *32*(3), 339.

Chamizo, V. D., Rodríguez, C. A., Espinet, A., & Mackintosh, N. (2012). Generalization decrement and not overshadowing by associative competition among pairs of landmarks in a navigation task. *Journal of Experimental Psychology: Animal Behavior Processes*, *38*(3), 255.

Chan, M. Y., Han, L., Carreno, C. A., Zhang, Z., Rodriguez, R. M., LaRose, M., Hassenstab, J., & Wig, G. S. (2021). Long-term prognosis and educational determinants of brain network decline in older adult individuals. *Nature aging*, *1*(11), 1053-1067.

Chapuis, N., Durup, M., & Thinus-Blanc, C. (1987). The role of exploratory experience in a shortcut task by golden hamsters (Mesocricetus auratus). *Animal learning & behavior*, *15*, 174-178.

Chattopadhyay, S., Zary, L., Quek, C., & Prasad, D. K. (2021). Motivation detection using EEG signal analysis by residual-in-residual convolutional neural network. *Expert Systems with Applications*, *184*, 115548.

Chen, A. C. N., Feng, W., Zhao, H., Yin, Y., & Wang, P. (2008). EEG default mode network in the human brain: Spectral regional field powers. *NeuroImage*, *41*(2), 561-574.

Chen, D., Kunz, L., Wang, W., Zhang, H., Wang, W.-X., Schulze-Bonhage, A., Reinacher, P. C., Zhou, W., Liang, S., & Axmacher, N. (2018). Hexadirectional modulation of theta power in human entorhinal cortex during spatial navigation. *Current Biology*, *28*(20), 3310-3315. e3314.

Chen, J. L., Ros, T., & Gruzelier, J. H. (2013). Dynamic changes of ICA-derived EEG functional connectivity in the resting state. *Human brain mapping*, *34*(4), 852-868.

Cheng, Y., He, C., Hegarty, M., & Chrastil, E. R. (2022). Who believes they are good navigators? A machine learning pipeline highlights the impact of gender, commuting time, and education. *Machine Learning with Applications*, *10*, 100419.

Chiu, T. C., Gramann, K., Ko, L. W., Duann, J. R., Jung, T. P., & Lin, C. T. (2012). Alpha modulation in parietal and retrosplenial cortex correlates with navigation performance. *Psychophysiology*, *49*(1), 43-55.

Chrastil, E. R., Rice, C., Goncalves, M., Moore, K. N., Wynn, S. C., Stern, C. E., & Nyhus, E. (2022). Theta oscillations support active exploration in human spatial navigation. *NeuroImage*, *262*, 119581.

Chrastil, E. R., & Warren, W. H. (2013). Active and passive spatial learning in human navigation: acquisition of survey knowledge. *Journal of Experimental Psychology: Learning, Memory, and Cognition*, *39*(5), 1520.

Cimadevilla, J. M., Fenton, A. A., & Bures, J. (2000). Functional inactivation of dorsal hippocampus impairs active place avoidance in rats. *Neuroscience Letters*, *285*(1), 53-56.

Civile, C., Chamizo, V., Mackintosh, N., & McLaren, I. P. (2014). The effect of disrupting configural information on rats' performance in the Morris water maze. *Learning and Motivation*, *48*, 55-66.

Clark, R. E., Broadbent, N. J., & Squire, L. R. (2005a). Hippocampus and remote spatial memory in rats. *Hippocampus*, *15*(2), 260-272.

Clark, R. E., Broadbent, N. J., & Squire, L. R. (2005b). Impaired remote spatial memory after hippocampal lesions despite extensive training beginning early in life. *Hippocampus*, *15*(3), 340-346.

Cockrell, J. R., & Folstein, M. F. (2002). Mini-mental state examination. *Principles and practice of geriatric psychiatry*, 140-141.

Cogné, M., Taillade, M., N'Kaoua, B., Tarruella, A., Klinger, E., Larrue, F., Sauzéon, H., Joseph, P.-A., & Sorita, E. (2017). The contribution of virtual reality to the diagnosis of spatial navigation disorders and to the study of the role of navigational aids: A

systematic literature review. *Annals of physical and rehabilitation medicine*, *60*(3), 164-176.
Cohen, L. (1995). *Time-frequency analysis* (Vol. 778). Prentice hall New Jersey.
Cohen, M. X. (2014). *Analyzing neural time series data: theory and practice*. MIT press.
Cohen, M. X. (2017). Where does EEG come from and what does it mean? *Trends in Neurosciences*, *40*(4), 208-218.
Cohen, M. X. (2019). A better way to define and describe Morlet wavelets for time-frequency analysis. *NeuroImage*, *199*, 81-86.
Cohen, S. J., Munchow, A. H., Rios, L. M., Zhang, G., Ásgeirsdóttir, H. N., & Stackman, R. W. (2013). The rodent hippocampus is essential for nonspatial object memory. *Current Biology*, *23*(17), 1685-1690.
Colgin, L. L. (2020). Five decades of hippocampal place cells and EEG rhythms in behaving rats. *Journal of Neuroscience*, *40*(1), 54-60.
Colgin, L. L., Denninger, T., Fyhn, M., Hafting, T., Bonnevie, T., Jensen, O., Moser, M.-B., & Moser, E. I. (2009). Frequency of gamma oscillations routes flow of information in the hippocampus. *Nature*, *462*(7271), 353-357.
Commins, S. (2018a). *Behavioural neuroscience*. Cambridge university press.
Commins, S. (2018b). Efficiency: an underlying principle of learning? *Rev Neurosci*, *29*(2), 183-197.
Commins, S., Coutrot, A., Hornberger, M., Spiers, H. J., & De Andrade Moral, R. (2023). Examining individual learning patterns using generalised linear mixed models. *Behavior research methods*, 1-16.
Commins, S., Coutrot, A., Hornberger, M., Spiers, H. J., & De Andrade, R. (2022). Examining individual learning patterns using generalized linear mixed models.
Commins, S., Duffin, J., Chaves, K., Leahy, D., Corcoran, K., Caffrey, M., Keenan, L., Finan, D., & Thornberry, C. (2020). NavWell: A simplified virtual-reality platform for spatial navigation and memory experiments. *Behavior research methods*, *52*(3), 1189-1207.
Commins, S., & Fey, D. (2019). Understanding the role of distance, direction and cue salience in an associative model of landmark learning. *Scientific reports*, *9*(1), 1-13.
Commins, S., & Kirby, B. P. (2019). The complexities of behavioural assessment in neurodegenerative disorders: A focus on Alzheimer's disease. *Pharmacological Research*, *147*, 104363.
Commins, S., McCormack, K., Callinan, E., Fitzgerald, H., Molloy, E., & Young, K. (2013). Manipulation of visual information does not change the accuracy of distance estimation during a blindfolded walking task. *Human Movement Science*, *32*(4), 794-807.
Committeri, G., Fragueiro, A., Campanile, M. M., Lagatta, M., Burles, F., Iaria, G., Sestieri, C., & Tosoni, A. (2020). Egocentric navigation abilities predict episodic memory performance. *Frontiers in Human Neuroscience*, *14*, 574224.
Compton, R. J., Gearinger, D., & Wild, H. (2019). The wandering mind oscillates: EEG alpha power is enhanced during moments of mind-wandering. *Cognitive, Affective, & Behavioral Neuroscience*, *19*, 1184-1191.
Convertino, L., Bush, D., Zheng, F., Adams, R. A., & Burgess, N. (2023). Reduced grid-like theta modulation in schizophrenia. *Brain*, *146*(5), 2191-2198.
Cooper, N. R., Croft, R. J., Dominey, S. J., Burgess, A. P., & Gruzelier, J. H. (2003). Paradox lost? Exploring the role of alpha oscillations during externally vs. internally directed attention and the implications for idling and inhibition hypotheses. *International Journal of Psychophysiology*, *47*(1), 65-74.
Cornwell, B. R., Arkin, N., Overstreet, C., Carver, F. W., & Grillon, C. (2012). Distinct contributions of human hippocampal theta to spatial cognition and anxiety. *Hippocampus*, *22*(9), 1848-1859.

Cornwell, B. R., Johnson, L. L., Holroyd, T., Carver, F. W., & Grillon, C. (2008). Human hippocampal and parahippocampal theta during goal-directed spatial navigation predicts performance on a virtual Morris water maze. *Journal of Neuroscience*, *28*(23), 5983-5990.

Cornwell, B. R., Salvadore, G., Colon-Rosario, V., Latov, D. R., Holroyd, T., Carver, F. W., Coppola, R., Manji, H. K., Zarate Jr, C. A., & Grillon, C. (2010). Abnormal hippocampal functioning and impaired spatial navigation in depressed individuals: evidence from whole-head magnetoencephalography. *American Journal of Psychiatry*, *167*(7), 836-844.

Coughlan, G., Laczó, J., Hort, J., Minihane, A. M., & Hornberger, M. (2018). Spatial navigation deficits - overlooked cognitive marker for preclinical Alzheimer disease? *Nat Rev Neurol*, *14*(8), 496-506.

Coughlan, G., Puthusseryppady, V., Lowry, E., Gillings, R., Spiers, H., Minihane, A.-M., & Hornberger, M. (2020). Test-retest reliability of spatial navigation in adults at-risk of Alzheimer's disease. *PLOS ONE*, *15*(9), e0239077.

Coutrot, A., Schmidt, S., Coutrot, L., Pittman, J., Hong, L., Wiener, J. M., Hölscher, C., Dalton, R. C., Hornberger, M., & Spiers, H. J. (2019). Virtual navigation tested on a mobile app is predictive of real-world wayfinding navigation performance. *PLOS ONE*, *14*(3), e0213272.

Crespo-Garcia, M., Cantero, J. L., & Atienza, M. (2012). Effects of semantic relatedness on age-related associative memory deficits: the role of theta oscillations. *NeuroImage*, *61*(4), 1235-1248.

Crespo-García, M., Zeiller, M., Leupold, C., Kreiselmeyer, G., Rampp, S., Hamer, H. M., & Dalal, S. S. (2016). Slow-theta power decreases during item-place encoding predict spatial accuracy of subsequent context recall. *NeuroImage*, *142*, 533-543.

Crusio, W. E., Schwegler, H., & Lipp, H.-P. (1987). Radial-maze performance and structural variation of the hippocampus in mice: a correlation with mossy fibre distribution. *Brain research*, *425*(1), 182-185.

Cummins, T. D. R., & Finnigan, S. (2007). Theta power is reduced in healthy cognitive aging. *International Journal of Psychophysiology*, *66*(1), 10-17.

D'Hooge, R., & De Deyn, P. P. (2001). Applications of the Morris water maze in the study of learning and memory. *Brain Research Reviews*, *36*(1), 60-90.

Daugherty, A. M., & Raz, N. (2017). A virtual water maze revisited: Two-year changes in navigation performance and their neural correlates in healthy adults. *NeuroImage*, *146*, 492-506.

Daugherty, A. M., Yuan, P., Dahle, C. L., Bender, A. R., Yang, Y., & Raz, N. (2015). Path Complexity in Virtual Water Maze Navigation: Differential Associations with Age, Sex, and Regional Brain Volume. *Cereb Cortex*, *25*(9), 3122-3131.

Dauwels, J., Vialatte, F., Musha, T., & Cichocki, A. (2010). A comparative study of synchrony measures for the early diagnosis of Alzheimer's disease based on EEG. *NeuroImage*, *49*(1), 668-693.

De Araújo, D. B., Baffa, O., & Wakai, R. T. (2002). Theta oscillations and human navigation: a magnetoencephalography study. *Journal of Cognitive Neuroscience*, *14*(1), 70-78.

de Bruin, J. P. C., Sanchez-Santed, F., Heinsbroek, R. P. W., Donker, A., & Postmes, P. (1994). A behavioural analysis of rats with damage to the medial prefrontal cortex using the Morris water maze: evidence for behavioural flexibility, but not for impaired spatial navigation. *Brain research*, *652*(2), 323-333.

de Cheveigné, A., & Nelken, I. (2019). Filters: when, why, and how (not) to use them. *Neuron*, *102*(2), 280-293.

De Stefano, P., Carboni, M., Marquis, R., Spinelli, L., Seeck, M., & Vulliemoz, S. (2022). Increased delta power as a scalp marker of epileptic activity: a simultaneous scalp and intracranial electroencephalography study. *European Journal of Neurology*, *29*(1), 26-35.

Deacon, R. M., Bannerman, D. M., Kirby, B. P., Croucher, A., & Rawlins, J. N. P. (2002). Effects of cytotoxic hippocampal lesions in mice on a cognitive test battery. *Behavioural Brain Research*, *133*(1), 57-68.

Deacon, R. M., & Rawlins, J. N. P. (2006). T-maze alternation in the rodent. *Nature Protocols*, *1*(1), 7-12.

Deceuninck, L., & Kloosterman, F. (2022). Awake hippocampal replay is not required for short-term memory. *bioRxiv*, 2022.2011. 2003.514989.

Deery, R., & Commins, S. (2023). Landmark Distance Impacts the Overshadowing Effect in Spatial Learning Using a Virtual Water Maze Task with Healthy Adults. *Brain Sciences*, *13*(9), 1287.

Delaux, A., de Saint Aubert, J. B., Ramanoël, S., Bécu, M., Gehrke, L., Klug, M., Chavarriaga, R., Sahel, J. A., Gramann, K., & Arleo, A. (2021). Mobile brain/body imaging of landmark-based navigation with high-density EEG. *European Journal of Neuroscience*, *54*(12), 8256-8282.

Delorme, A. (2023). EEG is better left alone. *Scientific reports*, *13*(1), 2372.

Després, O., Lithfous, S., Tromp, D., Pebayle, T., & Dufour, A. (2017). Gamma oscillatory activity is impaired in episodic memory encoding with age. *Neurobiology of aging*, *52*, 53-65.

Dhein, K. (2023). The cognitive map debate in insects: A historical perspective on what is at stake. *Studies in History and Philosophy of Science*, *98*, 62-79.

Di Liberto, G. M., Barsotti, M., Vecchiato, G., Ambeck-Madsen, J., Del Vecchio, M., Avanzini, P., & Ascari, L. (2021). Robust anticipation of continuous steering actions from electroencephalographic data during simulated driving. *Scientific Reports*, *11*(1), 23383.

Dimitrov, M., Granetz, J., Peterson, M., Hollnagel, C., Alexander, G., & Grafman, J. (1999). Associative learning impairments in patients with frontal lobe damage. *Brain and cognition*, *41*(2), 213-230.

Do, T.-T. N., Lin, C.-T., & Gramann, K. (2021). Human brain dynamics in active spatial navigation. *Scientific Reports*, *11*(1), 13036.

Dobbels, B., Mertens, G., Gilles, A., Moyaert, J., van de Berg, R., Fransen, E., Van de Heyning, P., & Van Rompaey, V. (2020). The Virtual Morris Water Task in 64 Patients With Bilateral Vestibulopathy and the Impact of Hearing Status [Original Research]. *Frontiers in Neurology*, *11*.

Doeller, C. F., & Burgess, N. (2008). Distinct error-correcting and incidental learning of location relative to landmarks and boundaries. *Proceedings of the National Academy of Sciences*, *105*(15), 5909-5914.

Dong, L., Zhao, L., Zhang, Y., Yu, X., Li, F., Li, J., Lai, Y., Liu, T., & Yao, D. (2021). Reference electrode standardization interpolation technique (RESIT): a novel interpolation method for scalp EEG. *Brain Topography*, *34*(4), 403-414.

Du, Y. K., Liang, M., McAvan, A. S., Wilson, R. C., & Ekstrom, A. D. (2023). Frontal-midline theta and posterior alpha oscillations index early processing of spatial representations during active navigation. *Cortex*, *169*, 65-80.

Dupret, D., O'neill, J., Pleydell-Bouverie, B., & Csicsvari, J. (2010). The reorganization and reactivation of hippocampal maps predict spatial memory performance. *Nature Neuroscience*, *13*(8), 995-1002.

Durteste, M., Delaux, A., Ariztégui, A., Cottereau, B. R., Sheynikhovich, D., Ramanoël, S., & Arleo, A. (2023). Age-related disparities in oscillatory dynamics within scene-selective regions during spatial navigation. *bioRxiv*, 2023.2010. 2016.562507.

Duval, A. (2019). The representation selection problem: Why we should favor the geometric-module framework of spatial reorientation over the view-matching framework. *Cognition*, *192*, 103985.

Duvelle, É., Grieves, R. M., Liu, A., Jedidi-Ayoub, S., Holeniewska, J., Harris, A., Nyberg, N., Donnarumma, F., Lefort, J. M., & Jeffery, K. J. (2021). Hippocampal place cells encode global location but not connectivity in a complex space. *Current Biology*, *31*(6), 1221-1233. e1229.

Düzel, E., Habib, R., Schott, B., Schoenfeld, A., Lobaugh, N., McIntosh, A. R., Scholz, M., & Heinze, H. J. (2003). A multivariate, spatiotemporal analysis of electromagnetic time-frequency data of recognition memory. *NeuroImage*, *18*(2), 185-197.

Düzel, E., Neufang, M., & Heinze, H.-J. (2005). The Oscillatory Dynamics of Recognition Memory and its Relationship to Event-related Responses. *Cerebral Cortex*, *15*(12), 1992-2002.

Dyer, F. C. (1991). Bees acquire route-based memories but not cognitive maps in a familiar landscape. *Animal Behaviour*, *41*(2), 239-246.

Ehinger, B. V., Fischer, P., Gert, A. L., Kaufhold, L., Weber, F., Pipa, G., & König, P. (2014). Kinesthetic and vestibular information modulate alpha activity during spatial navigation: a mobile EEG study. *Frontiers in human neuroscience*, *8*, 71.

Eichenbaum, H. (2014). Time cells in the hippocampus: a new dimension for mapping memories. *Nature Reviews Neuroscience*, *15*(11), 732-744.

Eichenbaum, H., Dudchenko, P., Wood, E., Shapiro, M., & Tanila, H. (1999). The hippocampus, memory, and place cells: is it spatial memory or a memory space? *Neuron*, *23*(2), 209-226.

Eichenbaum, H., Stewart, C., & Morris, R. (1990). Hippocampal representation in place learning. *Journal of Neuroscience*, *10*(11), 3531-3542.

Ekstrom, A. D., & Bookheimer, S. Y. (2007). Spatial and temporal episodic memory retrieval recruit dissociable functional networks in the human brain. *Learn Mem*, *14*(10), 645-654.

Ekstrom, A. D., Caplan, J. B., Ho, E., Shattuck, K., Fried, I., & Kahana, M. J. (2005). Human hippocampal theta activity during virtual navigation. *Hippocampus*, *15*(7), 881-889.

Ekstrom, A. D., & Hill, P. F. (2023). Spatial navigation and memory: A review of the similarities and differences relevant to brain models and age. *Neuron*, *111*(7), 1037-1049.

Ekstrom, A. D., Huffman, D. J., & Starrett, M. (2017). Interacting networks of brain regions underlie human spatial navigation: a review and novel synthesis of the literature. *J Neurophysiol*, *118*(6), 3328-3344.

Ekstrom, A. D., Kahana, M. J., Caplan, J. B., Fields, T. A., Isham, E. A., Newman, E. L., & Fried, I. (2003). Cellular networks underlying human spatial navigation. *Nature*, *425*(6954), 184-188.

Ekstrom, A. D., & Ranganath, C. (2018). Space, time, and episodic memory: The hippocampus is all over the cognitive map. *Hippocampus*, *28*(9), 680-687.

Ekstrom, A. D., Spiers, H. J., Bohbot, V. D., & Rosenbaum, R. S. (2018). *Human spatial navigation*. Princeton University Press.

Ekstrom, A. D., & Watrous, A. J. (2014). Multifaceted roles for low-frequency oscillations in bottom-up and top-down processing during navigation and memory. *NeuroImage*, *85*, 667-677.

Engel, A. K., & Fries, P. (2010). Beta-band oscillations—signalling the status quo? *Current Opinion in Neurobiology*, *20*(2), 156-165.

Enz, N., Ruddy, K. L., Rueda-Delgado, L. M., & Whelan, R. (2021). Volume of β-bursts, but not their rate, predicts successful response inhibition. *Journal of Neuroscience*, *41*(23), 5069-5079.

Epstein, R. A. (2008). Parahippocampal and retrosplenial contributions to human spatial navigation. *Trends in Cognitive Sciences*, *12*(10), 388-396.

Epstein, R. A., Patai, E. Z., Julian, J. B., & Spiers, H. J. (2017). The cognitive map in humans: spatial navigation and beyond. *Nature neuroscience*, *20*(11), 1504-1513.

Erkan, İ. (2018). Examining wayfinding behaviours in architectural spaces using brain imaging with electroencephalography (EEG). *Architectural Science Review*, *61*(6), 410-428.

Farina, F. R., Burke, T., Coyle, D., Jeter, K., McGee, M., O'Connell, J., Taheny, D., & Commins, S. (2015). Learning efficiency: The influence of cue salience during spatial navigation. *Behavioural processes*, *116*, 17-27.

Farina, F. R., & Commins, S. (2016). Differential expression of immediate early genes Zif268 and c-Fos in the hippocampus and prefrontal cortex following spatial learning and glutamate receptor antagonism. *Behavioural Brain Research*, *307*, 194-198.

Farina, F. R., & Commins, S. (2020). Hippocampal and prefrontal contributions to memory retrieval: Examination of immediate early gene, NMDA receptor and environmental interactions. *European Journal of Neuroscience*, *52*(3), 2982-2994.

Farzanfar, D., Spiers, H. J., Moscovitch, M., & Rosenbaum, R. S. (2023). From cognitive maps to spatial schemas. *Nature Reviews Neuroscience*, *24*(2), 63-79.

Fell, J., & Axmacher, N. (2011). The role of phase synchronization in memory processes. *Nature Reviews Neuroscience*, *12*(2), 105-118.

Fellner, M.-C., Volberg, G., Wimber, M., Goldhacker, M., Greenlee, M. W., & Hanslmayr, S. (2016). Spatial mnemonic encoding: theta power decreases and medial temporal lobe BOLD increases co-occur during the usage of the method of loci. *eneuro*, *3*(6).

Fellous, J. M., & Sejnowski, T. J. (2000). Cholinergic induction of oscillations in the hippocampal slice in the slow (0.5–2 Hz), theta (5–12 Hz), and gamma (35–70 Hz) bands. *Hippocampus*, *10*(2), 187-197.

Fellrath, J., Mottaz, A., Schnider, A., Guggisberg, A. G., & Ptak, R. (2016). Theta-band functional connectivity in the dorsal fronto-parietal network predicts goal-directed attention. *Neuropsychologia*, *92*, 20-30.

Fenton, A. A., Arolfo, M. P., & Bures, J. (1994). Place navigation in the Morris water maze under minimum and redundant extra-maze cue conditions. *Behavioral and neural biology*, *62*(3), 178-189.

Ferguson, T. D., Livingstone-Lee, S. A., & Skelton, R. W. (2019). Incidental learning of allocentric and egocentric strategies by both men and women in a dual-strategy virtual Morris Water Maze. *Behavioural Brain Research*, *364*, 281-295.

Fernández, T., Harmony, T., Rodríguez, M., Reyes, A., Marosi, E., & Bernal, J. (1993). Test-retest reliability of EEG spectral parameters during cognitive tasks: I absolute and relative power. *International Journal of Neuroscience*, *68*(3-4), 255-261.

Ferreira, C. S., Maraver, M. J., Hanslmayr, S., & Bajo, T. (2019). Theta oscillations show impaired interference detection in older adults during selective memory retrieval. *Scientific reports*, *9*(1), 9977.

Field, A. (2013). *Discovering statistics using IBM SPSS statistics*. sage.

Finnigan, S., & Robertson, I. H. (2011). Resting EEG theta power correlates with cognitive performance in healthy older adults. *Psychophysiology*, *48*(8), 1083-1087.

Fleck, J. I., Kuti, J., Mercurio, J., Mullen, S., Austin, K., & Pereira, O. (2017). The Impact of Age and Cognitive Reserve on Resting-State Brain Connectivity [Original Research]. *Frontiers in Aging Neuroscience*, *9*.

Fodor, Z., Marosi, C., Tombor, L., & Csukly, G. (2020). Salient distractors open the door of perception: alpha desynchronization marks sensory gating in a working memory task. *Scientific Reports*, *10*(1), 19179.

Foster, J. J., Sutterer, D. W., Serences, J. T., Vogel, E. K., & Awh, E. (2016). The topography of alpha-band activity tracks the content of spatial working memory. *Journal of neurophysiology*, *115*(1), 168-177.

Foxe, J. J., & Snyder, A. C. (2011). The role of alpha-band brain oscillations as a sensory suppression mechanism during selective attention. *Frontiers in Psychology*, *2*, 154.

Frank, L. M., Stanley, G. B., & Brown, E. N. (2004). Hippocampal Plasticity across Multiple Days of Exposure to Novel Environments. *The Journal of Neuroscience*, *24*(35), 7681-7689.

Frankland, P. W., & Bontempi, B. (2005). The organization of recent and remote memories. *Nature Reviews Neuroscience*, *6*(2), 119-130.

Frossard, J., & Renaud, O. (2021). Permutation tests for regression, ANOVA, and comparison of signals: the permuco package. *Journal of Statistical Software*, *99*, 1-32.

Fuentes-García, J. P., Villafaina, S., Collado-Mateo, D., Cano-Plasencia, R., & Gusi, N. (2020). Chess Players Increase the Theta Power Spectrum When the Difficulty of the Opponent Increases: An EEG Study. *International Journal of Environmental Research and Public Health*, *17*(1), 46.

Gagnon, K. T., Thomas, B. J., Munion, A., Creem-Regehr, S. H., Cashdan, E. A., & Stefanucci, J. K. (2018). Not all those who wander are lost: Spatial exploration patterns and their relationship to gender and spatial memory. *Cognition*, *180*, 108-117.

Gaillard, A., Fehring, D. J., & Rossell, S. L. (2021). A systematic review and meta-analysis of behavioural sex differences in executive control. *European Journal of Neuroscience*, *53*(2), 519-542.

Gallagher, M., Colantuoni, C., Eichenbaum, H., Haberman, R. P., Rapp, P. R., Tanila, H., & Wilson, I. A. (2006). Individual differences in neurocognitive aging of the medial temporal lobe. *Age*, *28*, 221-233.

Gammeri, R., Léonard, J., Toupet, M., Hautefort, C., Van Nechel, C., Besnard, S., Machado, M.-L., Nakul, E., Montava, M., & Lavieille, J.-P. (2022). Navigation strategies in patients with vestibular loss tested in a virtual reality T-maze. *Journal of neurology*, *269*(8), 4333-4348.

Garcia-Rill, E. (2015). Chapter 8 - The 10Hz Fulcrum. In E. Garcia-Rill (Ed.), *Waking and the Reticular Activating System in Health and Disease* (pp. 157-170). Academic Press.

Gehrke, L., & Gramann, K. (2021). Single-trial regression of spatial exploration behavior indicates posterior EEG alpha modulation to reflect egocentric coding. *European Journal of Neuroscience*, *54*(12), 8318-8335.

Goodman, M. S., Kumar, S., Zomorrodi, R., Ghazala, Z., Cheam, A. S. M., Barr, M. S., Daskalakis, Z. J., Blumberger, D. M., Fischer, C., Flint, A., Mah, L., Herrmann, N., Bowie, C. R., Mulsant, B. H., & Rajji, T. K. (2018). Theta-Gamma Coupling and Working Memory in Alzheimer's Dementia and Mild Cognitive Impairment [Original Research]. *Frontiers in Aging Neuroscience*, *10*.

Goodrich-Hunsaker, N. J., Livingstone, S. A., Skelton, R. W., & Hopkins, R. O. (2010). Spatial deficits in a virtual water maze in amnesic participants with hippocampal damage. *Hippocampus*, *20*(4), 481-491.

Gould, J. L. (1986). The locale map of honey bees: Do insects have cognitive maps? *Science*, *232*(4752), 861-863.

Goyal, A., Miller, J., Qasim, S. E., Watrous, A. J., Zhang, H., Stein, J. M., Inman, C. S., Gross, R. E., Willie, J. T., Lega, B., Lin, J.-J., Sharan, A., Wu, C., Sperling, M. R., Sheth, S. A., McKhann, G. M., Smith, E. H., Schevon, C., & Jacobs, J. (2020). Functionally distinct high and low theta oscillations in the human hippocampus. *Nature Communications*, *11*(1), 2469.

Grabner, R. H., Fink, A., Stipacek, A., Neuper, C., & Neubauer, A. C. (2004). Intelligence and working memory systems: evidence of neural efficiency in alpha band ERD. *Cognitive Brain Research*, *20*(2), 212-225.

Grady, C. (2012). The cognitive neuroscience of ageing. *Nature Reviews Neuroscience*, *13*(7), 491-505.

Gramann, K., Onton, J., Riccobon, D., Mueller, H. J., Bardins, S., & Makeig, S. (2010). Human Brain Dynamics Accompanying Use of Egocentric and Allocentric Reference Frames during Navigation. *Journal of Cognitive Neuroscience*, *22*(12), 2836-2849.

Grech, A. M., Nakamura, J. P., & Hill, R. A. (2018). The importance of distinguishing allocentric and egocentric search strategies in rodent hippocampal-dependent spatial memory paradigms: getting more out of your data. *The Hippocampus-Plasticity and Functions*.

Greenberg, J. A., Burke, J. F., Haque, R., Kahana, M. J., & Zaghloul, K. A. (2015). Decreases in theta and increases in high frequency activity underlie associative memory encoding. *NeuroImage*, *114*, 257-263.

Grieves, R. M., & Jeffery, K. J. (2017). The representation of space in the brain. *Behav Processes*, *135*, 113-131.

Griffiths, B., Mazaheri, A., Debener, S., & Hanslmayr, S. (2016). Brain oscillations track the formation of episodic memories in the real world. *NeuroImage*, *143*, 256-266.

Griffiths, B. J., Martín-Buro, M. C., Staresina, B. P., Hanslmayr, S., & Staudigl, T. (2021). Alpha/beta power decreases during episodic memory formation predict the magnitude of alpha/beta power decreases during subsequent retrieval. *Neuropsychologia*, *153*, 107755. https://doi.org/https://doi.org/10.1016/j.neuropsychologia.2021.107755

Gruber, T., Tsivilis, D., Giabbiconi, C.-M., & Müller, M. M. (2008). Induced Electroencephalogram Oscillations during Source Memory: Familiarity is Reflected in the Gamma Band, Recollection in the Theta Band. *Journal of Cognitive Neuroscience*, *20*(6), 1043-1053.

Guderian, S., Schott, B. H., Richardson-Klavehn, A., & Düzel, E. (2009). Medial temporal theta state before an event predicts episodic encoding success in humans. *Proceedings of the National Academy of Sciences*, *106*(13), 5365-5370.

Gyurkovics, M., Clements, G. M., Low, K. A., Fabiani, M., & Gratton, G. (2021). The impact of 1/f activity and baseline correction on the results and interpretation of time-frequency analyses of EEG/MEG data: A cautionary tale. *NeuroImage*, *237*, 118192.

Haegens, S., Luther, L., & Jensen, O. (2012). Somatosensory Anticipatory Alpha Activity Increases to Suppress Distracting Input. *Journal of Cognitive Neuroscience*, *24*(3), 677-685.

Hafting, T., Fyhn, M., Molden, S., Moser, M.-B., & Moser, E. I. (2005). Microstructure of a spatial map in the entorhinal cortex. *Nature*, *436*(7052), 801-806.

Hamilton, D. A., Driscoll, I., & Sutherland, R. J. (2002). Human place learning in a virtual Morris water task: some important constraints on the flexibility of place navigation. *Behavioural Brain Research*, *129*(1-2), 159-170.

Händel, B. F., Haarmeier, T., & Jensen, O. (2011). Alpha Oscillations Correlate with the Successful Inhibition of Unattended Stimuli. *Journal of Cognitive Neuroscience*, *23*(9), 2494-2502.

Hanninen, T., Hallikainen, M., Koivisto, K., Partanen, K., Laakso, M., Riekkinen Sr, M., PhD, PJ, & Soininen, H. (1997). Decline of frontal lobe functions in subjects with age-associated memory impairment. *Neurology*, *48*(1), 148-153.

Hanslmayr, S., Spitzer, B., & Bäuml, K.-H. (2009). Brain oscillations dissociate between semantic and nonsemantic encoding of episodic memories. *Cerebral Cortex*, *19*(7), 1631-1640.

Hanslmayr, S., Staresina, B. P., & Bowman, H. (2016). Oscillations and Episodic Memory: Addressing the Synchronization/Desynchronization Conundrum. *Trends in Neurosciences*, *39*(1), 16-25. https://doi.org/10.1016/j.tins.2015.11.004

Hanslmayr, S., Staudigl, T., & Fellner, M.-C. (2012). Oscillatory power decreases and long-term memory: the information via desynchronization hypothesis. *Frontiers in Human Neuroscience*, *6*, 74.

Harris, A. M., Dux, P. E., Jones, C. N., & Mattingley, J. B. (2017). Distinct roles of theta and alpha oscillations in the involuntary capture of goal-directed attention. *NeuroImage*, *152*, 171-183.

Harty, S., Murphy, P. R., Robertson, I. H., & O'Connell, R. G. (2017). Parsing the neural signatures of reduced error detection in older age. *NeuroImage*, *161*, 43-55.

Harvey, D. R., Brant, L., & Commins, S. (2009). Differences in cue-dependent spatial navigation may be revealed by in-depth swimming analysis. *Behav Processes*, *82*(2), 190-197.

Hassabis, D., Kumaran, D., & Maguire, E. A. (2007). Using imagination to understand the neural basis of episodic memory. *Journal of Neuroscience*, *27*(52), 14365-14374.

Hassabis, D., & Maguire, E. A. (2009). The construction system of the brain. *Philos Trans R Soc Lond B Biol Sci*, *364*(1521), 1263-1271.

Hebscher, M., Meltzer, J. A., & Gilboa, A. (2019). A causal role for the precuneus in network-wide theta and gamma oscillatory activity during complex memory retrieval. *Elife*, *8*, e43114.

Hegarty, M., He, C., Boone, A. P., Yu, S., Jacobs, E. G., & Chrastil, E. R. (2023). Understanding differences in wayfinding strategies. *Topics in Cognitive Science*, *15*(1), 102-119.

Heimrath, K., Sandmann, P., Becke, A., Müller, N. G., & Zaehle, T. (2012). Behavioral and electrophysiological effects of transcranial direct current stimulation of the parietal cortex in a visuo-spatial working memory task. *Frontiers in psychiatry*, *3*, 56.

Herrmann, C. S., Munk, M. H., & Engel, A. K. (2004). Cognitive functions of gamma-band activity: memory match and utilization. *Trends in Cognitive Sciences*, *8*(8), 347-355.

Herrmann, C. S., Strüber, D., Helfrich, R. F., & Engel, A. K. (2016). EEG oscillations: from correlation to causality. *International Journal of Psychophysiology*, *103*, 12-21.

Herrmann, W., Fichte, K., & Freund, G. (1979). Reflections on the topics: EEG frequency bands and regulation of vigilance. *Pharmacopsychiatry*, *12*(02), 237-245.

Herweg, N., & Kahana, M. (2018). Spatial Representations in the Human Brain. *Frontiers in Human Neuroscience*, *12*, 297.

Herweg, N. A., Sharan, A. D., Sperling, M. R., Brandt, A., Schulze-Bonhage, A., & Kahana, M. J. (2020). Reactivated Spatial Context Guides Episodic Recall. *The Journal of Neuroscience*, *40*(10), 2119-2128.

Herweg, N. A., Solomon, E. A., & Kahana, M. J. (2020). Theta Oscillations in Human Memory. *Trends in Cognitive Sciences*, *24*(3), 208-227.

Hill, P. F., Bermudez, S., McAvan, A. S., Garren, J. D., Grilli, M. D., Barnes, C. A., & Ekstrom, A. D. (2023). Age differences in spatial memory are mitigated during naturalistic navigation. *bioRxiv*.

Hirshhorn, M., Grady, C., Rosenbaum, R. S., Winocur, G., & Moscovitch, M. (2012). The hippocampus is involved in mental navigation for a recently learned, but not a highly familiar environment: a longitudinal fMRI study. *Hippocampus*, *22*(4), 842-852.

Hölscher, C. (1999). Stress impairs performance in spatial water maze learning tasks. *Behavioural Brain Research*, *100*(1-2), 225-235.

Honkanen, R., Rouhinen, S., Wang, S. H., Palva, J. M., & Palva, S. (2015). Gamma oscillations underlie the maintenance of feature-specific information and the contents of visual working memory. *Cerebral Cortex*, *25*(10), 3788-3801.

Hori, S., Matsumoto, J., Hori, E., Kuwayama, N., Ono, T., Kuroda, S., & Nishijo, H. (2013). Alpha- and Theta-Range Cortical Synchronization and Corticomuscular Coherence During Joystick Manipulation in a Virtual Navigation Task. *Brain Topography*, *26*(4), 591-605.

Horner, A. J., Bisby, J. A., Zotow, E., Bush, D., & Burgess, N. (2016). Grid-like processing of imagined navigation. *Current Biology*, *26*(6), 842-847.

Horner, A. J., & Burgess, N. (2013). The associative structure of memory for multi-element events. *Journal of Experimental Psychology: General*, *142*(4), 1370.

Horner, A. J., Gadian, D. G., Fuentemilla, L., Jentschke, S., Vargha-Khadem, F., & Duzel, E. (2012). A rapid, hippocampus-dependent, item-memory signal that initiates context memory in humans. *Current Biology*, *22*(24), 2369-2374.

Howett, D., Castegnaro, A., Krzywicka, K., Hagman, J., Marchment, D., Henson, R., Rio, M., King, J. A., Burgess, N., & Chan, D. (2019). Differentiation of mild cognitive impairment using an entorhinal cortex-based test of virtual reality navigation. *Brain*, *142*(6), 1751-1766.

Hoy, K. E., Bailey, N., Michael, M., Fitzgibbon, B., Rogasch, N. C., Saeki, T., & Fitzgerald, P. B. (2016). Enhancement of working memory and task-related oscillatory activity following intermittent theta burst stimulation in healthy controls. *Cerebral Cortex*, *26*(12), 4563-4573.

Hsieh, L.-T., & Ranganath, C. (2014). Frontal midline theta oscillations during working memory maintenance and episodic encoding and retrieval. *NeuroImage*, *85*, 721-729.

Huang, J. (2019). Greater brain activity during the resting state and the control of activation during the performance of tasks. *Scientific Reports*, *9*(1), 5027.

Ilardi, C. R., Menichelli, A., Michelutti, M., Cattaruzza, T., & Manganotti, P. (2023). Optimal MoCA cutoffs for detecting biologically-defined patients with MCI and early dementia. *Neurological Sciences*, *44*(1), 159-170.

Inostroza, M., Cid, E., Brotons-Mas, J., Gal, B., Aivar, P., Uzcategui, Y. G., Sandi, C., & Menendez de la Prida, L. (2011). Hippocampal-dependent spatial memory in the water maze is preserved in an experimental model of temporal lobe epilepsy in rats. *PLOS ONE*, *6*(7), e22372.

Insel, N., Patron, L. A., Hoang, L. T., Nematollahi, S., Schimanski, L. A., Lipa, P., & Barnes, C. A. (2012). Reduced Gamma Frequency in the Medial Frontal Cortex of Aged Rats during Behavior and Rest: Implications for Age-Related Behavioral Slowing. *The Journal of Neuroscience*, *32*(46), 16331-16344.

Ishii, R., Canuet, L., Aoki, Y., Hata, M., Iwase, M., Ikeda, S., Nishida, K., & Ikeda, M. (2018). Healthy and Pathological Brain Aging: From the Perspective of Oscillations, Functional Connectivity, and Signal Complexity. *Neuropsychobiology*, *75*(4), 151-161.

Jabès, A., Klencklen, G., Ruggeri, P., Antonietti, J.-P., Banta Lavenex, P., & Lavenex, P. (2021). Age-related differences in resting-state EEG and allocentric spatial working memory performance. *Frontiers in Aging Neuroscience*.

Jacobs, J. (2014). Hippocampal theta oscillations are slower in humans than in rodents: implications for models of spatial navigation and memory. *Philosophical Transactions of the Royal Society B: Biological Sciences*, *369*(1635), 20130304.

Jacobs, J., Hwang, G., Curran, T., & Kahana, M. J. (2006). EEG oscillations and recognition memory: theta correlates of memory retrieval and decision making. *NeuroImage*, *32*(2), 978-987.

Jacobs, J., Korolev, I. O., Caplan, J. B., Ekstrom, A. D., Litt, B., Baltuch, G., Fried, I., Schulze-Bonhage, A., Madsen, J. R., & Kahana, M. J. (2010). Right-lateralized Brain Oscillations in Human Spatial Navigation. *Journal of Cognitive Neuroscience*, *22*(5), 824-836.

Jai, Y. Y., & Frank, L. M. (2015). Hippocampal–cortical interaction in decision making. *Neurobiology of Learning and Memory*, *117*, 34-41.

Jaiswal, N., Ray, W., & Slobounov, S. (2010). Encoding of visual–spatial information in working memory requires more cerebral efforts than retrieval: Evidence from an EEG and virtual reality study. *Brain research*, *1347*, 80-89.

James, T., Strunk, J., Arndt, J., & Duarte, A. (2016). Age-related deficits in selective attention during encoding increase demands on episodic reconstruction during context retrieval: An ERP study. *Neuropsychologia*, *86*, 66-79.

Jankowski, M. M., & O'Mara, S. M. (2015). Dynamics of place, boundary and object encoding in rat anterior claustrum. *Frontiers in Behavioral Neuroscience*, *9*, 250.

Jaušovec, N., & Jaušovec, K. (2010). Resting brain activity: Differences between genders. *Neuropsychologia*, *48*(13), 3918-3925.

Jensen, O., Bonnefond, M., & VanRullen, R. (2012). An oscillatory mechanism for prioritizing salient unattended stimuli. *Trends in Cognitive Sciences*, *16*(4), 200-206.

Jensen, O., Goel, P., Kopell, N., Pohja, M., Hari, R., & Ermentrout, B. (2005). On the human sensorimotor-cortex beta rhythm: sources and modeling. *NeuroImage*, *26*(2), 347-355.

Jensen, O., & Lisman, J. E. (1996). Hippocampal CA3 region predicts memory sequences: accounting for the phase precession of place cells. *Learning and Memory-Plainview*, *3*(2), 279.

Jensen, O., & Tesche, C. D. (2002). Frontal theta activity in humans increases with memory load in a working memory task. *European Journal of Neuroscience*, *15*(8), 1395-1399.

Jeong, J. (2004). EEG dynamics in patients with Alzheimer's disease. *Clinical Neurophysiology*, *115*(7), 1490-1505.

Ji, D., & Wilson, M. A. (2007). Coordinated memory replay in the visual cortex and hippocampus during sleep. *Nature Neuroscience*, *10*(1), 100-107.

Jia, X., Wang, Z., Huang, F., Su, C., Du, W., Jiang, H., Wang, H., Wang, J., Wang, F., & Su, W. (2021). A comparison of the Mini-Mental State Examination (MMSE) with the Montreal Cognitive Assessment (MoCA) for mild cognitive impairment screening in Chinese middle-aged and older population: a cross-sectional study. *BMC psychiatry*, *21*(1), 1-13.

Jones, M. W., & Wilson, M. A. (2005). Theta Rhythms Coordinate Hippocampal–Prefrontal Interactions in a Spatial Memory Task. *PLOS Biology*, *3*(12), e402.

Joo, H. R., & Frank, L. M. (2018). The hippocampal sharp wave–ripple in memory retrieval for immediate use and consolidation. *Nature Reviews Neuroscience*, *19*(12), 744-757.

Jost, K., Bryck, R. L., Vogel, E. K., & Mayr, U. (2011). Are old adults just like low working memory young adults? Filtering efficiency and age differences in visual working memory. *Cerebral Cortex*, *21*(5), 1147-1154.

Julayanont, P., & Nasreddine, Z. S. (2017). Montreal Cognitive Assessment (MoCA): concept and clinical review. *Cognitive screening instruments: A practical approach*, 139-195.

Jung, R., & Kornmüller, A. E. (1938). Eine Methodik der Ableitung Iokalisierter Potentialschwankungen aus subcorticalen Hirngebieten [Article]. *Archiv für Psychiatrie und Nervenkrankheiten*, *109*(1), 1-30.

Jungnickel, E., Gehrke, L., Klug, M., & Gramann, K. (2019). Chapter 10 - MoBI—Mobile Brain/Body Imaging. In H. Ayaz & F. Dehais (Eds.), *Neuroergonomics* (pp. 59-63). Academic Press.

Kahana, M. J., Seelig, D., & Madsen, J. R. (2001). Theta returns. *Current Opinion in Neurobiology*, *11*(6), 739-744.

Kahana, M. J., Sekuler, R., Caplan, J. B., Kirschen, M., & Madsen, J. R. (1999). Human theta oscillations exhibit task dependence during virtual maze navigation. *Nature*, *399*(6738), 781-784.

Kam, J. W. Y., Rahnuma, T., Park, Y. E., & Hart, C. M. (2022). Electrophysiological markers of mind wandering: A systematic review. *NeuroImage*, *258*, 119372.

Kane, J., Cavanagh, J. F., & Dillon, D. G. (2019). Reduced Theta Power During Memory Retrieval in Depressed Adults. *Biol Psychiatry Cogn Neurosci Neuroimaging*, *4*(7), 636-643.

Kaplan, R., Bush, D., Bonnefond, M., Bandettini, P. A., Barnes, G. R., Doeller, C. F., & Burgess, N. (2014). Medial prefrontal theta phase coupling during spatial memory retrieval. *Hippocampus*, *24*(6), 656-665.

Kaplan, R., Doeller, C. F., Barnes, G. R., Litvak, V., Düzel, E., Bandettini, P. A., & Burgess, N. (2012). Movement-related theta rhythm in humans: coordinating self-directed hippocampal learning. *PLOS Biology*, *10*(2), e1001267.

Kardos, Z., Tóth, B., Boha, R., File, B., & Molnár, M. (2014). Age-related changes of frontal-midline theta is predictive of efficient memory maintenance. *Neuroscience*, *273*, 152-162.

Karlsson, A. E., Lindenberger, U., & Sander, M. C. (2022). Out of Rhythm: Compromised Precision of Theta-Gamma Coupling Impairs Associative Memory in Old Age. *The Journal of Neuroscience*, *42*(9), 1752-1764.

Keay, L., Coxon, K., Chevalier, A., Brown, J., Rogers, K., Clarke, E., & Ivers, R. Q. (2018). Sex differences evident in self-reported but not objective measures of driving. *Accident Analysis & Prevention*, *111*, 155-160.

Keizer, A. W., Verment, R. S., & Hommel, B. (2010). Enhancing cognitive control through neurofeedback: A role of gamma-band activity in managing episodic retrieval. *NeuroImage*, *49*(4), 3404-3413.

Kelly, D. M., & Gibson, B. M. (2007). Spatial navigation: Spatial learning in real and virtual environments. *Comparative Cognition & Behavior Reviews*, *2*.

Kennedy, J. P., Zhou, Y., Qin, Y., Lovett, S. D., Sheremet, A., Burke, S., & Maurer, A. (2022). A direct comparison of theta power and frequency to speed and acceleration. *Journal of Neuroscience*, *42*(21), 4326-4341.

Kentros, C. G., Agnihotri, N. T., Streater, S., Hawkins, R. D., & Kandel, E. R. (2004). Increased attention to spatial context increases both place field stability and spatial memory. *Neuron*, *42*(2), 283-295.

Kerrén, C., Linde-Domingo, J., Hanslmayr, S., & Wimber, M. (2018). An Optimal Oscillatory Phase for Pattern Reactivation during Memory Retrieval. *Curr Biol*, *28*(21), 3383-3392.e3386.

Ketz, N., O'Reilly, R. C., & Curran, T. (2014). Classification aided analysis of oscillatory signatures in controlled retrieval. *NeuroImage*, *85*, 749-760.

Khader, P. H., Jost, K., Ranganath, C., & Rösler, F. (2010). Theta and alpha oscillations during working-memory maintenance predict successful long-term memory encoding. *Neuroscience Letters*, *468*(3), 339-343.

Kilavik, B. E., Zaepffel, M., Brovelli, A., MacKay, W. A., & Riehle, A. (2013). The ups and downs of beta oscillations in sensorimotor cortex. *Experimental neurology*, *245*, 15-26.

Kim, M., & Maguire, E. A. (2019). Encoding of 3D head direction information in the human brain. *Hippocampus*, *29*(7), 619-629.

Kim, O., Pang, Y., & Kim, J.-H. (2019). The effectiveness of virtual reality for people with mild cognitive impairment or dementia: a meta-analysis. *BMC psychiatry*, *19*(1), 1-10.

Kim, S., Sapiurka, M., Clark, R. E., & Squire, L. R. (2013). Contrasting effects on path integration after hippocampal damage in humans and rats. *Proceedings of the National Academy of Sciences*, *110*(12), 4732-4737.

Kimura, D. (1996). Sex, sexual orientation and sex hormones influence human cognitive function. *Current Opinion in Neurobiology*, *6*(2), 259-263.

Kimura, K., Reichert, J. F., Olson, A., Pouya, O. R., Wang, X., Moussavi, Z., & Kelly, D. M. (2017). Orientation in virtual reality does not fully measure up to the real-world. *Scientific reports*, *7*(1), 18109.

Klencklen, G., Després, O., & Dufour, A. (2012). What do we know about aging and spatial cognition? Reviews and perspectives. *Ageing research reviews*, *11*(1), 123-135.

Klimesch, W. (1999). EEG alpha and theta oscillations reflect cognitive and memory performance: a review and analysis. *Brain Research Reviews*, *29*(2-3), 169-195.

Klimesch, W. (2012). Alpha-band oscillations, attention, and controlled access to stored information. *Trends in Cognitive Sciences*, *16*(12), 606-617.

Klimesch, W., Doppelmayr, M., Russegger, H., Pachinger, T., & Schwaiger, J. (1998). Induced alpha band power changes in the human EEG and attention. *Neuroscience Letters*, *244*(2), 73-76.

Klimesch, W., Doppelmayr, M., Schimke, H., & Ripper, B. (1997). Theta synchronization and alpha desynchronization in a memory task. *Psychophysiology*, *34*(2), 169-176.

Klimesch, W., Sauseng, P., & Hanslmayr, S. (2007). EEG alpha oscillations: the inhibition–timing hypothesis. *Brain Research Reviews*, *53*(1), 63-88.

Kline, J. E., Poggensee, K., & Ferris, D. P. (2014). Your brain on speed: cognitive performance of a spatial working memory task is not affected by walking speed. *Frontiers in Human Neuroscience*, *8*, 288.

Klinzing, J. G., Niethard, N., & Born, J. (2019). Mechanisms of systems memory consolidation during sleep. *Nature Neuroscience*, *22*(10), 1598-1610.

Knott, V., Mohr, E., Mahoney, C., & Ilivitsky, V. (2000). Electroencephalographic coherence in Alzheimer's disease: comparisons with a control group and population norms. *Journal of geriatric psychiatry and neurology*, *13*(1), 1-8.

Kober, S. E., & Neuper, C. (2011). Sex differences in human EEG theta oscillations during spatial navigation in virtual reality. *International Journal of Psychophysiology*, *79*(3), 347-355.

Kober, S. E., Reichert, J. L., Neuper, C., & Wood, G. (2016). Interactive effects of age and gender on EEG power and coherence during a short-term memory task in middle-aged adults. *Neurobiology of aging*, *40*, 127-137.

Kock, R., Ceolini, E., Groenewegen, L., & Ghosh, A. (2023). Neural processing of goal and non-goal-directed movements on the smartphone. *Neuroimage: Reports*, *3*(2), 100164.

Kolarik, B. S., Shahlaie, K., Hassan, A., Borders, A. A., Kaufman, K. C., Gurkoff, G., Yonelinas, A. P., & Ekstrom, A. D. (2016). Impairments in precision, rather than spatial strategy, characterize performance on the virtual Morris Water Maze: A case study. *Neuropsychologia*, *80*, 90-101.

Kolb, B., & Cioe, J. (1996). Sex-related differences in cortical function after medial frontal lesions in rats. *Behavioral Neuroscience*, *110*(6), 1271.

Konishi, K., Mckenzie, S., Etchamendy, N., Roy, S., & Bohbot, V. D. (2017). Hippocampus-dependent spatial learning is associated with higher global cognition among healthy older adults. *Neuropsychologia*, *106*, 310-321.

Korthauer, L. E., Nowak, N. T., Moffat, S. D., An, Y., Rowland, L. M., Barker, P. B., Resnick, S. M., & Driscoll, I. (2016). Correlates of virtual navigation performance in older adults. *Neurobiology of aging*, *39*, 118-127.

Köster, M., Friese, U., Schöne, B., Trujillo-Barreto, N., & Gruber, T. (2014). Theta–gamma coupling during episodic retrieval in the human EEG. *Brain research*, *1577*, 57-68.

Kota, S., Rugg, M. D., & Lega, B. C. (2020). Hippocampal Theta Oscillations Support Successful Associative Memory Formation. *J Neurosci*, *40*(49), 9507-9518.

Kropff, E., Carmichael, J. E., Moser, E. I., & Moser, M.-B. (2021). Frequency of theta rhythm is controlled by acceleration, but not speed, in running rats. *Neuron*, *109*(6), 1029-1039. e1028.

Kumar, J. S., & Bhuvaneswari, P. (2012). Analysis of Electroencephalography (EEG) Signals and Its Categorization–A Study. *Procedia Engineering*, *38*, 2525-2536.

Kunz, L., Brandt, A., Reinacher, P. C., Staresina, B. P., Reifenstein, E. T., Weidemann, C. T., Herweg, N. A., Patel, A., Tsitsiklis, M., & Kempter, R. (2021). A neural code for egocentric spatial maps in the human medial temporal lobe. *Neuron*, *109*(17), 2781-2796. e2710.

Kunz, L., Wang, L., Lachner-Piza, D., Zhang, H., Brandt, A., Dümpelmann, M., Reinacher, P. C., Coenen, V. A., Chen, D., & Wang, W.-X. (2019). Hippocampal theta phases organize the reactivation of large-scale electrophysiological representations during goal-directed navigation. *Science advances*, *5*(7), eaav8192.

Ladouce, S., Donaldson, D. I., Dudchenko, P. A., & Ietswaart, M. (2017). Understanding minds in real-world environments: toward a mobile cognition approach. *Frontiers in Human Neuroscience*, *10*, 694.

Lambe, S., Knight, I., Kabir, T., West, J., Patel, R., Lister, R., Rosebrock, L., Rovira, A., Garnish, B., & Freeman, J. (2020). Developing an automated VR cognitive treatment for psychosis: gameChange VR therapy. *Journal of Behavioral and Cognitive Therapy*, *30*(1), 33-40.

Lang, M., Colby, S., Ashby-Padial, C., Bapna, M., Jaimes, C., Rincon, S. P., & Buch, K. (2024). An imaging review of the hippocampus and its common pathologies. *Journal of Neuroimaging*, *34*(1), 5-25.

Laptinskaya, D., Fissler, P., Küster, O. C., Wischniowski, J., Thurm, F., Elbert, T., von Arnim, C. A. F., & Kolassa, I.-T. (2020). Global EEG coherence as a marker for cognition in older adults at risk for dementia. *Psychophysiology*, *57*(4), e13515.

Larson, M. J., & Carbine, K. A. (2017). Sample size calculations in human electrophysiology (EEG and ERP) studies: A systematic review and recommendations for increased rigor. *International Journal of Psychophysiology*, *111*, 33-41.

Laszlo, S., Ruiz-Blondet, M., Khalifian, N., Chu, F., & Jin, Z. (2014). A direct comparison of active and passive amplification electrodes in the same amplifier system. *Journal of Neuroscience Methods*, *235*, 298-307.

Lega, B. C., Jacobs, J., & Kahana, M. (2012). Human hippocampal theta oscillations and the formation of episodic memories. *Hippocampus*, *22*(4), 748-761.

Lester, A. W., Moffat, S. D., Wiener, J. M., Barnes, C. A., & Wolbers, T. (2017). The aging navigational system. *Neuron*, *95*(5), 1019-1035.

Lever, C., Burton, S., Jeewajee, A., O'Keefe, J., & Burgess, N. (2009). Boundary vector cells in the subiculum of the hippocampal formation. *Journal of Neuroscience*, *29*(31), 9771-9777.

Li, D., Zhao, C., Guo, J., Kong, Y., Li, H., Du, B., Ding, Y., & Song, Y. (2021). Visual Working Memory Guides Spatial Attention: Evidence from alpha oscillations and sustained potentials. *Neuropsychologia*, *151*, 107719.

Li, Z., Zhang, L., Zhang, F., Gu, R., Peng, W., & Hu, L. (2020). Demystifying signal processing techniques to extract resting-state EEG features for psychologists. *Brain Science Advances*, *6*(3), 189-209.

Liang, M., Starrett, M. J., & Ekstrom, A. D. (2018). Dissociation of frontal-midline delta-theta and posterior alpha oscillations: A mobile EEG study. *Psychophysiology*, *55*(9), e13090.

Liang, M., Zheng, J., Isham, E., & Ekstrom, A. (2021). Common and Distinct Roles of Frontal Midline Theta and Occipital Alpha Oscillations in Coding Temporal Intervals and Spatial Distances. *Journal of Cognitive Neuroscience*, *33*(11), 2311-2327.

Lifanov, J., Linde-Domingo, J., & Wimber, M. (2021). Feature-specific reaction times reveal a semanticisation of memories over time and with repeated remembering. *Nature Communications*, *12*(1), 3177.

Light, G. A., Williams, L. E., Minow, F., Sprock, J., Rissling, A., Sharp, R., Swerdlow, N. R., & Braff, D. L. (2010). Electroencephalography (EEG) and event-related potentials (ERPs) with human participants. *Curr Protoc Neurosci*, *Chapter 6*, Unit 6.25.21-24.

Lin, C. T., Chiu, T. C., & Gramann, K. (2015). EEG correlates of spatial orientation in the human retrosplenial complex. *NeuroImage*, *120*, 123-132.

Lin, J. J., Rugg, M. D., Das, S., Stein, J., Rizzuto, D. S., Kahana, M. J., & Lega, B. C. (2017). Theta band power increases in the posterior hippocampus predict successful episodic memory encoding in humans. *Hippocampus*, *27*(10), 1040-1053.

Lin, M.-H., Liran, O., Bauer, N., & Baker, T. E. (2022). Scalp recorded theta activity is modulated by reward, direction, and speed during virtual navigation in freely moving humans. *Scientific Reports*, *12*(1), 2041.

Lin, Y., Shu, I.-W., & Singh, F. (2023). Frontal gamma as a marker of effective training during neurofeedback to improve memory in patients with mild cognitive impairment. 2023 11th International IEEE/EMBS Conference on Neural Engineering (NER),

Lisman, J. E., & Jensen, O. (2013). The theta-gamma neural code. *Neuron*, *77*(6), 1002-1016.

Lissner, L. J., Wartchow, K. M., Toniazzo, A. P., Gonçalves, C.-A., & Rodrigues, L. (2021). Object recognition and Morris water maze to detect cognitive impairment from mild hippocampal damage in rats: A reflection based on the literature and experience. *Pharmacology Biochemistry and Behavior*, *210*, 173273.

Lithfous, S., Dufour, A., Bouix, C., Pebayle, T., & Després, O. (2018). Reduced parahippocampal theta activity during spatial navigation in low, but not in high elderly performers. *Neuropsychology*, *32*(1), 40.

Lithfous, S., Dufour, A., & Després, O. (2013). Spatial navigation in normal aging and the prodromal stage of Alzheimer's disease: Insights from imaging and behavioral studies. *Ageing research reviews*, *12*(1), 201-213.

Lithfous, S., Tromp, D., Dufour, A., Pebayle, T., Goutagny, R., & Després, O. (2015). Decreased theta power at encoding and cognitive mapping deficits in elderly individuals during a spatial memory task. *Neurobiol Aging*, *36*(10), 2821-2829.

Liu, J., Singh, A. K., Wunderlich, A., Gramann, K., & Lin, C.-T. (2022). Redesigning navigational aids using virtual global landmarks to improve spatial knowledge retrieval. *npj Science of Learning*, *7*(1), 17.

Logothetis, N. K. (2008). What we can do and what we cannot do with fMRI. *Nature*, *453*(7197), 869-878.

Lopez, A., O. Caffò, A., Spano, G., & Bosco, A. (2019). The Effect of Aging on Memory for Recent and Remote Egocentric and Allocentric Information. *Experimental Aging Research*, *45*(1), 57-73.

Luck, S. J., & Gaspelin, N. (2017). How to get statistically significant effects in any ERP experiment (and why you shouldn't). *Psychophysiology*, *54*(1), 146-157.

Lugo, F., Torres, M. N., & Chamizo, V. (2018). Two strategies used to solve a navigation task: A different use of the hippocampus by males and females? A preliminary study in rats. *Psicológica*, *39*(2), 319-339.

Luna, D., & Martínez, H. (2015). Spontaneous recovery of human spatial memory in a virtual water maze. *Psicologica: International Journal of Methodology and Experimental Psychology*, *36*(2), 283-308.

Lundqvist, M., Rose, J., Herman, P., Brincat, S. L., Buschman, T. J., & Miller, E. K. (2016). Gamma and beta bursts underlie working memory. *Neuron*, *90*(1), 152-164.

Lynn, P. A., & Sponheim, S. R. (2016). Disturbed theta and gamma coupling as a potential mechanism for visuospatial working memory dysfunction in people with schizophrenia. *Neuropsychiatric Electrophysiology*, *2*, 1-30.

Maei, H., Zaslavsky, K., Teixeira, C., & Frankland, P. (2009). What is the most sensitive measure of water maze probe test performance? [Original Research]. *Frontiers in Integrative Neuroscience*, *3*.

Maguire, E. A., Frackowiak, R. S., & Frith, C. D. (1997). Recalling routes around London: activation of the right hippocampus in taxi drivers. *Journal of Neuroscience*, *17*(18), 7103-7110.

Maguire, E. A., Gadian, D. G., Johnsrude, I. S., Good, C. D., Ashburner, J., Frackowiak, R. S. J., & Frith, C. D. (2000). Navigation-related structural change in the hippocampi of taxi drivers. *Proceedings of the National Academy of Sciences*, *97*(8), 4398-4403.

Maguire, E. A., Nannery, R., & Spiers, H. J. (2006). Navigation around London by a taxi driver with bilateral hippocampal lesions. *Brain*, *129*(11), 2894-2907.

Maguire, E. A., Spiers, H. J., Good, C. D., Hartley, T., Frackowiak, R. S. J., & Burgess, N. (2003). Navigation expertise and the human hippocampus: a structural brain imaging analysis. *Hippocampus*, *13*(2), 250-259.

Mainy, N., Kahane, P., Minotti, L., Hoffmann, D., Bertrand, O., & Lachaux, J. P. (2007). Neural correlates of consolidation in working memory. *Human brain mapping*, *28*(3), 183-193.

Mamashli, F., Hämäläinen, M., Ahveninen, J., Kenet, T., & Khan, S. (2019). Permutation Statistics for Connectivity Analysis between Regions of Interest in EEG and MEG Data. *Scientific Reports*, *9*(1), 7942.

Mao, D. (2023). Neural Correlates of Spatial Navigation in Primate Hippocampus. *Neuroscience Bulletin*, *39*(2), 315-327.

Marr, D., Willshaw, D., & McNaughton, B. (1991). *Simple memory: a theory for archicortex*. Springer.

Marshall, A. C., Cooper, N., Rosu, L., & Kennett, S. (2018). Stress-related deficits of older adults' spatial working memory: an EEG investigation of occipital alpha and frontal-midline theta activities. *Neurobiology of aging*, *69*, 239-248.

Mathewson, K. E., Basak, C., Maclin, E. L., Low, K. A., Boot, W. R., Kramer, A. F., Fabiani, M., & Gratton, G. (2012). Different slopes for different folks: alpha and delta EEG power predict subsequent video game learning rate and improvements in cognitive control tasks. *Psychophysiology*, *49*(12), 1558-1570.

Mathewson, K. E., Harrison, T. J., & Kizuk, S. A. (2017). High and dry? Comparing active dry EEG electrodes to active and passive wet electrodes. *Psychophysiology*, *54*(1), 74-82.

Maurer, U., Brem, S., Liechti, M., Maurizio, S., Michels, L., & Brandeis, D. (2015). Frontal midline theta reflects individual task performance in a working memory task. *Brain Topography*, *28*, 127-134.

McCormick, C., Barry, D. N., Jafarian, A., Barnes, G. R., & Maguire, E. A. (2020). vmPFC drives hippocampal processing during autobiographical memory recall regardless of remoteness. *Cerebral Cortex*, *30*(11), 5972-5987.

McCormick, C., Ciaramelli, E., De Luca, F., & Maguire, E. A. (2018). Comparing and contrasting the cognitive effects of hippocampal and ventromedial prefrontal cortex damage: a review of human lesion studies. *Neuroscience*, *374*, 295-318.

McCormick, C., Rosenthal, C. R., Miller, T. D., & Maguire, E. A. (2017). Deciding what is possible and impossible following hippocampal damage in humans. *Hippocampus*, *27*(3), 303-314.

McFarland, D. J., McCane, L. M., David, S. V., & Wolpaw, J. R. (1997). Spatial filter selection for EEG-based communication. *Electroencephalography and clinical Neurophysiology*, *103*(3), 386-394.

McGee, J. S., van der Zaag, C., Buckwalter, J. G., Thiébaux, M., Van Rooyen, A., Neumann, U., Sisemore, D., & Rizzo, A. A. (2000). Issues for the assessment of visuospatial skills in older adults using virtual environment technology. *Cyberpsychology & Behavior*, *3*(3), 469-482.

McLaren, I., & Mackintosh, N. (2002). Associative learning and elemental representation: II. Generalization and discrimination. *Animal learning & behavior*, *30*, 177-200.

Medendorp, W. P., Kramer, G. F. I., Jensen, O., Oostenveld, R., Schoffelen, J.-M., & Fries, P. (2007). Oscillatory activity in human parietal and occipital cortex shows hemispheric lateralization and memory effects in a delayed double-step saccade task. *Cerebral Cortex*, *17*(10), 2364-2374.

Meltzer, J. A., Fonzo, G. A., & Constable, R. T. (2009). Transverse patterning dissociates human EEG theta power and hippocampal BOLD activation. *Psychophysiology*, *46*(1), 153-162.

Menzel, R., Greggers, U., Smith, A., Berger, S., Brandt, R., Brunke, S., Bundrock, G., Hülse, S., Plümpe, T., & Schaupp, F. (2005). Honey bees navigate according to a map-like spatial memory. *Proceedings of the National Academy of Sciences*, *102*(8), 3040-3045.

Michel, C. M., & Brunet, D. (2019). EEG Source Imaging: A Practical Review of the Analysis Steps [Review]. *Frontiers in Neurology*, *10*.

Michelmann, S., Bowman, H., & Hanslmayr, S. (2018). Replay of stimulus-specific temporal patterns during associative memory formation. *Journal of Cognitive Neuroscience*, *30*(11), 1577-1589.

Miller, J., Watrous, A. J., Tsitsiklis, M., Lee, S. A., Sheth, S. A., Schevon, C. A., Smith, E. H., Sperling, M. R., Sharan, A., & Asadi-Pooya, A. A. (2018). Lateralized hippocampal oscillations underlie distinct aspects of human spatial memory and navigation. *Nature Communications*, *9*(1), 1-12.

Miller, J. F., Neufang, M., Solway, A., Brandt, A., Trippel, M., Mader, I., Hefft, S., Merkow, M., Polyn, S. M., & Jacobs, J. (2013). Neural activity in human hippocampal formation reveals the spatial context of retrieved memories. *Science*, *342*(6162), 1111-1114.

Miller, T. D., Chong, T. T., Aimola Davies, A. M., Johnson, M. R., Irani, S. R., Husain, M., Ng, T. W., Jacob, S., Maddison, P., & Kennard, C. (2020). Human hippocampal CA3 damage disrupts both recent and remote episodic memories. *Elife*, *9*, e41836.

Missonnier, P., Herrmann, F. R., Rodriguez, C., Deiber, M.-P., Millet, P., Fazio-costa, L., Gold, G., & Giannakopoulos, P. (2011). Age-related differences on event-related potentials and brain rhythm oscillations during working memory activation. *Journal of Neural Transmission*, *118*, 945-955.

Mitchell, D. J., McNaughton, N., Flanagan, D., & Kirk, I. J. (2008). Frontal-midline theta from the perspective of hippocampal "theta". *Progress in Neurobiology*, *86*(3), 156-185.

Miyakoshi, M., Gehrke, L., Gramann, K., Makeig, S., & Iversen, J. (2021). The AudioMaze: An EEG and motion capture study of human spatial navigation in sparse augmented reality. *European Journal of Neuroscience*, *54*(12), 8283-8307.

Moffat, S. D. (2009). Aging and spatial navigation: what do we know and where do we go? *Neuropsychology review*, *19*, 478-489.

Moffat, S. D., Elkins, W., & Resnick, S. M. (2006). Age differences in the neural systems supporting human allocentric spatial navigation. *Neurobiology of aging*, *27*(7), 965-972.

Moffat, S. D., & Resnick, S. M. (2002). Effects of age on virtual environment place navigation and allocentric cognitive mapping. *Behavioral Neuroscience*, *116*(5), 851.

Moffat, S. D., Zonderman, A. B., & Resnick, S. M. (2001). Age differences in spatial memory in a virtual environment navigation task. *Neurobiology of aging*, *22*(5), 787-796.

Montirosso, R., Piazza, C., Giusti, L., Provenzi, L., Ferrari, P. F., Reni, G., & Borgatti, R. (2019). Exploring the EEG mu rhythm associated with observation and execution of a goal-directed action in 14-month-old preterm infants. *Scientific Reports*, *9*(1), 8975.

Morales, S., & Bowers, M. E. (2022). Time-frequency analysis methods and their application in developmental EEG data. *Developmental Cognitive Neuroscience*, *54*, 101067.

Moretti, D. V., Babiloni, C., Binetti, G., Cassetta, E., Dal Forno, G., Ferreric, F., Ferri, R., Lanuzza, B., Miniussi, C., Nobili, F., Rodriguez, G., Salinari, S., & Rossini, P. M. (2004). Individual analysis of EEG frequency and band power in mild Alzheimer's disease. *Clinical Neurophysiology*, *115*(2), 299-308.

Morgan, L. K., MacEvoy, S. P., Aguirre, G. K., & Epstein, R. A. (2011). Distances between real-world locations are represented in the human hippocampus. *Journal of Neuroscience*, *31*(4), 1238-1245.

Morris, Garrud, P., Rawlins, J. N. P., & O'Keefe, J. (1982). Place navigation impaired in rats with hippocampal lesions. *Nature*, *297*(5868), 681-683.

Morris, R. (1984). Developments of a water-maze procedure for studying spatial learning in the rat [Article]. *Journal of Neuroscience Methods*, *11*(1), 47-60.

Morris, R. G. M. (1981). Spatial localization does not require the presence of local cues. *Learning and Motivation*, *12*(2), 239-260.

Morrow, A., Elias, M., & Samaha, J. (2023). Evaluating the Evidence for the Functional Inhibition Account of Alpha-band Oscillations during Preparatory Attention. *Journal of Cognitive Neuroscience*, *35*(8), 1195-1211.

Moscovitch, M., Nadel, L., Winocur, G., Gilboa, A., & Rosenbaum, R. S. (2006). The cognitive neuroscience of remote episodic, semantic and spatial memory. *Current Opinion in Neurobiology*, *16*(2), 179-190.

Moser, E. I., Kropff, E., & Moser, M.-B. (2008). Place cells, grid cells, and the brain's spatial representation system. *Annual review of neuroscience*, *31*(1), 69-89.

Moser, E. I., Moser, M.-B., & McNaughton, B. L. (2017). Spatial representation in the hippocampal formation: a history. *Nature Neuroscience*, *20*(11), 1448-1464.

Muela, P., Cintado, E., Tezanos, P., Fernández-García, B., Tomás-Zapico, C., Iglesias-Gutiérrez, E., Díaz Martínez, A. E., Butler, R. G., Cuadrado-Peñafiel, V., & De la Vega, R. (2022). A Multiple-Choice Maze-like Spatial Navigation Task for Humans Implemented in a Real-Space, Multipurpose Circular Arena. *Applied Sciences*, *12*(19), 9707.

Mueller, S. C., Jackson, C. P. T., & Skelton, R. W. (2008). Sex differences in a virtual water maze: An eye tracking and pupillometry study. *Behavioural Brain Research*, *193*(2), 209-215.

Muessig, L., Hauser, J., Wills, T., & Cacucci, F. (2016). Place cell networks in pre-weanling rats show associative memory properties from the onset of exploratory behavior. *Cerebral Cortex*, *26*(8), 3627-3636.

Muller, R. U., Kubie, J. L., & Ranck, J. B. (1987). Spatial firing patterns of hippocampal complex-spike cells in a fixed environment. *Journal of Neuroscience*, *7*(7), 1935-1950.

Murias, K., Kwok, K., Castillejo, A. G., Liu, I., & Iaria, G. (2016). The effects of video game use on performance in a virtual navigation task. *Computers in Human Behavior*, *58*, 398-406.

Musaeus, C. S., Engedal, K., Høgh, P., Jelic, V., Mørup, M., Naik, M., Oeksengaard, A. R., Snaedal, J., Wahlund, L. O., Waldemar, G., & Andersen, B. B. (2018). EEG Theta Power Is an Early Marker of Cognitive Decline in Dementia due to Alzheimer's Disease. *J Alzheimers Dis*, *64*(4), 1359-1371.

Mussel, P., Ulrich, N., Allen, J. J. B., Osinsky, R., & Hewig, J. (2016). Patterns of theta oscillation reflect the neural basis of individual differences in epistemic motivation. *Scientific Reports*, *6*(1), 29245.

Nadel, L., & Moscovitch, M. (1997). Memory consolidation, retrograde amnesia and the hippocampal complex. *Current Opinion in Neurobiology*, *7*(2), 217-227.

Nadel, L., Samsonovich, A., Ryan, L., & Moscovitch, M. (2000). Multiple trace theory of human memory: computational, neuroimaging, and neuropsychological results. *Hippocampus*, *10*(4), 352-368.

Nagelhus, A., Andersson, S. O., Cogno, S. G., Moser, E. I., & Moser, M.-B. (2023). Object-centered population coding in CA1 of the hippocampus. *Neuron*.

Nasreddine, Z. S., Phillips, N. A., Bédirian, V., Charbonneau, S., Whitehead, V., Collin, I., Cummings, J. L., & Chertkow, H. (2005). The Montreal Cognitive Assessment, MoCA: a brief screening tool for mild cognitive impairment. *Journal of the American Geriatrics Society*, *53*(4), 695-699.

Nelson, H. E., & Willison, J. (1991). *National adult reading test (NART)*. Nfer-Nelson Windsor.

Newhouse, P., Newhouse, C., & Astur, R. S. (2007). Sex differences in visual-spatial learning using a virtual water maze in pre-pubertal children. *Behavioural Brain Research*, *183*(1), 1-7.

Newson, J. J., & Thiagarajan, T. C. (2019). EEG Frequency Bands in Psychiatric Disorders: A Review of Resting State Studies [Review]. *Frontiers in Human Neuroscience*, *12*.

Nguyen, L. T., Marini, F., Shende, S. A., Llano, D. A., & Mudar, R. A. (2020). Investigating EEG theta and alpha oscillations as measures of value-directed strategic processing in cognitively normal younger and older adults. *Behavioural Brain Research*, *391*, 112702.

Nicolás, B., Wu, X., García-Arch, J., Dimiccoli, M., Sierpowska, J., Saiz-Masvidal, C., Soriano-Mas, C., Radeva, P., & Fuentemilla, L. (2021). Behavioural and neurophysiological signatures in the retrieval of individual memories of recent and remote real-life routine episodic events. *Cortex*, *141*, 128-143.

Nishiyama, N., Mizuhara, H., Miwakeichi, F., & Yamaguchi, Y. (2002). Theta episodes observed in human scalp EEG during virtual navigation-spatial distribution and task dependence. Proceedings of the 9th International Conference on Neural Information Processing, 2002. ICONIP'02.,

Noachtar, I., Harris, T.-A., Hidalgo-Lopez, E., & Pletzer, B. (2022). Sex and strategy effects on brain activation during a 3D-navigation task. *Communications Biology*, *5*(1), 234.

Nori, R., Grandicelli, S., & Giusberti, F. (2009). Individual differences in visuo-spatial working memory and real-world wayfinding. *Swiss Journal of Psychology/Schweizerische Zeitschrift für Psychologie/Revue Suisse de Psychologie*, *68*(1), 7.

Nunez, J. (2008). Morris Water Maze Experiment. *Journal of visualized experiments : JoVE*(19), 897.

Nyberg, N., Duvelle, É., Barry, C., & Spiers, H. J. (2022). Spatial goal coding in the hippocampal formation. *Neuron*.

Nyhus, E., & Curran, T. (2010). Functional role of gamma and theta oscillations in episodic memory. *Neuroscience & Biobehavioral Reviews*, *34*(7), 1023-1035.

O'Keefe, J. (1993). Hippocampus, theta, and spatial memory. *Current Opinion in Neurobiology*, *3*(6), 917-924.

O'Keefe, J., & Dostrovsky, J. (1971). The hippocampus as a spatial map: preliminary evidence from unit activity in the freely-moving rat. *Brain research*.

O'Keefe, J., & Nadel, L. (1978). *The hippocampus as a cognitive map*. Clarendon Press Oxford.

O'Keefe, J., Nadel, L., Keightley, S., & Kill, D. (1975). Fornix lesions selectively abolish place learning in the rat. *Experimental neurology*, *48*(1), 152-166.

O'Keefe, J., & Recce, M. L. (1993). Phase relationship between hippocampal place units and the EEG theta rhythm. *Hippocampus*, *3*(3), 317-330.

Ólafsdóttir, H. F., Bush, D., & Barry, C. (2018). The Role of Hippocampal Replay in Memory and Planning. *Curr Biol*, *28*(1), R37-r50.

Oliveira, A. S., Schlink, B. R., Hairston, W. D., König, P., & Ferris, D. P. (2016). Proposing metrics for benchmarking novel EEG technologies towards real-world measurements. *Frontiers in Human Neuroscience*, *10*, 188.

Olton, D. S. (1979). Mazes, maps, and memory. *American psychologist*, *34*(7), 583.

Olton, D. S., & Samuelson, R. J. (1976). Remembrance of places passed: spatial memory in rats. *Journal of Experimental Psychology: Animal Behavior Processes*, *2*(2), 97.

Onton, J., Westerfield, M., Townsend, J., & Makeig, S. (2006). Imaging human EEG dynamics using independent component analysis. *Neuroscience & Biobehavioral Reviews*, *30*(6), 808-822.

Ormond, J., & O'Keefe, J. (2022). Hippocampal place cells have goal-oriented vector fields during navigation. *Nature*, *607*(7920), 741-746.

Osipova, D., Takashima, A., Oostenveld, R., Fernández, G., Maris, E., & Jensen, O. (2006). Theta and gamma oscillations predict encoding and retrieval of declarative memory. *Journal of Neuroscience*, *26*(28), 7523-7531.

Owen, A. M., Downes, J. J., Sahakian, B. J., Polkey, C. E., & Robbins, T. W. (1990). Planning and spatial working memory following frontal lobe lesions in man. *Neuropsychologia*, *28*(10), 1021-1034.

Packard, M. G., & McGaugh, J. L. (1992). Double dissociation of fornix and caudate nucleus lesions on acquisition of two water maze tasks: further evidence for multiple memory systems. *Behavioral Neuroscience*, *106*(3), 439.

Padilla, L. M., Creem-Regehr, S. H., Stefanucci, J. K., & Cashdan, E. A. (2017). Sex differences in virtual navigation influenced by scale and navigation experience. *Psychonomic Bulletin & Review*, *24*(2), 582-590.

Page, H. J., & Jeffery, K. J. (2018). Landmark-based updating of the head direction system by retrosplenial cortex: a computational model. *Frontiers in Cellular Neuroscience*, *12*, 191.

Palma, G. R., Thornberry, C., Commins, S., & Moral, R. d. A. (2023). Understanding learning from EEG data: Combining machine learning and feature engineering based on hidden Markov models and mixed models. *arXiv preprint arXiv:2311.08113*.

Palmigiano, A., Geisel, T., Wolf, F., & Battaglia, D. (2017). Flexible information routing by transient synchrony. *Nature Neuroscience*, *20*(7), 1014-1022.

Pantazis, D., Nichols, T. E., Baillet, S., & Leahy, R. M. (2005). A comparison of random field theory and permutation methods for the statistical analysis of MEG data. *NeuroImage*, *25*(2), 383-394.

Park, H., Kang, E., Kang, H., Kim, J. S., Jensen, O., Chung, C. K., & Lee, D. S. (2011). Cross-frequency power correlations reveal the right superior temporal gyrus as a hub region during working memory maintenance. *Brain connectivity*, *1*(6), 460-472.

Park, J., Lee, H., Kim, T., Park, G. Y., Lee, E. M., Baek, S., Ku, J., Kim, I. Y., Kim, S. I., Jang, D. P., & Kang, J. K. (2014). Role of low- and high-frequency oscillations in the human hippocampus for encoding environmental novelty during a spatial navigation task. *Hippocampus*, *24*(11), 1341-1352.

Park, J. L., Dudchenko, P. A., & Donaldson, D. I. (2018). Navigation in real-world environments: New opportunities afforded by advances in mobile brain imaging. *Frontiers in Human Neuroscience*, 361.

Park, J. Y., Lee, K. S., An, S. K., Lee, J., Kim, J.-J., Kim, K. H., & Namkoong, K. (2012). Gamma oscillatory activity in relation to memory ability in older adults. *International Journal of Psychophysiology*, *86*(1), 58-65.

Park, Y. M., Park, J., Baek, J. H., Kim, S. I., Kim, I. Y., Kang, J. K., & Jang, D. P. (2019). Differences in theta coherence between spatial and nonspatial attention using intracranial electroencephalographic signals in humans. *Human brain mapping*, *40*(8), 2336-2346.

Pastalkova, E., Itskov, V., Amarasingham, A., & Buzsáki, G. (2008). Internally generated cell assembly sequences in the rat hippocampus. *Science*, *321*(5894), 1322-1327.

Pastötter, B., & Bäuml, K.-H. T. (2014). Distinct slow and fast cortical theta dynamics in episodic memory retrieval. *NeuroImage*, *94*, 155-161.

Pavlov, Y. G., Adamian, N., Appelhoff, S., Arvaneh, M., Benwell, C. S. Y., Beste, C., Bland, A. R., Bradford, D. E., Bublatzky, F., Busch, N. A., Clayson, P. E., Cruse, D., Czeszumski, A., Dreber, A., Dumas, G., Ehinger, B., Ganis, G., He, X., Hinojosa, J. A., Huber-Huber, C., Inzlicht, M., Jack, B. N., Johannesson, M., Jones, R., Kalenkovich, E., Kaltwasser, L., Karimi-Rouzbahani, H., Keil, A., König, P., Kouara, L., Kulke, L., Ladouceur, C. D., Langer, N., Liesefeld, H. R., Luque, D., MacNamara, A., Mudrik, L., Muthuraman, M., Neal, L. B., Nilsonne, G., Niso, G., Ocklenburg, S., Oostenveld, R., Pernet, C. R., Pourtois, G., Ruzzoli, M., Sass, S. M., Schaefer, A., Senderecka, M., Snyder, J. S., Tamnes, C. K., Tognoli, E., van Vugt, M. K., Verona, E., Vloeberghs, R., Welke, D., Wessel, J. R., Zakharov, I., & Mushtaq, F. (2021). #EEGManyLabs: Investigating the replicability of influential EEG experiments. *Cortex*, *144*, 213-229.

Pearce, J. M. (2009). The 36th Sir Frederick Bartlett lecture: An associative analysis of spatial learning. *Quarterly Journal of Experimental Psychology*, *62*(9), 1665-1684.

Pereira, J., Ofner, P., Schwarz, A., Sburlea, A. I., & Müller-Putz, G. R. (2017). EEG neural correlates of goal-directed movement intention. *NeuroImage*, *149*, 129-140.

Perrot-Sinal, T. S., Kostenuik, M. A., Ossenkopp, K.-P., & Kavaliers, M. (1996). Sex differences in performance in the Morris water maze and the effects of initial nonstationary hidden platform training. *Behavioral Neuroscience*, *110*(6), 1309.

Peters, E., Hess, T. M., Västfjäll, D., & Auman, C. (2007). Adult age differences in dual information processes: Implications for the role of affective and deliberative processes in older adults' decision making. *Perspectives on Psychological Science*, *2*(1), 1-23.

Peylo, C., Hilla, Y., & Sauseng, P. (2021). Cause or consequence? Alpha oscillations in visuospatial attention. *Trends in Neurosciences*, *44*(9), 705-713.

Pfeiffer, B. E., & Foster, D. J. (2013). Hippocampal place-cell sequences depict future paths to remembered goals. *Nature*, *497*(7447), 74-79.

Pfurtscheller, G., Neuper, C., Andrew, C., & Edlinger, G. n. (1997). Foot and hand area mu rhythms. *International Journal of Psychophysiology*, *26*(1-3), 121-135.

Pfurtscheller, G., Stancak Jr, A., & Neuper, C. (1996). Event-related synchronization (ERS) in the alpha band—an electrophysiological correlate of cortical idling: a review. *International Journal of Psychophysiology*, *24*(1-2), 39-46.

Piber, D., Nowacki, J., Mueller, S. C., Wingenfeld, K., & Otte, C. (2018). Sex effects on spatial learning but not on spatial memory retrieval in healthy young adults. *Behavioural Brain Research*, *336*, 44-50.

Pimentel, G. A., Crestani, A. M., & Florindo, L. H. (2022). Do spatial and recognition memories have a lateralized processing by the dorsal hippocampus CA3? *Behavioural Brain Research*, *416*, 113566.

Pineda, J. A. (2005). The functional significance of mu rhythms: Translating "seeing" and "hearing" into "doing". *Brain Research Reviews*, *50*(1), 57-68.

Piper, B. J., Acevedo, S. F., Craytor, M. J., Murray, P. W., & Raber, J. (2010). The use and validation of the spatial navigation Memory Island test in primary school children. *Behavioural Brain Research*, *210*(2), 257-262.

Pothakos, K., Kurz, M. J., & Lau, Y.-S. (2009). Restorative effect of endurance exercise on behavioral deficits in the chronic mouse model of Parkinson's disease with severe neurodegeneration. *BMC neuroscience*, *10*(1), 1-14.

Power, L., & Bardouille, T. (2021). Age-related trends in the cortical sources of transient beta bursts during a sensorimotor task and rest. *NeuroImage*, *245*, 118670.

Prabhakaran, V., Narayanan, K., Zhao, Z., & Gabrieli, J. (2000). Integration of diverse information in working memory within the frontal lobe. *Nature Neuroscience*, *3*(1), 85-90.

Prichep, L., John, E., Ferris, S., Rausch, L., Fang, Z., Cancro, R., Torossian, C., & Reisberg, B. (2006). Prediction of longitudinal cognitive decline in normal elderly with subjective complaints using electrophysiological imaging. *Neurobiology of aging*, *27*(3), 471-481.

Proskovec, A. L., Wiesman, A. I., Heinrichs-Graham, E., & Wilson, T. W. (2018). Beta Oscillatory Dynamics in the Prefrontal and Superior Temporal Cortices Predict Spatial Working Memory Performance. *Scientific Reports*, *8*(1), 8488.

Pu, Y., Cornwell, B. R., Cheyne, D., & Johnson, B. W. (2018). High-gamma activity in the human hippocampus and parahippocampus during inter-trial rest periods of a virtual navigation task. *NeuroImage*, *178*, 92-103.

Pu, Y., Cornwell, B. R., Cheyne, D., & Johnson, B. W. (2020). Gender differences in navigation performance are associated with differential theta and high-gamma activities in the hippocampus and parahippocampus. *Behavioural Brain Research*, *391*, 112664.

Quirk, G. J., Muller, R. U., & Kubie, J. L. (1990). The firing of hippocampal place cells in the dark depends on the rat's recent experience. *Journal of Neuroscience*, *10*(6), 2008-2017.

R Core Team, R. (2013). R: A language and environment for statistical computing.

Ramos-Loyo, J., & Sanchez-Loyo, L. M. (2011). Gender differences in EEG coherent activity before and after training navigation skills in virtual environments. *Human Physiology*, *37*(6), 700-707.

Raslau, F. D., Mark, I. T., Klein, A. P., Ulmer, J. L., Mathews, V., & Mark, L. P. (2015). Memory Part 2: The Role of the Medial Temporal Lobe. *American Journal of Neuroradiology*, *36*(5), 846-849.

Ray, S., & Maunsell, J. H. (2015). Do gamma oscillations play a role in cerebral cortex? *Trends in Cognitive Sciences*, *19*(2), 78-85.

Redhead, E. S., & Hamilton, D. A. (2009). Evidence of blocking with geometric cues in a virtual watermaze. *Learning and Motivation*, *40*(1), 15-34.

Reinhart, R. M. G., & Nguyen, J. A. (2019). Working memory revived in older adults by synchronizing rhythmic brain circuits. *Nature Neuroscience*, *22*(5), 820-827.

Reis, J., Portugal, A. M., Fernandes, L., Afonso, N., Pereira, M., Sousa, N., & Dias, N. S. (2016). An Alpha and Theta Intensive and Short Neurofeedback Protocol for Healthy Aging Working-Memory Training [Original Research]. *Frontiers in Aging Neuroscience*, *8*.

Reitan, R. M., & Wolfson, D. (1992). *Neuropsychological evaluation of older children*. Neuropsychology Press.

Reitan, R. M., & Wolfson, D. (1995). Category Test and Trail Making Test as measures of frontal lobe functions. *The Clinical Neuropsychologist*, *9*(1), 50-56.

Rejer, I., & Górski, P. (2015). Benefits of ICA in the case of a few channel EEG. 2015 37th Annual International Conference of the IEEE Engineering in Medicine and Biology Society (EMBC),

Rekkas, P., & Constable, R. T. (2005). Evidence that autobiographic memory retrieval does not become independent of the hippocampus: an fMRI study contrasting very recent with remote events. *Journal of Cognitive Neuroscience*, *17*(12), 1950-1961.

Rempe, M. P., Ott, L. R., Picci, G., Penhale, S. H., Christopher-Hayes, N. J., Lew, B. J., Petro, N. M., Embury, C. M., Schantell, M., & Johnson, H. J. (2023). Spontaneous cortical dynamics from the first years to the golden years. *Proceedings of the National Academy of Sciences*, *120*(4), e2212776120.

Reynolds, N. C., Zhong, J. Y., Clendinen, C. A., Moffat, S. D., & Magnusson, K. R. (2019). Age-related differences in brain activations during spatial memory formation in a well-learned virtual Morris water maze (vMWM) task. *NeuroImage*, *202*, 116069.

Riddle, J., Scimeca, J. M., Cellier, D., Dhanani, S., & D'Esposito, M. (2020). Causal evidence for a role of theta and alpha oscillations in the control of working memory. *Current Biology*, *30*(9), 1748-1754. e1744.

Riečanský, I., & Katina, S. (2010). Induced EEG alpha oscillations are related to mental rotation ability: The evidence for neural efficiency and serial processing. *Neuroscience Letters*, *482*(2), 133-136.

Robbins, K. A., Touryan, J., Mullen, T., Kothe, C., & Bigdely-Shamlo, N. (2020). How sensitive are EEG results to preprocessing methods: a benchmarking study. *IEEE transactions on neural systems and rehabilitation engineering*, *28*(5), 1081-1090.

Roberts, B. M., Clarke, A., Addante, R. J., & Ranganath, C. (2018). Entrainment enhances theta oscillations and improves episodic memory. *Cognitive neuroscience*, *9*(3-4), 181-193.

Roberts, B. M., Hsieh, L. T., & Ranganath, C. (2013). Oscillatory activity during maintenance of spatial and temporal information in working memory. *Neuropsychologia*, *51*(2), 349-357.

Robin, J., & Moscovitch, M. (2017). Details, gist and schema: hippocampal–neocortical interactions underlying recent and remote episodic and spatial memory. *Current opinion in behavioral sciences*, *17*, 114-123.

Robinson, N. T., Descamps, L. A., Russell, L. E., Buchholz, M. O., Bicknell, B. A., Antonov, G. K., Lau, J. Y., Nutbrown, R., Schmidt-Hieber, C., & Häusser, M. (2020). Targeted activation of hippocampal place cells drives memory-guided spatial behavior. *Cell*, *183*(6), 1586-1599. e1510.

Rodgers, M. K., Sindone III, J. A., & Moffat, S. D. (2012). Effects of age on navigation strategy. *Neurobiology of aging*, *33*(1), 202. e215-202. e222.

Rodriguez, P. F. (2010). Neural decoding of goal locations in spatial navigation in humans with fMRI. *Human brain mapping*, *31*(3), 391-397.

Rogers, J., Churilov, L., Hannan, A. J., & Renoir, T. (2017). Search strategy selection in the Morris water maze indicates allocentric map formation during learning that underpins spatial memory formation. *Neurobiology of Learning and Memory*, *139*, 37-49.

Rolls, E. T., Stringer, S. M., & Elliot, T. (2006). Entorhinal cortex grid cells can map to hippocampal place cells by competitive learning. *Network: Computation in Neural Systems*, *17*(4), 447-465.

Rondina Ii, R., Olsen, R. K., Li, L., Meltzer, J. A., & Ryan, J. D. (2019). Age-related changes to oscillatory dynamics during maintenance and retrieval in a relational memory task. *PLOS ONE*, *14*(2), e0211851.

Rosenbaum, R. S., Priselac, S., Köhler, S., Black, S. E., Gao, F., Nadel, L., & Moscovitch, M. (2000). Remote spatial memory in an amnesic person with extensive bilateral hippocampal lesions. *Nature Neuroscience*, *3*(10), 1044-1048.

Roux, F., & Uhlhaas, P. J. (2014). Working memory and neural oscillations: α-γ versus θ-γ codes for distinct WM information? *Trends Cogn Sci*, *18*(1), 16-25.

Roux, F., Wibral, M., Mohr, H. M., Singer, W., & Uhlhaas, P. J. (2012). Gamma-band activity in human prefrontal cortex codes for the number of relevant items maintained in working memory. *Journal of Neuroscience*, *32*(36), 12411-12420.

Salthouse, T. A., & Babcock, R. L. (1991). Decomposing adult age differences in working memory. *Developmental psychology*, *27*(5), 763.

Sanders, A. E., Holtzer, R., Lipton, R. B., Hall, C., & Verghese, J. (2008). Egocentric and exocentric navigation skills in older adults. *The Journals of Gerontology Series A: Biological Sciences and Medical Sciences*, *63*(12), 1356-1363.

Sandstrom, N. J., Kaufman, J., & Huettel, S. A. (1998). Males and females use different distal cues in a virtual environment navigation task. *Cognitive Brain Research*, *6*(4), 351-360.

Sanei, S., & Chambers, J. A. (2013). *EEG signal processing*. John Wiley & Sons.

Santos, B. S., Dias, P., Silva, S., Capucho, L., Salgado, N., Lino, F., Carvalho, V., & Ferreira, C. (2008). Usability Evaluation in Virtual Reality: A User Study Comparing Three Different Setups. EGVE (Posters),

Sauseng, P., Klimesch, W., Heise, K. F., Gruber, W. R., Holz, E., Karim, A. A., Glennon, M., Gerloff, C., Birbaumer, N., & Hummel, F. C. (2009). Brain oscillatory substrates of visual short-term memory capacity. *Current Biology*, *19*(21), 1846-1852.

Sauseng, P., Klimesch, W., Schabus, M., & Doppelmayr, M. (2005). Fronto-parietal EEG coherence in theta and upper alpha reflect central executive functions of working memory. *International Journal of Psychophysiology*, *57*(2), 97-103.

Sauseng, P., Klimesch, W., Stadler, W., Schabus, M., Doppelmayr, M., Hanslmayr, S., Gruber, W. R., & Birbaumer, N. (2005). A shift of visual spatial attention is selectively associated with human EEG alpha activity. *European Journal of Neuroscience*, *22*(11), 2917-2926.

Scally, B., Burke, M. R., Bunce, D., & Delvenne, J.-F. (2018). Resting-state EEG power and connectivity are associated with alpha peak frequency slowing in healthy aging. *Neurobiology of aging*, *71*, 149-155.

Schapiro, A. C., Reid, A. G., Morgan, A., Manoach, D. S., Verfaellie, M., & Stickgold, R. (2019). The hippocampus is necessary for the consolidation of a task that does not require the hippocampus for initial learning. *Hippocampus*, *29*(11), 1091-1100.

Scheeringa, R., Bastiaansen, M. C., Petersson, K. M., Oostenveld, R., Norris, D. G., & Hagoort, P. (2008). Frontal theta EEG activity correlates negatively with the default mode network in resting state. *International Journal of Psychophysiology*, *67*(3), 242-251.

Schlesiger, M. I., Cressey, J. C., Boublil, B., Koenig, J., Melvin, N. R., Leutgeb, J. K., & Leutgeb, S. (2013). Hippocampal activation during the recall of remote spatial memories in radial maze tasks. *Neurobiology of Learning and Memory*, *106*, 324-333.

Schneider, D., Barth, A., & Wascher, E. (2017). On the contribution of motor planning to the retroactive cuing benefit in working memory: Evidence by mu and beta oscillatory activity in the EEG. *NeuroImage*, *162*, 73-85.

Schoenfeld, R., Foreman, N., & Leplow, B. (2014). Ageing and spatial reversal learning in humans: Findings from a virtual water maze. *Behavioural Brain Research*, *270*, 47-55.

Schoenfeld, R., Moenich, N., Mueller, F.-J., Lehmann, W., & Leplow, B. (2010). Search strategies in a human water maze analogue analyzed with automatic classification methods. *Behavioural Brain Research*, *208*(1), 169-177.

Schoenfeld, R., Schiffelholz, T., Beyer, C., Leplow, B., & Foreman, N. (2017). Variants of the Morris water maze task to comparatively assess human and rodent place navigation. *Neurobiology of Learning and Memory*, *139*, 117-127.

Sederberg, P. B., Gauthier, L. V., Terushkin, V., Miller, J. F., Barnathan, J. A., & Kahana, M. J. (2006). Oscillatory correlates of the primacy effect in episodic memory. *NeuroImage*, *32*(3), 1422-1431.

Seeber, M., Scherer, R., Wagner, J., Solis-Escalante, T., & Müller-Putz, G. R. (2014). EEG beta suppression and low gamma modulation are different elements of human upright walking [Original Research]. *Frontiers in Human Neuroscience*, *8*.

Seger, S. E., Kriegel, J. L., Lega, B. C., & Ekstrom, A. D. (2023). Memory-related processing is the primary driver of human hippocampal theta oscillations. *Neuron*, *111*(19), 3119-3130. e3114.

Sestieri, C., Shulman, G. L., & Corbetta, M. (2017). The contribution of the human posterior parietal cortex to episodic memory. *Nature reviews neuroscience*, *18*(3), 183-192.

Shanks, D. R., Charles, D., Darby, R. J., & Azmi, A. (1998). Configural processes in human associative learning. *Journal of Experimental Psychology: Learning, Memory, and Cognition*, *24*(6), 1353.

Shanks, D. R., Darby, R. J., & Charles, D. (1998). Resistance to interference in human associative learning: evidence of configural processing. *Journal of Experimental Psychology: Animal Behavior Processes*, *24*(2), 136.

Shine, J., Valdes-Herrera, J. P., Tempelmann, C., & Wolbers, T. (2019). Evidence for allocentric boundary and goal direction information in the human entorhinal cortex and subiculum. *Nature Communications*, *10*(1), 4004.

Shine, J. P., Valdés-Herrera, J. P., Hegarty, M., & Wolbers, T. (2016). The human retrosplenial cortex and thalamus code head direction in a global reference frame. *Journal of Neuroscience*, *36*(24), 6371-6381.

Shires, K. L., & Aggleton, J. P. (2008). Mapping immediate-early gene activity in the rat after place learning in a water-maze: the importance of matched control conditions. *Eur J Neurosci*, *28*(5), 982-996.

Skarsfeldt, T. (1996). Differential effect of antipsychotics on place navigation of rats in the Morris water maze. *Psychopharmacology*, *124*(1), 126-133.

Small, W. S. (1901). Experimental study of the mental processes of the rat. II. *The American Journal of Psychology*, 206-239.

Smallwood, J., Bernhardt, B. C., Leech, R., Bzdok, D., Jefferies, E., & Margulies, D. S. (2021). The default mode network in cognition: a topographical perspective. *Nature Reviews Neuroscience*, *22*(8), 503-513.

Smith, A. D. (2014). Age differences in encoding, storage, and retrieval. In *New Directions in Memory and Aging (PLE: Memory)* (pp. 23-45). Psychology Press.

Smith, D. M., & Mizumori, S. J. (2006). Hippocampal place cells, context, and episodic memory. *Hippocampus*, *16*(9), 716-729.

Smyrnis, N., Protopapa, F., Tsoukas, E., Balogh, A., Siettos, C. I., & Evdokimidis, I. (2014). Amplitude spectrum EEG signal evidence for the dissociation of motor and perceptual

spatial working memory in the human brain. *Experimental brain research*, *232*(2), 659-673.

Solomon, E. A., Stein, J. M., Das, S., Gorniak, R., Sperling, M. R., Worrell, G., Inman, C. S., Tan, R. J., Jobst, B. C., & Rizzuto, D. S. (2019). Dynamic theta networks in the human medial temporal lobe support episodic memory. *Current Biology*, *29*(7), 1100-1111.

Solstad, T., Boccara, C. N., Kropff, E., Moser, M.-B., & Moser, E. I. (2008). Representation of geometric borders in the entorhinal cortex. *Science*, *322*(5909), 1865-1868.

Soltani Zangbar, H., Ghadiri, T., Seyedi Vafaee, M., Ebrahimi Kalan, A., Fallahi, S., Ghorbani, M., & Shahabi, P. (2020). Theta oscillations through hippocampal/prefrontal pathway: importance in cognitive performances. *Brain connectivity*, *10*(4), 157-169.

Sosa, M., & Giocomo, L. M. (2021). Navigating for reward. *Nature reviews neuroscience*, *22*(8), 472-487.

Spiers, H., & Maguire, E. (2007). The neuroscience of remote spatial memory: a tale of two cities. *Neuroscience*, *149*(1), 7-27.

Spiers, H. J., Burgess, N., Maguire, E. A., Baxendale, S. A., Hartley, T., Thompson, P. J., & O'Keefe, J. (2001). Unilateral temporal lobectomy patients show lateralized topographical and episodic memory deficits in a virtual town. *Brain*, *124*(12), 2476-2489.

Spiers, H. J., & Maguire, E. A. (2008). The dynamic nature of cognition during wayfinding. *Journal of environmental psychology*, *28*(3), 232-249.

Spitzer, B., & Haegens, S. (2017). Beyond the Status Quo: A Role for Beta Oscillations in Endogenous Content (Re)Activation. *eneuro*, *4*(4).

Squire, L. R. (1992). Memory and the hippocampus: a synthesis from findings with rats, monkeys, and humans. *Psychological review*, *99*(2), 195.

Squire, L. R., Genzel, L., Wixted, J. T., & Morris, R. G. (2015). Memory consolidation. *Cold Spring Harbor perspectives in biology*, *7*(8), a021766.

Stachenfeld, K. L., Botvinick, M. M., & Gershman, S. J. (2017). The hippocampus as a predictive map. *Nature Neuroscience*, *20*(11), 1643-1653.

Stark, C. E., & Squire, L. R. (2003). Hippocampal damage equally impairs memory for single items and memory for conjunctions. *Hippocampus*, *13*(2), 281-292.

Staudigl, T., & Hanslmayr, S. (2013). Theta Oscillations at Encoding Mediate the Context-Dependent Nature of Human Episodic Memory. *Current Biology*, *23*(12), 1101-1106.

Staufenbiel, S. M., Brouwer, A. M., Keizer, A. W., & van Wouwe, N. C. (2014). Effect of beta and gamma neurofeedback on memory and intelligence in the elderly. *Biological Psychology*, *95*, 74-85.

Steiger, T. K., Sobczak, A., Reineke, R., & Bunzeck, N. (2022). Novelty processing associated with neural beta oscillations improves recognition memory in young and older adults. *Annals of the New York Academy of Sciences*, *1511*(1), 228-243.

Steinvorth, S., Wang, C., Ulbert, I., Schomer, D., & Halgren, E. (2010). Human entorhinal gamma and theta oscillations selective for remote autobiographical memory. *Hippocampus*, *20*(1), 166-173.

Stern, Y., Habeck, C., Moeller, J., Scarmeas, N., Anderson, K. E., Hilton, H. J., Flynn, J., Sackeim, H., & Van Heertum, R. (2005). Brain networks associated with cognitive reserve in healthy young and old adults. *Cerebral Cortex*, *15*(4), 394-402.

Stoewer, P., Schilling, A., Maier, A., & Krauss, P. (2023). Neural network based formation of cognitive maps of semantic spaces and the putative emergence of abstract concepts. *Scientific Reports*, *13*(1), 3644.

Strunk, J., James, T., Arndt, J., & Duarte, A. (2017). Age-related changes in neural oscillations supporting context memory retrieval. *Cortex*, *91*, 40-55.

Sutherland, R. J., Lee, J. Q., McDonald, R. J., & Lehmann, H. (2020). Has multiple trace theory been refuted? *Hippocampus*, *30*(8), 842-850.

Sutherland, R. J., & Rudy, J. W. (1989). Configural association theory: The role of the hippocampal formation in learning, memory, and amnesia. *Psychobiology*, *17*(2), 129-144.

Sutterer, D. W., Foster, J. J., Serences, J. T., Vogel, E. K., & Awh, E. (2019). Alpha-band oscillations track the retrieval of precise spatial representations from long-term memory. *Journal of neurophysiology*, *122*(2), 539-551.

Tadel, F., Baillet, S., Mosher, J. C., Pantazis, D., & Leahy, R. M. (2011). Brainstorm: a user-friendly application for MEG/EEG analysis. *Computational intelligence and neuroscience*, *2011*.

Takehara-Nishiuchi, K. (2020). Prefrontal–hippocampal interaction during the encoding of new memories. *Brain and Neuroscience Advances*, *4*, 2398212820925580.

Taube, J. S. (2007). The head direction signal: origins and sensory-motor integration. *Annu. Rev. Neurosci.*, *30*, 181-207.

Taube, J. S., Muller, R. U., & Ranck, J. B., Jr. (1990). Head-direction cells recorded from the postsubiculum in freely moving rats. II. Effects of environmental manipulations. *J Neurosci*, *10*(2), 436-447.

Tempel, T., Frings, C., & Pastötter, B. (2020). EEG beta power increase indicates inhibition in motor memory. *International Journal of Psychophysiology*, *150*, 92-99.

Teng, E., & Squire, L. R. (1999). Memory for places learned long ago is intact after hippocampal damage. *Nature*, *400*(6745), 675-677.

Thornberry, C. (2019). *An Examination of the Influence of Landmarks in Human Spatial Navigation Using a Virtual Water Maze* National University of Ireland, Maynooth (Ireland)].

Thornberry, C., Caffrey, M., & Commins, S. (2023). Theta oscillatory power decreases in humans are associated with spatial learning in a virtual water maze task. *European Journal of Neuroscience*, *58*(11), 4341-4356.

Thornberry, C., Cimadevilla, J. M., & Commins, S. (2021). Virtual Morris water maze: opportunities and challenges. *Reviews in the Neurosciences*, *32*(8), 887-903.

Thornberry, C., Clarke, A., & Commins, S. (2022). The Impact of Covid-19 Lockdown Restrictions on Attention and Activities of Daily Living in the Republic of Ireland. *PsyPag Quarterly (British Psychological Society)*(123), 8-21.

Thorndyke, P. W., & Hayes-Roth, B. (1982). Differences in spatial knowledge acquired from maps and navigation. *Cognitive psychology*, *14*(4), 560-589.

Thut, G., Nietzel, A., Brandt, S. A., & Pascual-Leone, A. (2006). α-Band electroencephalographic activity over occipital cortex indexes visuospatial attention bias and predicts visual target detection. *Journal of Neuroscience*, *26*(37), 9494-9502.

Tolman, E. C. (1948). Cognitive maps in rats and men. *Psychological review*, *55*(4), 189.

Tolman, E. C., Ritchie, B. F., & Kalish, D. (1946). Studies in spatial learning. I. Orientation and the short-cut. *Journal of experimental psychology*, *36*(1), 13.

Tombaugh, T. N. (2004). Trail Making Test A and B: normative data stratified by age and education. *Archives of clinical neuropsychology*, *19*(2), 203-214.

Trivedi, M. A., & Coover, G. D. (2004). Lesions of the ventral hippocampus, but not the dorsal hippocampus, impair conditioned fear expression and inhibitory avoidance on the elevated T-maze. *Neurobiology of Learning and Memory*, *81*(3), 172-184.

Tröndle, M., Popov, T., Pedroni, A., Pfeiffer, C., Barańczuk-Turska, Z., & Langer, N. (2023). Decomposing age effects in EEG alpha power. *Cortex*, *161*, 116-144.

Tse, D., Langston, R. F., Kakeyama, M., Bethus, I., Spooner, P. A., Wood, E. R., Witter, M. P., & Morris, R. G. M. (2007). Schemas and Memory Consolidation. *Science*, *316*(5821), 76-82.

Tu, S., Wong, S., Hodges, J. R., Irish, M., Piguet, O., & Hornberger, M. (2015). Lost in spatial translation - A novel tool to objectively assess spatial disorientation in Alzheimer's disease and frontotemporal dementia. *Cortex; a journal devoted to the study of the nervous system and behavior*, *67*, 83-94.

Tucker, L. B., Velosky, A. G., & McCabe, J. T. (2018). Applications of the Morris water maze in translational traumatic brain injury research. *Neuroscience & Biobehavioral Reviews*, *88*, 187-200.

Tuladhar, A. M., Huurne, N. t., Schoffelen, J. M., Maris, E., Oostenveld, R., & Jensen, O. (2007). Parieto-occipital sources account for the increase in alpha activity with working memory load. *Human brain mapping*, *28*(8), 785-792.

Umbach, G., Kantak, P., Jacobs, J., Kahana, M., Pfeiffer, B. E., Sperling, M., & Lega, B. (2020). Time cells in the human hippocampus and entorhinal cortex support episodic memory. *Proceedings of the National Academy of Sciences*, *117*(45), 28463-28474.

Unsworth, N., Redick, T. S., McMillan, B. D., Hambrick, D. Z., Kane, M. J., & Engle, R. W. (2015). Is playing video games related to cognitive abilities? *Psychological science*, *26*(6), 759-774.

Urcelay, G. P., & Miller, R. R. (2014). The functions of contexts in associative learning. *Behavioural processes*, *104*, 2-12.

van de Vijver, I., Cohen, M. X., & Ridderinkhof, K. R. (2014). Aging affects medial but not anterior frontal learning-related theta oscillations. *Neurobiology of aging*, *35*(3), 692-704.

van der Ham, I. J. M., & Claessen, M. H. G. (2020). How age relates to spatial navigation performance: Functional and methodological considerations. *Ageing research reviews*, *58*, 101020.

Van Ede, F., De Lange, F., Jensen, O., & Maris, E. (2011). Orienting attention to an upcoming tactile event involves a spatially and temporally specific modulation of sensorimotor alpha-and beta-band oscillations. *Journal of Neuroscience*, *31*(6), 2016-2024.

Van Gerven, D. J., Ferguson, T., & Skelton, R. W. (2016). Acute stress switches spatial navigation strategy from egocentric to allocentric in a virtual Morris water maze. *Neurobiology of Learning and Memory*, *132*, 29-39.

van Schie, H. T., Mars, R. B., Coles, M. G. H., & Bekkering, H. (2004). Modulation of activity in medial frontal and motor cortices during error observation. *Nature Neuroscience*, *7*(5), 549-554.

Vanderwolf, C. H. (1969). Hippocampal electrical activity and voluntary movement in the rat. *Electroencephalogr Clin Neurophysiol*, *26*(4), 407-418.

Vann, S. D. (2024). Effects of experimental brain lesions on spatial navigation. In *Reference Module in Neuroscience and Biobehavioral Psychology*. Elsevier.

Vass, L. K., Copara, M. S., Seyal, M., Shahlaie, K., Farias, S. T., Shen, P. Y., & Ekstrom, A. D. (2016). Oscillations go the distance: low-frequency human hippocampal oscillations code spatial distance in the absence of sensory cues during teleportation. *Neuron*, *89*(6), 1180-1186.

Vecchiato, G., Tieri, G., Jelic, A., De Matteis, F., Maglione, A. G., & Babiloni, F. (2015). Electroencephalographic Correlates of Sensorimotor Integration and Embodiment during the Appreciation of Virtual Architectural Environments [Original Research]. *Frontiers in Psychology*, *6*.

Vivekananda, U., Bush, D., Bisby, J. A., Baxendale, S., Rodionov, R., Diehl, B., Chowdhury, F. A., McEvoy, A. W., Miserocchi, A., Walker, M. C., & Burgess, N. (2021). Theta

power and theta-gamma coupling support long-term spatial memory retrieval. *Hippocampus*, *31*(2), 213-220.
Vlahou, E. L., Thurm, F., Kolassa, I.-T., & Schlee, W. (2014). Resting-state slow wave power, healthy aging and cognitive performance. *Scientific reports*, *4*(1), 5101.
Vorhees, C. V., & Williams, M. T. (2006). Morris water maze: Procedures for assessing spatial and related forms of learning and memory [Article]. *Nature Protocols*, *1*(2), 848-858.
Vorhees, C. V., & Williams, M. T. (2014a). Assessing Spatial Learning and Memory in Rodents. *ILAR Journal*, *55*(2), 310-332.
Vorhees, C. V., & Williams, M. T. (2014b). Value of water mazes for assessing spatial and egocentric learning and memory in rodent basic research and regulatory studies. *Neurotoxicology and Teratology*, *45*, 75-90.
Vorhees, C. V., & Williams, M. T. (2024). Tests for learning and memory in rodent regulatory studies. *Current Research in Toxicology*, *6*, 100151.
Vysata, O., Kukal, J., Prochazka, A., Pazdera, L., Simko, J., & Valis, M. (2014). Age-related changes in EEG coherence. *Neurologia i neurochirurgia polska*, *48*(1), 35-38.
Wagner, A. R., & Rescorla, R. A. (1972). Inhibition in Pavlovian conditioning: Application of a theory. *Inhibition and learning*, 301-336.
Waldhauser, G. T., Bäuml, K.-H. T., & Hanslmayr, S. (2015). Brain oscillations mediate successful suppression of unwanted memories. *Cerebral Cortex*, *25*(11), 4180-4190.
Waldhauser, G. T., Johansson, M., & Hanslmayr, S. (2012). Alpha/beta oscillations indicate inhibition of interfering visual memories. *Journal of Neuroscience*, *32*(6), 1953-1961.
Wallet, G., Sauzéon, H., Larrue, F., & N'Kaoua, B. (2013). Virtual/real transfer in a large-scale environment: impact of active navigation as a function of the viewpoint displacement effect and recall tasks. *Adv. in Hum.-Comp. Int.*, *2013*, Article 8.
Wang, J., Barstein, J., Ethridge, L. E., Mosconi, M. W., Takarae, Y., & Sweeney, J. A. (2013). Resting state EEG abnormalities in autism spectrum disorders. *Journal of neurodevelopmental disorders*, *5*, 1-14.
Ward, A. M., Mormino, E. C., Huijbers, W., Schultz, A. P., Hedden, T., & Sperling, R. A. (2015). Relationships between default-mode network connectivity, medial temporal lobe structure, and age-related memory deficits. *Neurobiology of aging*, *36*(1), 265-272.
Watrous, A. J., Fried, I., & Ekstrom, A. D. (2011). Behavioral correlates of human hippocampal delta and theta oscillations during navigation. *Journal of neurophysiology*, *105*(4), 1747-1755.
Watrous, A. J., Lee, D. J., Izadi, A., Gurkoff, G. G., Shahlaie, K., & Ekstrom, A. D. (2013). A comparative study of human and rat hippocampal low-frequency oscillations during spatial navigation. *Hippocampus*, *23*(8), 656-661.
Weisberg, S. M., Newcombe, N. S., & Chatterjee, A. (2019). Everyday taxi drivers: Do better navigators have larger hippocampi? *Cortex*, *115*, 280-293.
Weiss, E. M., Kemmler, G., Deisenhammer, E. A., Fleischhacker, W. W., & Delazer, M. (2003). Sex differences in cognitive functions. *Personality and Individual Differences*, *35*(4), 863-875.
Werkle-Bergner, M., Müller, V., Li, S.-C., & Lindenberger, U. (2006). Cortical EEG correlates of successful memory encoding: implications for lifespan comparisons. *Neuroscience & Biobehavioral Reviews*, *30*(6), 839-854.
Wessel, J. R. (2020). β-bursts reveal the trial-to-trial dynamics of movement initiation and cancellation. *Journal of Neuroscience*, *40*(2), 411-423.
Whelan, R., Barbey, F. M., Cominetti, M. R., Gillan, C. M., & Rosická, A. M. (2022). Developments in scalable strategies for detecting early markers of cognitive decline. *Translational Psychiatry*, *12*(1), 473.

Whishaw, I. Q. (1991). Latent learning in a swimming pool place task by rats: Evidence for the use of associative and not cognitive mapping processes. *The Quarterly Journal of Experimental Psychology Section B*, *43*(1b), 83-103.

White, D. J., Congedo, M., Ciorciari, J., & Silberstein, R. B. (2012). Brain Oscillatory Activity during Spatial Navigation: Theta and Gamma Activity Link Medial Temporal and Parietal Regions. *Journal of Cognitive Neuroscience*, *24*(3), 686-697.

Wichert, S., Wolf, O. T., & Schwabe, L. (2011). Reactivation, interference, and reconsolidation: Are recent and remote memories likewise susceptible? *Behavioral Neuroscience*, *125*(5), 699.

Wiener, J. M., Carroll, D., Moeller, S., Bibi, I., Ivanova, D., Allen, P., & Wolbers, T. (2020). A novel virtual-reality-based route-learning test suite: Assessing the effects of cognitive aging on navigation. *Behavior research methods*, *52*(2), 630-640.

Wilson, M. A., & McNaughton, B. L. (1994). Reactivation of hippocampal ensemble memories during sleep. *Science*, *265*(5172), 676-679.

Winocur, G., Moscovitch, M., & Bontempi, B. (2010). Memory formation and long-term retention in humans and animals: Convergence towards a transformation account of hippocampal–neocortical interactions. *Neuropsychologia*, *48*(8), 2339-2356.

Winterling, S. L., Shields, S. M., & Rose, M. (2019). Reduced memory-related ongoing oscillatory activity in healthy older adults. *Neurobiology of aging*, *79*, 1-10.

Wolff, M. J., Jochim, J., Akyürek, E. G., & Stokes, M. G. (2017). Dynamic hidden states underlying working-memory-guided behavior. *Nature Neuroscience*, *20*(6), 864-871. https://doi.org/10.1038/nn.4546

Woods, D. L., Wyma, J. M., Herron, T. J., & Yund, E. W. (2015). The effects of aging, malingering, and traumatic brain injury on computerized trail-making test performance. *PLOS ONE*, *10*(6), e0124345.

Woollett, K., & Maguire, E. A. (2010). The effect of navigational expertise on wayfinding in new environments. *Journal of environmental psychology*, *30*(4), 565-573.

Woolley, D. G., Vermaercke, B., de Beeck, H. O., Wagemans, J., Gantois, I., D'Hooge, R., Swinnen, S. P., & Wenderoth, N. (2010). Sex differences in human virtual water maze performance: Novel measures reveal the relative contribution of directional responding and spatial knowledge. *Behavioural Brain Research*, *208*(2), 408-414.

Wu, C.-T., Haggerty, D., Kemere, C., & Ji, D. (2017). Hippocampal awake replay in fear memory retrieval. *Nature Neuroscience*, *20*(4), 571-580.

Wunderlich, A., & Gramann, K. (2021). Eye movement-related brain potentials during assisted navigation in real-world environments. *European Journal of Neuroscience*, *54*(12), 8336-8354.

Yaffe, R. B., Shaikhouni, A., Arai, J., Inati, S. K., & Zaghloul, K. A. (2017). Cued memory retrieval exhibits reinstatement of high gamma power on a faster timescale in the left temporal lobe and prefrontal cortex. *Journal of Neuroscience*, *37*(17), 4472-4480.

Yang, C. S., Liu, J., Singh, A. K., Huang, K. C., & Lin, C. T. (2021). Brain Dynamics of Spatial Reference Frame Proclivity in Active Navigation. *IEEE transactions on neural systems and rehabilitation engineering*, *29*, 1701-1710.

Yao, D., Qin, Y., Hu, S., Dong, L., Bringas Vega, M. L., & Valdés Sosa, P. A. (2019). Which reference should we use for EEG and ERP practice? *Brain Topography*, *32*, 530-549.

Yao, J., & Dewald, J. P. (2005). Evaluation of different cortical source localization methods using simulated and experimental EEG data. *NeuroImage*, *25*(2), 369-382.

Yassa, M. A. (2018). Brain rhythms: higher-frequency theta oscillations make sense in moving humans. *Current Biology*, *28*(2), R70-R72.

Yassa, M. A., & Reagh, Z. M. (2013). Competitive trace theory: a role for the hippocampus in contextual interference during retrieval. *Frontiers in Behavioral Neuroscience*, *7*, 107.

Yavuz, E., He, C., Gahnstrom, C. J., Goodroe, S., Coutrot, A., Hornberger, M., Hegarty, M., & Spiers, H. J. (2024). Video gaming, but not reliance on GPS, is associated with spatial navigation performance. *Journal of environmental psychology*, *96*, 102296. https://doi.org/https://doi.org/10.1016/j.jenvp.2024.102296

Yu, S., Boone, A. P., He, C., Davis, R. C., Hegarty, M., Chrastil, E. R., & Jacobs, E. G. (2021). Age-related changes in spatial navigation are evident by midlife and differ by sex. *Psychological science*, *32*(5), 692-704.

Zadikoff, C., Fox, S. H., Tang-Wai, D. F., Thomsen, T., De Bie, R. M., Wadia, P., Miyasaki, J., Duff-Canning, S., Lang, A. E., & Marras, C. (2008). A comparison of the mini mental state exam to the Montreal cognitive assessment in identifying cognitive deficits in Parkinson's disease. *Movement disorders*, *23*(2), 297-299.

Zakrzewska, M. Z., & Brzezicka, A. (2014). Working memory capacity as a moderator of load-related frontal midline theta variability in Sternberg task. *Frontiers in Human Neuroscience*, *8*, 399.

Zhang, H., Lee, A., & Qiu, A. (2017). A posterior-to-anterior shift of brain functional dynamics in aging. *Brain Structure and Function*, *222*, 3665-3676.

Zhong, J. Y., Magnusson, K. R., Swarts, M. E., Clendinen, C. A., Reynolds, N. C., & Moffat, S. D. (2017). The application of a rodent-based Morris water maze (MWM) protocol to an investigation of age-related differences in human spatial learning. *Behavioral Neuroscience*, *131*(6), 470.

Zielinski, M. C., Tang, W., & Jadhav, S. P. (2020). The role of replay and theta sequences in mediating hippocampal-prefrontal interactions for memory and cognition. *Hippocampus*, *30*(1), 60-72.

Zou, Q., Ross, T. J., Gu, H., Geng, X., Zuo, X. N., Hong, L. E., Gao, J. H., Stein, E. A., Zang, Y. F., & Yang, Y. (2013). Intrinsic resting-state activity predicts working memory brain activation and behavioral performance. *Human brain mapping*, *34*(12), 3204-3215.

Zúñiga, R. G., Davis, J. R., Boyle, R., De Looze, C., Meaney, J. F., Whelan, R., Kenny, R. A., Knight, S. P., & Ortuño, R. R. (2023). Brain connectivity in frailty: Insights from The Irish Longitudinal Study on Ageing (TILDA). *Neurobiology of aging*, *124*, 1-10.

# Appendices

Appendix A: EEG Standard Operating Procedure during COVID-19.

Appendix B: Participant Information Sheet.

*Appendix A*

**Department of Psychology**

**Specific health precautions for EEG testing**

As EEG experiments will require close proximity to the participant at certain times, extra precautions to those laid out in the general document will need to be followed.

**Cubicle area/laboratory space**

- Separate areas should be used for EEG preparation and recording.
- No other experiments should take place in the cubicle/EEG area during this time.
- Only one participant and one experimenter should be present in the laboratory area.
- Keep the area well ventilated.

**Equipment**

- EEG cap.

Use separate EEG caps for each participant where possible. All caps must be disinfected thoroughly following use. Allow 3 days between use of the same cap.

- Face mask

A face mask **must** be worn throughout the entire procedure.

- A log book

A log of names, contact details of all participants and the relevant experimenter should be kept. The date and time of entry/exit of the participants should also be noted. This will be used for contact tracing.

**Procedure**

<u>Prior to participant arrival</u>

- Note, if the participants are not students or staff the experimenter further covid protocols may be needed to be completed before the experiment can be done. Ensure all relevant paperwork is done. Contact the Return to Campus Office for further information.
- The experimenter should sign into the log book upon entry to the laboratory area.
- Lay out as much of the equipment prior to the arrival of the participant. This includes a EEG cap, gel-filled syringe, syringe tips, towels, electrodes, gloves, alcohol wipes etc.
- Participants may need to be warned that some gel may remain in their hair following the experiment, if the wash area is not in use or if the participant is not willing to avail of this facility.
- Both the participant and experimenter should wash hands for at least 20 seconds (or apply hand sanitizer) upon entry to the laboratory.

During the experiment and application of electrodes

- The experimenter should already be wearing gloves, a lab coat, and mask. The participant should also be wearing a mask (see general rules) before entering the building.
- Upon arrival the participant should log their name and contact details and time of entry.
- Ensure that both parties continue to wear face masks when applying the electrodes at the beginning of the session, while making any adjustments to the electrodes during the session, and while removing them at the end of the session.
- To the extent possible, the experimenter should stand behind the subject while attaching the electrodes.
- Keep social distance at all times apart from when applying the electrodes.

Post testing

- Participant hair washing is not recommended. Gel should be wiped from the hair as much as possible with a tissue. This is done by the participant. If the wash room is used, it must be entirely disinfected after the participant leaves.
- The participant should be signed out and walked to the exit, while maintaining social distance.
- The participant must re-apply hand sanitizer, and keep wearing the mask until he/she leaves the building.
- The experimenter should then apply hand sanitizer.
- Disinfect the electrodes and electrode caps in Envirocide solution for 3 minutes. This disinfecting procedure is recommended for the Brain Products actiCAP system.
- As usual, used syringes and tips are discarded.
- Disinfect chairs, computers, all equipment, response pad, mouse, door handles - anything that might be touched by the subject or the experimenter using disinfection wipes.
- The experimenter's gloves can be discarded and the lab coat can be removed once the participant has departed.
- Laboratory coats must be laundered at least once per week on a hot wash (>60°C) and can't be shared with others.
- The experimenter's mask should be discarded and a new one used in the rest of the building.
- Hands should be sanitized when leaving the laboratory/cubicle area. The experimenter should then sign out using the log book.

*Appendix B*

Maynooth University
National University of Ireland Maynooth

Roinn Síceolaíochta Ollscoil Mhá Nuad
Maynooth University Department of Psychology

**Information Sheet:**

# An examination of the neural correlates of spatial navigation and memory in humans

**Postgraduate Researcher**:
Conor Thornberry
Michelle Caffrey
Roisin Deery

conor.thornberry@mu.ie
michelle.caffrey@mu.ie
roisin.deery@mu.ie

**Supervisor:**
Dr. Sean Commins
Department of Psychology
Maynooth University,
Co. Kildare,
Ireland.

Sean.Commins@mu.ie

Ph 017086182

Your participation is requested in an experimental study taking place with the Department of Psychology at Maynooth University examining the brains electrical activity underlying learning and recall in humans using a task that depends on navigation and recall of the environment.

***What is the study about?***

The brains electrical activity during our daily navigation has been relatively unexplored. Most daily tasks involve understanding the space and location of objects, being able to recall them and using them to navigate our environment. Therefore, using two tasks that involve this type of associative learning and recall, we wish to examine brain activity as humans learn and remember using non-invasive Electroencephalography (EEG). EEG is a safe, harmless method of recording the electrical activity of the brain.

***What does it involve? What would I have to do?***

There would be two parts to your involvement, all of which will take place in a quiet location free from distraction.

1. You will be set-up with the EEG cap and connected to our monitoring software. This will take about 15 minutes.

2. You will then be asked to perform a computerized task. This will be a computer-based task - NavWell – which will involve learning the spatial position of a goal in relation to the environment. The researcher will then organize a time that suits you to return to see if you can recall the spatial location again. This will be greater than 24 hours but no longer than 1 month.

3. In your follow-up session, you will be set-up with our EEG system again. Your ability to recall the goal location will be examined using NavWell. This should take up to 20 minutes. You will then be asked to complete 4 brief cognitive tasks. These consist of the National Adult Reading Test (NART) for general intelligence, the Trail Making Task (TMT) for executive functioning, the Rey Auditory Verbal Learning Task (RAVLT) for memory and the Montreal Cognitive Assessment (MoCA). These tasks will take about 10 minutes and are only carried out to ensure participants are cognitively matched. The specific aims of the study will be explained as soon as you have completed the experiment.

***Are there any risks to me?***

There are no risks associated with this study. The procedure involves very little discomfort and should be an enjoyable experience for most participants. This procedure is safe, painless, and non-invasive; it does not involve radiation, x-rays, magnetic fields or any other dangerous elements, so you should consider it similar to having your heart rate or blood-pressure measured. The procedure involves applying a conductive gel to your scalp to help us get a clear signal from the brain, so you will need to wash your hair afterwards – washing and drying facilities will be provided for you.

Roinn Síceolaíochta Ollscoil Mhá Nuad, Ollscoil Mhá Nuad, Maigh Nuad, Co. Chill Dara, Éire.
Maynooth University Department of Psychology, Maynooth University, Maynooth, Co. Kildare, Ireland.

**T** +353 1 708 6311 **E** psychology.dept@nuim.ie **W** maynoothuniversity.ie/psychology

The questionnaires will involve either verbally answering questions or filling in answers with pen and paper. The NavWell software involves joystick controlled first-person navigation of a virtual environment, very similar to playing a computer game.

In the unlikely event that you experience any distress, discomfort or if you have any concerns about any aspect of your performance on these tasks, you should feel free to contact Dr. Sean Commins or contact your own GP with these concerns. Should you be a student of the University you may also avail of the Student Counseling Service (01 708 3554) or Student Health Service (01 708 3878); both are on campus and located very close to the Psychology Department.

We hope to provide a baseline of healthy neural activity during everyday navigation learning tasks, which could be used for comparison with at-risk older adults suffering from memory-related disorders such as dementia.

***What happens to my test scores?***

The printed data from your participation (i.e., test scores) will be strictly confidential and will be kept in a locked cabinet in the Psychology Department. Your results will be kept confidential by assigning a random number to each participant instead of your name. Aside from your age, no other personal data will be recorded. Except for the researcher(s) involved in running this study, nobody will be allowed to see or discuss any of your data. Your data will be combined with many others and reported in group form – averages etc. – in a scientific paper, but your own data will be available to you at your discretion.

Roinn Síceolaíochta Ollscoil Mhá Nuad, Ollscoil Mhá Nuad, Maigh Nuad, Co. Chill Dara, Éire.
Maynooth University Department of Psychology, Maynooth University, Maynooth, Co. Kildare, Ireland.

**T** +353 1 708 6311 **E** psychology.dept@nuim.ie **W** maynoothuniversity.ie/psychology

***Can I withdraw from the study?***

Yes, you may withdraw your data and involvement in the study at any time up until the completion of your participation.

If you are willing to help us by participating in this study, we will ask you to sign a **Letter of Consent**, which accompanies this information sheet. We are very grateful for your participation.

***I have some health issues – am I still eligible to take part?***

Finally, if you suffer from **any** of the following, you may not be eligible to take part:

- severe visual impairments;
- history of psychological/neurological impairment;
- history of motion or simulator sickness;
- history of epilepsy or memory issues;
- history of drug or alcohol abuse;
- currently taking psychoactive medication;
- other relevant medical conditions; such as **vertigo** or **claustrophobia**

Do you suffer from/have suffered from any of the above?

Yes ☐ No ☐

You are welcome to discuss this decision with us, but you are under no obligation to do so. Please feel free to study these criteria during a cooling off period of up to one week. Should you choose not to participate, no further action is required. If you have any doubts as to whether or not you are eligible to take place in this study, please inform us so we may determine your eligibility.

Roinn Síceolaíochta Ollscoil Mhá Nuad, Ollscoil Mhá Nuad, Maigh Nuad, Co. Chill Dara, Éire.
Maynooth University Department of Psychology, Maynooth University, Maynooth, Co. Kildare, Ireland.

**T** +353 1 708 6311 **E** psychology.dept@nuim.ie **W** maynoothuniversity.ie/psychology

**INFORMED CONSENT FORM**

**In agreeing to participate in this research I understand the following:**

This research is being conducted by Conor Thornberry, a postgraduate student at the Department of Psychology, Maynooth University. The method proposed for this research project adheres in principle to the Psychological Society of Ireland (PSI) code of professional ethics. It is, however, the above-named student's responsibility to adhere to ethical guidelines in their dealings with participants and the collection and handling of data. If I have any concerns about participation, I understand that I may refuse to participate or withdraw at any stage.

I have been informed as to the general nature of the study and agree voluntarily to participate.

The total time for your participation will be approximately 2 hours in total across two sessions. The follow up session is carried out no less than 24 hours later. There are no known expected discomforts or risks associated with participation.

The results of my participation will be documented by participant number only. No names or individual identifying information will be recorded. Except for the researcher(s) involved in running this study, nobody will be allowed to see or discuss any of the individual responses. My responses will be combined with many others and reported in group form in a scientific paper and/or a report submitted to the Department of Psychology. My own data will be available to me at my discretion. I may withdraw my data and involvement in the study at any time, up until the completion of your participation.

**Please Note:** students participating in this research as part of the Year 2 Research Credit Participation Scheme (connected to the modules PS256 and PS260) should be aware that, while you may withdraw your participation at any stage, this may mean you will have to complete a short-written assignment in lieu of participation. You may also withdraw and choose to not receive credit also. The credit system is managed independently of the researchers. Should you have any concerns please refer to the module description in your Year 2 Handbook (https://www.maynoothuniversity.ie/psychology/resources).

At the conclusion of my participation, any questions or concerns I have will be fully addressed.
I may withdraw from this study at any time and may withdraw my data at the conclusion of my participation if I still have concerns.

Signed:

_____Participant

_____Researcher

_____Date

Roinn Síceolaíochta Ollscoil Mhá Nuad, Ollscoil Mhá Nuad, Maigh Nuad, Co. Chill Dara, Éire.
Maynooth University Department of Psychology, Maynooth University, Maynooth, Co. Kildare, Ireland.

**T** +353 1 708 6311 **E** psychology.dept@nuim.ie **W** maynoothuniversity.ie/psychology